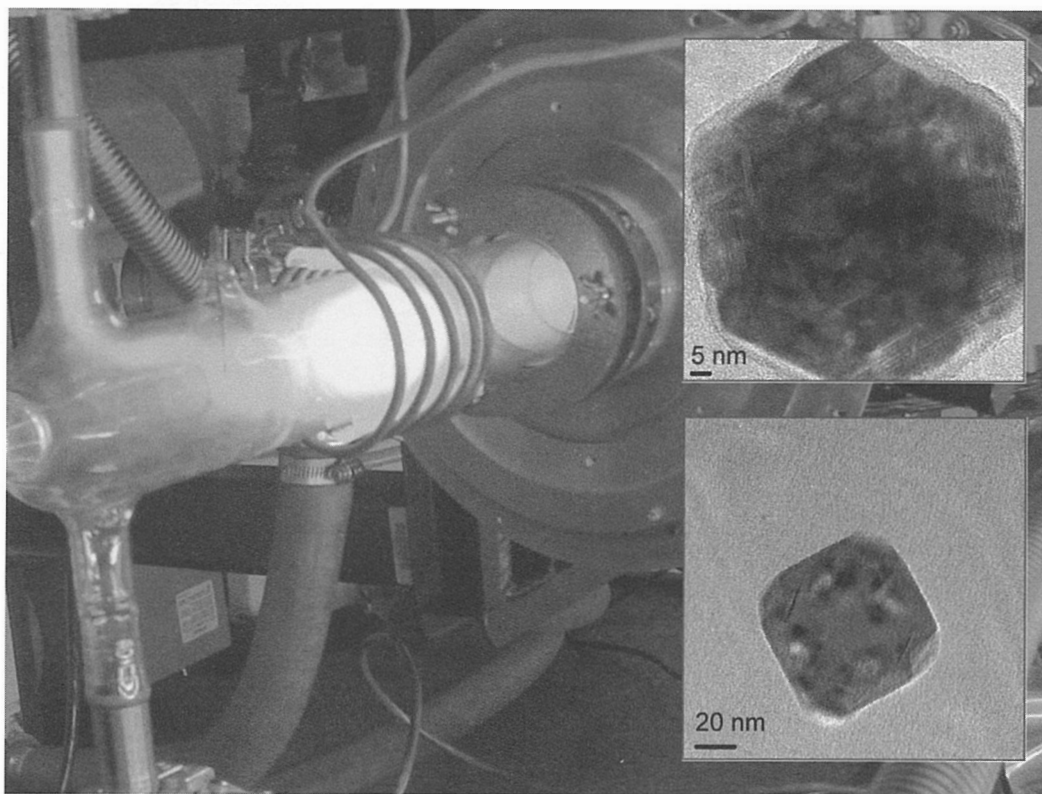


BULLETIN

OF THE AMERICAN PHYSICAL SOCIETY

PROGRAM OF THE 55th ANNUAL
GASEOUS ELECTRONICS CONFERENCE



October 15–18, 2002
Minneapolis, Minnesota

October 2002

Volume 47, No. 7

BULLETIN

OF THE AMERICAN PHYSICAL SOCIETY

Coden BAPSA6

Series II, Vol. 47, No. 7

ISSN: 0003-0503

October 2002

APS COUNCIL 2002

President

William F. Brinkman,* *Bell Labs-Lucent Technologies*

President-Elect

Myriam P. Sarachik,* *City College of New York-CUNY*

Vice President

Helen R. Quinn,* *Stanford Linear Accelerator Center*

Executive Officer

Judy R. Franz,* *University of Alabama, Huntsville (on leave)*

Treasurer

Thomas McIlrath,* *University of Maryland (emeritus)*

Editor-in-Chief

Martin Blume,* *Brookhaven National Laboratory*

Past-President

George H. Trilling,* *Lawrence Berkeley National Laboratory*

General Councillors

Jonathan A. Bagger, Philip Bucksbaum,* L. Craig Davis, Stuart Freedman,* Frances Houle, Leon Lederman,* Gerald Mahan, Margaret Murnane,* Cherry Ann Murray, Philip Phillips,* Jin-Joo Song, James Trefil

International Councillor

T. Maurice Rice

Chair, Nominating Committee

Susan Nan Coppersmith

Chair, Panel on Public Affairs

James C. H. Tsang

Division, Forum and Section Councillors

Edward Kolb (*Astrophysics*), Harold Metcalf (*Atomic, Molecular & Optical*), Robert Eisenberg (*Biological*), Sylvia Ceyer (*Chemical*), E. Dan Dahlberg,* Allen Goldman* (*Condensed Matter Physics*), Steven White (*Computational*), Jerry Gollub* (*Fluid Dynamics*), Peter Zimmerman (*Forum on Education*), Stuart Wolf (*Forum on Industrial and Applied Physics*), Gloria Lubkin (*Forum on History of Physics*), James Vary (*Forum on International Physics*), Ed Gerjuoy (*Forum on Physics and Society*), Timothy P. Lodge (*Polymer Physics*), W. Carl Lineberger (*Laser Science*), G. Slade Cargill, III (*Materials*), Bunny C. Clark (*Nuclear*), Sally Dawson, Peter Meyers (*Particles & Fields*), Stephen Holmes (*Physics of Beams*), Richard Hazeltine (*Plasma*), Kannan Jagannathan (*New England*), Joe Hamilton (*Southeast Section*)

*Members of the APS Executive Board

ADVISORS

Representatives from Other Societies

Christopher J. Chiaverina, *AAPT*; Marc Brodsky, *AIP*

International Advisors

Gerardo C. Puente, *Mexican Physical Society*;
W. J. McDonald, *Canadian Association of Physicists*

Editor: Donna M. Baudrau, CMP

Meetings Publications Coordinator:

Vinaya K. Sathyasheelappa

APS MEETINGS DEPARTMENT

One Physics Ellipse

College Park, MD 20740-3844

Telephone: (301) 209-3286

FAX: (301) 209-0866

Donna Baudrau, *Director of Meetings & Conventions*

Terri Adorjan, *Senior Meeting Planner*

Karen MacFarland, *Meeting Planner*

Don Wise, *Registrar*

Staff Representatives

Alan Chodos, *Associate Executive Officer*; Irving Lerch, *Director of International Affairs*; Fredrick Stein, *Director of Education and Outreach*; Robert L. Park, *Director, Public Information*; Michael Lubell, *Director, Public Affairs*; Stanley Brown, *Editorial Director*; Charles Muller, *Director, Journal Operations*; Michael Stephens, *Controller and Assistant Treasurer*

Administrator for Governing Committees

Ken Cole

The *Bulletin of The American Physical Society* is published 11X in 2002—March, April, May, July, August, October (3X), November (2X), and December—by The American Physical Society through the American Institute of Physics. It contains information about meetings of the Society, including abstracts of papers to be presented, as well as transactions of past meetings. Reprints of papers can be obtained only by writing directly to the authors.

The *Bulletin* is delivered, on subscription, by Periodicals mail. Complete volumes are also available on microfilm. **APS Members** may subscribe to individual issues, or for the entire year. **Nonmembers** may subscribe to the *Bulletin* at the following rates: Domestic \$600; Foreign Surface \$620; Air Freight \$645. Information on prices, as well as subscription orders, renewals, and address changes, should be addressed as follows: **For APS Members**—Membership Department, The American Physical Society, One Physics Ellipse, College Park, MD 20740-3844. **For Nonmembers**—Circulation and Fulfillment Division, The American Institute of Physics, Suite 1N01, 2 Huntington Quadrangle, Melville, NY 11747-4502. Allow at least 6 weeks advance notice. For address changes, please send both the old and new addresses, and, if possible, include a mailing label from a recent issue. Requests from subscribers for missing issues will be honored without charge only if received within 6 months of the issue's actual date of publication.

The *Bulletin of The American Physical Society* (ISSN: 0003-0503) is published eleven times a year for The American Physical Society by the American Institute of Physics. 2002 subscription rate is \$600 for domestic nonmembers. Postmaster: Send address changes to *Bulletin of The American Physical Society*, AIP, Suite 1N01, 2 Huntington Quadrangle, Melville, NY 11747-4502. Periodicals postage paid at Huntington Station, NY, and additional mailing offices.

BULLETIN

OF THE AMERICAN PHYSICAL SOCIETY

Vol. 47, No. 7, October 2002

55th Annual Gaseous Electronics Conference

TABLE OF CONTENTS

General Information	3
Special Sessions and Events	3
<i>Sessions</i>	3
<i>Presentation Formats</i>	4
<i>GEC Student Award for Excellence</i>	4
Registration	5
Banquet and Reception	5
E-mail and Other Business Services	5
Audio-Visual Equipment	5
Dining Options	5
Guest Program	5
Call for Nominations for GEC General and Executive Committees	5
<i>GEC02 Executive Committee</i>	6
<i>Conference Secretary</i>	6
Please Note	6
Epitome	7
Main Text	10
<i>Tuesday, October 15, 2002</i>	10
<i>Wednesday, October 16, 2002</i>	35
<i>Thursday, October 17, 2002</i>	56

<i>Friday, October 18, 2002</i>	69
Author Index	79
Maps and Floor Plan	At End of Issue

55th Annual Gaseous Electronics Conference

October 15–18, 2002

University of Minnesota Minneapolis, Minnesota

GENERAL INFORMATION

Welcome to the 55th Annual Gaseous Electronics Conference (GEC) of the American Physical Society (APS). The GEC02 program includes the APS Will Allis Prize Lecture, the GEC Foundation Talk, and the annual GEC Student Award for Excellence. Oral sessions with both invited and contributed papers and two poster sessions will address a broad range of topics. The Millennium Hotel in downtown Minneapolis will serve as headquarters for the conference.

SPECIAL SESSIONS AND EVENTS

The GEC Executive Committee is pleased to announce the *Allis Prize Lecture* at the GEC02. The lecture will be given by Dr. Alan Garscadden, U.S. Air Force Research Laboratory, and is entitled "*Gaseous Electronics Physics Inside*." The Will Allis Prize for the Study of Ionized Gases was established in 1989 in recognition of the outstanding contributions of Will Allis to the study of ionized gases. The prize includes a \$5000 award and was established through contributions from AT&T, GE, GTE, IBM, and Xerox. GEC participants are well represented among the previous winners of this prize, and include Arthur Phelps (JILA, U. Colorado), Jim Lawler (U. Wisconsin), Chun Lin (U. Wisconsin), Ray Flannery (Georgia Tech), and John Waymouth (Sylvania). Further information, including nomination guidelines, can be found on the APS website (www.aps.org).

The Executive Committee is also pleased to announce the *Foundation Talk* at the GEC02. The talk will be given by Prof. Emil Pfender, University of Minnesota, and is entitled "*What do we know about the anode region of thermal plasmas?*" The GEC Foundation Talk is a plenary talk at each GEC. Its aim is to present a cogent overview of a topical area and to put it into context for the very cross-disciplinary audience that attends the GEC. The talk covers both introductory

material to guide students and newcomers, as well as cutting edge work from the speaker's own experience to engage the expert.

A special *workshop on "The Bohm criterion and sheath formation"* will be held in the evening of Tuesday, October 15, 2002. This informal workshop will cover current understanding of this aspect of gas discharges in the variety of gases now of interest particularly in processing plasmas. There will be a short scene-setting historical presentation followed by others covering recent work which may have been published in the past year, be currently in the process of publication, or is work still in progress. Contributions are solicited particularly covering complex situations, e.g., non-local treatments, multiplicity of ion species and the transition to a collisional sheath. No abstracts will be required for participation in the workshop; hence there can be no citations to material presented. The workshop is organized by Profs. Mike Lieberman, U.C. Berkeley, and Raoul Franklin, Open University.

Three tutorials will be offered as pre-GEC activity in the afternoon of Monday, October 14, 2002. The tutorials are intended to provide non-experts and students with a broad, introductory overview of emerging fields of plasma applications.

Laboratory Tours are planned for Wednesday, October 16, at 15:30. Conference participants will have an opportunity to visit selected research laboratories at the University of Minnesota. Among the laboratories to be included in the tour are the High Temperature and Plasma Laboratory (<http://www.me.umn.edu/divisions/tht/highT/>), laboratories participating in the NSF-IGERT for Nanoparticle Science and Engineering (<http://www.nanoigert.umn.edu>), and the University of Minnesota Microtechnology Laboratory (<http://www.mtl.umn.edu>).

SESSIONS

- Tutorial I: Biomedical Applications of Plasmas (*Session AMT*)
- Tutorial II: The Physics of Filamentary, Regularly-

- Patterned and Diffuse Barrier Discharges (*Session BMT*)
- Tutorial III: Nanoparticles and Plasmas (*Session CMT*)
- Reception and Registration (*Session DM*)
- Plasma Modeling (*Session ET1*)
- Ionization of Atoms and Molecules (*Session ET2*)
- Plasma Boundaries: Sheaths and Boundary Layers (*Session FT1*)
- Thermal Plasmas (*Session FT2*)
- Poster Session I (*Session GTP*)
 - Electron and Positron Collisions with Atoms and Molecules
 - Materials and Device Processing
 - Plasma-Surface Interactions
 - Capacitively Coupled Plasmas and Negative-Ion Plasmas
 - Computational Methods for Plasmas
 - Plasma Boundaries, Sheaths and Presheaths I
 - Plasma Diagnostics I
 - Plasma for Nanostructured Materials and Dusty Plasmas
 - Light Sources I
 - High-Pressure Nonthermal Plasmas I
 - Thermal Plasmas and Arcs
 - Atmospheric Plasma Chemistry
- Plasma Processing (*Session HT1*)
- Biological and Emerging Applications of Plasmas (*Session HT2*)
- Workshop: The Bohm Criterion and Sheath Formation (*Session JTW*)
- Plenary Lecture: GEC Foundation Talk (*Session KW*)
- Plenary Lecture: APS Will Allis Prize Talk (*Session LW*)
- GEC Business Meeting (*Session MW*)
- Diagnostics of Reactive Plasmas (*Session NW1*)
- Thermal Plasmas: Lamps and Electrodes (*Session NW2*)
- Laboratory Tours (*Session PW*)
- Poster Session II (*Session QWP*)
 - Electron, Positron and Photon Interactions
 - Heavy Particle Interactions
 - Distribution Functions and Transport Coefficients
 - Glows: dc, pulsed, rf, microwave, other
 - Inductively Coupled Plasmas
 - Magnetically Enhanced Plasmas
 - Plasma Boundaries, Sheaths, Presheaths II
 - Plasma Diagnostics II
 - Laser Media and Kinetics
 - Light Sources II
 - High-Pressure Nonthermal Plasmas II
 - Biological Applications of Plasmas
- Instabilities (*Session RRI*)
- Collisions with Complex Targets (*Session RR2*)
- Plasmas for Nanostructured Materials (*Session SRI*)
- Near Threshold Processes (*Session SR2*)
- Plasma Diagnostics: Electrical and Optical (*Session TRI*)
- Recombination and Dissociation (*Session TR2*)
- Inductively Coupled Plasmas and Plasma Sources (*Session URI*)
- Atmospheric Pressure Nonthermal Plasmas I (*Session UR2*)
- Banquet and Reception (*Session VR*)
- Plasma Surface Interactions (*Session WFI*)
- Nonequilibrium Light Sources (*Session WF2*)
- Plasmas for Nanostructures and Dusty Plasmas (*Session XF1*)
- Atmospheric Pressure Nonthermal Plasmas II (*Session XF2*)
- Plasma Diagnostics: Optical Emission (*Session YFI*)
- Plasma Propulsion and Plasma Aerodynamics (*Session YF2*)

PRESENTATION FORMATS

Papers that have been accepted for presentation are listed in the technical program. Invited papers are allotted 25 minutes, with 5 additional minutes for questions and discussions. Oral contributed presentations are allotted 12 minutes, with 3 additional minutes for discussion. Poster sessions will be provided with 96" by 48" posterboards. Presenters may mount their posters anytime earlier in the day upon which their presentation is scheduled. Poster materials must be removed the evening of the scheduled presentation.

GEC STUDENT AWARD FOR EXCELLENCE

In order to recognize the outstanding contributions students make to the GEC and encourage further student participation, the GEC will continue to award a prize for the best paper presentation by a student. A subcommittee of the GEC Executive Committee will choose the award winner. Students competing for the \$500 award, in the order of their appearance in the program, are:

E. Ghedini, nominated by V. Colombo (University of Bologna), "Fully 3D Modeling of Inductively Coupled Plasma Torches."

J. P. Marler, nominated by Cliff Surko (University of California, San Diego), "Positron Scattering from Noble Gas Atoms."

A. Gidwani, nominated by Steve Girshick (University of Minnesota), "Hypersonic Plasma Particle Deposition of Nanostructured Films and Patterns."

Tae Won Kim, nominated by Eray Aydil (University of California, Santa Barbara), "Two-dimensional Spatial Distributions of Ion Flux Impinging on the Wafer Surface in Discharges Maintained in Inductively Coupled Plasma Etching Reactors."

Sebastien Dine, nominated by Jacques Jolly (École Polytechnique), "Frequency effects in a RF capacitive discharge in hydrogen."

Lorenzo Mangolini, nominated by Joachim Heberlein (University of Minnesota), "Experimental and numerical study of an atmospheric pressure glow discharge in helium."

L. Moskwinski, nominated by Kurt Becker (Stevens Institute of Technology), "Al Surface Cleaning Using a Capillary Plasma Electrode Discharge (CPED) Plasma."

Badri Ramamurthy, nominated by Igor Kaganovich (University of Houston), "Effect of non-local electron conductivity on power absorption and plasma density profiles for low pressure inductively coupled discharges."

REGISTRATION

The registration desk will be located in the Millennium Hotel. Registration hours will be 12:30 to 21:00 on Monday, October 14, 7:30 to 15:00 Tuesday, October 15, and 7:30 to 13:00 Wednesday through Friday, October 16-18, 2002. The on-site conference registration fee is \$310 for regular registrations and \$190 for students and retirees.

BANQUET AND RECEPTION

An opening reception will be held on the evening of Monday, October 14, 2002, in the Millennium Hotel, starting at 19:00, on the 14th floor of the Millennium Hotel.

The conference banquet will be held in the Forum Ballroom of the Millennium Hotel on Thursday evening, October 17, starting with a reception at 18:45. Conference participants are encouraged to attend the reception and the banquet.

E-MAIL AND OTHER BUSINESS SERVICES

Free e-mail access will be available to conference participants in the Millennium Hotel in the Avenue 3 meeting room located on the lower level. Fax, photocopy services, and office supplies will also be available from the hotel business center.

AUDIO-VISUAL EQUIPMENT

Each conference room will be equipped with an overhead projector and a LCD projector. If additional equipment is required, please contact the conference secretary.

DINING OPTIONS

A list with dining options in the vicinity of the Millennium Hotel is included in the registration packet provided to each conference participant.

GUEST PROGRAM

Minneapolis downtown and the broader Twin Cities area offer a wide variety of attractions for guests. Many cultural attractions are in walking distance from the Millennium Hotel. The hotel also offers a shuttle service to the Mall of America. A meeting room for accompanying persons will be available throughout the conference. Please check the GEC website <http://www.me.umn.edu/gec> for links to some area attractions.

CALL FOR NOMINATIONS FOR GEC GENERAL AND EXECUTIVE COMMITTEES

The GEC Executive Committee (ExComm) is the governing body of the GEC. It is the responsibility of ExComm to oversee all aspects of the conference. This includes selection of meeting sites, budgetary decisions, selection of special topics and invited speakers, accepting/rejecting abstracts, and arranging of the program. The General Committee and ExComm meet during the GEC, and the ExComm meets again during the

summer to plan the program of the next GEC. There are numerous communications between members of the ExComm (usually e-mail) during the year to insure the successful completion of their duties. We have been fortunate over the years to have a dedicated group of volunteers who have been willing to take on these very necessary roles.

The by-laws of the Gaseous Electronics Conference describe the process whereby members of the ExComm are elected. At the GEC Business Meeting (to be held on Wednesday, October 16, at 11:15 in the Forum Ballroom in the Millennium Hotel) nominations are accepted for members of the GEC General Committee (GenComm).

The GenComm consists of the ExComm and 6 at-large members elected at the Business Meeting. The eligible voting membership of the GEC (defined as those attending the Business Meeting) elect these 6 at-large members. The GenComm then meets to fulfill its only duty: to elect new members of the ExComm.

The ExComm membership consists of the Chair, Treasurer, Past-Secretary, Secretary, Secretary-elect, past or incoming Chair and 4 at-large members. The Chair is a 4-year term (1-year incoming, 2-years chair, 1-year past-chair), the secretary is a 3-year term (1-year incoming, 1-year secretary, 1-year past-secretary), and all other ExComm members serve 2 years. (The secretary is the person who manages the local arrangements for the meeting and is usually "recruited" and appointed to the ExComm.)

The ExComm welcomes nominations, including self-nominations, for both the GenComm and ExComm. Becoming a GenComm and/or ExComm member provides a unique opportunity to see both how the GEC is run and to influence its future direction by helping to define the programs and choose future sites.

Please submit your nominations to the GEC Chair or any member of the ExComm. The ExComm also welcomes inquiries on hosting future GECs.

GEC02 EXECUTIVE COMMITTEE

Tim Sommerer, Chair
GE Research

Leposava Vuskovic, Chair-Elect

Old Dominion University

Uwe Kortshagen, Secretary

University of Minnesota

Robert McGrath, Past-Secretary

Pennsylvania State University

Helen Hwang, Secretary-Elect

NASA Ames

Winifred Huo, Treasurer

NASA Ames

Klaus Bartschat

Drake University

Jean-Paul Booth

École Polytechnique

Steven Buckman

Australian National University

Akihiro Kono

Nagoya University

Ann Orel

UC Davis

Bish Ganguly

Wright Patterson Air Force Base

CONFERENCE SECRETARY

Prof. Uwe Kortshagen

University of Minnesota

Mechanical Engineering

111 Church Street S.E.

Minneapolis, MN 55455

Voice: (612) 625 4028

FAX: (612) 625 4344

Email: gec@me.umn.edu

PLEASE NOTE

The APS has made every effort to provide accurate and complete information in this *Bulletin*. However, changes or corrections may occasionally be necessary and may be made without notice after the date of publication. To ensure that you receive the most up-to-date information, please check the meeting Corrigenda distributed with this *Bulletin*.

Epitome of the 55th Gaseous Electronics Conference of The American Physical Society

13:00 MONDAY AFTERNOON
14 OCTOBER 2002

AMT **Tutorial I: Biomedical
Applications of Plasmas**
Satellites 6,7, Millennium Hotel

14:45 MONDAY AFTERNOON
14 OCTOBER 2002

BMT **Tutorial II: The Physics of
Filamentary, Regularly-Patterned
and Diffuse Barrier Discharges**
Satellites 6,7, Millennium Hotel

16:30 MONDAY AFTERNOON
14 OCTOBER 2002

CMT **Tutorial III: Nanoparticles and
Plasmas**
Satellites 6,7, Millennium Hotel

19:00 MONDAY EVENING
14 OCTOBER 2002

DM **Reception and Registration**
Horizons/Dome, Millennium Hotel

8:00 TUESDAY MORNING
15 OCTOBER 2002

ET1 **Plasma Modeling**
North Forum, Millennium Hotel

ET2 **Ionization of Atoms and
Molecules**
Dorn, Whelan
Center Forum, Millennium Hotel

10:00 TUESDAY MORNING
15 OCTOBER 2002

FT1 **Plasma Boundaries: Sheaths and
Boundary Layers**
North Forum, Millennium Hotel

FT2 **Thermal Plasmas**
Center Forum, Millennium Hotel

13:15 TUESDAY AFTERNOON
15 OCTOBER 2002

GTP **Poster Session I**
Horizons/Satellites, Millennium
Hotel

15:30 TUESDAY AFTERNOON
15 OCTOBER 2002

HT1 **Plasma Processing**
Boswell
North Forum, Millennium Hotel

HT2 **Biological and Emerging
Applications of Plasmas**
Ohl, Shard, Favia
Center Forum, Millennium Hotel

19:15 TUESDAY EVENING
15 OCTOBER 2002

JTW **Workshop: The Bohm Criterion
and Sheath Formation**
Dome, Millennium Hotel

8:15 WEDNESDAY MORNING
16 OCTOBER 2002

KW **GEC Foundation Talk**
Pfender
North/Center Forum, Millennium
Hotel

10:00 WEDNESDAY MORNING
16 OCTOBER 2002

LW **APS Allis Prize Talk**
Garscadden
North/Center Forum, Millennium
Hotel

11:15 WEDNESDAY MORNING
16 OCTOBER 2002

MW **GEC Business Meeting**
North/Center Forum, Millennium
Hotel

13:15 WEDNESDAY AFTERNOON
16 OCTOBER 2002

NW1 **Diagnostics of Reactive Plasmas**
North Forum, Millennium Hotel

NW2 **Thermal Plasmas: Lamps and
Electrodes**
Mentel, Hechtfisher
Center Forum, Millennium Hotel

15:30 WEDNESDAY AFTERNOON
16 OCTOBER 2002

PW **Laboratory Tours**
University of Minnesota

19:15 WEDNESDAY EVENING
16 OCTOBER 2002

QWP **Poster Session II**
Horizons/Satellites, Millennium
Hotel

8:00 THURSDAY MORNING
17 OCTOBER 2002

RR1 **Instabilities**
Chabert
North Forum, Millennium Hotel

RR2 **Collisions with Complex Targets**
Brunger, Orlando
Center Forum, Millennium Hotel

10:00 THURSDAY MORNING
17 OCTOBER 2002

SR1 **Plasmas for Nanostructured
Materials**
Shih, Hatakeyama
North Forum, Millennium Hotel

SR2 **Near Threshold Processes**
Allan, Thumm
Center Forum, Millennium Hotel

13:30 THURSDAY AFTERNOON
17 OCTOBER 2002

TR1 **Plasma Diagnostics: Electrical
and Optical**
North Forum, Millennium Hotel

TR2 **Recombination and Dissociation**
Greene, Djuric
Center Forum, Millennium Hotel

15:30 THURSDAY AFTERNOON
17 OCTOBER 2002

UR1 **Inductively Coupled Plasmas and
Plasma Sources**
North Forum, Millennium Hotel

UR2 **Atmospheric Pressure
Nonthermal Plasmas I**
Wagner
Center Forum, Millennium Hotel

18:45 THURSDAY EVENING
17 OCTOBER 2002

VR **Reception and Banquet**
Millennium Hotel

8:00 FRIDAY MORNING
18 OCTOBER 2002

WF1 **Plasma Surface Interactions**
Toyoda
North Forum, Millennium Hotel

WF2 **Nonequilibrium Light Sources**
Center Forum, Millennium Hotel

10:00 FRIDAY MORNING
18 OCTOBER 2002

- XF1 **Plasmas for Nanostructures and
Dusty Plasmas**
North Forum, Millennium Hotel
- XF2 **Atmospheric Pressure
Nonthermal Plasmas II**
Fridman, Okazaki
Center Forum, Millennium Hotel

13:30 FRIDAY AFTERNOON
18 OCTOBER 2002

- YF1 **Plasma Diagnostics: Optical
Emission**
North Forum, Millennium Hotel
- YF2 **Plasma Propulsion and Plasma
Aerodynamics**
Bouchoule
Center Forum, Millennium Hotel

MAIN TEXT

SESSION ET1: PLASMA MODELING

Tuesday morning, 15 October 2002

North Forum, Millennium Hotel at 8:00

H. Akashi, National Defense Academy of Japan, presiding

8:00

ET1 1 Modeling of Electron Kinetics in Magnetically Enhanced Inductively Coupled Plasmas* ALEX VASENKOV, MARK J. KUSHNER, *University of Illinois/Urbana-Champaign* Collisionless electron heating is often the dominant process in inductively coupled plasmas (ICPs) when the anomalous skin effect is important. Owing to their high ionization and power deposition efficiencies magnetically enhanced inductively coupled plasma (MEICP) sources are being investigated for use in the semiconductor industry. The mechanisms through which these higher efficiencies are obtained are not well understood. In this paper we report on a computational study of non-collisional electron heating in MEICPs sustained in C_4F_8/Ar gas mixtures at low pressures (< 10 mTorr) where the skin layer is anomalous. A detailed plasma chemical reaction mechanism was developed to address the complex surface and gas-phase processes of this plasma system. The spatial dependences of electron energy distributions (EEDs) and power deposition were investigated for magnetic fields up to 100s G using a 2-dimensional plasma hydrodynamics model containing a Monte Carlo based kinetic electron transport module which includes electron-electron collisions. The angular anisotropy of the EEDs will also be discussed.

*Work supported by Sematech, CFD Research Corp., SRC and the National Science Foundation (CTS99-74962).

8:15

ET1 2 Modeling of magnetically enhanced inductive plasmas DEEPAK BOSE, *Eloret Corp.* T. R. GOVINDAN, *NASA Ames Research Center, Moffett Field, CA 94035* M. MEYYAPPAN, *NASA Ames Research Center, Moffett Field, CA 94035* Magnetically enhanced inductive sources are of interest since they achieve high plasma densities via electron confinement. Also, the presence of a dc magnetic field allows the rf antenna to launch helicon waves which results in power deposition well within the discharge volume. Many authors have studied propagation of helicons in uniform and non uniform plasmas. However, a self-consistent model of wave propagation and plasma generation and transport is rare in the literature. A dc magnetic field not only causes strong anisotropy in electron mobility, diffusion, thermal and electrical conductivity, but also gives rise to cross-directional effects. These cross-directional terms are difficult to model implicitly in a numerical scheme. In this work we will present a robust numerical technique to self-consistently model 2d, axisymmetric helicon mode (with 3d wave components) with plasma generation and transport in a commercial tool. We will compare our results with available experimental data and theoretical estimates.

8:30

ET1 3 A Numerical Model for Magnetically Enhanced Plasma in 3-D Reactors NING ZHOU, *CFD Research Corp* Magnetically enhanced plasma have recently attracted interest from semiconductor industry due to its higher ionization efficiency and more uniform ion flux to wafer. Based on our existent ICP model implemented in commercial code CFD-ACE+, the effect of magneto-static field is simulated by employing the electric conductivity tensor for eddy current, and the electron mobility tensor for drift current. Magnetostatic and electromagnetic (in frequency domain) fields are both solved for the 3-dimensional components in 2-D and 3-D geometry. Quasi-neutrality and ambipolarity are assumed for electron density and electrostatic field, respectively. Numerical demonstration and parametric study are performed for magnetically enhanced ICP, and ECR plasma.

8:45

ET1 4 Hybrid Simulation of Inductively/Capacitively Coupled Plasmas RALF PETER BRINKMANN, *Ruhr-Universitaet Bochum* THEORETICAL ELECTRICAL ENGINEERING COLLABORATION A simulation tool is presented which allows to study electrodynamic and kinetic phenomena in RF driven low pressure plasmas (CCP and/or ICP). The code differs from a first-principles approach, as it is constructed from a number of specialized modules which focus on particular aspects of the dynamics (heavy species, sheath behavior, surface chemistry, electromagnetic field). The distribution functions of the electrons in the bulk and the ions in the sheath are calculated by means of a Monte Carlo simulations. The time and length scale assumptions which underlie the approach hold for typical process plasmas. The model is completely self-consistent on the hydrodynamic level; its systematic error on the kinetic level can be monitored and was found sufficiently small. The tool was used to investigate the effect of various parameters on the details of the EEDF. For purely inductively coupled plasmas, one remarkable result is the formation of a pronounced spatial structure of the EEDF. The distribution under the coils can be characterized by a two-temperature model (a near-Maxwellian depleted at high energies), while the distribution in the discharge center has a three-temperature form, indicating a sizable fraction of cold electrons trapped in the potential maximum.

9:00

ET1 5 Standing Wave and Skin Effects in Large Area, High Frequency Capacitive Discharges M.A. LIEBERMAN, *U.C. Berkeley* J.P. BOOTH, P. CHABERT, J.M. RAX, *Ecole Polytechnique, France* M.M. TURNER, *Dublin City University, Ireland* Large area capacitive discharges driven at frequencies higher than the usual industrial frequency of 13.56 MHz have attracted recent interest for materials etching and thin film deposition on large area substrates. Standing wave and skin effects can be important limitations for plasma processing uniformity, which cannot be described by conventional electrostatic theory. An electromagnetic theory is developed for a discharge having two plates of radius R and separation $2l$, which accounts for the propagation of surface and evanescent waves from the discharge edge into the center and the role of capacitive and inductive fields in driving the power absorption. Examples of discharge fields are given having substantial standing wave and/or skin effects. The conditions for a uniform discharge without significant standing wave and skin effects are found to be, respectively, $\lambda_0 \gg 2.6(l/s)^{1/2}R$ and $\delta \gg 0.45(dR)^{1/2}$, where λ_0 is the free space wavelength, s is the sheath width, $\delta = c/\omega_p$ is the collisionless skin depth, with c the

speed of light and ω_p , the plasma frequency, and $d = l - s$ is the plasma half-width. Taking the equality for these conditions for a discharge radius of 50 cm, plate separation of 4 cm, and sheath width of 2 mm, there is a substantial skin effect for plasma densities $> 10^{10} \text{ cm}^{-3}$, and there is a substantial standing wave effect for frequencies $f > 70 \text{ MHz}$.

9:15

ET1 6 1-D Electrostatic Modeling of dual frequency Capacitive Plasma Sources PAUL BOYLE, *Dublin City University* ALBERT R. ELLINGBOE, *Dublin City University* MILES M. TURNER, *Plasma Research Laboratory School of Physical Sciences and National Center for Plasma Science and Technology Dublin City University, Dublin 9, Ireland* Particle-in-cell simulations are used to study the structure of dual frequency capacitive

coupled Plasma sources. One of the electrodes is grounded, whereas the other electrode is driven with a variable amplitude current source, which is the summation of a 100MHz component combined with a 1MHz component. As the (LF) voltage is increased the sheath expands resulting in decreased plasma density; but the ion flux is found to remain nearly constant. The dc-bias and plasma potential are both dependent on the (LF) voltage, and the mean ion energy at the electrodes is nearly linearly dependent on the (LF) voltage, in agreement with the voltage difference between the time-averaged plasma potential and the DC bias on the electrode. The increasing sheath width results in bulk electron temperature being linearly dependent of the (LF) voltage. By manipulating the power supplied by the high and low frequencies it is possible to control the ion current and energy independently. Work Supported by EURATOM.

SESSION ET2: IONIZATION OF ATOMS AND MOLECULES

Tuesday morning, 15 October 2002; Center Forum, Millennium Hotel at 8:00; John Boffard, University of Wisconsin-Madison, presiding

Invited Papers

8:00

ET2 1 Kinematically complete studies of electron-impact double ionization using the COLTRIMS technique.

ALEXANDER DORN,* *Max-Planck-Institut für Kernphysik, PF 103980, 69029 Heidelberg, Germany*

A full understanding of the correlated many-body dynamics in atomic and molecular reactions is one of the major aims of atomic collision physics. Experimentally an important break-through in the investigation of atomic fragmentation has been achieved 1994 with the development of the "reaction microscope," a combined recoil-ion - multi-electron spectrometer. With this instrument for the first time final-state vector momenta of several electrons and of the recoiling target ion can be accessed with high resolution and to a large extent independent of their relative energies and emission directions. In the following years this technique has been applied to the investigation of a large number of break-up reactions induced by projectiles as different as photons from threshold to tens of keV, ions ranging from keV protons to GeV/u U^{92+} , antiprotons and positrons. In the present paper we discuss the application to electron impact ionization of atoms. Kinematically complete experiments for double ionization of helium are presented for high energy (2 keV) and moderate energy (500 eV) electron impact. The results allow to critically test theoretical models and give detailed insight into the collision dynamics and contributing reaction mechanisms. In future we will extend this technique to low energy collisions down to threshold using monochromatic and spin-polarized electron beams.

*In collaboration with Conny Höhr, Georgi Sakhelashvili, Claus-Dieter Schröter, Bennaceur Najjari, Robert Moshhammer, Joachim Ullrich, Max-Planck-Institut für Kernphysik, PF 103980, 69029 Heidelberg, Germany.

8:30

ET2 2 Ionization with two active target electrons.

COLM T. WHELAN, *Physics Department, Old Dominion University, Virginia*

In this talk I will give an overview of electron and photon ionization processes where there are two active target electrons. Examples of such processes are excitation ionization and double ionization. These processes are presently being studied experimentally using multiple coincidence techniques, i.e. in kinematically complete measurements and a wealth of new data is becoming available. As been shown,[1], these processes are extremely sensitive to correlation effects both in the target and post collisional interactions. I will first review the commonly used perturbative approach pioneered in [1] and then present a novel non perturbative approach based on the variational determination of a 2-electron R operator, a linear operator that relates functions to their normal derivatives on a bounding surface inside which the functions satisfy the Schrödinger equation.[2] This method will be applied to $(\gamma, 2e)$ on Helium [1] Marchalant P J, Whelan C T and Walters H R J(1997), in Whelan and Walters edited, *Coincidence Studies of Electron and Photon Impact Ionization*, Plenum, New York [2] Roche P J P, Nesbet R K and Whelan C T(2002) in Mason and Whelan edited, *Electron Scattering from Atoms, Molecules, Nuclei and Bulk Matter*, Plenum/Kluwer, New York.

Contributed Papers

9:00

ET2 3 Simultaneous electron-impact ionization–excitation of helium* K. BARTSCHAT,[†] *ITAMP, Harvard Smithsonian Center for Astrophysics* A. N. GRUM-GRZHIMAILO,[‡] *Drake University* As a highly correlated process, simultaneous electron-impact ionization–excitation presents a major challenge, experimentally because of relatively low count rates and theoretically because of the need to account for strong correlation effects between all three electrons. We report new results calculated for this process using a hybrid method, in which the interaction of a “fast” projectile with the target is treated perturbatively by first-order and second-order distorted-wave models, while a convergent close-coupling-type description is applied to generate the initial bound state and to describe the interaction between a “slow” ejected electron and the residual ion. The quality of the method is assessed by comparison with various experimental data, and the sensitivity of the theoretical results on various parameters (order of perturbation theory, plane waves vs. distorted waves, number of states in the close-coupling expansion) will be analyzed.

*Work supported by the NSF and NATO.

[†]permanent address: Drake University

[‡]permanent address: Moscow State University

9:15

ET2 4 Dissociative ionization of pyridine by electron impact CHRISTOPHER DATEO, *Eloret Corporation* WINIFRED HUO, *NASA Ames Research Center* In order to understand the damage of biomolecules by electrons, a process important in radiation damage, we undertake a study of the dissociative ionization (DI) of pyridine (C_5H_5N) from the low-lying ionization channels. The methodology used is the same as in the benzene study. While no experimental DI data are available, we compare the dissociation products from our calculations with the dissociative photoionization measurements of Tixier et al.¹ using dipole (e,e^+ ion) coincidence spectroscopy. Comparisons with the DI of benzene is also made so as to understand the difference in DI between a heterocyclic and an aromatic molecule.

¹S. Tixier, G. Cooper, R. Feng, C.E. Brion, J. Electron Spectrosc. Relat. Phenom. **123**, 185 (2002)

SESSION FT1: PLASMA BOUNDARIES: SHEATHS AND BOUNDARY LAYERS

Tuesday morning, 15 October 2002

North Forum, Millennium Hotel at 10:00

Pascal Chabert, Ecole Polytechnique, presiding

10:00

FT1 1 Stability of an active plasma-sheath RAOUL FRANKLIN, *The Open University* Conventional treatments of the stability of a plasma-sheath system examine the system for micro-instability i.e. against the generation of ion waves and electron plasma waves. These suffer from the difficulty that they use uniform plasma theory and it is then applied in situations where the plasma is far from uniform. A recent treatment by Slemrod [1] examines the macro-stability of a collisional plasma-collisionless

sheath, concluding that it is stable to any arbitrary perturbation. That treatment did not include explicitly generation of the plasma in the volume. Here we extend that treatment by including ionization so that the plasma is an active plasma. Slemrod's conclusions are confirmed analytically in the case when the ratio of the ion collision frequency to the ionisation frequency is small and also when it is large. It is conjectured that computations will show them to be true when they are comparable. [1] Slemrod M Euro. J. Appl. Math. (2002) (in the press).

10:15

FT1 2 Inductively coupled plasmas: one big presheath? CAROLE MAURICE, *TUE JAAP FEIJEN, TUE ARVIND SHANKARAN, UI MARK J. KUSHNER, UI GERRIT KROESEN, TUE TUE: EINDHOVEN UNIVERSITY OF TECHNOLOGY COLLABORATION, UI: UNIVERSITY OF ILLINOIS COLLABORATION* In a planar-coil inductively coupled plasma, the ion velocity distributions in the plasma bulk have been measured as a function of the position in the plasma with Doppler-shifted laser induced fluorescence (DS-LIF). Furthermore, the ion energy distribution of ions arriving at the surface of the electrode has been measured with energy-resolved mass spectrometry. In parallel, the Plasma Equipment Model, a 2-D hybrid fluid/Monte Carlo approach, has been adapted to fit this plasma geometry. From the results it can be concluded that the plasma is in fact one large pre-sheath. Acceleration of the ions starts in the center. The ion velocity then steadily increases until the Bohm velocity (3100 ms/ for these plasma conditions) is reached. In the sheath, the ions then acquire an amount of energy which roughly corresponds to the plasma potential.

10:30

FT1 3 Quasineutrality in Electronegative Plasmas* RICHARD F. FERNSLER, *Plasma Physics Division, Naval Research Laboratory* As is well known, plasmas are good conductors and thus usually keep the electric field small inside. The field is small because most of the voltage, whether developed naturally or applied externally, appears across narrow sheaths at the boundaries. The charge density is therefore high in the sheaths but low in the plasma middle. Most plasmas can thus be viewed as a quasineutral middle surrounded by a non-neutral sheath. Using this model, Bohm derived a condition in 1949 for the minimum flow velocity at which positive ions enter the sheath at the boundary of electropositive plasmas, and versions of this condition apply wherever quasineutrality fails. The Bohm condition has since been extended to electronegative plasmas by assuming the negative ions, as well as the electrons, obey the Boltzmann relationship. More recently, that assumption has led to the conclusion that non-neutral sheaths can form inside electronegative plasmas, as well as at the boundaries. Such claims are surprising, given the shielding capability of plasmas. The present paper addresses the formation of both internal sheaths and double layers by reexamining the Bohm condition and the Boltzmann assumption.

*Work supported by the Office of Naval Research

10:45

FT1 4 Comparison of the Discrete Plasma-Sheath Model with the Full Hydrodynamic Description VALERY GODYAK, *Osram Sylvania, Beverly, MA 01915* NATALIA STERNBERG, *Clark University, Worcester, MA 01610* The relationship between the bounded gas discharge plasma and the space-charge sheath at the plasma-sheath boundary is of great importance for a number of problems such as electrostatic plasma probes, and electrode phe-

nomena in dc and rf discharges. In those applications, the electrical characteristics of bounded plasma-sheath systems are, either to a large extent or entirely, defined by the behavior of the sheath at the plasma boundary. The plasma and the sheath are described by different models, which need to be joined in some way. The boundary condition that separates the quasi-neutral plasma with low electric field from the space-charge ion sheath with large electric field was proposed in Ref. 1 as a specified value of electric field $E_1 = kT_e / e\lambda_D$ at the plasma-sheath interface. This boundary condition permits one to construct a discrete plasma-sheath hydrodynamic model with a smooth transition from the plasma to the sheath for arbitrary plasma non-neutrality and collisionality, and without singularities inherent to asymptotic plasma and sheath models. As a result, the sheath parameters are uniquely defined by the plasma parameters in the center and by the electrical potential at the wall. A comparison with a numerical solution of the full hydrodynamic plasma-wall problem is given in this presentation demonstrating a reasonable agreement in the corresponding data. [1] V. A. Godyak, Phys. Lett. 89A, 80 (1982).

11:00

FT1 5 How fast do ions fall out of a weakly collisional two species plasma? NOAH HERSHKOWITZ, XU WANG, EUN-SUK KO, *University of Wisconsin-Madison* GREG SEVERN, *University of San Diego* In plasmas with two or more ion species, it is usually assumed that ions leave plasma at their individual Bohm velocities. In collisionless plasmas, this result can be achieved if ions fall through a presheath with a plasma potential drop of $T_e/2e$. If ionization is ignored, such a potential drop cannot exist. If ionization is included with the same profile for each species, a solution can exist, but the presheath length will equal the chamber length and the potential drop must exceed $T_e/2e$. With weakly collisional plasmas, mobility limited flow can be assumed for weak electric fields but not for velocities close to the individual species Bohm velocities. In the absence of presheath ionization, ion flux conservation gives a better solution. Experimental data from emissive probes, LIF and ion acoustic wave propagation in an argon/helium plasma suggest another solution to the problem. It appears that at the presheath/sheath boundary neither ion leaves at their individual Bohm velocity. For one specific example it appears that both ion species leave at the same velocity, the system ion acoustic velocity. *Work Supported by US DOE grant DE-FG02-97ER54437

11:15

FT1 6 Electric field induced energy level shifts of Argon D states GREG HEBNER, *Sandia National Laboratories* The characteristic of the plasma sheath around structures immersed in plasma is of fundamental interest. In particular, the details of the sheath structure in the presheath region or around objects immersed in flowing ion fields are not well characterized. A key aspect of this work is obtaining the required spatial, temporal and electric field sensitivity. Argon is a commonly used rare gas in a number of discharges. As such it is an ideal candidate for spectroscopic based electric field measurements within the sheath and bulk discharge regions. This talk will discuss the use of an atomic beam system combined with pulsed laser spectroscopy to directly calibrate the electric field induced shift of high lying energy levels. Prior work has used the F states in argon. We demonstrate a two-laser technique that probes the D states with demonstrated high spatial and temporal resolution. Several D states have been

identified with usable electric field induced energy level shifts. This work was performed at Sandia National Laboratories and supported by DoE Office of Science and the United States Department of Energy (DE-AC04-94AL85000).

11:30

FT1 7 Numerical velocity distributions of positive and negative ions incident on a wafer in a pulsed 2f-CCP in CF₄/Ar for SiO₂ etching T. YAGISAWA, K. MAESHIGE, T. MAKABE, *Keio University at Yokohama, Japan* Charging damage during plasma etching of insulator will be still interesting issue with further decreasing the size of elements of ULSI. Recently, we reported the experimental evidence of the reduction of charging voltage during etching by using a pulsed two-frequency capacitively coupled plasma(2f-CCP)¹. In this work, we will focus on the charging free plasma etching in a pulsed 2f-CCP system with rf sources used for sustaining a high density plasma at VHF (100MHz) and biasing a wafer at high energy positive ion at LF (1MHz). A particle trace method (Monte Carlo simulation) is used to estimate a time-dependent ion velocity distribution, on the basis of the 2D-t plasma structure predicted by the RCT model²³. Typical velocity distribution with non-linear time-dependence, modulated at low frequency bias power at 1MHz or 500kHz is shown. The characteristics of the impact energy and angle, which act as the element to reduce charges accumulated inside the hole/trench in SiO₂ with high aspect ratio, are discussed for positive and negative ions in a pulsed 2f-CCP in CF₄(5%)/Ar.

¹T.Fujita and T.Makabe; Plasma Sources Sci.Technol.11,142 (2002) T.Ohmori *et al* ; submitted

²K.Maeshige,G.Washio,T.Yagisawa,T.Makabe;J.Appl.Phys. 91,9494(2002)

³T.Makabe and K.Maeshige; Appl.Surf.Sci. 192,176(2002)

SESSION FT2: THERMAL PLASMAS

Tuesday morning, 15 October 2002

Center Forum, Millennium Hotel at 10:00

Thierry Renault, University of Minnesota, presiding

10:00

FT2 1 Plasma Characteristics of Supersonic Ammonia and Nitrogen/Hydrogen-Mixture DC Plasma Jets for Nitriding under a Low Pressure Environment HIROKAZU TAHARA, *Graduate School of Engineering Science, Osaka University* TAKAO YOSHIKAWA, *Graduate School of Engineering Science, Osaka University* Spectroscopic and electrostatic probe measurements were carried out to understand the plasma features inside and outside a 10-kW-class direct-current arc plasma jet generator with a supersonic expansion nozzle for nitriding. Ammonia and a mixture of nitrogen and hydrogen were used as the working gas. The NH₃ and N₂+3H₂ plasmas in the expansion nozzle and in the downstream plume were in thermodynamical nonequilibrium state although those in the throat were nearly in a temperature equilibrium condition. As a result, the H-atom excitation temperature and the N₂ rotational excitation temperature decreased from 11000 K in the throat to 4000 K and to 2000 K, respectively, on the nozzle exit at 0.2 g/s, although the NH rota-

tional temperature did not show an axial decrease even in the nozzle. On the other hand, several temperatures were almost kept some ranges in the downstream plume under an ambient pressure 130 Pa except for the NH rotational temperature for NH₃ working gas.

10:15

FT2 2 Plasma Characteristics of an Electromagnetic Acceleration Plasma Jet for Titanium-Nitride Reactive Spray Coatings

HIROKAZU TAHARA, *Graduate School of Engineering Science, Osaka University* TAKAO YOSHIKAWA, *Graduate School of Engineering Science, Osaka University* In magneto-plasma-dynamic (MPD) arcjet generators, plasma is accelerated by electromagnetic body forces. A cathode-ablation-type MPD arcjet generator was developed for titanium nitride reactive spray coating. The coating characteristics were evaluated; plasma diagnostic measurement and flowfield analysis were also conducted. Large amounts of chemically active particles of N and N⁺ were expected to be exhausted with high velocities from the MPD generator. Both the electron temperature and the electron number density were kept high even at an enough downstream position, i.e., at the substrate position, compared with those for conventional low-pressure thermal sprayings. A chemically active plasma with excited particles of N⁺, Ti, Ti⁺ and Ti²⁺ were expected to contribute to the titanium nitride reactive spray coatings. The emission spectral intensities of titanium relatively decreased with increasing cathode diameter compared with those of N⁺. This agreed with the coating characteristics. Hence, when the spectral intensities of N⁺ are relatively high and those of titanium are very low; that is, with a larger diameter cathode, high-quality titanium nitride films, i.e., TiN-rich films are expected to be created.

10:30

FT2 3 Cathode Erosion in a Plasma Cutting Torch

JOHN PETERS, *University of Minnesota (Twin Cities)* JOACHIM HEBERLEIN, *University of Minnesota (Twin Cities)* CHARLES HACKETT, *Centricut* The erosion of hafnium from a water-cooled cutting torch has been investigated. Observations of the cathode during operation indicate that hafnium erosion is a result of the ejection of liquid metal droplets from the molten cathode surface. These droplet ejections occur at specific times during arc operation and are usually associated with changes in the operating conditions. In order to obtain quantitative, time resolved erosion rates, ejected droplets were collected while the torch was operated. The mass of the collected droplets was measured to determine the relative importance of the various ejection types. Results show that the dominant source of droplet ejection is a fast current shut-off. The arc start is also a significant source of erosion. Hypotheses for the causes of the ejections have also been developed.

10:45

FT2 4 Observation of the glow-to-arc transitions

SHIGERU WATANABE, SHIGEKI SAITO, KUNIO TAKAHASHI, TADAO ONZAWA, *Tokyo Institute of Technology* Researches of the glow-to-arc transitions have been required for a new development of the welding technology in low current. It is important to clarify the characteristics of plasma in the transitions because there have been few reports investigated the transitions in detail. The glow-to-arc transitions were observed in argon at atmospheric pressure. The Th-W electrodes of 1 mm in a diameter are used. Both of the electrodes are needle-shaped and set in a quartz tube coaxially. Plasma is generated between the electrodes with the gap spacing of 1 mm. A DC power supply has been applying constant

voltage of 600 V during the discharge. A high-speed camera is used to record the images of plasma in the transitions with the measurement of voltage and current between the electrodes. As a result, two things were confirmed for the behavior of the glow-to-arc transition. First, plasma extended over the cathode surface in the transition from the glow to the arc. Second, temperature in the tip of the cathode would increase gradually during the glow and decrease during the arc.

11:00

FT2 5 Modeling of low-current non-LTE discharges in atmospheric-pressure air and its mixtures with hydrocarbons*

M.S. BENILOV, *Departamento de Física, Universidade da Madeira, 9000 Funchal, Portugal* G.V. NAIDIS, *Institute for High Temperatures RAS, Moscow 127412, Russia* A modeling approach based on the LTE assumption is justified for DC discharges if the electric current is higher than approximately 0.1 A. Recently, a considerable attention has been paid in the literature to experimental investigation of atmospheric-pressure DC discharges in the range 0.01-0.1 A. In this work, a model of low-current DC discharges in air is developed. It is found out that a change of mechanism of ionization occurs at currents of about 0.1 A: while the associative ionization in atomic collisions is the dominating mechanism at higher currents, the direct ionization of molecules by electron impact dominates at lower currents. While the electron number density in the core of the discharge is close to the LTE value corresponding to the gas temperature at higher currents, at lower currents it is governed mainly by the reduced electric field and may strongly exceed the LTE value. Results of calculation of discharge parameters in a wide current range, covering both LTE and non-LTE regimes, are presented. Calculated plasma parameters are in a good agreement with available experimental data. A kinetic model is developed also for discharges in mixtures of air with hydrocarbon gases.

*The work was supported by EC through the project N ENK5-CT-2000-00346

11:15

FT2 6 OPTICAL AND ELECTRICAL MEASUREMENTS IN ATMOSPHERIC PRESSURE ARCS: A COMPARISON

CARLO FANARA, *School of Industrial and manufacturing Science, Cranfield University* LOURIEL OLIVEIRA VILARINHO, *School of Industrial and manufacturing Science, Cranfield University and Universidade Federal de Uberlandia, Brazil* Atmospheric pressure arcs are investigated by emission spectroscopy and electric exploration techniques. Temperature maps for arc currents in the range 100-200 A show good agreement with previously published data. An extended study on Langmuir probes in arcs has been performed and a multi-wire apparatus was constructed. The probes characteristic curve is distorted at high pressure and as a consistent theory is lacking, interpretation difficulties are outlined. Comparison with temperatures obtained from optical spectroscopy is made in order to correct for "cooler" probe temperatures. Arc radii in biased and floating conditions are examined and estimates of the axial electric field are presented. Data from carbon diamond partially coated probes suggest a differential charge capture. The investigation of the anode region can be performed using a split-anode technique and the prototype is described of a modified apparatus, which avoids the two-dimensional Abel inversion needed to reconstruct local information.

11:30

FT2 7 Fully 3D Modeling of Inductively Coupled Plasma Torches D. BERNARDI, V. COLOMBO, E. GHEDINI, A. MENTRELLI, A. VERTUAN, *University of Bologna, D.I.E.M. and C.I.R.A.M., Via Saragozza 8, 40123 Bologna, Italy* A fully 3D model for ICPTs is presented, using the FLUENT code and taking into account the coil actual shape and asymmetric secondary gas injection, so showing effects on plasma discharge for various geometric, electric and operating conditions. Steady laminar flow, energy and EM field equations are solved for an optically thin, LTE, argon plasma. 3D vector potential equation is solved in an extended grid [1-2] and using FLUENT capabilities as done in [3] for a 2D domain. Improvements of this approach, already performed in [4] for 2D cases, can be foreseen also for 3D ones, using an external routine that allows one to restrict the fluid-dynamics domain to the torch region. The relative importance of various 3D effects on plasma temperature and flow fields are compared with results obtainable from conventional and improved 2D models [5]. [1] Colombo et al., *IEEE Trans. Plasma Sci.* Vol. 25 1073, 1997 [2] Bernardi, et al., *Eur. Phys. J. D*, Vol. 14, 337, 2001 [3] Xue et al., *J. Phys. D: Appl. Phys.* Vol. 34, 1897, 2001 [4] Bernardi et al., *Comparison of Different Techniques for the Treatment of the Electromagnetic Field for Studying Inductively-Coupled Plasma Torches by Means of the Fluent Code*, TPP7, Strasbourg, June 2002 [5] Xue, Proulx, Boulos, *Proc. of ISPC15*, 1221-1226, Orleans, July 2001

SESSION GTP: POSTER SESSION I

Tuesday afternoon, 15 October 2002

Horizons/Satellites, Millennium Hotel at 13:15

GTP 1 ELECTRON AND POSITRON COLLISIONS WITH ATOMS AND MOLECULES

GTP 2 Scaling behavior of the fully differential cross section for ionization of hydrogen atoms by the impact of fast elementary charged particles¹ S. JONES, D. H. MADISON, *Laboratory for Atomic, Molecular and Optical Research and Physics Department, University of Missouri-Rolla, Rolla MO 65409-0640* Ionization of hydrogen atoms by the impact of fast charged particles can be accurately treated theoretically using simple two-center wave functions to describe the scattering system both initially and finally. For the final state, we use a continuum-distorted wave (CDW) that contains the product of three Coulombic distortion factors (one for each two-body subsystem), hence it is called the 3C wave function. This CDW (3C) wave function is ideal for studying fast collisions since it is asymptotically correct in all asymptotic domains of momentum space for all configurations of the three particles in coordinate space. Coulomb distortion in the entrance channel is provided by an eikonal initial state (EIS), and this CDW-EIS approximation has proven to be the most accurate perturbative method ever devised within a two-state approxima-

tion. The first fully differential cross sections for ion-atom ionization in the CDW-EIS approximation will be presented. In addition, by considering projectiles of different mass and charge, it will be shown that although the charge of the projectile is important, the mass of the projectile plays virtually no role in the vast majority of fast ionizing collisions.

¹Work supported by the NSF

GTP 3 Importance of Correlation and Exchange in Electron-Impact Ionization of Krypton¹ A. PRIDEAUX, D. H. MADISON, *University of Missouri-Rolla, USA* M. A. HAYNES, B. LOHMANN, *Griffith University, Australia* It has been known for more than a decade that the final-state electron-electron interaction (known as correlation) plays an important role in electron-impact ionization of hydrogen. For heavier atoms, additional many-particle effects such as exchange between the projectile electron and atomic electrons can also play an important role. We have recently studied the importance of correlation and exchange in electron-impact ionization of the inner 3s shell of argon and it was found that both effects become increasingly important with decreasing incident-electron energy. For low energy symmetric collisions, theories neglecting correlation often predict completely nonsense results. Here we report a similar study for ionization of the inner 4s shell of krypton. Experimental and theoretical results for krypton will be compared with the earlier argon results.

¹Work supported by the NSF

GTP 4 ELECTRON AND POSITRON SCATTERING FROM CHLORINE MOLECULES IN THE ENERGY REGION FROM 0.8 eV TO 600 eV C. MAKOCHEKANWA, H. KAWATE, O. SUEOKA, MINEO KIMURA, *Grad. School of Sci., & Eng., Yamaguchi University* Total scattering cross sections for chlorine molecules by electron impact are determined experimentally for the impact energies from 0.8 eV to 600 eV. Elastic scattering cross sections are also determined theoretically. The results above 23 eV are the first report on these processes. The present results are in good accord in the energy-dependence with the previous measurements, although the absolute magnitude is found to be about 30% smaller than that of Gulley et al. [*J. Phys.* B31, 2971 (1998)]. Strong sharp peaks around 7.8 eV and 12 eV are observed and well separated, and the one at 7.8 eV is attributed to dissociative electron attachment, while the one at 12 eV is speculated to be due to ion-pair formation through direct dissociation. The present elastic cross sections are found to show the similar shape to the TCS although the magnitude is smaller by a few % below 30 eV to a factor of two at 100 eV. Small-scale experimental study is also carried out for determining total and positronium formation cross sections by positron impact as well to carry out the comparative study.

GTP 5 Electron collisions with SF₆ (sulfur hexafluoride)* CARL WINSTEAD, VINCENT MCKOY, *California Institute of Technology* Despite the importance of sulfur hexafluoride, SF₆, in both switching and plasma processing applications, there remain many gaps in our knowledge of its electron cross sections. To assist in constructing an improved cross section set, we have stud-

ied low-energy electron collisions with SF₆ using the Schwinger multichannel method. We will present results for elastic scattering and for selected electronic excitation channels, and we will discuss these results in the context of experimental data and previous calculations.

*Work supported in part by DOE and Sematech, Inc.

GTP 6 Electron Impact Cross Section Data for Cesium Obtained using a MOT* JOHN MACASKILL, WLADEK KEDZIERSKI, JOSEPH BORBELY, WILLIAM MCCONKEY, *University of Windsor, Canada* JOLANTA DOMYSLAWSKA, *Nicholas Copernicus University, Poland* IGOR BRAY, *Murdoch University, Australia* A magneto-optical trap coupled to a pulsed electron beam system has been used to obtain cross sections for electron impact on cesium at energies up to 400 eV. Good agreement is obtained between CCC calculations and the experimental measurements of the total cross section for both the ground and excited 6P states. A long-standing question regarding the energy variation of the total cross section for ground state targets is resolved. For energies above 10 eV, total cross sections involving the first excited 6P state are about 1.5 times those of the ground state at the same energy. Full details of these and ongoing measurements will be presented at the Conference.

*Financial support from NSERC and CIPI is gratefully acknowledged

GTP 7 Low-energy electron collisions with molybdenum atoms* K. BARTSCHAT,† *ITAMP, Harvard Smithsonian Center for Astrophysics* A. DASGUPTA, *Naval Research Laboratory* J. L. GIULIANI, *Naval Research Laboratory* Reliable cross-section data for electron collisions with molybdenum atoms are important for various applications, such as monitoring the impurity influx in tokamaks or the modeling of a high-intensity metal-oxide discharge that represents a promising candidate for mercury-free lighting concepts. We have therefore extended our recent work on electron collisions with Mo I atoms in their ground state [1] and will present new results for electron-induced transitions between the lowest 15 septet and quintet states of neutral molybdenum. The dependence of our results from a non-relativistic *R*-matrix (close-coupling) approach on the details of the theoretical model, particularly on the structure description and the number of coupled states, is analyzed, with particular emphasis on the relevant transitions in a moly-oxide discharge lamp. [1.] K. Bartschat, A. Dasgupta, and J.L. Giuliani, *J. Phys. B* **35**, in press (scheduled for July 2002).

*Work supported, in part, by the NSF and the Office of Naval Research.

†permanent address: Drake University

GTP 8 Resonances in low-energy electron scattering on atomic Rb, Cs, and Fr* U. THUMM, *Dept. of Physics, Kansas State University, Manhattan* C. BAHRIM, *Depts. of Physics, Kansas State University and Lamar University, Beaumont, TX* I. I. FABRIKANT, *Dept. of Physics and Astronomy, University of Nebraska, Lincoln* Within the relativistic Dirac *R*-matrix method and a model based on an effective two-electron approach¹, we analyze the spectra of Rb⁻, Cs⁻, and Fr⁻ ions in electron scattering by

Rb, Cs, and Fr targets at incident electron energies below 2.8 eV. Our calculations predict the same ³P^{o,e}, ³F^o, and ¹P^o resonances for all three anions² in calculations of angle-dependent, momentum transfer, and total cross sections. We discuss relativistic effects in the resonance profiles. Our 1⁺ partial cross sections show pronounced Ramsauer-Townsend (RT) minima at 41/46/32 meV for Rb/Cs/Fr, caused by the strong atomic polarizability and related to a ³S^e virtual state³. In the total converged cross section these RT minima are shifted to lower energies (4.6/1.1 meV for Rb/Cs, and below 1 meV for Fr) due to the nearby ³P^o resonance. We also discuss our spin-flip and spin-exchange cross sections for e⁻ + Rb, Cs, and Fr collisions in comparison with experimental data.

*Supported by the Science Division, Office of Fusion Energy, Office of Energy Research, US DOE

¹U. Thumm and D.W. Norcross *Phys.Rev.A* **45**, 6349 (1992).

²C. Bahrim, U. Thumm, and I.I. Fabrikant *Phys.Rev.A* **63**, 042710 (2001); C. Bahrim and U. Thumm, *Phys.Rev.A* **64**, 022716 (2001)

³C. Bahrim, U.Thumm, and I.I. Fabrikant, *J. Phys. B* **34**, L195 (2001)

GTP 9 Photodetachment of Rb⁻, Cs⁻, and Fr⁻: A new boundary-corrected Pauli equation approach* U. THUMM, *Dept. of Physics, Kansas State University, Manhattan* C. BAHRIM, *Depts. of Physics Kansas State University, Manhattan and Lamar University, Beaumont, TX* I. I. FABRIKANT, *Dept. of Physics and Astronomy, University of Nebraska, Lincoln* As a weak relativistic limit of the exact Dirac equation, the Pauli equation includes the spin-dependent potential *V*_{LS} added to the non-relativistic, spin-independent Coulomb potential *V*. For a Coulomb potential, *V*_{LS} has a non-physical singularity 1/*r*³ at *r* = 0, and the PE-approach breaks down. Various regularization functions have been suggested to remove this singularity [1]. Based on the exact analytic solution of the Dirac equation near the nucleus, we formulated boundary conditions for solving the PE for an electron interacting with an atom [1]. By integrating the PE using an effective potential *V*_{eff} that is adjusted to reproduce scattering phase shifts provided by exact Dirac *R*-matrix calculations, we calculated angle-differential and total photodetachment (PD) cross sections. Our ³P₁^o resonance contribution to the PD cross section of Cs⁻ agrees (in position and width) with recent experiments [2], after fine-tuning *V*_{eff}. [1] C. Bahrim, I.I. Fabrikant, and U. Thumm, *Phys. Rev. Lett.* **87**, 123003 (2001), and Refs. therein. [2] M. Scheer et al., *Phys. Rev. Lett.* **80**, 684 (1998).

*Supported by the Office of Fusion Energy, US DOE

GTP 10 Dissociative Recombination of Hydrocarbon Ions at CRYRING S.T. ARNOLD, A.A. VIGGIANO, *Air Force Research Laboratory, Hanscom AFB, MA* M. LARSON, S. KALHORI, S. ROSEN, A. DERKATCH, *Department of Physics, University of Stockholm, Sweden* J. SEMANIAC, *Institute of Physics, Swietokrzyska Academy, Poland* M.AF. UGGLAS, *Manne Siegbahn Laboratory, Sweden* Dissociative recombination (DR) is a significant loss mechanism for many types of plasmas. Measurements have demonstrated previously that DR reactions are very rapid; however, little is known about the product distributions of these reactions due to the difficulty of detecting low concentrations of neutral species. This situation has begun to change in

recent years, with the advent of heavy ion storage rings. Here we report on the rate constants and product distributions for DR of several organic ions: $C_2H_2^+$, $C_2H_3^+$, $C_2H_4^+$, $C_2H_5^+$, and $C_3H_7^+$. The experiments were performed at CRYRING, the heavy ion storage ring at the University of Stockholm. The data clearly show surprises. In particular, production of three products from DR is found to be more prevalent than previously thought. Applications of these results to interstellar cloud chemistry and plasma-enhanced combustion will be discussed.

GTP 11 Measurement of the Contribution of CO* Triplet States to the Total Yield of CO(a³Π) in the Dissociative Recombination of CO₂⁺ and HCO⁺ Ions with Electrons RICHARD E. ROSATI, MICHAEL F. GOLDE, RAINER JOHNSEN, *University of Pittsburgh** The flowing afterglow technique, in conjunction with absolute spectroscopy, has been applied to the dissociative recombination of CO₂⁺ + e⁻. The goal was to determine the radiative cascading contribution from high energy triplet states to the total observed yield of the long-lived CO(a³Π) state. The absolute yield of the triplet states was found to be 0.13 ± 0.03. When combined with our previously reported value¹ of 0.29 ± 0.10 for the total spectroscopic yield of CO(a), this implies that approximately 45CO(a) yield results from radiative cascading rather than direct formation. A similar, but more complicated analysis has been performed on HCO⁺/HOC⁺ recombination. The results so far show that CO(a³Π) is again an important product state and that it appears to be populated mainly by the lower energy isomer, HCO⁺.

*The authors would like to thank the NASA Planetary Atmospheres Program for their support of this work.

¹M. P. Skrzypkowski et al., *J. Chem. Phys.* **108** 8400 (1998).

GTP 12 MATERIALS AND DEVICE PROCESSING

GTP 13 Field Emission Property of Boron-Doped Amorphous Carbon Thin Films by Pulsed Laser Deposition* Y. SUGANUMA, Y. SUDA, Y. SAKAI, *Hokkaido University, Sapporo, 060-8628, Japan* Recently, carbon materials that have high electron yield and low threshold voltage for field emission due to low electron affinity have attracted attention for an application of electron emitter of flat panel displays.¹ In this report, we will present the electron emission property of amorphous carbon (a-C) and boron-doped a-C films prepared by pulsed laser deposition. An experimental setup is described elsewhere.² Focused ArF excimer laser beam is irradiated on a sintered graphite (or boron) target, and the thin film is deposited on a silicon substrate. Boron doping into a-C films is performed by alternative deposition of carbon and boron on the substrate. The chemical composition of films is analyzed by an X-ray photoelectron spectroscopy and secondary ion mass spectrometry. The effect of boron-doping on the electron emission property is discussed.

*Work in part supported by the Inamori Foundation.

¹Y. Suda, *Appl. Surf. Sci.*, in press

²Y. Suda, *Thin Solid Films*, in press

GTP 14 Thermal Plasma Chemical Vapor Deposition of Silicon Carbide Films FENG LIAO, SOONAM PARK, MICHAEL ZACHARIAH, STEVEN GIRSHICK, *University of Minnesota* Nanocrystalline silicon carbide films were deposited by radio frequency thermal plasma chemical vapor deposition. The reactants, CH₄ and vapor-phase SiCl₄, were injected into an argon-hydrogen RF plasma operating at 3.3 MHz with a generator plate power of 10-20 kW. Substrate temperature was varied from 650°C to 1300°C, with chamber pressure in the range 20 to 33 kPa. Film growth rates up to 900 μm/h were obtained, and were found to vary linearly with the SiCl₄ flow rate. The films were primarily β-phase SiC, and exhibit a columnar structure with hemispherical surfaces and nanocrystalline (5-100 nm) grain size. Studies of the plasma and film growth chemistry were conducted using a custom-designed molecular beam mass spectrometry system to characterize the composition of gas sampled through a small orifice in the substrate. This system was shown to provide a high quality molecular beam (beam-to-background ratios better than 10 under film growth conditions) and to have minimum detectabilities below 100 ppb, allowing quantitative measurements of radicals and other unstable species.

GTP 15 Ablation Plasma Ion Implantation Optimization and Deposition of Compound Coatings M.C. JONES, B. QI, R.M. GILGENBACH, M.D. JOHNSTON, Y.Y. LAU, *University of Michigan, Ann Arbor, MI 48109-2104* G.L. DOLL, A. LAZARIDES, *Timken Research, The Timken Corp., Canton, OH 44706-0939* Ablation Plasma Ion Implantation (APII) utilizes KrF laser ablation plasma plumes to implant ions into pulsed, negatively-biased substrates [1]. Ablation targets are Ti foils and TiN disks. Substrates are Si wafers and Al, biased from 0 to 10 kV. Optimization experiments address: 1) configurations that reduce arcing, 2) reduction of particulate, and 3) deposition/implantation of compounds (e.g. TiN). Arcing is suppressed by positioning the target perpendicular (previously parallel) to the substrate. Thus, bias voltage can be applied at the same time as the KrF laser, resulting in higher ion current. This geometry also yields lower particulate. APII with TiN has the goal of hardened coatings with excellent adhesion. SEM, AFM, XPS, TEM, and scratch tests characterize properties of the thin films. Ti APII films at 4kV are smoother with lower friction. 1. B. Qi, R.M. Gilgenbach, Y.Y. Lau, M.D. Johnston, J. Lian, L.M. Wang, G. L. Doll and A. Lazarides, *APL*, **78**, 3785 (2001) * Research funded by NSF

GTP 16 Ion mass and energy distributions in Ar/C₄F₈/O₂ and Xe/ Ar/C₄F₈/O₂ capacitively-coupled plasmas JEAN-PAUL BOOTH, *LPTP, Ecole Polytechnique, France* NICOLAS BULCOURT, *LPTP, Ecole Polytechnique, France* JACQUES JOLLY, *LPTP, Ecole Polytechnique, France* Capacitively-coupled plasmas in gas mixtures of the type Ar/C₄F₈/O₂ (90 % Ar) have become the standard in the microelectronics industry for the etching of contact holes in SiO₂ thin films, displacing inductively-coupled sources. However, small changes in the gas composition can have dramatic effects on the process results (narrow "process window"). We have investigated the ion mass and energy distributions in a 27 MHz parallel plate system using a quadrupole mass spectrometer with energy analyzer. The dominant ions include Ar⁺, C₂F₅⁺, C₃F₅⁺, CF₃⁺, C₄F₇⁺, COF⁺ and CF⁺. The Ar⁺ energy distribution functions are strongly degraded to low energies due to charge exchange collisions in the sheath. Increasing RF power increases the degree of fragmentation, leading to more low-

mass molecular ions. The effect of replacing 50 % of the Ar with Xe was investigated. The principal effect is to replace the majority Ar^+ ion by Xe^+ . The Xe^+ energy distribution functions are less degraded to low energies than is the case for Ar^+ .

GTP 17 TREATMENT OF a-C:H AND a-C:Si:H FILMS BY PLASMA IMMERSION ION IMPLANTATION ELIDIANE C. RANGEL, ROBERTO Y. HONDA, DEBORAH C. R. SANTOS, NILSON C. CRUZ, *Laboratório de Plasmas, Faculdade de Engenharia UNESP, 12516-410, Guaratinguetá, SP, Brazil* This work reports an investigation on the surface properties of plasma polymer films treated by PIII (Plasma Immersion Ion Implantation) technique. The effect of the work parameters on the wettability and free surface energy of the films was determined. Samples were prepared from hexamethyldisiloxane (HMDSO), acetylene-argon and benzene glow discharges. Ion implantation was carried out varying the PIII parameters, namely the plasma composition (nitrogen, helium or argon) and exposure time (t). Sample wettability was investigated by contact angle (θ) measurements, using de-ionized water. Temporal evolution of θ was determined measuring it periodically after the treatment. Free-surface energy was evaluated from contact angle data acquired using water and methylene iodide. After the treatment θ drops with t for all the samples. However, the fall is more pronounced in films deposited from organosilicon compounds. Indeed, θ does not vary significantly with t in the hydrocarbon prepared samples. However, treated hydrocarbon samples demonstrated higher stability of θ than organosilicon films. Such behavior is ascribed to different abilities to crosslink the carbon chain in each material.

GTP 18 PRODUCTION AND CHARACTERIZATION OF POLYMER FILMS DEPOSITED BY PLASMA IMMERSION ION IMPLANTATION AND DEPOSITION TECHNIQUE ELIDIANE C. RANGEL, *Laboratório de Plasmas, Faculdade de Engenharia UNESP, 12516-410, Guaratinguetá, SP, Brazil* MANFREDO H. TABACNIKS, *LAMFI, IFUSP, São Paulo, SP, Brazil* CARLOS A. ACHETE, *PEMM/COPPE/UFRJ, Rio de Janeiro, Brazil* SÉRGIO C. JUNIOR, *PEMM/COPPE/UFRJ, Rio de Janeiro, Brazil* MILTON E. KAYAMA, NILSON C. CRUZ, *Laboratório de Plasmas, Faculdade de Engenharia UNESP, 12516-410, Guaratinguetá, SP, Brazil* Plasma immersion ion implantation and deposition (PIID) technique combines film deposition and ion bombardment in the same procedure. According to that, high voltage negative pulses are supplied to substrates exposed to organic compound containing plasmas. During the pulse on-time, positive ions from the glow discharge are attracted and implanted into the solid. While the pulse is off, the substrate is coated with a layer by the conventional PECVD process. In this work, polymer films were deposited and treated by PIID using radiofrequency (13.56 MHz, 20 W) plasmas of methane and argon mixtures. Partial pressures of Ar and CH_4 were 1.3 and 0.8 Pa, respectively. To avoid the growth of an unmodified film/substrate interface, the sample holder was biased with 25 kV negative pulses simultaneously to the plasma ignition. Exposure time to the plasma was 3600 s and the pulse frequency, ν , ranged from 2 to 125 Hz. Chemical composition of the samples was determined from RBS measurements, using a 3.5 MeV He^+ beam. The adhesion of the deposited layer to glass substrates, α , was evaluated by the pull-off technique. Contact angle measurements were used to evaluate surface wettability and free energy. The later was calculated measuring contact angles of a polar and an apolar liquid, namely water and methylene iodide, respectively. Nanoindentation

technique was used to determine film hardness and reduced elastic modulus. Increasing the pulse frequency from 0 to 60 Hz produced improvement in the film/substrate adhesion. Further increasing ν induced a fall tendency in α . On the other hand, hardness, surface free energy and water wettability continuously increased with ν . Contact angles as low as 40° and hardnesses about 5.5 GPa have been obtained with films treated at 125 Hz.

GTP 19 Focused ion beams using a high-brightness plasma source SAMAR GUHARAY, *FM Technologies, Inc.* High-brightness ion beams, with low energy spread, have merits for many new applications in microelectronics, materials science, and biology. Negative ions are especially attractive for the applications that involve beam-solid interactions. When negative ions strike a surface, especially an electrically isolated surface, the surface charging voltage is limited to few volts [1]. This property can be effectively utilized to circumvent problems due to surface charging, such as device damage and beam defocusing. A compact plasma source, with the capability to deliver either positive or negative ion beams, has been developed. H- beams from this pulsed source showed brightness within an order of magnitude of the value for beams from liquid-metal ion sources. The beam angular intensity is $> 40 \text{ mAsr}^{-1}$ and the corresponding energy spread is $< 2.5 \text{ eV}$ [2]. Using a simple Einzel lens with magnification of about 0.1, a focused current density of about 40 mAcm^{-2} is obtained. It is estimated that an additional magnification of about 0.1 can yield a focused current density of $> 1 \text{ Acm}^{-2}$ and a spot size of 100 nm. Such characteristics of focused beam parameters, using a dc source, will immediately open up a large area of new applications. [1] P. N. Guzdar, A. S. Sharma, S. K. Guharay, "Charging of substrates irradiated by particle beams". *Appl. Phys. Lett.* 71, 3302 (1997). [2] S. K. Guharay, E. Sokolovsky, J. Orloff, "Characteristics of ion beams from a Penning source for focused ion beam applications" *J. Vac. Sci. Technol.* B17, 2779 (1999).

GTP 20 PLASMA-SURFACE INTERACTIONS

GTP 21 Wall charging in a low pressure high density oxygen-silane plasma CHRISTINE CHARLES,* *The Australian National University* A low pressure high density oxygen/silane radiofrequency (13.56 MHz) plasma coupled in a helicon reactor used for silicon dioxide deposition is characterized by using an energy selective mass spectrometer situated at the wall of the processing chamber: measurements of positive and negative ion energy distribution functions and mass spectra ($1 < \text{a.m.u} < = 150$) are obtained for various flowrate ratios ($R = O_2/SiH_4 = 1$ to 10 but constant total flow rate of 30 sccm), and for constant radiofrequency power and magnetic field of 800 W, and 70 G, respectively. Plasma potentials between 35 ($R=10$) and 60 V ($R=1$) are measured depending on the silane and oxygen flows showing charging of the silica-covered diffusion chamber wall. The magnitude of the wall charging most likely depends on the effective capacitance formed by the silica layer (which results from months of deposition) and on the imbalance between the positively and negatively charged particles which impinge onto

the sidewalls at the discharge initiation until equilibrium of fluxes is reached. This imbalance is a result of the magnetic field configuration generated by the four coils surrounding the reactor and of the subsequent cross-field diffusion of the positively and negatively charged particles to the sidewalls. Maximum wall charging is observed when the silane flow is maximum ($R < 2$), a situation where polymerisation is observed in the mass spectrum of the positive ions, and where a minimum density of negative ions (O^- , OH^- and H^-) are detected close to the walls. Although the polymerisation appeared to be a primary candidate for the increase of the plasma potential to ~ 60 V, its presence does not significantly change the total positive ion density at equilibrium but is accompanied by a dramatic decrease (two orders of magnitude for the O^- ions) in the negative ion density close to the walls when R is increased from 1 to 10. The change in the degree of electronegativity close to the walls affects the global plasma equilibrium and appears as an indirect factor in the magnitude of the wall charging.

*also at the "Dpartement Sciences Pour l'Ingénieur," CNRS, France

GTP 22 The modified Gaseous Electronics Conference (mGEC) research reactor MATTHEW J. GOECKNER, *Electrical Engineering Program, University of Texas at Dallas* E.A. JOSEPH, *Electrical Engineering Program, University of Texas at Dallas* YONGHUA LIU, *Electrical Engineering Program, University of Texas at Dallas* L.J. OVERZET, *Electrical Engineering Program, University of Texas at Dallas* SANKET SANT, *Electrical Engineering Program, University of Texas at Dallas* BAO ZHOU, *Electrical Engineering Program, University of Texas at Dallas* The modified Gaseous Electronics Conference (mGEC) research reactor is a tool designed to study plasma-surface interactions and chamber geometry. Specifically, the tool is designed such that the plasma source can be moved axially, from 0.95 cm to 16.19 cm above a wafer chuck, which is in turn 3.81 cm above the bottom surface. Additionally there are a series of internal walls of various radii and surfaces that can be inserted into the chamber. This system can be used to examine a wide variety of phenomenon. For example if the source is moved from approximately the center of its axial motion, $z = 8.7$ cm, to the maximum separation, $z = 16.2$ cm, the peak of the electron temperature for a 20 mTorr Ar plasma will drop from 5 eV to 4 eV. Further, the axial variation of the temperature (over 7 cm) will decrease from 2 eV to 0.75 eV. Similar variations are observed in the density and potentials. This paper will serve as an overview of the mGEC design parameters as well as of the data gathered from the tool. This work is supported by a grant from NSF / DOE, CTS-0078669.

GTP 23 Studies of plasma chemistry in a modified Gaseous Electronics Conference (mGEC) research reactor BAO ZHOU, E.A. JOSEPH, YONGHUA LIU, L.J. OVERZET, M.J. GOECKNER, *Electrical Engineering Program, University of Texas at Dallas* The mGEC research reactor has been designed to study plasma chemistry-surface interactions. Often, to obtain general chemistry parameters a Fourier transform infrared (FTIR) spectrometer using a single pass IR beam is employed. Such arrangements suffer from low signal to noise ratio for low density chemical species. The signal to noise ratio can be improved by increasing the path length of the IR beam through the discharge. This can be done by adding a multi-pass system, such as a White cell. We have added such a system to the mGEC. We use it to examine radial species concentrations in CF_4 discharges, with various internal chamber configurations. This work is supported by a grant from NSF / DOE, CTS-0078669.

GTP 24 Simulation of plasma chemistry in a modified Gaseous Electronics Conference (mGEC) research reactor SANKET SANT, E.A. JOSEPH, YONGHUA LIU, L.J. OVERZET, BAO ZHOU, M.J. GOECKNER, *Electrical Engineering Program, University of Texas at Dallas* In this paper, we make use of the Hybrid Plasma Equipment Model (HPEM) [1] and Langmuir probes to examine the mGEC. The mGEC was designed to study the interactions of the radicals created in a high density low pressure plasma with the chamber walls. The tool has the ability to change its geometrical structure in various dimensions, allowing us to closely inspect various plasma-wall interactions. This ability can be imperative in deciding the exact wall conditions necessary for optimal yield in a real time process. This paper presents a part of this project by matching Langmuir probe results taken in the mGEC cell when a highly polymerizing gas, CF_4 , is used to create a high density low pressure plasma. The results are compared to the theoretical results derived from modeling the chamber conditions using the Hybrid plasma equipment model (HPEM). [1] R. Kinder and M.J. Kushner, 'Non-Collisional Heating and Electron Energy Distributions in Magnetically Enhanced Inductively Coupled and Helicon Plasma Sources', *J. Appl. Phys.* 90, 3699 (2001). This work is supported by a grant from NSF / DOE, CTS-0078669.

GTP 25 Dependence of Ti Surface Nitriding Degree by Nitrogen Plasma Irradiation on Plasma Parameters HIROYUKI KOBORI, SHUJI KOIKE, SOU WATANABE, MITSUO MATSUZAKI, HARUAKI MATSUURA, HIROSHI AKATSUKA, *Research Laboratory for Nuclear Reactors, Tokyo Institute of Technology* Degree of nitriding of Ti surface is experimentally investigated by applying two kinds of nitrogen plasma source. The one is microwave discharge plasma source, and the other is magnetically confined expanding arc jet. As the plasma parameters, we measured electron temperature and density by Langmuir probe, and vibrational and rotational temperature by spectroscopic observation. Relationship between the nitriding degree and various plasma parameters is systematically studied. It is found that the effect of the vibration temperature is the most essential for the surface nitriding, whereas the effect of electron temperature, density and rotation temperature is less remarkable. It is also found that the temperature of the irradiated Ti surface increases as the vibration temperature increases. Higher vibration temperature of the nitrogen plasma makes the target temperature higher, and consequently, the degree of nitriding remarkably increased.

GTP 26 Cold Cathode Electron Beam Injection to Substrates Employed in an Inductively Coupled Plasma* MASAHIRO WATANABE, *Veeco Instruments Inc., Fort Collins, Colorado* KATSUMI HOSHIMIYA, *Dept. of Electrical and Computer Engineering, Colorado State University, Fort Collins, CO 80523* ZENGQI YU, *Dept. of Electrical and Computer Engineering, Colorado State University, Fort Collins, CO 80523* GEORGE COLLINS, *Dept. of Electrical and Computer Engineering, Colorado State University, Fort Collins, CO 80523* A cold cathode electron beam, generated in the inductively coupled plasma discharge, has shown its charge neutralization performance on etch surface in the reactive ion etching. The electron beam is created by ion impact secondary electron emission from the cold cathode. This electron beam source produces an electron flux up to 1 mA/cm². The electron energy can be separately controlled from 300 eV up to 1.2 keV. The electron energy spectra of the transmitted beam in a variety of gas species with different applied rf

frequency have been studied. The dielectric coating on cathode surface is shown to play an important role in e-beam generation as described below. Finally we report the effects of oxide coating thickness on the energy distribution of the generated electron beam. The dielectric layer on cathode surface acts, to a first approximation, as a voltage divider for the applied rf. The oxide layer thickness allows fine tuning of the beam voltage. Beam voltage is also a function of the applied rf frequency.

*This work is supported by NSF grant #ECS - 0097061

GTP 27 Surface Modification of Aluminium by Dielectric Barrier Discharges J.F. BEHNKE, V. LEBEDV, A. SONNENFELD, H. STEFFEN, *University of Greifswald, Institute of Physics, Germany* R. FOEST, M. SCHMIDT, *Institute of Low Temperature Plasma Physics Greifswald, Germany* The application of the DBD (filamentary mode, $f=7$ kHz, U : 2-6 kV, P : 30-100 W) for the cleaning of hydrocarbon contaminated surfaces, for the modification of metallic surfaces by oxidation and for deposition of silicon organic films will be reported. 2 dielectric electrode with an area of $80 \times 20 \text{ mm}^2$ was positioned above the substrate. The arrangement allowed the motion of the substrate relatively to the electrode at a discharge gap of 1 mm. The surface cleaning, oxidation and deposition (admixture of 0.1% TEOS) experiments were carried out in dry air at atmospheric pressure. It will be demonstrated, that hydrocarbon-containing films up to a thickness of 100 nm were removed within 10 s. The cleaning process was succeeded by the growth of a compact oxid layer (15 nm). The results were verified by gravimetric, ellipsometric and angle resolved XPS investigations. The protective properties of the deposited silicon organic films will be discussed in relation to the growth rate and the chemical structure derived from FTIR absorption measurements.

GTP 28 CAPACITIVELY COUPLED PLASMAS AND NEGATIVE-ION PLASMAS

GTP 29 Comparison between One-Dimensional and Two-Dimensional Models of Ar Plasma with Asymmetric Geometry SOON-YOUL SO, MASAKAZU UEDA, HIROTAKE SUGAWARA, YOSUKE SAKAI, *Hokkaido University, Japan* RF capacitively coupled plasmas with asymmetric electrode geometries are widely used in plasma processes that require very high ion bombardment energies. In order to appropriately simulate such asymmetric systems, we have to use a two-dimensional (2D) model. However, one-dimensional (1D) models assuming equal parallel-plate electrodes are actually used in many investigations to understand the essential plasma properties. In this work, for pure argon plasmas at 500 mTorr, we developed 1D fluid models for taking account of asymmetric electrode systems in cylindrical geometries, and we compared their results with those obtained by 2D models. The symmetric models showed that the plasmas in a harmonic steady state have single-peaked structure symmetric with respect to the midpoint between the electrodes. On the other hand, in the asymmetric models, the maximum plasma density appears at an off-centered position and dc self-bias is generated by the blocking condenser. We also investigated an asymmetric

model without blocking condenser and compared the results with the other models. Furthermore, the plasma properties and the dc self-bias are examined at various electrode area ratios and RF source voltages. The applicable limit of a 1D model is discussed.

GTP 30 Power dissipation mode transition by a magnetic field SHINJAE YOU, *KAIST in Korea* CHINWOOK CHUNG, *KAIST in Korea* KUENHEE BAI, *KAIST in Korea* HONGYOUNG CHANG, *KAIST in Korea* We measured electrical characteristics of transversely magnetized capacitively coupled plasma at low pressure (10 mTorr). From these measurements, we found that the power characteristics of the magnetized discharge were different from those of the unmagnetized discharge. As the magnetic field increases, a square dependence of power characteristic at high current changes to a linear dependence. This can be understood as a power dissipation mode transition by a magnetic field. A calculation from a simple sheath model agrees well with the experimental data.

GTP 31 Standing wave and skin effects in high frequency capacitive discharges: Self-consistent calculations of fields and plasma density MILES M. TURNER, *Dublin City University, Ireland* MICHAEL A. LIEBERMAN, *University of California at Berkeley* PASCAL CHABERT, *Ecole Polytechnique, France* JEAN-PAUL BOOTH, *Ecole Polytechnique, France* JEAN-MARCEL RAX, *Ecole Polytechnique, France* We show in another presentation that electromagnetic effects may be expected to produce appreciable non-uniformity in high frequency capacitive discharges under conditions of practical interest. In this paper, we show self-consistent calculations of the plasma density and electromagnetic fields, illustrating in more detail the extent of the effect. The calculations use results from a one-dimensional particle in cell calculation and a two-dimensional solution of Maxwell's equations, coupled together using the assumption that the electron energy relaxation length is small compared with the characteristic length of electromagnetic disturbances. These calculations show that, as expected, there can be substantial non-uniformities produced by electromagnetic effects.

GTP 32 Anomalous Capacitive Sheath with Deep Radio Frequency Electric Field Penetration IGOR D. KAGANOVICH, *Plasma Physics Laboratory, Princeton University, Princeton, NJ 08543* A novel nonlinear effect of anomalously deep penetration of an external radio frequency electric field into a plasma is described. A self-consistent kinetic treatment reveals a transition region between the sheath and the plasma. Because of the electron velocity modulation in the sheath, bunches in the energetic electron density are formed in the transition region adjacent to the sheath. The width of the region is of order V_T/ω , where V_T is the electron thermal velocity, and ω , is frequency of the electric field. The presence of the electric field in the transition region results in a cooling of the energetic electrons and an additional heating of the cold electrons in comparison with the case when the transition region is neglected. The total deposited power in the sheath region does not change considerably. Additional information on the subject is posted in <http://www.pppl.gov/pub/report/2002/PPPL-3649.pdf> <http://arxiv.org/abs/physics/0203042> Work supported by the Princeton Plasma Physics Laboratory through a University Research Support Program.

GTP 33 Analysis of Heating Mechanisms in Capacitively-Coupled Plasma using PIC Simulation T. R. CHUNG, H. C. KIM, S. E. PARK, J. K. LEE, J. W. SHON, *Plasma Application Modeling Group, Lam Research Corporation* Recently, variations of capacitively coupled plasma are becoming mainstream plasma sources for dielectric etchers. Hardware variations include with or without magnetic fields, the single or multiple power sources for different RF frequency, various electrode spacing and materials. The results of PIC simulation is compared with single and double Langmuir probe measurements, which have shown a good agreement. Independent delivered RF power measurements have compared well with PIC simulation results. We have analyzed their plasma heating mechanisms using a Particle-In-Cell (PIC) simulation. Electron energy distribution functions, absorbed power between ions and electrons are compared and found that depending on driving frequency and power, more power can be put into electrons or ions by sheath heating. Variations in EEDF and IEDF will be described depending on plasma parameters.

GTP 34 Energetics of secondary electrons in a model of an RF sheath FRED HAAS, *The Open University* LAURA LAUROTARONI, *The Open University* NICK BRAITHWAITE, *The Open University* An idealised model of an RF sheath is used to study the energetics of secondary electrons emitted with an initial energy from an electrode. The sheath potential is spatially quadratic (particle simulations suggest that this is a satisfactory assumption) and comprises a steady part and two harmonics. Space charge and currents arising from secondary electrons are neglected. The transit time takes account of the phase between the electron motion and the sheath current. To examine the relation between them, the phases are separated into two groups: (a) values of excluding π , and (b) those close to π . In case (a) the transit time is of order the electron plasma period and independent of initial energy and sheath potential. In case (b) there is a dependence on potential and initial energy. The electron energy at the plasma-sheath boundary is a function of phase and potential. The electron energy is conserved; at the plasma-sheath boundary it is equivalent to the potential energy at the electrode upon emission. The resulting secondary electron distribution in the bulk plasma has two singularities and a minimum. Taking parameters typical of an argon plasma the orderings are shown to be consistent. Observations of secondary electron trajectories in a self-consistent particle simulation [1] are in agreement with the analytical approach. The model provides insight and is a useful way of specifying the energy distribution of secondary electrons in the bulk plasma. [1] PIC code by Miles Turner, Dublin City University

GTP 35 Emissive Probe Measurements in a Dual-Frequency-Confined Capacitively-Coupled-Plasma System* SHANE LINNANE, *Dublin City University* ALBERT R. ELLINGBOE, *Dublin City University* Dual frequency confined capacitively coupled plasmas (DFC-CCP) are increasingly used in semiconductor manufacturing for dielectric etching, allowing greater (and independent) control of ion energies and ion flux on the etched substrate. The powered electrode is driven with the summation of 27MHz and 2MHz sinusoidal voltages, while the other electrode is grounded. The electrode areas are similar in size, giving an electrode aspect ratio less than 2. Because of this low aspect ratio, there are large oscillations in the plasma potential. The expectation is for sinusoidal oscillations at the higher driving frequency, due to capacitive sheaths, while a rectified oscillation is expected at the lower driving frequency.¹ Measurements of rf oscillation in the

plasma potential taken with a floating emissive probe will be presented. The emissive probe and circuitry allows direct realtime measurement of plasma potential oscillation at both driving frequencies and the harmonics of each, thus allowing measurement of the actual potential on the driven electrode and ion energy incident on grounded electrode.

*E. Kawamura, V. Vahedi, M. A. Lieberman and C. K. Birdsall, *Plasma Sources Sci. Technology*. 8 (1999) R45-R64

¹E. Kawamura, V. Vahedi, M. A. Lieberman and C. K. Birdsall, *Plasma Sources Sci. Technology*. 8 (1999) R45-R64 Work Supported by EURATOM.

GTP 36 FTIR Analysis of Etch Products in Ion-Ion and Electron-Ion Cl₂ Discharges ASHISH JINDAL, MATTHEW GOECKNER, LAWRENCE OVERZET, *University of Texas at Dallas, Electrical Engineering Program* The volatile etch products that result from the etching of single crystalline Si, poly-Si, SiO₂, and photoresist in a Cl₂ discharge are analyzed downstream from the turbo-pump, via FTIR spectroscopy. An independently controlled chuck is rf biased to produce an alternating flux of negative and positive ions or electrons and positive ions at the silicon substrate. Plasma power is either pulsed to produce ion-ion plasmas or continuous to produce electron-ion plasmas. Various biasing schemes are utilized including continuous wave, asynchronous, and synchronous. Asynchronous and synchronous modes apply to 1 kHz, 50 percent duty ratio pulsed regimes of the discharge in which the former implies continuous biasing throughout the entire pulse cycle and the latter to only the afterglow, where an ion-ion plasma exists. FTIR spectroscopy is used to investigate various etch products released as pump exhaust that may play a role in environmental degradation.

GTP 37 COMPUTATIONAL METHODS FOR PLASMAS

GTP 38 A numerical scheme to speed up PIC simulations of radio-frequency plasma discharges ROBERTO ZORAT, *Dublin City University* DAVID VENDER, *Dublin City University* MILES TURNER, *Dublin City University* ALBERT R. ELLINGBOE, *Dublin City University* Plasma Research Laboratory and National Centre for Plasma Science and Technology, DCU, Dublin Ireland A numerical scheme coupling a Particle-In-Cell Monte Carlo Collisions (PIC/MCC) simulation code with a suitably modified version of a global model code is presented. The two codes cyclically interact in a suitable way by exchanging information. The scheme is used to model an rf capacitively coupled hydrogen plasma discharge. It is shown that the computational time needed to reach the steady state of the simulated plasma discharge with a conventional PIC/MCC simulation is significantly reduced if this new scheme is used instead. Besides, plasmas with complex chemistry can in principle be handled by this scheme thanks to the input of the global model code on the PIC/MCC code. As an example the negative ion production by dissociative electron attachment on vibrationally excited states of molecular hydrogen is included in the model of the same plasma discharge. Work Supported by EURATOM

GTP 39 PLASMA BOUNDARIES, SHEATHS AND PRESHEATHS I

GTP 40 An efficient solution of the Boltzmann equation OLEG POLOMAROV, CONSTANTINE THEODOSIOU, *University of Toledo* We have developed an efficient computational method of solving the Boltzmann equation for electrons using a multi-term expansion of the distribution function with explicit inclusion of anisotropic elastic scattering as well as anisotropic ionizing collisions (creating secondary electrons). The temporal development and steady-state electron distribution functions and corresponding transport coefficients have been obtained for various gases. We have addressed the importance of accurate accounting of different scattering processes and their influence on the distribution function. Our findings will be presented at the conference.

GTP 41 Transition from a collisionless to a collisional sheath K.-U. RIEMANN, *Theoretische Physik 1, Ruhr-University, D-44780 Bochum, Germany* The subdivision of the plasma boundary layer into a quasi-neutral presheath and a collision-free sheath is strictly valid only in the asymptotic limit $\lambda_D/\lambda \rightarrow 0$, where λ_D is the electron Debye length and λ the ion mean free path. This trivial fact requires to discuss the applicability and correct interpretation of the plasma-sheath concept for finite ratios λ_D/λ . Various questionable attempts have been made (and are still made) to re-define the sheath edge and to derive a modified Bohm criterion accounting for ion collisions. In a previous fluid analysis [1] (based on the charge exchange model) we had demonstrated that such modifications of the Bohm criterion are neither necessary nor justified. The former conclusions are improved by a corresponding kinetic analysis and by generalisations with respect to the presheath mechanism. [1mm] [1] K.-U. Riemann, *Phys. Plasmas* 4, 4158 (1997)

GTP 42 The plasma-sheath transition in multiple ion species plasmas K.-U. RIEMANN, TH. WELLIE, *Theoretische Physik 1, Ruhr-University, D-44780 Bochum, Germany* In a separate plasma and sheath analysis, the plasma boundary conditions are represented by the breakdown of the quasi-neutral solution at the "sheath edge." Mathematically, the sheath edge definition is closely related to the marginal validity of the Bohm criterion. In a multi-component system we are confronted with the problem to formulate the boundary conditions for various ion components from one Bohm criterion [1]. We discuss this problem hydrodynamically and kinetically with explicit examples. In particular we show that the kinetic analysis of generalized Tonks-Langmuir type problems can be reduced under very general conditions to the corresponding one-component problem. In a hydrodynamic analysis, in contrast, the boundary condition problem of multi-component systems proves to be rather involved. [1mm] [1] K.-U. Riemann, *IEEE Trans. Plasma Sci.* 23, 709 (1995)

GTP 43 On the Consistency of the Collisionless Sheath Model VALERY GODYAK, *Osram Sylvania, Beverly, MA, 01915* NATALIA STERNBERG, *Clark University, Worcester, MA 01610* The sheath that occurs at a plasma boundary is defined in textbooks as a thin (several Debye lengths λ_D) space charged layer where the electron density is much less than the ion density (n_e

$\ll n_p$). Since the sheath length is much smaller than the plasma length ($s \ll d$) and $n_e \ll n_p$, there is practically no ionization in the sheath, and ion flux, injected from the adjacent plasma into the sheath, is constant throughout. A common approach to mathematically model a collisionless sheath, for an ion mean free path $\lambda_p \gg s$, is to apply Poisson's equation including the space charge of ions and electrons, assuming an ion speed equal to the Bohm velocity along with a zero electrostatic potential and electric field at the plasma-sheath interface. Such a sheath model leads to physical inconsistencies for real plasma with finite non-neutrality ($\lambda_D/d \neq 0$). First, this model results in an infinite sheath width ($s \approx \infty$). Second, throughout most of the sheath n_e is infinitely close to n_p , which implies that total ionization in the sheath is much larger than that in the adjacent plasma and contradicts the basic assumption of zero ionization in the sheath. Third, the Bohm criterion requires ion acceleration before entering the sheath and thus requires a non-zero electric field in the plasma that vanishes at the sheath edge. The reason for these inconsistencies, as well as for mathematical difficulties in this model, stems from the unrealistic zero field assumption at the plasma-sheath interface. Different approaches to resolve the inconsistencies are discussed in this presentation.

GTP 44 HOW TO PATCH ACTIVE PLASMA AND COLLISIONLESS SHEATH: PRAGMATICAL GUIDE IGOR D. KAGANOVICH, *Plasma Physics Laboratory, Princeton University, Princeton, New Jersey, 08543, USA* Most plasmas have very thin sheath compared with plasma dimension. This necessitates separate calculation of plasma and sheath. Bohm criterion provides boundary condition for calculation of plasma profiles. To calculate sheath properties a value of electric field at the plasma-sheath interface has to be specified in addition to Bohm criterion. The value of the boundary electric field and robust procedure to approximately patch plasma and collisionless sheath with a very good accuracy is reported. Additional information on the subject is posted on the web <http://www.pppl.gov/pub/report/2002/> <http://arxiv.org/abs/physics/0208041>. Work supported by the Department of Energy via the University Research Support Program of Princeton Plasma Physics Laboratory.

GTP 45 Dynamics of the Debye-Sheath with Weak RF-Coupling V.A. KADETOV, U. CZARNETZKI, *Institut for Plasma and Atomic Physics, Bochum University, 44780 Bochum, Germany* H.F. DOEBELE, *Institut for Experimental Physics, Essen University, 45117 Essen, Germany* At low sheath voltages ($eU =$ a few kT_e), the electron density within the sheath is not negligible. These kind of sheaths are found e.g. close to surfaces (floating potential) in DC or inductively coupled RF (ICP) discharges. In the latter case the DC-potential can be superimposed by a weak capacitive coupling, especially at powers just above the threshold for ICP operation. The dynamic of this intermediate type of sheath is investigated by laser spectroscopic electric field measurements (fluorescence-dip spectroscopy in atomic hydrogen) and mass resolved determination of the ion energy distribution (plasma monitor). From spatially and temporally resolved electric field distributions a number of further quantities can be deduced: electron and ion density and energy distributions, electron temperature, temporal development of the sheath potential and the individual contributions to the sheath current (ion, electron, and displacement current). Further analysis even allows an insight to the weak ion dynamics. In general, good agreement is found between the electric field and ion energy measurements.

GTP 46 Energy Distribution and Sheath Formation in a Cylindrical Self-sustained Surface-wave Discharge at Low Pressures L.L. ALVES, *CFP, IST, Portugal* G. GOUSSET, P. LEPINCE, *LPGP, Univ. Paris-Sud, France* The paper analyses the radial distribution of the plasma mean energy in a cylindrical discharge created and maintained by a TM_{00} surface wave at frequency $\omega/2\pi = 2.45$ GHz, pressures $p = 1 - 100$ mTorr and average electron densities $n_e \approx 10^{11} - 10^{12} \text{ cm}^{-3}$. The electron energy transfer is described using a fluid model that takes into account the energy gained from the surface-wave e.m. field, and the energy lost in convection, friction and diffusion against the static space-charge electric field (resulting from charge separation within the sheath region near the wall). The latter contribution to energy losses is associated with the sheath formation. A special attention is given to the energy coupling between the wave and the plasma, which occurs mainly at the electron plasma resonance where $\omega_p \approx \omega$ (ω_p is the electron plasma frequency). This region is located in the vicinity of the plasma-sheath threshold, and is characterized by a strong variation of the electron density and thus of the plasma permittivity. Simulation results show that the energy absorbed by the electrons within the resonance region is radially transported in two opposite directions: towards the discharge axis, where is dissipated by collisions, and towards the wall where is used to maintain the space-charge sheath, the latter being the dominant energy loss process. The paper will discuss the influence of pressure and average electron density on the results.

GTP 47 Mitigation Process of Negative Charging by Plasma Flow HIROKAZU TAHARA, *Graduate School of Engineering Science, Osaka University* TAKAO YOSHIKAWA, *Graduate School of Engineering Science, Osaka University* In order to simply and clearly understand phenomena of negative charging and its mitigation by plasma flow, equivalent electrical circuits between a substrate and the plasma around it were made. The substrate was found to have the hazard of electrical breakdown between the conductive main body and the insulating surface during the mitigation. A segmented ion collector in series with negatively charged condensers were exposed to argon plasma flows with changing plasma velocity under a constant plasma number density. The time variations of neutralization current and ion sheath shape were measured. The mitigation process was expected to depend on plasma velocity and plasma number density, i.e., ion velocity and ion flux, and their dependence intensively changed with the attack angle of plasma flow to the negatively charged surface by effect of inertia of ions. In cases that a negatively-charged insulating surface disappears from a plasma source; in the shade on view from a plasma source; i.e., at wake condition, particularly with a high plasma velocity, electrical breakdown fears occurring by a large difference in mitigation time between the absolute charging of the conductive main body and the local charging of the insulating surface, as predicted from the equivalent electrical circuits.

GTP 48 PLASMA DIAGNOSTICS I

GTP 49 Techniques for measurement of electric fields in microplasmas MARK BOWDEN, BRAM VISSER, TAO JIANG, GERRIT KROESEN, *Applied Physics, Eindhoven University of Technology, Netherlands* Electric field is an important parameter in determining the efficiency of the microplasma light sources that make up a plasma display panels. Measurement of the field, how-

ever, is difficult because of the lack of suitable techniques and the size of the discharge itself. At Eindhoven, we have developed a measurement method for the purpose of measuring fields in such discharges. The method is based on Stark spectroscopy of xenon atoms. The development of the method had two initial stages. Firstly, measurements of Stark spectra were made in the sheath region of a glow discharge using laser spectroscopy. These measurements then were compared with theoretical spectra calculated by solving the Schrödinger equation for the case of a xenon atom in the presence of an electric field. In this presentation, the measurement technique will be explained, with results of both experiments and theoretical calculations being presented. Preliminary measurements in a microdischarge will also be discussed.

GTP 50 Stark spectra of argon Rydberg states measured by laser-induced fluorescence-dip spectroscopy under well-defined electric fields K. TAKIZAWA, K. SASAKI, K. KADOTA, *Department of Electronics, Nagoya University, Japan* V. P. GAVRILENKO, *Center for Surface and Vacuum Research, Russian State Committee for Standards, Russia* Electric fields in front of solid surfaces play essential roles in plasma processing of materials. After an innovative work by Czarnetzki *et al.*, many researchers are trying sensitive detection of electric fields in plasmas using advanced laser-spectroscopic methods. For the sensitive measurement of electric field, we have adopted laser-induced fluorescence-dip (LIF-dip) spectroscopy to Ar Rydberg states. To date, we have succeeded in detecting Rydberg states with a principal quantum number of $n = 59$. This paper reports the change in the spectral distribution of Ar Rydberg states due to the Stark effect under well-defined electric fields. The LIF-dip spectra were obtained by two-step excitation from a metastable state to Rydberg states. Ar atoms at the metastable state were produced in a remote microwave plasma source, and were transported to plasma-free region sandwiched by two plane electrodes. The experimental results indicate that the Stark effect of Ar Rydberg states is very sensitive to electric field. The highest sensitivity we obtained experimentally was ~ 1 V/cm, which was realized by detecting a Rydberg state with $n \approx 50$. The authors would like to thank U. Czarnetzki for providing helpful information on the microwave plasma source.

GTP 51 Phase resolved emission spectroscopy of RF discharges: Measurement of rotational temperatures in inductively coupled hydrogen plasmas T. GANS, *Plasma Research Laboratory, Dublin City University, Ireland* V. SCHULZ-VON DER GATHEN, M. ABDEL-RAHMAN, H.F. DÖBELE, *Institut f. Laser- und Plasmaphysik, Universität Essen, 45117 Essen, Germany* Phase and space resolved optical emission spectroscopy (OES) has to the potential to unravel the population dynamics of excited states in RF excited discharges. The method allows—in combination with an analytical model—quantitative measurements of time and space resolved rotational temperatures. The method is applied to an inductively coupled discharge of dimensions similar to the GEC reference cell. Measurements of rotational temperature distributions are presented from which commonly gas temperatures are deduced. Both the power (150-600 W RF power) and the pressure (3-75 Pa) are varied. Comparison with a capacitively coupled discharge demonstrates that time variations of populations within one excitation cycle exist but are not as pronounced as in the capacitive case. Furthermore, the effect is limited to the high power case. This work was supported by the DFG in the frame of SFB 191.

GTP 52 Phase resolved emission spectroscopy of RF discharges: Measurement of quenching coefficients and EEDFs in capacitively coupled hydrogen plasmas T. GANS, *Plasma Research Laboratory, Dublin City University, Ireland* V. SCHULZ-VON DER GATHEN, H.F. DOBELE, *Institut f. Laser- und Plasmaphysik, Universität Essen, 45117 Essen, Germany* Phase and space resolved optical emission spectroscopy (OES) has the potential to unravel the population dynamics of excited states in RF excited discharges. The method allows, in combination with an analytical model, quantitative measurements of: a) lifetimes and collisional quenching coefficients; b) time and space resolved electron densities and EEDFs of energetic electrons ($> 12\text{eV}$). The phase resolved OES measurements of quenching coefficients are—in contrast to laser measurements—not limited by optical selection rules or large energy gaps. The phase and space resolved access to the EEDF of energetic electrons by phase resolved OES is of particular interest, since these electrons dominate excitation and ionisation processes. Other electron specific diagnostic methods—e.g. Thomson scattering or probe measurements—have no access to these energetic electrons in view of their very low densities ($10^7\text{-}10^9\text{cm}^{-3}$), the transient character, and perturbations by the strong RF field—in particular in the sheath region. This work was supported by the DFG in the frame of SFB 191.

GTP 53 Perturbed optical emission and electron heating in capacitively coupled plasmas PIERRE BARROY, *The Open University* ALEC GOODYEAR, *The Open University* NICK BRAITHWAITE, *The Open University* Studies have been conducted to observe directly the dominant heating processes in a capacitively coupled plasma (GEC reference cell). The ground electrode incorporates a 25 mm diameter planar embedded test surface flush with the electrode face. Controlled pulses of radio-frequency voltage were applied to the test surface in addition to the main 13.56 MHz reactor driving voltage. Spatially resolved measurements, adjacent to the test surface, of the enhanced optical emission that coincides with the RF excitation were made using an intensified CCD camera [1]. Correlation between the parameters of the controlled perturbation and enhanced emission give insight into heating processes within the plasma. To distinguish between stochastic processes, ohmic heating and heating through secondary electrons, the effects of the amplitude, frequency, phase and timing of the perturbing RF pulses are being examined. [1] PRJ Barroy, A Goodyear, and N St J Braithwaite, *IEEE Trans Plasma Science* Vol 30, 148-149, 2002 Work supported by the EPSRC, Grant No. GR/L82380.

GTP 54 Spatio-temporal Characterization of Pulsed, Electron Beam Produced Plasmas* SCOTT WALTON, DAVID BLACKWELL, *SFA Inc., Largo, MD* DARRIN LEONHARDT, RICHARD FERNLSER, ROBERT MEGER, *Naval Research Laboratory* In plasma-based materials modification, determining the flux of ion, neutral, and radical species at the substrate surface is a critical component of process control. In pulsed plasmas, the flux of plasma produced species is directly related to the spatial and temporal variations in the plasma density and electron temperature. In this paper, mass and time-resolved measurements of ion and neutral fluxes sampled from pulsed, electron beam-generated plasmas will be presented as well as temporally-resolved ion energy distributions. The results are correlated to measurements of the plasma density and electron temperature. Previous works have shown that energetic electron beams are efficient at producing high-density plasmas ($n_e > 10^{11}\text{cm}^{-3}$) with

low electron temperatures ($T_e < 1.0\text{eV}$) over the volume of the beam. Outside the beam, ion-neutral and electron-ion interactions alter ion densities and the electron temperature. Temporal variations in the density, electron temperature, and flux have also been observed during all phases of pulsed plasma production. Measurements are presented as a function of operating pressure and electron beam-electrode separation for plasmas produced in argon and nitrogen. The results are discussed in terms of the important gas-phase kinetics.¹

*Work supported by the Office of Naval Research

¹S.G. Walton, D. Leonhardt, D.D. Blackwell, D.P. Murphy, R.F. Fernsler and R.A. Meger, *Phys. Rev. E* 65, 046412 (2002).

GTP 55 Measurements of Electron Number Density and Electron Collision Frequency in a One Atmosphere Uniform Glow Discharge Plasma Using a Microwave Network Analyzer* MOSTOFA HOWLADER, YUNQIANG YANG, J. REECE ROTH, *ECE Department, University of Tennessee* UT PLASMA SCIENCES LABORATORY COLLABORATION Measuring the electron number density and collision frequency is crucial to understanding the behavior and transport coefficients of an atmospheric pressure plasma. We describe a technique to characterize these parameters in a quantitative and non-perturbing way. The technique uses a microwave network analyzer system to measure the absorption and phase shift of a propagating 15 GHz microwave signal. These measured quantities are related to the real and imaginary parts of the plasma index of refraction, which is described by Appleton's equation. Since the electron number density and collision frequency can be numerically derived from the absorption and phase shift that are measured quantities, one need not know the electron energy distribution function, the electron kinetic temperature, or the electron energy-dependent cross section for the collision process. The electron collision frequency is sufficient to determine the transport coefficients, including the diffusion coefficient, the viscosity, and the thermal and electrical conductivity.

*Supported in part by AFOSR contract AF F49620-01-1-0425 (Roth)

GTP 56 Resonant and Non-resonant Deactivation of Ar 4s', 4p', and 6s in a SF₆/Ar/O₂ rf Discharge JAMES M. WILLIAMSON, *Innovative Scientific Solutions, Inc., Dayton, OH* BISWA N. GANGULY, *Air Force Research Laboratory, Wright-Patterson Air Force Base, OH* The change in metastable Ar density as a function of SF₆ and O₂ concentration in a rf-powered, SF₆/Ar/O₂ discharge used for reactive ion etching of SiC was measured. The line-integrated Ar 4s' [$\frac{1}{2}$]^o metastable population density was measured by the absorption of an external-cavity tuned diode-laser operating at 772.4 nm. The plasma emission of excited Ar at 641.6, 750.4, and 772.4 nm as well as the emission of F-atoms at 703.7 nm and O-atoms at 777 and 845 nm were simultaneously recorded with the metastable Ar absorption for 40 W rf power at 0.8 Torr pressure. The SF₆ fraction in the gas mixture was varied from 5 to 50% and the O₂ varied from 0 to 20%. The line-integrated Ar metastable population density decreased, although E/n increased, with SF₆ and O₂ addition. Likewise, the plasma emission of excited Ar at 750 and 772 nm decreased with O₂ addition but the emission of Ar at 641 nm deviated from the Ar emission at 750 and 772 nm and the deviation increased with SF₆ addition. Both the non-resonant deactivation of the 4s' [$\frac{1}{2}$]^o, 4p' [$\frac{1}{2}$], and 6s[$1\frac{1}{2}$]^o states of Ar by SF₆ and resonant deactivation by O-atoms were determined from the combination of the line-integrated absorption density measurements and the plasma emission from excited Ar.

GTP 57 Diode laser induced fluorescence of argon ion metastable SANGHYUN JUN, *Department of Physics, KAIST, South Korea* SANG-WON LEE, *Department of Physics, KAIST, South Korea* HONG-YOUNG CHANG, *Department of Physics, KAIST, South Korea* VDF (Velocity Distribution Function) of argon ion metastable state in magnetized ICP (inductively coupled plasma) are studied by diode LIF (Laser Induced Fluorescence) system. The VDFs are measured from the Doppler effect. Ion temperature, density, and convection velocity are derived from the measured VDF. The density linearly increases from 50 to 150 gauss and abruptly decreases above 200 gauss about 2mTorr and 300Watts. Ion temperature is about 0.1 eV in this region. We have investigated the relation between the argon ion characteristics by LIF technique and plasma parameters by a electrical probe.

GTP 58 PLASMA FOR NANOSTRUCTURED MATERIALS AND DUSTY PLASMAS

GTP 59 Stability of multi-layer plasma dust crystals GREG HEBNER, *Sandia National Laboratories* MERLE RILEY, *Sandia National Laboratories* Single layer, 2D plasma dust crystals can form a number of stable and well-defined arrangements. In general, the 2D crystals have a hexagonal closed pack structure that is strongly influenced by the confining potential. However, multi-layer or 3D structures are notoriously unstable. In most cases, the addition of a 2D plasma crystal layer above or below an existing 2D layer can introduce changes and instabilities into both the upper and lower layer that produce an amorphous arrangement as opposed to a stable multi layer arrangement with well defined order. The stability of multi-layer structures appears to depend on the characteristics of an attractive potential between the negatively charged particles. The attractive potential is formed by the ion flow past the particles that results in ion focusing and creation of a positive space charge region downstream from the object. In this poster, the details of the interparticle potential will be discussed. The particle motion will be illustrated using a number of short video clips. This work was performed at Sandia National Laboratories and supported by DoE Office of Science and the United States Department of Energy (DE-AC04-94AL85000).

GTP 60 Contact charging of dusts on surfaces ZOLTAN STERNOVSKY, *Department of Physics, University of Colorado, Boulder, CO 80309-0390* MIHALY HORANYI, *Department of Physics, University of Colorado, Boulder, CO 80309-0390* SCOTT ROBERTSON, *Department of Physics, University of Colorado, Boulder, CO 80309-0390* Dust particles play an important role in plasma, planetary and space physics. Numerous interesting phenomena involving dust particles are related to their charge. Along with charging in plasma, considerable dust charge may result from contact processes with other objects. An experimental method has been developed to investigate dust charging on surfaces. Dust samples are loaded onto clean metal surfaces that are agitated by a small electromagnet. Single dust particles drop through a small hole into a Faraday cap for charge measurements. The dust samples investigated are of large variety including metallic and insulating grains and lunar (JSC-1) and Martian (JSC-

Mars-1) regolith simulants. A typical contact charge on a 100 micron sized insulating dust particle is $10E5 - 10E6$ elementary charges and increases with repeated contacts. The contact charging of metallic grains is significantly lower. The contact charge varies linearly with the work function of the surfaces and with dust size. Oxidized metal surfaces charge the dust particles in a similar way independent of the metal's work function. By contacting the dust samples with different surfaces, the effective work function of the dust samples is determined. External electric fields applied above the surface influence contact charging and may alter the sign of the resulting dust charge.

GTP 61 Numerical simulation of particle transport in a plasma sheath SARAH WARTHESEN, UWE KORTSHAGEN, STEVEN GIRSHICK, *Dept. of Mechanical Eng., University of Minnesota, Minneapolis, MN, 55455* During chemical vapor deposition of silicon films from silane plasmas, particles formed from the gas phase may contribute to film deposition, causing film defects. In other cases, the deposition of nanoparticles can actually enhance the electronic properties of deposited films, improving their performance in photovoltaic cells. The study of particle transport in various plasma conditions is essential in controlling the deposition of particles in films. In this study, a numerical simulation is used to predict the temporal evolution of axial particle position and charge distribution in the sheath of a capacitive RF plasma. The particle transport mechanisms included in this model are convection, diffusion, thermophoresis, and electrostatic force. Simulations are carried out for various particle sizes and plasma conditions. The effects of pressure and temperature on particle transport are explored. Results from this model provide insight on establishing parameters to control or prevent particle deposition. This work is supported by NSF (grant CTS-9909563) and the Minnesota Supercomputing Institute.

GTP 62 Plasma Enhanced Chemical Vapor Deposition of Nanostructured Hydrogenated Silicon Thin Films* SIRI THOMPSON, UWE KORTSHAGEN, *Dept. of Mechanical Engineering, University of Minnesota, Minneapolis, MN 55455* JAMES KAKALIOS, *School of Physics and Astronomy, University of Minnesota, Minneapolis, MN 55455* Thin films of hydrogenated silicon with nanocrystalline inclusions (nc-Si:H) have demonstrated enhanced electronic properties and improved medium range order over standard amorphous silicon films, thereby indicating the potential for their application in photovoltaic cell manufacturing. We study the deposition of these films by means of a radio frequency capacitively-coupled plasma discharge using a mixture of dilute Silane (SiH₄) in Helium (He) and Hydrogen (H₂), with discharge conditions at the boundary of powder formation. The dependence of the film properties on the temperature gradient between the electrodes is analyzed. The effects of the discharge conditions (pressure, RF power) are investigated and the resulting material properties are discussed. Using the constant photocurrent method, the optical absorption coefficient of the film is studied as a function of photon energies, yielding information about the density of the electronic states (extended states, localized/band tail states, and defect states).

*This research is supported by NSF under IGERT grant DGE-0114372.

GTP 63 Parameter dependence of particle growth in silane discharges GREGORY BANO, KAROLY ROZSA, ALAN GALLAGHER, *JILA, University of Colorado and NIST** The dependence of silicon particle formation and growth on discharge parameters will be reported for silane RF discharges. Particles of

6-60 nm diameter are studied by light scattering, and their size is established from their afterglow diffusion [1]. The particle growth rate (Gp) has a strong dependence on higher silanes (HS) generated in the discharge, whereas the HS do not influence film growth rates (Gf). Gp also increases(decreases) rapidly with increasing pressure(temperature), whereas Gf has very little dependence on these parameters. Since the same silyl radical dominates film and particle growth, this lack of Gp-Gf correlation is surprising. It may result from H-atom activation of the particle surfaces, as will be explained. Hydrogen added to the silane strongly increases Gp, consistent with this conjecture. The RF voltage has a similar effect on Gp and Gf, consistent with simple expectations for silyl induced growth. [1] M.A.Childs and A. Gallagher, *J. Appl. Phys.* 87,1076(2000)

*corresponding and attending author

GTP 64 Effects of dust particles on the dust-free regions in argon-diluted silane plasmas S. PARK, W. CHOE, *Department of Physics, Korea Advanced Institute of Science and Technology* G. S. EOM, C. W. PARK, *Laser Metrology Group, Korea Research Institute of Standards and Science* J. W. HAHN, *Department of Mechanical Engineering, Yonsei University* Dusty particles were generated in a capacitively-coupled, argon-diluted silane discharge. Two regions free from the dust particles were observed near the electrode sheath and in the bulk plasma (dust void). These regions evolved with time and were periodic with approximately (6-7) minutes of period at $P_{gas}=30$ mTorr. In the initial phase of the discharge, the thickness of the dust-free region near the electrode became narrower, and it became wider again after a few minutes. In addition, the evolution of the dust void structure was also observed. The evolution of the sheath and dust void structure is likely to be due to the temporal change of the dust particle size as well as its density. By solving the continuity equation, momentum transfer equation, and Poisson equation including the dust particle contribution, the observed temporal change of the 1-D sheath structure and the particle equilibrium position were explained, and the details will be discussed. Measurement of particle size using laser diagnostics will also be described.

GTP 65 Influences of Plasma Parameters on Synthesis of Single-Walled Carbon Nanotubes by Transferred Plasma Torch Method SHIN IL CHOI, CHAN MIN LEE, JUN HO SEO, JUN SEOK NAM, SOO SEOK CHOI, SANG HEE HONG, *Seoul National University, Seoul, Korea* Single-walled carbon nanotubes (SWNTs) have a great potential of their practical applications to good conductor, semiconductor, field effect transistor, nano-devices, hydrogen storage medium, and so on. In conventional processes of carbon nanotubes synthesis by the dc arc discharge method, SWNTs have been observed in the carbon soot evaporated from the carbon anode, and more than 50% of evaporated materials have been directly deposited onto the cathode surface with no SWNTs contained. In order to increase the synthesized soot of SWNTs while reducing the quantity of the cathode deposit, we have developed a synthesis method using the dc transferred plasma torch, which has been generally used for melting and vitrification in the waste treatment. And in this experimental work, we have investigated the effects of arc current and gas flow rate on the synthesis of single-walled carbon nanotubes by the transferred

plasma torch method. The evaporation rate from the carbon anode and the generation rate of carbon soot are measured in order to evaluate the quantity of synthesized SWNTs. TEM and SEM images and Raman spectroscopy of synthesized SWNTs are analyzed to evaluate the quality of SWNTs.

GTP 66 LIGHT SOURCES I

GTP 67 Breakdown Properties of Cold Metal Halide Lamps*

RICHARD S. MOSS, ANANTH BHOJ, MARK J. KUSHNER, *University of Illinois/Urbana-Champaign* Breakdown during starting of metal halide lamps is of interest for optimizing the reliability of restart of warm lamps and reducing the erosion of electrodes during starting of cold lamps. These breakdown processes were experimentally and computationally investigated using a model metal halide lamp. The lamp is 1 cm diameter with an adjustable electrode separation of approximately 1.6 cm. Breakdown was investigated in argon and Penning mixtures of Ar/Xe over pressures of 10-100 Torr with 1-3 μ s voltage pulses of up to 2 kV. To minimize statistical jitter, an external UV lamp was used to provide a small seed electron density enabling reliable measurements to be made at low repetition rates of 0.1 to 1 Hz. Experiments were analyzed using a 2-dimensional plasma hydrodynamics computer model using a boundary fitting mesh. Time to breakdown smoothly increased with increasing pressure and reduced applied voltage until a minimum E/N. This E/N increased with decreasing pressure suggesting that wall charging effects are important in the breakdown process.

*Work was supported by General Electric and the National Science Foundation (CTS99-74962). The authors thank J. G. Eden and S. McCain for their advice during this work.

GTP 68 Modelling of a Low-Pressure Discharge in He-Xe Mixtures

SERGUEI GORTCHAKOV, HARTMUT LANGE, DETLEF LOFFHAGEN, DIRK UHRLANDT, *Institut für Niedertemperatur-Plasmaphysik, 17489 Greifswald, Germany* Helium-xenon mixtures are at present very promising for mercury-free low-pressure VUV radiation and light sources. Both DC and AC operation are of interest for industrial applications. Optimum output characteristics and operation conditions can be evaluated by an appropriate self-consistent analysis of the plasma of such glow discharges. Two models of the cylindrical column plasma in helium-xenon mixtures are presented each comprising a kinetic treatment of the plasma electrons, a detailed balance description of the excited states in xenon as well as a self-consistent determination of the axial heating field. The first model is based on a spatially resolved treatment of the plasma components and of the radial space-charge field in steady state. The second one uses a time-dependent, radially averaged description of electron and heavy particle kinetics and can be applied to studies of DC and AC discharge operation. In its framework, steady state plasma parameters are determined by means of a temporal relaxation procedure.

By comparing results for DC discharges, advantages and disadvantages of both models are discussed. As a reference, results of probe and spectroscopic measurements have been used. Perspectives for the modelling of the AC discharge operation are considered.

GTP 69 Luminous efficiency of narrowed positive column cell of DC plasma display panel KEIJI ISHII, YUKIO MURAKAMI, *NHK Science & Technical Research Laboratories* YOSHIMICHI TAKANO, *NHK Nagoya Station* A positive column cell of DC plasma display panel, which radiates the vacuum-ultraviolet light from the positive column region, has high luminous efficiency. However its luminous efficiency decreases with the increase in discharge current. To investigate this phenomenon, we measured the spatial density distribution of excited Xe atoms in the positive column region by laser spectroscopy absorption technique¹. For the measurement, we experimentally produced a rectangular parallelepiped discharge cell whose discharge path was formed on the diagonal line. Though the density of excited Xe atoms increased with the increase in discharge current, the positive column region contracted toward the anode side. Next, we investigated the density of excited Xe atoms of the narrowed cell, which varies the cell width from 0.19 to 0.36 mm under the same discharge current density. The density of excited Xe atoms increased with the decrease in cell width. Therefore, when the cell width is narrowed, the luminous efficiency of the positive column cell does not decrease.

¹K. Tachibana et al., *Appl. Phys.* **88**, 4967(2000)

GTP 70 Influence of electrode heating by laser radiation on the cathode fall voltage of mercury high-pressure discharges*

MICHAEL SIEG, BERND NEHMZOW, MANFRED KETTLITZ, HELMUT HESS, *INP Greifswald, Fr.-L.-Jahn-Str. 19, D-17489 Greifswald, Germany* The influence of external heating of electrodes in mercury high-pressure discharges is investigated. The quartz discharge lamps have an inner diameter of 12 mm and an electrode gap of 10 mm. The pure tungsten electrodes have a diameter of 0.5 and 0.7 mm and a length of 10 mm without any surrounding coil. The lamps contain 20 mg Hg and 40 mbar Ar, and they are vertically operated with a 50 Hz sinusoidal rms-current of 1.8 A which leads to a pressure of 6 bar. The arc attachment to the electrodes is diffuse. The lower electrode is heated by the IR radiation at 808 nm of a 40 W diode laser. Nearly 18 and lead only to a small increase of the tip temperature of the cathode of about 200 K to 3100 K. While there are only minor changes of the arc voltage during the anode phase a noticeable decrease of the voltage in the cathode phase is measured. This decrease depends directly on the laser power, varies during the cathode phase and is nearly 5 V for the max. laser power. That means that the laser heating of the cathode reduces the cathode fall.

*This work is supported by the VDI (FKZ 13N7762)

GTP 71 Spatially-Resolved Absorption Spectroscopy on an MH-HID Lamp G.A. BONVALLET, *Univ. of Wisconsin-Madison* J.E. LAWLER, *Univ. of Wisconsin-Madison*

We performed spatially-resolved absorption spectroscopy on a 250 W Metal Halide High Intensity Discharge (MH-HID) lamp using the High Sensitivity Absorption Spectroscopy (HSAS) experiment at the Synchrotron Radiation Center in Stoughton, WI. In the HSAS

experiment a stable, high radiance broadband beam of optical-UV synchrotron radiation is sent through an MH-HID lamp and is dispersed and detected using a 3 m focal length echelle spectrometer equipped with a CCD detector array. In diagnosing low- and high-pressure plasmas, HSAS provides superb sensitivity, spectral resolution, and spatial resolution as well as absolute column densities. Absorption measurements on the neutral scandium (Sc I) lines at 530.2 nm, 454.5 nm, and 470.9 nm and the Sc II line at 383.3 nm were used to determine absolute column densities of ground state (0.0 eV) Sc atoms, excited (1.8 eV & 2.3 eV) Sc atoms, and ground state (0.0 eV) Sc ions. The absorption measurements were Abel inverted and analyzed assuming LTE to determine the absolute density of Sc atoms, Sc ions, and electrons and the arc temperature as a function of radius.

GTP 72 One Dimensional Fluid Modeling of the Anode Layer in High Intensity Discharge Lamps ALAN LENEFF, *Osram Sylvania, Beverly, MA 01915*

Determination of the heat flux on the anode surface from the anode plasma layer in high-intensity discharge lamps (HID) is an important problem. This is needed for accurate modeling of electrode temperature distributions. We have performed 1D fluid simulations of the anode layer to investigate anode sheath formation and analyze the heat flux contributions to the anode surface. The simulations account for radiation and radial losses approximately without assumptions of quasi-neutrality. Our results show that the anode layer can have either net positive or negative potential, normally less than one volt for our conditions, and depend on the contributions of a positive sheath and the ambipolar diffusion region. We also show that anode heating appears to come primarily from the electron enthalpy flux in the positive column and ohmic heating in the sheath region. The ambipolar region appears to contribute less to the overall heating because the electric field reverses there. We will also compare these solutions with quasi-neutral solutions and discuss additional important effects such as radial contraction of anode layer.

GTP 73 Pulse Compression of CO₂ laser by Optical Free Induction Decay (OFID) Effect in Dymel Gas DECHANG YI, *Electrical and Computer Engineering, TTU, Cookeville TN 38505*

SATISH MAHAJAN, *Electrical and Computer Engineering, TTU, Cookeville, TN, 38505* Pulse compression of a laser can be accomplished by using OFID technique in IR gases such as ammonia and CH₃F [1]. Earlier work used OFID effect at the falling edge (ON to OFF) of a laser pulse. Results of a CO₂ laser pulse compression in Dymel gas are reported in the present paper. A unique feature of this experimental investigation is the presence of OFID effect on a rising edge (OFF to ON). This feature requires minimum instrumentation as compared to the conventional OFID set up. A pulsed CO₂ laser, test cell with Dymel (1,1 DI-Fluoroethane, C₂H₄F₂), a beam splitter, a digital oscilloscope, and a fast IR pulse detector were used to compress and record pulses of the CO₂ laser. Average of 40 pulses was recorded for a typical pressure of Dymel varying from 0 to 25 torr. Results indicate that the original laser pulse (at vacuum condition) could be compressed to one quarter of its width by adding merely 6 torr of Dymel gas in the test cell. The ratio of intensity to pulsewidth indicated a four times sharper pulse at a pressure of 6 torr of Dymel. These results and explanation of rising edge OFID mechanisms based upon polarization of gas molecules will be presented. [1] E. Yablonovitch, and J. Goldher, Short CO₂ Laser Pulse Generation by Optical Free Induction Decay, *Applied Physics Letters*, Vol. 25. No. 10, Nov. 1974, pp. 580-582.

GTP 74 HIGH-PRESSURE NONTHERMAL PLASMAS I

GTP 75 Selforganization in Microdischarges WENHUI SHI, MOHAMED MOSELHY, KARL H. SCHOENBACH, *Physical Electronics Research Institute, Old Dominion University* Optical studies of microhollow cathode discharges in xenon in the visible and VUV have shown that for high pressure and/or low current the plasma is confined in the microhole. With increasing current and/or decreasing pressure, however, it begins to expand into the cathode area outside the hole [1]. The discharge behaves during this expansion like a normal glow with constant voltage. It changes into an abnormal glow discharge when the plasma reaches physical boundaries, such as a dielectric enclosure of the cathode area. In the transition range from normal to abnormal glow two-dimensional current density patterns begin to evolve. For low pressure, on the order of 100 Torr, these patterns consist of regularly arranged domains of increased luminosity with characteristic dimensions of less than 100 μm . With increasing pressure and current the pattern becomes less regular, and the density of the individual luminescent domains increases. During this phase the patterns are similar to those observed in silent discharges [2]. Eventually, the patterns merge beginning at the center of the circular area, and form a homogeneous plasma layer. Measurements of the excimer intensity of these patterns show that the plasma emits excimer radiation at 172 nm with an efficiency of almost 10%. This material was supported by NSF (CTS-0078618).[1] Mohamed Moselhy, Wenhui Shi, Robert H. Stark, and Karl H. Schoenbach, *IEEE Trans. Plasma Science* 30, 198 (2002).[2] W. Breazeal, K.M. Flynn, and E.G. Gwinn, *Phys. Rev. E* 52, 1503 (1995).

GTP 76 Effect of Rare Gas Addition on O₃ Production Rate in Barrier Discharge Ozonizer T. KIMURA, T. YOSHIGOE, A. ODA, *Nagoya Institute of Technology, Japan* A barrier discharge of planar disk-type with a thin gap is one of successful attempts to obtain high O₃ production at atmospheric pressure. In this study, the rare gas content(x) dependence of the O₃ production rate was investigated in a planar-disk type barrier discharge using a 60 Hz power source, with keeping the total flow rate $F_T=2(\ell/\text{min})$. Ar and Ne were mainly used in this experiment. The discharge was produced between the pyrex glass with 1.0 mm thickness, which was installed below the upper electrode (150mm ϕ stainless steel), and lower electrode (220mm ϕ stainless steel) in the discharge gap (d) range from 0.3 mm to 3.0 mm. A typical O₃ concentration and the production rate for $x = 0$, $d = 1$ mm and the dissipated power of 2 W were about 1600 ppm and 190 g/kWh. In case of $d=1$ mm, O₃ production rate was independent of x at $x \leq 0.5$ and then decreased gradually with increase in x , while the gap voltage estimated from the voltage-charge Lissajous figure gradually decreased from 2.7 kV at $x=0$ to about 1.0 kV at $x = 0.9$ with increase in x . This work is partially supported by Grant-in-Aid from Japan Society for the Promotion of Science.

GTP 77 Physical processes in a homogeneous barrier discharge in helium YU.B. GOLUBOVSKII, V.A. MAIOROV, *St. Petersburg State University, Russia* J. BEHNKE, J.F. BEHNKE, *Ernst-Moritz-Arndt University, Institute of Physics, Domstrasse 10a, D-17487 Greifswald, Germany* A theoretical description of a homogeneous barrier discharge in helium at atmospheric pressure is performed with the help of the fluid model. Various mechanisms

of ionization are analyzed by studying their influence over the characteristics of a glow mode. It is shown that currently available data on the rate constants of elementary processes do not allow to obtain a periodic glow discharge in pure helium. A small impurity (0.0005% of nitrogen) is necessary to get the results corresponding with the experimental data available in literature. With the help of the model constructed, the dynamics of a homogeneous barrier discharge at various external parameters is studied. It is possible to obtain a glow mode and a multi-peak Townsend mode of the barrier discharge. Both of them are observed in experiment. The number of peaks in the Townsend mode depends on the value of the electron desorption current. The calculated discharge characteristics agree well with the experimental results available in literature.

GTP 78 Analysis of the radial instability of a barrier discharge in nitrogen YU.B. GOLUBOVSKII, V.A. MAIOROV, *St. Petersburg State University, Russia* J. BEHNKE, J.F. BEHNKE, *Ernst-Moritz-Arndt University, Institute of Physics, Domstrasse 10a, D-17487 Greifswald, Germany* The evolution of a small gaussian-like radial perturbation in a homogeneous barrier discharge in nitrogen is studied with the help of the two-dimensional fluid model. The external voltage is chosen to be linearly increasing with time to simulate the phase of field growth in real discharge. This simple model allows to obtain a simple criterion of the discharge instability. Namely, the Townsend mode of a discharge is always stable; the evolution of the perturbation consists of damped oscillations. A perturbation of any radius become unstable simultaneously with the transition from Townsend to glow mode.

GTP 79 Simulations of Cold Atmospheric Plasmas VLADIMIR KOLOBOV, DEBASIS SENGUPTA, ROBERT ARSLANBEKOV, *CFD Research Corp.* Non-equilibrium (cold) atmospheric pressure plasmas have recently been generated in a variety of gases in dielectric barrier discharges, hollow cathode discharges, dielectric plate discharges, etc. Operating regimes for the existence of cold plasma under different conditions are not totally clear. In this work, we will report on simulations of atmospheric pressure non-equilibrium plasmas in Helium and Nitrogen for different discharge geometries. We shall analyze effects of driving frequency and discharge geometry on plasma characteristics. Electron kinetics and the influence of non-Maxwellian electron energy distribution function on the plasma chemistry and discharge maintenance will be investigated using a deterministic Boltzmann solver. Comparison with available experimental data will be presented.

GTP 80 Influence of O₂ Addition on Discharge Properties in Xe Dielectric Barrier Discharges AKINORI ODA, TAKASHI KIMURA, *Nagoya Institute of Technology, 466-8555, Japan* The influence of O₂ addition on discharge properties of Xe dielectric barrier discharges at the total pressure of 40 kPa was investigated using one-dimensional fluid model. The model consists of the continuity equations for 7 charged species and 14 neutrals, the electron energy balance equation and Poisson's equation. The discharges were produced between the dielectrics with 2.0 mm thickness and dielectric constant of 4 in the discharge gap of 4.0 mm, by applying the sinusoidal voltage with amplitude of 4.8 kV and frequency of 100 kHz to the metallic electrodes. With increasing in mixture ratio(r_{O_2}) of O₂ up to 1 %, the efficiency of $h\nu(172 \text{ nm})$ emission from Xe₂^{*} rapidly decreased from 50 % ($r_{\text{O}_2} = 0 \%$)

to 22 % ($r_{O_2} = 1$ %), because the loss of $Xe^*(^3P_2)$, which is a precursor of Xe_2^* , drastically increased due to the de-excitation collisions between $Xe^*(^3P_2)$ and O_2 . For $r_{O_2} \geq 1$ %, the r_{O_2} dependence of discharge properties was weak. This work was partially supported by Grant-in-Aid from Japan Society for the Promotion of Science.

GTP 81 Over atmospheric pressure flowing afterglow MIHAI GANCIU, *National Institute for Laser, Plasma and Radiation Physics, Institute of Atomic Physics, Bucharest, Romania* JOHANNES ORPHAL, MICHEL VERVLOET, *Photophysique Molculaire, Universit Paris-Sud, Orsay, France* ANNE-MARIE POINTU, MICHEL TOUZEAU, *Laboratoire de Physique des Gaz et des Plasmas, Universit Paris-Sud, Orsay, France* FRENCH RESEARCH MINISTRY PPF COLLABORATION A Tabletop discharge * created above atmospheric pressure in a N_2 gas flow, uses some 10 kV very fast high voltage pulses applied between needle electrodes with some 10 kHz repetition rate. It is followed by a post-discharge, in a plastic tube with 6-mm internal diameter. Adjusting the flow and the repetition rate, the post-discharge exhibits a surprisingly long size, 9-10 m, as shown by the tube fluorescence. Preliminary spectroscopic measurements demonstrate that fluorescence is due to internal gas excited molecules (CN and NH) that are locally created by active species interaction with organic impurities. The discharge emission spectrum evidences a high nitrogen atom production rate, much higher than attainable rate with a Dielectric Barrier Discharge with same applied voltage pulses. For small air quantities added in the post-discharge, spectrum exhibits rich UV range corresponding to NO excited states. Further studies will be devoted to the post-discharge kinetics and to possible applications to medical sterilization. *M. Ganciu, private communication

GTP 82 VUV Emission Characteristics of High-Pressure Microgap Discharge Excited by Microwave A. KONO, T. KANO, T. SUGIYAMA, *Nagoya University, Nagoya 464-8603, Japan* It was shown that a stable atmospheric-pressure nonthermal air plasma could be produced at a high density ($>10^{15} \text{cm}^{-3}$) in the microgap ($\sim 100 \mu\text{m}$) between two knife edge electrodes by using microwave excitation [Jpn. J. Appl. Phys. 40 (2001) L238]. In the present work, Ar_2 and Xe_2 excimer emission characteristics of the microgap discharge were studied. The apparatus was installed in a pressure chamber and the total gas pressure was varied from 0.5 to 2.5 atm. Admixture of He with Ar or Xe was necessary to obtain a uniform discharge extending along the electrode length. The Ar_2 emission ($\sim 130 \text{ nm}$) or Xe_2 emission ($\sim 170 \text{ nm}$) dominated in the optical emission in the VUV region, but their intensities depended only weakly on the microwave power as well as on the total pressure. To understand the reasons for the results and to increase the VUV emission intensity, measurements of the gas temperature, electron temperature and electron density are in progress, as well as a modification of the apparatus for introducing gas flow through the microgap.

GTP 83 Enhanced Plasma Lifetime of Air Plasmas Generated by Electron Beam Excitation ROBERT VIDMAR, *University of Nevada, Reno* KENNETH STALDER, *Stalder Technologies and Research* A kinetic model with an improved set of reaction rate coefficients for air constituents will be discussed. The model includes rates that vary with E/N for electron temperature, momentum transfer, three body attachment, singlet-delta formation, elec-

tron detachment from O_2^- , and ionization of O_2 . The electric field is assumed uniform and sustained either by external electrodes or return currents generated in an electron beam. Calculations show the plasma lifetime increases as E/N increases by reducing attachment, increasing detachment, and increasing ionization. Electric-field-free plasma lifetimes of 10-20 ns for air at sea level (depending on initial electron density) can be increased by a factor of almost 5 with an E/N of about $2 \times 10^{-16} \text{ volt cm}^2$. The plasma lifetime at altitudes of 30,000 feet corresponds to 60-100 ns without electric field and increases by a factor of 5-20 with an E/N of $5 \times 10^{-17} \text{ volt cm}^2$. The power to maintain these E/N values and to sustain a given level of plasma density will be discussed. This research is sponsored by the Air Force Research Laboratory, under agreement number F49620-01-1-0414.

GTP 84 Tantalum Etching with an Atmospheric Pressure Plasma Jet HILARY TESLOW, HANS HERRMANN, LOUIS ROSOCHA, *Los Alamos National Laboratory* The APPJ is a non-thermal, atmospheric-pressure, glow discharge. A feedgas, composed of an inert carrier gas (e.g., He) and small concentrations of additives (e.g., O_2 or CF_4), flows between closely spaced electrodes powered at 13.56 MHz rf in a coaxial or parallel plate arrangement. The plasma has $T_e \sim 2 \text{ eV}$ and $n_e \sim 10^{11} \text{ cm}^{-3}$. Electrons are not in thermal equilibrium with ions and neutrals: the electrons are "hot," while the overall gas temperature is quite "cold," typically 50-300 C. In the plasma, the gas is excited, dissociated or ionized by energetic electron impact. As the gas exits the discharge volume, ions and electrons are rapidly lost by recombination, leaving metastables (e.g. O_2^* , He^*) and radicals (e.g. O, F, OF, O_2F , CFO). These reactive species are then directed onto a surface to be processed. The APPJ has been developed for decontaminating nuclear, chemical, and biological agents. Atomic fluorine, and possibly other reactive species, can be used to convert actinides (e.g., U and Pu), into volatile fluorides (e.g., UF_6 , PuF_6) that can be trapped, resulting in significant volume reduction of radioactive waste. In this talk, we will present results on using Ta as a surrogate for Pu in He/ O_2 / CF_4 etching plasmas. Results of experimental measurements of Ta etch rates for various gas mixtures and plasma jet standoff distance will be compared with plasma chemistry modeling of the concentrations of several active species produced in the plasma.

GTP 85 THERMAL PLASMAS AND ARCS

GTP 86 High Pressure Discharges with Hydrodynamically Imposed Stability and Reduced Power Requirements N.H. BROOKS, *General Atomics* T.H. JENSEN, *General Atomics* C.P. MOELLER, *General Atomics* High pressure discharges with long, straight plasma columns have been formed in open-ended and sealed systems, utilizing rotation of the confinement envelope to generate a rigid rotor flow of the gas inside. With the externally imposed stability conferred by this technique, a one-meter-long, electric arc in argon at atmospheric pressure has been sustained in steady-state with 1 A of current and only 5 W/cm of input power.

In this argon arc, heat conduction to the wall is reduced to that arising from collisional processes alone. In radiatively dominated discharges, exemplified by a commercial medium-pressure, mercury-vapor arc lamp, rotational stabilization leads to a near-linear relationship between the cross sectional area of the plasma column and the arc current. Model calculations duplicate the observed experimental scaling. Suitability of the technique to electrodeless discharges as well as electroal ones, has been demonstrated by operation of a microwave torch at 2.45 GHz and rf input powers up to 3 kW.

GTP 87 Influence of plasma cooling on the anode fall in anode region of the arc discharge DENIS GLOUCHKOV, *Ruhr-Universitaet-Bochum* VLADIMIR IVANOV, K.N. KOSHELEV, ISAN K.-U. RIEMANN, *Ruhr-Universitaet-Bochum* In contrast to the cathode, the anode plays apparently no vital role in the discharge operation. There is, however, a serious difficulty to produce a sufficient number of ions in the anode region. This difficulty is enhanced by the cooling effect of the anode resulting in a decrease of the electron temperature. Actually, this difficulty might be reduced by a constriction of the discharge and a corresponding enhancement of the electrical field. This enhanced field gives a positive contribution to anode fall. We investigate this problem by a 2-fluid quasi-2D model of the plasma radial energy transport with an axial heat loss component.

GTP 88 Prediction of liquid spray evaporation in RF inductively coupled plasmas Y. SHAN, J. MOSTAGHIMI, *Centre for Advanced Coating Technologies, University of Toronto* In some chemical vapor deposition applications using high pressure radio-frequency inductively coupled plasmas or plasma jets, precursors are introduced via a liquid spray. Understanding evaporation and dissociation of the spray is important in the deposition process. We present a new model for liquid sprays injected into radio frequency inductively coupled plasmas (rf-ICPs). The model is used to study the thermal and dynamic behavior of liquid spray. The model considers the evolution of the spray equation as the liquid spray travels through the discharge. The spray is comprised of many thousands of single liquid droplets. To calculate the mass, momentum and energy exchange between the gas and the spray, we consider the evolution of the spray distribution function and predict droplet sizes, velocities, and temperatures. Droplet collision and breakup also were considered. The spray equation was solved using the Monte Carlo method and discrete particle method by sampling randomly from assumed probability distributions that govern droplet properties at injection and droplet behavior after injection. For plasma, the time-dependent equations for the conservation of mass, momentum and energy, along with Maxwell's equations were solved numerically. The coupling source terms were calculated by summing the rates of change of mass, momentum, and energy of all droplets. Effects of liquid spray on plasma gas were studied for the injection of water spray into a typical rf-ICP torch. Results show that droplet's properties (such as spray flow rates droplet sizes distribution, injection velocity and angle of injection cone) have significant effects on plasma fields.

GTP 89 Effect of Nozzle Length on Arc Attachment and Heat Transfer on The Anode in A Transferred Plasma Torch for Waste Melting Process CHAN MIN LEE, SHIN IL CHOI, SOO SEOK CHOI, SANG HEE HONG, *Seoul National University, Seoul, Korea* The effects of nozzle length on arc attachment and heat transfer on a water-cooled copper anode plate in a transferred arc plasma torch for its application to melting and vitrification of

solid wastes are discussed on the basis of experimental investigations. In the previous study¹, the input power fractions to the anode is very rapidly decreased with increasing the arc length in a torch of short nozzle type compared to one of long nozzle type. In the present work, different modes of the arc attachment are experimentally identified by measuring arc voltage fluctuations and arc column images with a CCD camera. The different features of heat transfer rate obtained by the torch nozzle type are explained by its correlation with the arc anode attachment modes. In addition, the arc length ranges maintaining a diffuse mode according to arc current and gas flow rate are compared for the two types of plasma torches.

¹M. Hur, T. H. Hwang, W. T. Ju, C. M. Lee, and S. H. Hong, *Thin Solid Films* **390** (2001) 186.

GTP 90 Development of a transferred plasma torch for the efficient vitrification treatment for hazardous wastes MIN HUR, *Department of Mechanical Engineering, University of Minnesota, 111 Church Street Southeast, Minneapolis, Minnesota 55455* CHAN-MIN LEE, SANG-HEE HONG, *Department of Nuclear Engineering, Seoul National University, San 56-2 Shilim-dong Gwanak-gu Seoul, Korea, 151-744* A transferred plasma torch with rod type cathode has been designed and fabricated with six different cathode-nozzle arrangements to determine an optimum torch structure for the efficient vitrification process. Numerical results show that not only the operating conditions, such as input current, gas flow rate, and arc length, but also the design variables like nozzle diameter and nozzle length give considerable influences on the argon plasma temperature and velocity generated by the transferred torch. In the measurements of temporal fluctuations of arc voltage, the arc discharge is found to become unstable by lowering input current and increasing arc length. Moreover, the torch with a long nozzle tends to play a better role in maintaining the stable arc than that with a short nozzle under the same operating conditions. The measured results of the fraction of input power transferred to the waste anode reveal that the fraction decreases with gas flow rate, but is hardly influenced by the input current. The higher fraction of transferred power is achievable by the torch with a long nozzle compared with the torch with a short one. The thermal plasma temperatures are measured by using the optical emission spectroscopy based on the absolute intensities of ArI line. Good agreement is obtained between the measured and calculated results of the plasma temperature and heat quantity transferred to the anode, which verifies the accuracy of the calculation. Finally, a vitrification system adopting the transferred torch with a long nozzle is set up and experimental tests for vitrification treatment are carried out.

GTP 91 ATMOSPHERIC PLASMA CHEMISTRY

GTP 92 Decomposition of Carbon Dioxide with Aim to Produce Oxygen on Mars T. DINH, S. POPOVIC, L. VUSKOVIC, *Department of Physics, Old Dominion U., Norfolk, VA 23529* Decomposition of CO₂ was studied in a capacitively coupled radio frequency discharge. The experiment was performed in a mixture similar to Mars atmosphere with 95% of CO₂ at gas pressure of 5-7 Torr and a low discharge power regime. Since the main

mechanism of CO₂ decomposition process is the electron impact dissociation collisions, the rate of process is directly influenced by the electron density, N_e, the concentration of CO₂, and the reduced electric field, E/N. A self-consistent model was established to describe the CO₂ decomposition process based on these parameters. The model gave a description from microscopic processes of electron transport coefficients to macroscopic processes of gas phase chemical kinetics. The validity of the model was successfully verified by comparing the numerical results with the experimental data. The discharge characteristics such as T_e, N_e, and E/N, were determined by using the Langmuir probe technique, while the discharge temperature, T_g, was determined by using the CO rotational temperature that was obtained from the CO rotational emission spectrum, and compared with results obtained from the thermocouple measurements. The steady-state gas composition was measured using a quadrupole mass spectrometer. Measurement of gas composition in the discharge condition was within 5% of the prediction from the model. The results present a foundation for O₂ extraction *in situ* on Mars or CO₂ reduction in the industry.

GTP 93 Ambient non-thermal plasma for metal surface treatment* PRASAD NUAMATHA, *Electrical Engineering, Southern Illinois University* BIJAN PASHAIE, *Southeast Missouri University* SHIRSHAK DHALI, *Electrical Engineering, Southern Illinois University* BAKUL DAVE, *Chemistry, Southern Illinois University* Atmospheric pressure discharge in Argon/Hydrogen and Argon/Oxygen mixture is used to clean metal surfaces prior to applying coating. Dielectric barrier discharges

driven by low frequency (4 kHz) and RF (13.45 MHz) are used for the treatment. Plasma treatment removes organic contaminants from the surface of the steel and could provide an alternative to chemical cleaning. Peel tests indicate that Argon/Hydrogen plasma produces the strongest coatings. This would suggest that hydrogen plays a role in etching the surface of the metal. XPS results of surfaces coated with adhesives show that plasma treatment is capable of removing ester like compounds without the need for chemicals. The effect of both oxidizing and reducing atmosphere will be discussed.

*Supported by the National Science Foundation

GTP 94 Ozone production by bent tip hollow needles to plate electrical discharge at atmospheric pressure VITEZSLAV KRIHA, *Czech Technical University, Faculty of Electrical Engineering, Dep. of Physics* The ozone production is studied in a atmospheric pressure non-thermal plasma source with a plate anode and a cathode consisting of hollow needles, through which air is flown. If the tips of the needles are cut obliquely only, this results in an asymmetric flow pattern that changes with the distance between the needles, however, the discharge burns mostly outside of the direct flow from each needle. Additional bend of the tips of the needles prevents overheating of the tips and, from the other side, it enhances the direct flow-discharge interaction. Concentrations of ozone as functions of needles diameters and positions, discharge currents and flow rates are discussed in presented paper.

SESSION HT1: PLASMA PROCESSING

Tuesday afternoon, 15 October 2002; North Forum, Millennium Hotel at 15:30; M. Hori, Nagoya University, presiding

Invited Papers

15:30

HT1 1 Fabrication of planar waveguides using PECVD/RIE.

ROD BOSWELL, *Australian National University*

Existing optical fibre and fibre-device fabrication techniques have been complemented recently by the development of new processes for the fabrication of planar optical waveguides and devices. These processes rely on new forms of plasma reactors and diagnostic systems which allow in-situ control of optical parameters such as refractive index. Recent technical developments in the micro-electronics industry now allow the fabrication of very compact and highly complex optical circuitry which can be produced on a single photonic chip. They also offer the potential to integrate photonic devices with semiconductor sources and detectors to realise a compact, hybrid photonic-optoelectronic chip, complete with fibre pig-tailing. Because of their compactness and potential low cost, these types of photonic chips are attractive components for future high-capacity optical telecommunications and other networks now being planned. This paper presents the general techniques used in the plasma processing of thin films of silicate glasses including Plasma Enhanced Chemical and Plasma Etching (RIE).

Contributed Papers

16:00

HT1 2 Pulsed two-frequency capacitively coupled plasma simulation with H₂/N₂ mixtures for the etching of low-k materials

C.H. SHON, T. MAKABE, *Keio University at Yokohama, Japan* As the critical dimension of integrated circuit is scaled down, the resistance-capacitance (RC) delay of signals through interconnection materials becomes important. As a solution, the

new materials like Cu and low-k dielectric polymers have been used to reduce the signal delay in interconnect. As a result, low-k materials etching becomes a big issue in the plasma etching process. In this research, we present the simulation results of a pulsed two-frequency capacitively coupled plasma (2f-CCP)[1,2] based on relaxation continuum (RCT) model[3,4] in H₂/N₂ mixtures. The electrons, ions of each gas and NH_x radicals are followed in the model. The characteristics of a pulsed plasma are investigated. In addition, the flux of ions and radicals toward the biased substrate which has great importance in etching process is also dis-

cussed. sep = -1mm [[1]] T.Fujita and T.Makabe, *Plasma Sources Science and Technol.* **11**, 142(2002). [[2]] K.Maeshige, G.Washio, T.Yagisawa and T.Makabe, *J.Appl.Phys.* **91**, 9494(2002). [[3]] K.Okazaki, T.Makabe and Y.Yamaguchi, *Appl.Phys.Lett.* **54**, 1742(1989). [[4]] T.Makabe, N.Nakano and Y.Yamaguchi, *Phys. Rev. A* **45**, 2520(1992).

16:15

HT1 3 Ion Energy Control for Selective Etching of Low-k Dielectrics* RARDCHAWADEE SILAPUNT, *University of Wisconsin-Madison* AMY WENDT, *University of Wisconsin-Madison* Organosilicate glass (OSG) is a low-k dielectric material under development for high speed interconnects in integrated circuit manufacturing. Selective etching of OSG over etch stop layers, SiC and SiN, has proven challenging. The energy of ions bombarding the substrate has been shown to play an important role in etch selectivity, and improving ion energy control may enable more selective etching. However, the conventional sinusoidal substrate bias voltage waveform leads to a broad ion energy distribution (IED), allowing control only over average ion energy. A narrow IED can significantly enhance selectivity, when the ions have energy above the etching threshold energy of one material, but below that of the other. We have applied a technique for producing a narrow IED to improve OSG etch selectivity. This method replaces the sinusoidal substrate bias voltage waveform with a specially tailored waveform consisting of a short voltage spike in combination with longer periods of constant voltage, producing a nearly constant voltage drop across the substrate sheath. Experiments in a helicon plasma with a $C_4F_8/Ar/N_2$ gas mixture show that with the tailored bias voltage waveform, infinite selectivity is possible at reasonable etch rates. A comparison between tailored and sinusoidal waveforms shows significantly different etch rates for some process conditions, and comparable etch rates for others. Basic mechanisms will be discussed.

*Supported by SRC (TI custom funding)

16:30

HT1 4 Integrated Reactor and Feature Scale Plasma Processing Simulation Tool J. VERNON COLE, VLADIMIR I. KOLOBOV, J. C. SHEU, *CFD Research Corporation* We will present a computer aided process design environment for plasma-enhanced semiconductor fabrication steps. This environment includes the CFD-ACE+ reactor scale plasma simulation capability, with a Monte-Carlo transport option for ions and energetic neutrals. Both continuum and Monte-Carlo transport simulations are coupled with sheath models to provide the energy and angular distributions needed for feature scale simulation of the process. Fluxes of neutral and ionic species, as well as the energy and angular distributions, are passed automatically to a profile evolution simulator which predicts the process results within two or three dimensional feature geometries using a level set algorithm for surface movement. Integrated analysis of the effects of reactor design and process conditions on the resulting feature evolution during etching will be used to demonstrate the application of this process analysis tool.

16:45

HT1 5 ICP Etching of Tantalum Nitride using Cl₂, BCl₃ and CF₄ E.D. LUCKOWSKI, M.V. RAYMOND, D.R. ROBERTS, A. MARTINEZ, B. STEMILE, C.T. HAPP, S. STRAUB, T.P. REMMEL, S. KALPAT, M. SADD, R. RAMPRASAD, C.C. BARRON, M. MILLER, P. ELLAPPAN, P. ZURCHER, *APDER, Digital DNA Laboratories, Motorola Semiconductor Products Sector, 3501 Ed Bluestein Blvd, Austin, TX 78721* Tantalum nitride (TaN) is becoming an increasingly common material in semiconductor fabrication, finding a variety of uses such as: metal gates in CMOS technology, electrode materials for capacitors and precision thin film resistors. In patterning TaN films, redeposition of non-volatile etch by-products at the edge of a pattern generates undesirable topography (etch veils) that requires a separate plasma or wet chemical step for removal (deveil). Because deveil processes can have a negative impact on underlying films, it is important to select an etch process whereby sidewall deposits are minimized. We present a study of veil formation during patterned etch of TaN, where the etch terminates on different dielectrics and where different hardmask materials are used. In addition, we present TaN etch rate and selectivity to various materials as a function of processing conditions using Cl₂, CF₄, and BCl₃ gases in an ICP reactor.

17:00

HT1 6 Response of CHARM-2 Wafers and Surface Potential Measurements to VUV* J.L. LAUER, J.L. SHOHET, R.W. HANSEN, *Univ. of Wisconsin-Madison* During plasma processing, UV and VUV radiation are present, but their effects on gate-oxide damage, and damage to dielectrics in general are difficult to separate from those due to charged particle flux. To eliminate particle flux, unpatterned oxide-coated and Charm-2 wafers were exposed to UV/VUV at the UW-Madison synchrotron. The effects of UV/VUV were measured using two techniques: (1) surface potential and (2) EEPROMs (Charm-2 Wafers). Also, current flowing to the wafer and the substrate voltage were monitored. Both techniques showed positive charge appearing on the surfaces of dielectrics and conductors during VUV exposure. The UV monitors on Charm-2 wafers did not respond to VUV, but their charge monitors indicated positive charge instead. Thus, the results from both plasma-damage measurement techniques must be analyzed carefully, especially in situations where VUV generation is important, such as in processing plasmas.

*The authors thank W. A. Lukaszek of Wafer Charging Monitors and J. Hu of LSI for the loan of the Charm-2 wafers and the analysis. This work was supported in part by the National Science Foundation under grant DMR-0084402.

17:15

HT1 7 Etch By-Products in Plasma Etching MATTHEW T. RADTKE, *University of California-Berkeley* J.W. COBURN, *University of California-Berkeley* DAVID B. GRAVES, *University of California-Berkeley* Etch byproducts commonly play a major role in plasma composition, influencing etch rate, anisotropy, critical dimension control, and selectivity. Environmental implications associated with the etching process and subsequent chamber cleans are also a concern for new materials. In this work, experimental diagnostics were used to study silicon etch byproduct chemistry in Cl₂/O₂ plasmas as a model case. We report studies using an inductively coupled plasma reactor equipped with a

cooled, rf-biased chuck, a downstream FTIR spectrometer, a quartz crystal microbalance, a Langmuir probe, an ion flux wall probe, an ion mass spectrometer, a separate threshold ionization mass spectrometer for neutral radical detection, and an optical emission spectrometer. Neutral mass spectrometer measurements in pure SiCl_4 were used to measure the SiCl_4 electron impact

direct ionization cross section and dissociative ionization thresholds for SiCl_x^+ ions. Ion and neutral mass spectrometry were used to measure plasma composition in order to demonstrate the relative importance of etch byproducts. Specie wall fluxes were then calculated and compared with in-situ wall deposition and ex-situ XPS measurements to study the wall deposition mechanism.

SESSION HT2: BIOLOGICAL AND EMERGING APPLICATIONS OF PLASMAS

Tuesday afternoon, 15 October 2002; Center Forum, Millennium Hotel at 15:30; S. Popovic, Old Dominion University, presiding

Invited Papers

15:30

HT2 1 Plasma assisted chemical micropatterning of polymeric biomaterials.

ANDREAS OHL, *Institut für Niedertemperatur-Plasmaphysik, Greifswald, Germany*

In recent years a number of micro-lithographic methods received growing attention in biomedical research and technology which enable chemical micropatterning, i.e. the creation of patterns of chemical bond properties on flat surfaces. It was shown, that this way it is possible to control the attachment of biomolecules and living cells on surfaces in prescribed microscopic structures which are similar to e.g. microscopic tissue structures or biomolecule assemblies. Gas discharge plasmas are well known to exhibit distinct advantages for biomaterials surface modification, especially since most biomaterials are polymers. Different plasma based surface modification procedures are known which allow to improve attachment as well as to prevent this. Therefore, it suggests itself to investigate the potential of plasma processes for the purpose of chemical micropatterning. Here, an overview over existing experimental approaches to this subject is given. Results of investigations which were aimed at largely plasma based processes are discussed in detail. The basic process in these investigations consists of two plasma steps. First, the whole polymer surface is modified by an ammonia plasma treatment to get improved attachment. Then, a hydrogen plasma which causes a strongly reduced attachment surface is applied to surface regions that were selected by a micromasking technology. Well defined processing conditions are essential, in particular for the ammonia plasma process. The present state of plasma processes to generate functional surfaces of controlled amino group density is discussed. In summary plasma assisted chemical micropatterning appears to be a rather versatile, universal method with respect to different materials and applications.

16:00

HT2 2 Application of Plasma Technology in the Life Sciences.

A. G. SHARD, *University of Sheffield, Department of Engineering Materials*

This paper explores the versatility of plasma polymerization in the fabrication of surfaces for use in the Life Sciences and Tissue Engineering, highlighting three successful applications of plasma polymerized surfaces. 1. Plasma polymerized acrylic acid surfaces have been used as substrates for the culture and delivery of keratinocytes (skin cells) to chronic wounds. In proof of concept studies weekly delivery of keratinocytes have promoted healing in previously non-healing wounds. These include diabetic foot ulcers and wounds where skin grafts would normally be considered, but were contra-indicated. 2. Surface chemical patterning on the micrometer scale-length, by use of pre-fabricated masks, has been used to control the spatial binding of proteins and cells. This technology makes possible a significant reduction in size of biological assays, reducing the amount of material (e.g. antibody) or cells required. 3. Surface chemical potential gradients, from a few tens of micrometers to a few centimeters, have been fabricated by "plasma writing," a technique currently being developed in Sheffield. These gradients are being developed to separate mixtures of biomolecules or cells.

Contributed Papers

16:30

HT2 3 Electrosurgical Plasma Discharges K. R. STALDER, *Stalder Technologies and Research* J. WOLOSZKO, *ArthroCare Corp.* Electrosurgical instruments employing plasmas to volumetrically ablate tissue are now enjoying widespread use in medical applications. We have studied several commercially available instruments in which luminous plasma discharges are formed near electrodes immersed in saline solutions when sufficiently large amplitude bipolar voltage waveforms are applied. Different aqueous salt solutions have been investigated, including isotonic NaCl

solution as well as solutions of KCl, and BaCl_2 . With strong driving voltage applied, a vapor layer is formed as well as visible and UV optical emissions. Spectroscopic measurements reveal the predominant emissions are from the low ionization potential salt species, but significant emissions from electron impact dissociated water fragments such as OH and H-atoms also are observed. The emissions also coincide with negative bias on the active electrode. These optical emissions are consistent with an electron density of about 10^{12}cm^{-3} and an electron temperature of about 4 eV. Experimental results and model calculations of the vapor layer formation process and plasma formation in the high-field region will be discussed.

16:45

HT2 4 Biological decontamination by oxygen plasma A.A. BOL'SHAKOV,* B.A. CRUDEN,† R. MOGUL, M.V.V.S. RAO², S.P. SHARMA, M. MEYYAPPAN, *NASA Ames Research Center, Moffett Field, CA 94035* Oxygen plasma sustained at 13.56 MHz in a standardized reactor with a planar induction coil was used for biological sterilization experiments. Optical emission and mass spectrometry was applied for detection of excited species and ion energy/flux analysis. A plasma mode transition in the ranges of 13-67 Pa and 100-330 W was observed. At higher pressure and lower power, the plasma was in a dim mode (primarily stray capacitive coupling). A primarily inductive bright mode was

attained at lower pressure and higher power. This transition was identified using combined diagnostics and then recognized by emission spectroscopy on a scaled down reactor for biological degradation tests. Plasmid DNA removal was 25% more efficient in the bright versus dim mode at the same power. The fast degradation was attributed to photo- and ion-assisted etching by oxygen atoms and perhaps O₂ metastable molecules. Volatilization rates of the decomposition products (CO₂, CO, N₂, OH, H) evolving from the *Deinococcus radiodurans* microbe and polypeptide samples were compared.

*NRC/NASA Senior Research Associate

†Eloret Corp.

Invited Papers

17:00

HT2 5 Modulated plasma deposition of super hydrophobic fluorinated coatings.*

PIETRO FAVIA, *Department of Chemistry, University of Bari and Istituto di Metodologie Inorganiche e dei Plasmi (IMIP)-CNR, Bari*

Modulated (pulsed) RF glow discharges fed with unsaturated fluorocarbons originate often films with superior characteristics and remarkable monomer structure retention degree. Properties such as low dielectric constant, low friction coefficient, high flexibility and high hydrophobic character can be granted by such coatings, as well as applications in textiles, packaging, biomaterials, microelectronics and other fields [1-4]. Albeit the surface chemistry of fluorinated films has been extensively analysed, very few works deal with the investigation of the plasma phase and of the material morphology and crystalline. We present our last results on the plasma deposition of coatings from modulated glow discharges fed with tetrafluoroethylene. Period and Duty Cycle (DC) have been changed in the range 20-200 ms and 2-100%, respectively. Chemical composition and structure of the coatings were determined by means of XPS, SIMS, FT-IR and XRD measurements; SEM and AFM allowed morphological investigations. The diagnostics of the gas phase was carried out by time resolved (TR) OES [5] and by IR-AS diagnostics [6]. At low DC (< 10%) a unique morphology is observed at the surface of the films, in form of ribbon-like features many microns long and hundreds of nanometers wide, whose surface density increases at lower DC values. XPS has been used to determine the surface fluorine to carbon ratio of the coatings; best-fitting procedures of the C1s signals have been also carried out. XPS and SIMS results show a high F/C ratio and a chemical structure close to conventional PTFE for samples with ribbon-like features. Due to the combined presence of structures and high fluorination degree, structured surfaces revealed very high hydrophobic character (Water Contact Angle > 150°). XRD patterns of the structured coatings exhibited a diffraction peak at $2\theta = 18^\circ$, characteristic of crystalline PTFE [4, 6]; this finding, and the presence of the structures, open questions about the deposition mechanism of such unique materials, which still need to be rationalized. In order to understand the deposition mechanism of unstructured and structured coatings, spectroscopic diagnostics of the plasma phase has been carried out by TR-OES and IR-AS. TR-OES results reveals only CF₂ emitting radicals ($A16B_1 - X^1A_1 230 - 340nm$; $^3B_1 - ^1A_1 340 - 450 nm$ systems), whose evolution trends during time on of the discharge are clearly dependent on the DC value. TR-OES allowed to distinguish between two different deposition regimes which give origin (low DC) or not (high DC) to structured coatings, respectively. References [1] V. Panchalingam, B. Poon, H.H. Huo, C.R. Savage, R.B. Timmons, R.C. Eberhart; *J. Biomat. Sci. Polym. Ed.* **5**, (1993) 131, [2] S.J. Limb, K.K. Gleason, D.J. Edell, E.F. Gleason; *J. Vac. Sci. Tech. A* **15**, (1997) 1814, [3] S.R. Coulson, I.S. Woodward, S.A. Brewer, C. Willis, J.P.S. Badyal; *Chem. Mater.* **12**, (2000) 2031, [4] S.J. Limb, K.K.S. Lau, D.J. Edell, E.F. Gleason, K.K. Gleason; *Plasmas and Polymers* **4**, (1999) 21 [5] M. Creatore, F. Palumbo, R. d'Agostino P. Fayet - *Surface & Coatings Technology* **142**, (2001) 163 [6] G. Cicala, A. Milella, F. Palumbo, P. Favia and R. d'Agostino *Appl. Phys. Lett.* (submitted).

*In collaboration with: Fabio Palumbo, Grazia Cicala, Istituto di Metodologie Inorganiche e dei Plasmi (IMIP) - CNR, Bari; Antonella Milella, Riccardo d'Agostino, Department of Chemistry, University of Bari.

SESSION KW: GEC FOUNDATION TALK

Wednesday morning, 16 October 2002; North/Center Forum, Millennium Hotel at 8:15; Joachim Heberlein, University of Minnesota, presiding

8:15**KW 1 GEC Foundation Talk: What do we know about the anode region of high-intensity arcs?**

EMIL PFENDER, *University of Minnesota*

Over the past 20 years, the properties and the behavior of the anode region in atmospheric pressure high-intensity arcs attracted increasing attention, because of their importance for a number of arc applications ranging from well-established technologies such as arc welding and cutting to new developments in plasma spraying and plasma chemical vapor deposition. The anode region of an arc, defined as the region that includes the anode surface, the anode sheath or anode space charge zone immediately in front of the anode, and the anode boundary layer, is characterized by complex interactions of fluid dynamic, electric, magnetic and thermal fields. This is the main reason for the rather poor understanding of this region for many years. After a brief tutorial, experimental as well as analytical studies reported over the past 20 years will be summarized with emphasis on some unusual effects such as negative anode falls which have been theoretically predicted and experimentally verified. A similar argument applies to the strong deviations from kinetic ($T_e > T_h$) as well as from chemical equilibrium in the anode boundary layer. The thickness and the properties of the anode boundary layer are strongly affected by macroscopic flows that, in many cases, are induced by the arc itself. The effects of plasma flow fields interacting with the anode boundary layer will be discussed in detail, because of its importance for applications. The flow fields and the corresponding properties of the anode may determine the size of the anode arc root (constricted or diffuse) that, in turn, determines anode heat fluxes.

SESSION LW: APS ALLIS PRIZE TALK

Wednesday morning, 16 October 2002; North/Center Forum, Millennium Hotel at 10:00; Raymond Flannery, Georgia Institute of Technology, presiding

10:00**LW 1 Allis Prize Lecture: Gaseous Electronics Physics Inside.**

ALAN GARSCADDEN, *Propulsion Directorate Air Force Research Laboratory, WPAFB, OH and EAFB, CA*

I was fortunate to enjoy the advice of K. G. Emeleus during my graduate studies and for many years afterwards. He introduced me to the papers of Will Allis and later I was privileged to correspond with Professor Allis. At this time I had moved from the Queens university environment to work at a large Air Force base. There I have worked with a lot of smart people, including several who also come to the GEC each year to be refreshed and calibrated. A personal overview is presented on a few of the many roles that atomic, molecular and optical physics, including gaseous electronics, play in programs of the Air Force Research Laboratory and subsequently on AF systems and operations. While there have been misses, overall there have been many successes with impacts that provide more effective systems, as recent experiences have demonstrated. Some example studies, involving primarily electron collision physics, successful and unsuccessful in being chosen for application, are discussed.

SESSION NW1: DIAGNOSTICS OF REACTIVE PLASMAS

Wednesday afternoon, 16 October 2002

North Forum, Millennium Hotel at 13:15

Greg Hebner, Sandia National Laboratories, presiding

13:15

NW1 1 Submillimeter Absorption Spectroscopy of Fluorocarbon Plasmas ERIC BENCK, GUERMAN GOLUBIANTNIKOV, GERALD FRASER, DAVID PLUSQUELLIC, TIMOTHY KORTER, RICH LAVRICH, VYATCHESLAV BYCHKOV, *National Institute of Standards and Technology* Submillimeter (300 GHz to 1 THz) absorption spectroscopy is being developed as a diagnostic for measuring radical densities and temperatures in processing plasmas for microelectronics. Most molecules, radicals, and ions have transitions suitable for detection at these frequencies and the necessary spectroscopic data is available in the literature for determining the absolute radical densities. In addition, the narrow linewidths of < 10 kHz of these continuous-wave sources are suitable for measuring rotational, vibrational and translational temperatures of radicals. Initial measurements are being conducted with a backward-wave-oscillator (BWO) source and a liquid-H₂-cooled bolometer detector. Radical density measurements have been made in inductively and capacitively coupled GEC Reference Reactors. The influence of wafer coatings on plasma chemistry has been measured for several different fluorocarbon (C₄F₈, C₄F₆, and C₅F₈) / oxygen etching gas mixtures. In addition, a comparison of results obtained with the BWO and a new photomixer radiation source will be presented.

13:30

NW1 2 Neutral Heating and Neutral Temperature Measurement in Inductively Coupled Fluorocarbon Discharges BRETT CRUDEN,* DAVID HASH, M. V. V. S. RAO,† SURENDRA SHARMA, M. MEYYAPPAN, *NASA Ames Research Center* Over the past few years, large neutral temperatures (600-1500 K) have been measured in inductively coupled discharges. Maintaining these high temperatures requires significant power dissipation into neutral heating, thereby reducing the attainable electron density. Consequently, it becomes very important to characterize the neutral temperature in an inductively coupled plasma before performing a quantitative analysis. This paper will review work characterizing neutral heating phenomena as they pertain to inductively coupled fluorocarbon plasmas, including mechanisms, modeling, and experimental measurements. In addition, our results on optical characterization of neutral temperatures in CF₄ and CF₄/O₂/Ar mixtures will be presented. The disparity between different optical measurement techniques will be examined. Absorption techniques are shown to underpredict neutral temperature due to spatial averaging of temperatures. Temperature measurements through the fit of emission spectra are examined for several species. It is found that the temperature measurements can vary widely depending on the species chosen for measurement. Pressure dependencies of temperature indicate that some species are not well equilibrated with other species in the plasma.

*Eloret Corporation

†Eloret Corporation

13:45

NW1 3 Temperature effects on CF_x kinetics in a pulsed ICP in CF₄ JEAN-PAUL BOOTH, *LPTP, Ecole Polytechnique, France* HANA ABADA, *LPTP, Ecole Polytechnique, France* PASCAL CHABERT, *LPTP, Ecole Polytechnique, France* Laser Induced fluorescence (LIF) was used to determine axial profiles of CF and CF₂ density and gas temperature in an inductively-coupled plasma in CF₄ (2 to 33 mTorr). The gas temperature can reach 800 K in the reactor centre, causing considerable gas rarefaction at constant pressure. The steady-state CF and CF₂ density profiles (LIF signals corrected for gas temperature) are hollow. Even after allowing for thermo-diffusion, the net radical fluxes are away from the reactor surfaces (where they are produced) towards the reactor centre (where they are destroyed). In the post-discharge the gas cools in about a millisecond. The CF density drops rapidly due to gas-phase reactions, whereas the CF₂ density initially increases (by a factor of about 3) for the first millisecond, before decaying slowly. The mechanisms responsible for this initial increase will be discussed, including gas convection induced by gas cooling, chemical reactions and vibrational relaxation.

14:00

NW1 4 Temperature Mapping in CF₄ Plasmas using Planar Laser-Induced Fluorescence KRISTEN L. STEFFENS, *National Institute of Standards and Technology* MARK A. SOBOLEWSKI, *National Institute of Standards and Technology* Fluorocarbon plasmas are commonly used for dielectric etching. As model-based reactor design and process development become more prevalent, more data is needed for model validation. Spatial variations in translational temperatures can lead to spatial variations in gas density and reaction rates. Mapping of these temperature variations would provide useful information for modelers. In this work, 2-D temperature maps in CF₄ plasmas were measured in a capacitively-coupled GEC cell using planar laser-induced fluorescence (PLIF) of the CF radical. In PLIF the species is excited with a laser sheet and the fluorescence, imaged with an ICCD camera, is related to the radical density. For temperature mapping, multiple density maps were imaged, probing different CF rotational levels. The image intensities were used to calculate the rotational temperature of CF, which is expected to be in equilibrium with the plasma's translational temperature under these conditions. Temperatures ranging from 300 to 500 K were measured for pressures of 200 to 800 mTorr and powers of 10 to 30 W. Temperatures were lowest near the water-cooled electrodes and increased with power. At low pressures, plasmas were cooler in the center, becoming hotter and more radially uniform as pressure increased.

14:15

NW1 5 Measurement of hydrogen atom density in high-density CF₄/H₂ plasmas by (2+1)-photon laser-induced fluorescence spectroscopy K. SASAKI, M. OKAMOTO, K. KADOTA, *Department of Electronics, Nagoya University, Japan* The addition of H₂ is widely used for controlling the density ratio of CF_x radicals to F atoms in fluorocarbon plasmas. Although much effort has been concentrated on the diagnostics of CF_x radicals, the investigation on H atom density in fluorocarbon plasmas is insufficient. In the present work, we measured the distribution and the temporal variation of H atom density in high-density CF₄/H₂ plasmas by (2+1)-photon laser-induced fluorescence spectroscopy. The experiment was carried out in a pulsed helicon-wave plasma source. The instantaneous rf power, the discharge duration, and the repetition rate were 1 kW, 10 ms, and 5 Hz, respectively. The CF₄ pressure was fixed at 5 mTorr, and the partial pressure of H₂

was varied from 0 to 5 mTorr. After the partial pressure of H_2 was changed from 20% to 25%, the H atom density increased slowly during 100 minutes. The slow increase suggests that surface chemistry plays an important role in the determination of the gas-phase H atom density. When the feedstock gas was changed to pure CF_4 after sufficient discharge at an H_2 percentage of 50 %, we observed considerable amount of H atoms in the plasma. In addition, the H atom density in the region neighboring the chamber wall was higher than that in the plasma column. These results strongly suggest that hydrogenated fluorocarbon film deposited on the chamber wall was a source of H atoms.

14:30

NW1 6 Kinetics of $SiF_x(x=0-2)$ and SiF_4 molecule in RF 60MHz parallel-plate capacitively coupled plasma employing SiF_4 MASARU HORI, TAKAYUKI OHTA, KENICHIRO HARA, TOSHIO GOTO, *Dept. of Quantum Eng., Nagoya Univ., Japan* MASAHUMI ITO, *Dept. of Opto-Mechatronics Faculty of Systems Eng., Wakayama Univ., Japan* SATOSHI KAWAKAMI, *Tokyo Electron Tohoku Co. Ltd., Japan* NOBUO ISHII, *Central Research Lab., Tokyo Electron Co. Ltd., Japan* In the fabrication of ULSIs, SiF_4 based gases have been employed for the deposition of low-k thin films such as fluorine-doped silicon oxide and fluorine-doped silicon nitride. In this study, in order to clarify behaviours of species in RF 60MHz SiF_4 CCP, we have measured the spatial distribution of SiF_4 density using infrared diode laser absorption spectroscopy (IRLAS), SiF_2 and SiF densities using laser induced fluorescence (LIF). Si density was also measured by ultraviolet absorption spectroscopy (UVAS) using ring dye laser. The plasma was produced by RF 60MHz CCP employing SiF_4

gas. SiF_4 flow rate and the pressure were fixed at 90 sccm and 40 mTorr, respectively. SiF_2 density was increased with increasing electron density and decreased at electron densities above $1.2 \cdot 10^{11} \text{ cm}^{-3}$, while F, Si and SiF densities were increased. SiF_4 density was depleted at electron densities above $8.7 \cdot 10^{10} \text{ cm}^{-3}$, resulting in further dissociation of SiF_2 with electron impact. The kinetics of species in RF 60MHz SiF_4 plasma are discussed on the basis of measured results of densities of reactive species and electron, and electron temperature.

14:45

NW1 7 A Combined Diode Laser Absorption and Optical Emission Spectroscopic Studies of Free Radicals in $N_2/SiCl_4$ Discharges PENG LI, WAI YIP FAN, *Department of Chemistry, National University of Singapore, 3 Science Drive 3, Singapore, 117543* Infrared diode laser absorption and uv/visible optical emission spectroscopies have been applied to the study of transient species in the $N_2/SiCl_4$ dc plasmas which were used for growing SiN semiconductor films. Infrared absorption spectrum of SiN radical around 2017 cm^{-1} and emission spectrum of $SiCl_2$, $SiCl$, Si, Cl, N_2 and N_2^+ at uv/visible region were detected. The behaviour of these chemical species were studied with respect to the ratio of $N_2/SiCl_4$ and it was found that the highest concentration of SiN was obtained when the $N_2/SiCl_4$ ratio was around 10, at which point the concentrations of excited state $SiCl_2$, $SiCl$, Si, Cl and N_2 also reach the highest values. The electron impact dissociation of $SiCl_4$ is also essential in the growth of SiN film where higher concentrations of SiN radical were detected at higher electron densities.

SESSION NW2: THERMAL PLASMAS: LAMPS AND ELECTRODES

Wednesday afternoon, 16 October 2002; Center Forum, Millennium Hotel at 13:15; Vikas Midha, GE Research, presiding

Invited Papers

13:15

NW2 1 On the Physics of High Intensity Discharge Lamp Electrodes.*
JUERGEN MENDEL, *Ruhr-University of Bochum, Germany*

To optimize the electrodes of high intensity discharge (HID) lamps a detailed physical understanding of the interaction between the arc column and the cathode and anode has to be achieved. For this purpose a model lamp was developed in which a large variety of electrodes can be operated in noble gases at pressures up to 1 MPa. Separate values of the cathode and the anode fall are determined from Langmuir-probe measurements. Spatially resolved temperature distributions are measured pyrometrically along the electrodes. Their analysis yields the power fed into the electrodes. Relations are deduced between the electrode falls and the power removed by the electrodes from the power balances of the current transfer zones. Their outcomes are compared with the results of electrical measurements. In addition the electrodes and the plasma boundary layers in front of them are investigated by high speed photography, by spectroscopy and SEM after lamp operation. At the cathode at least three different modes of arc attachment are observed: a diffuse mode, a spot mode and a so called super spot mode. The diffuse mode which envelops the whole electrode tip is favored by high currents, low gas pressure and a poor electrode cooling, the spot mode by the opposite conditions. It attaches the cathodic end face in a small but very hot area of high current density. It is the starting point of a plasma jet which is propelled by self-magnetic forces. The super spot mode characterized by a very low cathode fall occurs on tiny electrode tips which may be formed during spot mode operation at a molten surface area. But also at the anode different though less pronounced modes of arc attachment occur. Comparison between detailed measurements and modelling shows that the ion balances in the electrode boundary layers are essential for an understanding of HID electrodes.

*Supported by the German BMBF, project No. 13N7763.

13:45

NW2 2 Physics and Chemistry of Ultra-High-Pressure Mercury Discharge Lamps.ULRICH HECHTFISCHER,* *Philips Research Laboratories, Weissshausstrasse 2, D-52066 Aachen, Germany*

In the last years Ultra-High-Pressure (UHP) mercury discharge lamps have gained increasing importance as a key-component of modern, light-weight LCD projectors. This is because UHP lamps are the only light sources combining high arc luminance ($> 1 \text{ Gcd/m}^2$) and long lifetime ($> 10,000$ hrs). The high luminance is a consequence of using highly pressurized (> 200 bar) mercury vapor as discharge medium at high power densities, e.g. 120W into an 1.2mm arc gap. This high Hg pressure is also causing a large amount of continuum radiation which leads to an improved color efficiency of the lamp spectrum. The electrode distance is kept stable during lifetime by a regenerative chemical cycle which uses oxygen and bromine to transport evaporated tungsten back to the electrodes. This cycle is keeping the quartz wall clean which is also advantageous for the thermal balance of the vessel. The compact, optimized discharge vessel is designed carefully to fulfil the various thermal requirements. This is the domain of modern HID lamp modeling tools solving the vessel's heat balance coupled to the discharge power balance including the effects of convection and radiation transport.

*E. Fischer, A. Koerber and T. Kruecken.

Contributed Papers

14:15

NW2 3 X-ray Absorption Imaging of High-Intensity Discharge Lamps Using Monochromatic Synchrotron Radiation*

JOHN J. CURRY, *National Institute of Standards and Technology, Gaithersburg, MD 20899* CRAIG J. SANSONETTI, *National Institute of Standards and Technology, Gaithersburg, MD 20899* ULRICH HECHTFISCHER, *Philips Research, Aachen, Germany* HELMAR G. ADLER, *Osram Sylvania, Beverly, MA 01915* We will report results from the imaging of Hg vapor in high-intensity discharge lamps using synchrotron radiation and digital detectors. These measurements extend previous work on x-ray absorption imaging in arc lamps using an x-ray tube and a passive phosphor image plate detector¹. The large x-ray flux obtained from the Advanced Photon Source (Argonne National Laboratory) combined with the electronic gating capabilities of an intensified charge-coupled device detector have allowed us to obtain time-resolved Hg distributions with high spatial resolution. Monochromatic synchrotron radiation improves the accuracy over what can be obtained with quasi-continuum radiation from an x-ray tube source. ¹J. J. Curry, M. Sakai, and J. E. Lawler, *Journal of Applied Physics* 84, 3066 (1998).

*Funded in part by the Advanced Light Source Research Consortium (ALITE) of the Electric Power Research Institute.

14:30

NW2 4 Self-consistent modeling of diffuse and spot modes on thermionic arc cathodes*

M. S. BENILOV, M. D. CUNHA, *Departamento de Física, Universidade da Madeira, Largo do Município, 9000 Funchal, Portugal* A model of the near-cathode layer in a plasma under a pressure of the order of one or several bars is reconsidered on the basis of recent theoretical and experimental results. It is found that a non-monotony of the dependence of the energy flux density on the surface temperature at fixed values of the near-cathode voltage drop is caused by one of the three mechanisms: overcoming of the increase of combined ion and plasma electron heating by the increase of thermionic cooling as the plasma approaches full ionization; non-monotony of the dependence of the ion current on the electron temperature which is caused by the deviation of the ion current from the diffusion value;

rapid increase of the plasma electron heating which is subsequently overcome by thermionic cooling. A closed description of the plasma-cathode interaction is obtained by numerically solving a nonlinear boundary-value problem governing the temperature distribution inside the cathode body. Results of numerical calculation of diffuse and spot modes are given in a wide range of arc currents and a general pattern of current-voltage characteristics is analyzed. The other questions addressed include properties of the solitary-spot mode, of a transition from the solitary-spot mode to a spot mode on a finite cathode, and of appropriate definitions of diffuse and spot modes.

*The work was supported by the projects 32411/99 of FCT and FEDER and NNE5/2001/282 of the EC and by the action COST 529 of the EC

14:45

NW2 5 Infrared emission in metal-halide arc lamps

D. J. SMITH, *Univ. of Wisconsin-Madison* G. A. BONVALLET, *Univ. of Wisconsin-Madison* J. E. LAWLER, *Univ. of Wisconsin-Madison* Spatially-resolved measurements of the visible and near infrared emission of a commercial metal-halide arc lamp (Sylvania Metalarc M250U) have been performed using a Fourier Transform IR spectrometer. The goal of the investigation is to identify and understand the IR losses from metal-halide lamps. Temperature profiles have been obtained using a Boltzmann analysis of the emission as a function of position and compared with the profile determined by analysis of self-reversed lines using Bartel's method. These results have also been compared with those obtained from a complementary study of a similar lamp, which employs absorption measurements using a synchrotron radiation source. Combined with IR emission measurements, this has allowed determination of the total power output from the near IR, which is principally due to emission on the $3d^2(^3F)4s^4F - 3d4s(^3D)4p^4F^o$ and $3d^2(^3F)4s^4F - 3d4s(^3D)4p^4D^o$ neutral atomic Scandium transitions, occurring in the range 2.2-2.5 microns.

SESSION QWP: POSTER SESSION II
 Wednesday evening, 16 October 2002
 Horizons/Satellites, Millennium Hotel at 19:15

QWP 1 ELECTRON, POSITRON AND PHOTON
 INTERACTIONS

QWP 2 Explicit demonstration of the slow convergence of the Bethe-Born theory for ionization¹ S. JONES, D. H. MADISON, *Laboratory for Atomic, Molecular and Optical Research and Physics Department, University of Missouri-Rolla, Rolla, MO 65409-0640* It is usually assumed that the first Born approximation (FBA) for electron-atom ionization becomes valid at sufficiently high impact energies for the fully differential cross section, at least for asymmetric collisions where the projectile suffers only a small energy loss and is scattered by only a small angle. Here we investigate this assumption quantitatively for ionization of hydrogen atoms.

¹Work supported by the NSF

QWP 3 Total and elastic cross sections of electron scattering from C₃H₄ isomers MINEO KIMURA, *Graduate School of Science and Engineering, Yamaguchi University* YAMAGUCHI UNIVERSITY TEAM Total and elastic cross sections of electron scattering from C₃H₄ isomers (allene and propyne) C. Makoche-kanwa, O. Sueoka and M. Kimura *Graduate School of Science and Engineering, Yamaguchi University, Ube 755-8611, Japan* Total cross sections (TCSs) for electron and positron scattering from C₃H₄ isomers (allene and propyne) have been determined by the linear transmission method in the energy range from 0.7 eV to 600 eV for positron and from 0.8 eV to 600 eV for electrons. Elastic cross sections for electron scattering from these isomers have also been measured by a crossed-beam experiment in the energy region of 1.5 - 100 eV. For electron scattering, both allene and propyne are found to possess sharp peaks due to resonance at around 3.6 eV and 8 eV for propyne and 2.5 eV and 11 eV for allene in TCSs. For positron scattering, both TCSs are found to be smaller in magnitude, and less eventful and smoother compared to the electron cases.

QWP 4 Resonant vibrational excitation of CO₂ by electron impact* THOMAS N. RESCIGNO, *LBNL/LLNL* C. WILLIAM MCCURDY, *LBNL/UC Davis* We present the results of a first-principles study of resonant excitation of the lowest Fermi dyad in CO₂ by low-energy electron impact. Slow electrons are captured by the target CO₂ molecule into a ²Π_u anion state. Upon bending, the degeneracy of the electronic state is lifted and the resonance splits into two non-degenerate states of ²A₁ and ²B₁ symmetry. The resonance surfaces and lifetimes are first extracted from the results of extensive ab initio fixed-nuclei variational calculations. The nuclear dynamics is then studied using multi-dimensional time-dependent wavepacket propagation techniques, taking into account the effects of both symmetric stretching and bending mo-

tions. These are the first ab initio studies to examine the effects of resonant vibrational excitation in multiple dimensions involving two complex electronic surfaces that are dynamically coupled by a non-adiabatic Coriolis interaction, similar to the Renner-Teller effect well-known in molecular spectroscopy.

*Work performed under the auspices of the US DOE by the University of California Lawrence Berkeley and Lawrence Livermore National Laboratories under contract Nos. DE-AC03-76SF00098 and W-7405-Eng-48, respectively.

QWP 5 Slow electron collisions with Na Rydberg atoms NAGESHA KANNADAGULI, KEITH B. MACADAM, *Department of Physics and Astronomy, University of Kentucky, Lexington, KY 40506, USA** Slow electron impact with Rydberg atoms leading to capture, ionization and inelastic processes such as *n*- and *ℓ*-change influence strongly the properties of plasmas of laboratory, astrophysical and technological interest. In this report, we present initial results on *n*- and *ℓ*-changing in Na Rydberg states (*n* = 22 - 40, *ℓ* = 0, 1 and 2) upon low energy e⁻ impact. In our experiments, Na atoms are excited by simultaneous yellow and blue nanosecond dye laser pulses. A magnetically collimated low energy electron beam impinges upon the cloud of these Na Rydberg atoms. After a few μs of electron exposure, the Rydberg atoms are sampled by state-selective field ionization (SFI). Population loss from the target state and gain in energetically close states are analyzed by comparing the results of an *electrons-on minus electrons-off* measurement with the initial SFI signal shapes of the interacting Rydberg states. Such experiments have been performed extensively with eV to keV positive-ion projectiles and fast e⁻s in this laboratory. Slow-e⁻ collisions with Rydberg atoms, however, have not been investigated before. We have also observed slow e⁻-impact ionization of the Na Rydberg atoms. These investigations are in progress.

*The authors thank M.J. Cavagnero, R.G. Rolfe and M. Ciocca for helpful discussions and assistance. This work was supported in part by NSF Grant No. PHY-9987954.

QWP 6 Elastic electron scattering from alkaline earth atoms MEHRDAD ADIBZADEH, CONSTANTINE THEODOSIU, *University of Toledo* NICHOLAS HARMON, *Wooster University* We present theoretical results for differential, total, and momentum transfer cross sections for the elastic scattering of electrons by alkaline earth atoms and the subsequent determination of the Sherman functions, for energies below 1 keV. Our work was motivated by our successful results for inert gases. We used a fully relativistic approach with explicit inclusion of electron exchange and core-polarization effects. Since there is little experimental information on the alkaline earth atoms, with the exception of barium, we used barium as a test case. Our barium differential cross section results are in good agreement with experimental data and the theoretical close coupling calculations. Based upon our thus developed approach and acquired experience, we provide a set of recommended differential, total, and momentum transfer cross sections and Sherman functions for elastic electron scattering from all alkaline earth atoms. We hope that this work will motivate more experimental and theoretical research on these elements.

QWP 7 Dissociation and Coulomb explosion of molecular hydrogen ions by one and two short laser pulses BERNOLD FEUERSTEIN, UWE THUMM, *Dept. of Physics, Kansas State University, Manhattan, KS 66506* We have investigated the interaction of 25 fs, 0.2 PW/cm², 780 nm laser pulses with H₂⁺ within a reduced dimensionality model, representing both, the nuclear

and electronic motion by one degree of freedom. We carefully adjusted adiabatic molecular electronic potentials to reproduce accurate 3D results for i) the known number of 19 bound vibration states in the electronic ground state and ii) the dipole oscillator strength over a large range of internuclear distances. We solve the time-dependent Schrödinger equation within a Crank-Nicholson split-operator scheme and "measure" the flux of emitted electrons and protons using a novel "virtual detector" approach. Our results reproduce the main features of measured kinetic-energy release spectra, support a "charge resonant enhanced" ionization mechanism, and allow us to clearly distinguish between molecular dissociation (MD) into different field-dressed final channels and fast, ionization-induced Coulomb explosion (CE). Two pulses with variable delay allow us to resolve in time the interesting interplay between MD and CE. B. Feuerstein and U. Thumm, to be published. *Supported in parts by DOE, NSF, and DFG.*

QWP 8 Low-Energy Electron Scattering from the Water Ion

A. E. OREL, *University of California, Davis Complex* Kohn variational calculations have been carried out on the low-energy electron scattering from the water ion. These calculations have been restricted to C_{2v} geometries. Scattering in all symmetries (A_1 , A_2 , B_1 and B_2) for both singlet and triplet spin states were considered. The elastic and excitation cross-sections and the eigenphase sum were calculated as a function of the O-H bond distance and bond angle. The eigenphase sum was fit to a Breit-Wigner form and the resonance parameters were abstracted. In each symmetry a number of core-excited state resonances, that is, Rydberg states converging to excited states of the water ion, were observed. One resonance was found to cross near the equilibrium geometry of the ion. The implications of these results for the dissociative recombination of water ion with low-energy electrons will be discussed. Work supported by the National Science Foundation, PHY-99-87877. Computer time supplied by NERSC, Lawrence Berkeley Lab.

QWP 9 Near-Threshold Electron Impact Multiple Ionization of the Rare Gases

B. GSTIR, S. DENIFL, G. HANEL, M. RUEMMELE, T. FIEGELE, P. CICMAN, P. SCHEIER, T. MAERK, *Universitat Innsbruck, Austria* M. STANO, S. MATEJCIK, *Comenius University, Bratislava, Slovakia* A. STAMATOVIC, *Institute of Physics, Belgrade, Yugoslavia* K. BECKER, *Stevens Institute of Technology, Hoboken, USA* We report the results of the experimental determination of the appearance energy values for the formation of multiply charged rare gas ions He (up to charge state $n=2$), Ne ($n=4$), Ar and Kr ($n=6$), and Xe ($n=8$) using a high-resolution electron impact ionization mass spectrometer. The data analysis uses an iterative, non-linear least-squares fitting routine in with either a 2-function or a 3-function fit based on a power threshold law. This allows the us to extract the appearance energy values and the corresponding exponents for a Wannier-type power law in the near-threshold region. A detailed comparison of our data with other measured appearance energies (incl. spectroscopic values, where available) and with other measured Wannier exponents is made as well as a comparison of our exponents with the predictions for exponents derived from various Wannier-type power law models. Work supported in part by FWF, OENB, OEAU, and NASA.

QWP 10 Calculated Cross Sections for the Electron Impact Ionization of Molecular Ions

H. DEUTSCH, *Universitat Greifswald, Germany* K. BECKER, *Stevens Institute of Technology, Hoboken, USA* P. DEFRANCE, *Universite Catholique de Louvain, Belgium* U. ONTHONG, R. PARAJULI, M. PROBST, S. MATT-LEUBNER, T. MAERK, *Universitat Innsbruck, Austria* We report the results of the application of the semi-classical Deutsch-Mrk (DM) formalism to the calculation of the absolute electron-impact ionization cross section of the molecular ions H_2^+ , N_2^+ , O_2^+ , CD^+ , CO^+ , CO_2^+ , H_3O^+ , and CH_4^+ for which experimental data have been reported. Where available, we also compare our calculated cross sections with calculated cross sections using the BEB method of Kim and co-workers. The level of agreement between the experimentally determined and calculated cross section is satisfactory in some cases. In all cases, the calculated cross sections exceed the measured cross sections which is not surprising in view of the experimental complications in measuring ionization cross sections of molecular ions due to the presence of competing channels such as ionization dissociative ionization, and dissociative excitation. Work supported in part by FWF, OEAU, and NASA.

QWP 11 HEAVY PARTICLE INTERACTIONS

QWP 12 Theoretical and Experimental Fully differential Cross Sections for $C^{6+} + He$ collisions at Large Perturbation¹

D. H. MADISON, *University of Missouri-Rolla, USA* D. FISCHER, *Max-Planck-Institut Für Kernphysik, Heidelberg, Germany* M. SCHULZ, M. FOSTER, S. JONES, *University of Missouri-Rolla, USA* R. MOSHAMMER, J. ULLRICH, *Max-Planck-Institute für Kernphysik, Heidelberg, Germany* Recently absolute fully differential measurements were reported for 100 MeV/amu C^{6+} projectiles ionizing He. These experimental cross sections were in very good agreement with 3C-HF (3 Coulomb wave-Hartree-Fock) theoretical calculations in the scattering plane. However, significant discrepancies between experiment and theory were found outside the scattering plane and perpendicular to the momentum transfer direction. In terms of the perturbation parameter q/v (projectile charge/velocity), the above collisions corresponded to a relatively small perturbation. We have now extended this investigation to a much larger perturbation. Absolute experimental fully differential cross sections will be compared with theoretical results for 2 MeV/amu $C^{6+} + He$ collisions both in and out of the scattering plane. Different physical mechanisms will be investigated to determine the source of the discrepancies between experiment and theory out of the scattering plane.

¹Work supported by the NSF

QWP 13 Effect of charge exchange on electrical characteristics of discharges in mixtures of inert gas

ROMAIN GANTER, MARK CAPPELLI, *Stanford University* In a Plasma Display Panel cell, as in some fluorescent lamps the light is produced by glow discharges in mixtures of xenon with other inert gases such as neon and/or helium. In this study, the current-voltage characteristics of various mixtures of helium, xenon and neon have been measured in DC discharges between stainless steel electrodes at pd

=3D 5 torr-cm. In the abnormal part of the glow discharge regime, the discharge voltages are higher in mixtures of helium and xenon than in pure xenon. In order to understand this behavior, comparisons with a one-dimensional fluid model have been performed. Good agreement between simulated and experimental characteristics in He-Xe is obtained when the charge exchange reaction: $\text{He} + \text{Xe} = \text{AE He} + \text{Xe}^+$ is taken into account, using a rate constant of $10^{-9} \text{ cm}^3 \cdot \text{s}^{-1}$, as reported in the literature for moderately high temperatures of around 1 eV. We discuss how such ion energies are not uncommon, since in our DC conditions the cathode sheath electric field accelerates He ions to drift velocities corresponding to a few eV's when E/p 600 V/torr/cm at the cathode surface.

QWP 14 Effects of Inelastic Collisions on Transport Cross Sections for Helium Atoms A.V. PHELPS, JILA, U. of Colorado and NIST We review experimental and theoretical cross sections for elastic and inelastic collisions between ground state helium atoms from 0.01 eV to 10 keV. Pure elastic scattering is calculated using potentials from thermal transport coefficients, beam attenuation data, and theory. Inelastic collisions cause rapid decreases in measured elastic differential cross sections at angle times energy products greater than ~ 3 degree keV for collision energies above 100 eV.¹ At these angles, the sum of the inelastic differential cross sections is roughly half theory for elastic scattering only. The inelastic collisions extrapolate to a ≈ 40 eV threshold and significantly decrease viscosity cross sections at higher energies. The change in total cross section is small. We correct the normalization of experimental ionization and excitation to theory.²

¹R. Morgenstern *et al.*, J. Phys. B 4, L330 (1973); M. Barat *et al.*, J. Phys. B 6, 1206 (1973); J. C. Brenot *et al.*, Phys. Rev A 11, 1245 (1975).

²V. Kempter, in *The Physics of Electronic and Atomic Collisions*, ed. by J. S. Risley and R. Geballe (U. Washington, Seattle, 1975) p. 327; J. P. Gauyacq, J. Phys. B 9, 3067 (1976).

QWP 15 Formation of Negative Ions from Nitromethane* C.Q. JIAO, Innovative Scientific Solutions, Inc., Dayton, OH C.A. DEJOSEPH, JR., A. GARSCADDEN, Air Force Research Laboratory, Wright-Patterson AFB, OH Fourier-transform mass spectrometry (FTMS) has been used to study the formation of negative ions from nitromethane via electron impact and the subsequent ion/molecule reactions. Nitromethane has recently attracted attention from researchers because of its use as a fuel and as a prototypical molecule for a class of high-energy materials. It is well known that nitromethane is sensitized toward detonation by amines, but the sensitization mechanism is still unclear. Recent studies have pointed out the importance of CH_2NO_2^- which is believed to be involved in the rate-limiting step of the detonation. A reaction pathway from CH_2NO_2^- to form NO_2^- has been proposed¹ but it is found to be highly endothermic². Our FTMS study on the reactions of CH_2NO_2^- and other negative ions permits us to identify another possible reaction pathway that is thermochemically allowed. Details of the FTMS experiment and the resulting data will be presented.

*This work supported by Air Force Office of Scientific Research.

¹Y. A. Gruzdov and Y. M. Gupta, J. Phys. Chem. A, 102 (1998) 2322.

²E. Woods, III, Y. Dessiaterik, R. E. Miller, and T. Baer, J. Phys. Chem. A, 105 (2001) 8273.

QWP 16 DISTRIBUTION FUNCTIONS AND TRANSPORT COEFFICIENTS

QWP 17 Evaluation of Synergy Effect in Electron Capture Mechanism of SF_6/N_2 Mixtures* HIROTAKE SUGAWARA, TAKUYA ISHIGAKI, YOSUKE SAKAI, Hokkaido University, Japan In a recent trend that reduction of use of SF_6 for electric power equipment is considered to avoid global warming, SF_6/N_2 mixture is a potential alternative of less environmental load, because insulating gas superior to SF_6 is hardly developed. The limiting E/N values of SF_6/N_2 are higher than the values of linear interpolation between those of pure SF_6 and N_2 , thus SF_6 can be diluted with N_2 without commensurate decrease in limiting E/N . This feature called synergy effect is explained from a collaboration between SF_6 and N_2 in the electron capture mechanism: N_2 molecules rob electrons of energy by inelastic collisions and SF_6 molecules capture the depressed electrons. The aim of this work is to find a quantitative guideline of choosing combinations of components for insulating gas mixtures through attempts to evaluate the synergy effect. We calculated the energy loss rates of electron swarms in SF_6/N_2 using a propagator method. The collaborative roles of SF_6 and N_2 were indicated by the result that the ratio of the electron energy loss concerning N_2 exceeds the N_2 content ratio. This tendency was remarkable at low N_2 content at low E/N .

*Work supported by JSPS under Grant-in-Aid 14750200

QWP 18 Self-consistent system of equations for kinetic description of low-pressure discharges accounting for nonlocal and collisionless electron dynamics IGOR D. KAGANOVICH, Plasma Physics Laboratory, Princeton University, Princeton, NJ 08543 For low-pressure discharges, when electron mean free path is larger or comparable with discharge length, the electron dynamics is essentially nonlocal. Moreover, the electron energy distribution function (EEDF) deviates considerably from a Maxwellian. Therefore, accurate kinetic description of low-pressure discharges requires knowledge of nonlocal conductivity operator and calculation of nonMaxwellian EEDF. The previous treatments made use of simplifying assumptions: uniform density profile or Maxwellian EEDF, etc. In the present study a self-consistent system of equations for kinetic description of nonlocal, nonuniform, collisionless plasmas of low-pressure discharges is derived. It consists of the nonlocal conductivity operator and the averaged kinetic equation for calculation of nonMaxwellian EEDF. The importance of accounting for nonuniform plasma density profile on both current density profile and EEDF is demonstrated. Additional information on the subject will be posted in <http://www.pppl.gov/pub/report/2002/> <http://arxiv.org/abs/physics/> Work supported by the Princeton Plasma Physics Laboratory through a University Research Support Program.

QWP 19 Spatial transition of the electron gas through a field reversal into a field-free region DETLEF LOFFHAGEN, FLORIAN SIGENEGGER, ROLF WINKLER, Institut für Niedertemperatur-Plasmaphysik, 17489 Greifswald, Germany The possible occurrence of an electric field reversal in glow discharge plasmas at certain discharge conditions has repeatedly been suggested in the literature. To investigate the impact of such a field

reversal on the electron gas its behavior was studied by solving the electron Boltzmann equation as well as by Monte Carlo simulations. The one-dimensional model comprises the transition of the electron gas from an active, homogeneous neon plasma into a field-free region in front of an absorbing wall. In a small transition region the electric field goes from its steady-state value through zero to a reversed field and back to zero. For comparison the field reversal is omitted in a second case. To get a continuous time-independent transition of the electron gas a spatially narrow electron sink, describing e.g. the electron extraction by a grid, is additionally included. The results show an enormous impact of the field reversal on the velocity distribution function (VDF) and the macroscopic quantities of the electrons in the whole region considered. A strong increase of the density and decrease of the mean energy is caused by the trapped electrons. The anisotropic part of the VDF has a complicated structure which is mainly induced by the backflow of low energy electrons towards the sink.

QWP 20 On the kinetics of the electron gas in the Franck-Hertz experiment FLORIAN SIGENEGER, ROLF WINKLER,

Institut für Niedertemperatur-Plasmaphysik, 17489 Greifswald, Germany The famous Franck-Hertz experiment very convincingly demonstrates the existence of discrete energy states in atomic systems. It has been described in many textbooks and repeated very frequently in various variants. However, most of these explanations are based on simplifying assumptions concerning the energy distribution and the elastic collisions of the electrons. Therefore, a study of the behavior of the electron gas on a rigorous kinetic basis has been performed considering a mercury vapor in a cylindrical Franck-Hertz tube. In the model the radially inhomogeneous Boltzmann equation is solved taking into account an accelerating field between the central cathode and the grid and a retarding one between the grid and the anode. Furthermore, the extraction of electrons which are trapped around the grid is included by a spatially narrow lifetime term. After solving the Boltzmann equation for a series of cathode-grid voltages and analyzing the anode current the well-known Franck-Hertz curve is obtained. The analysis of the electron power balance reveals the impact of the energy loss in elastic collisions as well as of the changing importance of the two lowest exciting states of the mercury atom on the maxima positions of the Franck-Hertz curve. The significant changes of the latter with the pressure can be explained by these effects.

QWP 21 Thomson Scattering Measurements in an Inductively Coupled Plasma—Ar/O₂ Mixtures GARY CRAIG, CATHERINE THOMPSON, PHILIP STEEN, TOM MORROW, BILL GRAHAM,

Queens University Belfast Electron energy distribution functions (EEDF) are central to the understanding of the physics and chemistry of low temperature plasmas. Here we use Thomson Scattering to measure the eedf's in Argon/Oxygen mixtures, using the second harmonic of the ND:Yag laser at 532nm and an ICCD detector. The Rayleigh scattering component is also detected and used in calibration. In an inductively coupled GEC reference reactor operating at a pressure of 100mT and a power of 300W with 100% Argon, we find the eedf is best represented by a Maxwellian distribution which when fitted yields an electron density of $1.9 \times 10^{13} \text{ cm}^{-3}$ and an electron temperature of 1.7 eV. With increasing oxygen percentage the electron density decreases and the distribution becomes more bi-Maxwellian in appearance.

QWP 22 Effective ionization coefficients and electron drift velocities in C₂F₆ and C₂F₆ - Ar mixtures J. DE URQUIJO,

Centro de Ciencias Fisicas, UNAM, Mexico A. CASTREJON, *Facultad de Ciencias, UNAM, Mexico* E. BASURTO, *Depto. de Ciencias Basicas, UAM-A, Mexico* G. HINOJOSA, *Centro de Ciencias Fisicas, UNAM, Mexico* J. L. HERNANDEZ-AVILA, *Depto. de Energia, UAM-A, Mexico* We have used the pulsed Townsend technique to measure the effective ionization coefficient $(\alpha - \eta)/N$ and the electron drift velocity v_e in C₂F₆ and its mixture with Ar, with C₂F₆ concentrations of 0.1, 1, 2, 5, 10, and 20%. The electron drift velocities display well defined Ramsauer-Townsend maxima, which become more pronounced with the share of Ar in the mixture. The overall E/N range covered was 0.1-400 Td (1 Td = 10^{-17} V cm^2). For C₂F₆, our v_e values are in good agreement with those recommended over the range $10 < E/N < 100$ Td. For the 0.1% and 10% C₂F₆ concentrations, we found good agreement with previously reported data. As regards the values of $(\alpha - \eta)/N$, the present set covers a wider E/N range (40-400 Td) than that recently surveyed [1]. Below E/N 300 Td, the present values disagree strongly with those previously reported. [1] L.G. Christophorou and J.K. Olthoff, *J. Phys. Chem. Ref. Data* 27, 1 (1998) Project supported by DGAPA IN104501

QWP 23 GLOWS: DC, PULSED, RF, MICROWAVE, OTHER

QWP 24 LANGMUIR PROBE DIAGNOSTICS OF PULSED PLASMA DOPING SYSTEM YU LEI,

Electrical Engineering Department, The University of Texas at Dallas LAWRENCE J. OVERZET, *Electrical Engineering Department, The University of Texas at Dallas* SUSAN B. FELCH, *Varian Semiconductor Equipments Associates, Inc* ZIWEI FANG, *Varian Semiconductor Equipments Associates, Inc* BON-WOONG KOO, *Varian Semiconductor Equipments Associates, Inc* MATTHEW J. GOECKER, *Electrical Engineering Department, The University of Texas at Dallas* Pulsed plasma doping (P2LAD) is a potential solution to implement ultra-shallow junctions. In this study, Langmuir probe diagnostics techniques were investigated thoroughly for its application to P2LAD system, and the current sensing scheme using batteries and a 'downstairs' load resistor turned out to be the most reliable. Severe limitations of current transformers were found in diagnostics of pulsed plasma. A floating probe was proven to be good at monitoring the disturbances of the Langmuir probe and the cathode voltage. With the above technique, time-resolved Langmuir probe measurements have been carried out in a P2LAD system. The Langmuir probe data in Ar plasma indicate that during a 20 microns long implant pulse the plasma density ranges from $1\text{E}9$ to $1\text{E}10 \text{ cm}^{-3}$ and the electron temperature ranges from 0.4 to 14 eV. Between the pulses, the density keeps at the high level for 30 ms and then decays exponentially until reaching the range of $3\text{E}8$ to $1\text{E}9 \text{ cm}^{-3}$, which demonstrates the presence of residual plasma between pulses. A non-zero plasma density during the afterglow is also observed for BF₃ plasma. Significant amounts of primary electron and electron beams are present during the ignition and ensuing steady region in both Ar and BF₃ plasmas while they are much stronger in BF₃ plasma. Plasma density is observed to in-

crease with cathode voltage and pressure while the electron temperature is mainly influenced by the pressure. An overshoot of the cathode voltage during the afterglow region was found, and it significantly influences the plasma potential during the afterglow.

QWP 25 RF hollow cathode discharge with mini-slot at high gas pressure* ZENGQI YU, KATSUMI HOSHIMIYA,

GEORGE COLLINS, *Dept. of Electrical and Computer Engineering, Colorado State University, Fort Collins, CO 80523* The hollow cathode discharge (HCD) has been widely used for spectral light sources, low-vacuum electron beam sources and gas lasers due to its ability provide a low voltage plasma discharge. Traditional HCD operates with a DC power supply to drive the discharge. The HCD, however, has a tendency to arc, which limits its maximum operating power without arc control provisions in the power supply. K. Schoenbachs group reported the most detailed progress to achieve pulsed micro hollow cathode discharge at Hundreds Torr of noble gases for VUV source. CSU has explored a rectangular shape HCD, which also demonstrates its stable operation at RF discharge mode. The rf HCD devices consist of a water-cold cathode with a proximity anode, controllable spacer, and rf matching elements. As with other HCD the cathode cooling mechanism is important to assure long device life time due to the high-density plasma achieved and associated heat build-up, especially at the narrow (100 micron) slot several centimeter length. Tailored dielectric coatings, with controlled thickness, on top of the metallic cathode surface play an important role in creating the characteristics of the discharge plasma. Alternatively, the cold cathode can be made from metal-ceramic composite for the additional capability of high secondary electron emission. Cathode slot size of 0.1 0.5 mm has been tested at slot length of 3 cm, and it operates at the gas pressure up to atmospheric pressure.

*This work is supported by NSF grant #ECS-0097061

QWP 26 A microdischarge device with a long active length

BERT BASTIAENS, KLAUS BOLLER, *Chair of Laser Physics, University of Twente, PO. Box 217, 7500AE Enschede, The Netherlands* Microhollow cathode discharge devices are very suitable for the generation of stable DC glow discharges in high pressure excimer laser gases. Strong XeCl excimer emission at 308 nm is reported. However the active length of these devices is limited to a few hundreds of micrometers resulting in a gain-length product that is too small to obtain laser operation. We present a new configuration of a microdischarge device that allows the extension of the discharge length up to tens of cm's. In this device stable DC glow discharges are generated between the anode and a slit in the cathode. A specific power deposition (volume averaged) of up to 120 kW/cm³ is obtained. The electrical characteristics as well as the XeCl fluorescence from He:Xe:HCl gas mixtures up to 1 bar total pressure are studied for different input powers and slit widths. The optimum small signal gain coefficient is estimated to be in the order of 0.05

QWP 27 Factors affecting production of singlet delta oxygen in glow discharges DAVID S. STOKER, *University of Texas at Austin* CRAIG W. McCLUSKEY, *University of Texas at Austin* JOHN W. KETO, *University of Texas at Austin*

Production of ¹Δ_g O₂ was investigated with coherent anti-Stokes Raman spectroscopy (CARS) in a low pressure linear DC glow discharge cell at

pressures up to 110 Torr. Singlet delta production was maximized at pressures below 10 Torr and near the wall of the discharge cell, as well as by adding helium and argon buffer gases and pulsing the discharge current. Results are compared with theoretical investigations and suggest there are other factors that can influence the production of ¹Δ_g O₂.

QWP 28 A graphical solution of the linear-field, source-

function model of the cathode fall A.V. PHELPS, *JILA, U. of Colorado and NIST L.C. PITCHFORD, CPAT, U. Paul Sabatier, Toulouse* We present graphical solutions to a simplified model¹ of the abnormal cathode fall that yield the operating voltage, current density, and cathode fall thickness for an assumed pressure and electron yield per ion at the cathode. The parallel-plane model is applied to fully developed cathode fall and negative glow discharges in He and Ar. A linear variation of the electric field near the cathode relates the space-charge limited, positive-ion current density to the cathode fall voltage, cathode fall thickness, ion mobility, and gas density. Secondly, the reciprocal electron yield per ion at the cathode equals the ions produced per electron emitted, i.e., the integrated "source function." The source function² depends on the cathode fall voltage and the cathode fall thickness times pressure pd_c . We use the local-field model at large pd_c , Monte Carlo results in the transition region, and a free-fall model at small pd_c . Superposition of plots of these two relations allows predictions of operating conditions.

¹A. V. Phelps, *Plasma Sources Sci. Technol.* **10**, 329 (2001).

²I. Pérès, N. Ouadoudi, L. C. Pitchford, and J. P. Boeuf, *J. Appl. Phys.* **72**, 4533 (1992).

QWP 29 Shock Wave Dispersions in Microwave Discharges P.

KESSARATIKOON, A. MARKHOTOK, G. BROOKE IV, S. POPOVIĆ, L. VUŠKOVIĆ, *Department of Physics, Old Dominion U., Norfolk, VA 23529* Dispersion of acoustic shock waves in ionized gas has been a subject of intensive debate.^{1,2,3} Most reported observations were made in positive columns of dc glow discharges. Among other effects, the excessive increase of propagation velocity in the cathode region and the polarity dependence of shock waves in the positive column were observed. In order to eliminate a possible influence of the electrodes on shock modification, we performed extensive measurements with a spark-generated shock propagating through a microwave discharge in a cylindrical cavity. Our observations show a distinctive difference in shock dispersion compared to the dc glow results. The difference in shock dispersion phenomenology can be explained by the absence of electrodes and by the absence of strong gradients between the discharge and neutral gas. We will explain the details of out diagnostics and present of the temperature, pressure, and power. Also, we will present EM mode dependence of dispersion and propagation of shock wave.

¹S. Popović and L. Vušković, *Physics of Plasmas* **6** 1448 (1999).

²S. O. Macheret, Y. Z. Ionikh, N. V. Chernysheva, A. P. Yalin, L. Martinelli, and R. B. Miles, *Phys. Fluids* **13** 2693 (2001).

³B. N. Ganguly and P. Bletzinger, *AIAA-2002-2182* (2002).

QWP 30 Power Balance and Non-Local Properties of a Neon DC Column Plasma DIRK UHRLANDT, *Institut für Niedertemperatur-Plasmaphysik, 17489 Greifswald, Germany*

The column plasma of dc glow discharges in neon is self-consistently analysed by a new hybrid method. The comprehensive spatially resolved description allows a detailed study of the

variation of the space-charge confinement, the non-local electron kinetic properties, and the population of the excited states in neon. The analysis deals with the impact of discharge parameter variations over larger ranges, of an admixture of a molecular gas as well as of the superposition of a longitudinal magnetic field on the spatial plasma structure. Among others, the non-local properties of the electron power balance and their influence on the overall power budget and the radiation efficiency of the plasma are discussed. The largest influence of energy transport processes in the electron power balance has been observed in the range of the pressure times radius values from about 200 to 400 Pa cm, which nearly coincides with the range where the maximum efficiency of the resonance radiation occurs. Such an analysis can help to determine optimal operation conditions of discharges used in low-pressure inert-gas radiation sources.

QWP 31 A Novel Microwave Beam Steering Technique Using Plasma PETER LINARDAKIS, GERARD G. BORG, JEFFREY H. HARRIS, *Plasma Research Laboratory, Research School of Physical Sciences and Engineering, Australian National University, Canberra Australia ACT 0200* NOEL M. MARTIN, *Weapons Systems Division, Defense Science and Technology Organisation, P.O. Box 1500 Salisbury Australia SA 5108** At frequencies above the plasma frequency, electromagnetic waves propagate through plasma with a wavelength longer than the free space wavelength. As a result, a plasma with a centrally peaked density profile can deflect rather than focus electromagnetic waves. We present a plasma device designed specifically to deflect a microwave beam as an alternative to conventional beam deflectors based on antenna arrays. A 22° deflection of K_a band microwave has been achieved using a laboratory plasma, with no detrimental effect on the beam-width or side-lobe level and structure. The use of a simple WKB model shows agreement and that the deflection can be increased with appropriate design. Results indicate the potential for increases in dynamic range, in power handling (for example from a gyrotron) and for the reduction of insertion losses over current beam steering systems. A "plasma lens" demonstrator device has also been designed to test practical performance aspects such as phase noise and to test optimization parameters.

*The authors would like to acknowledge the support of the Australian Defence Science and Technology Organisation (DSTO)

QWP 32 Plasma RF Switching Elements for Cell Phone Applications PETER LINARDAKIS, GERARD G. BORG, JEFFREY H. HARRIS, *Research School of Physical Sciences and Engineering, Australian National University, Canberra Australia** The functionality of modern multi-band, multi-system cell phones is provided by a large number of RF switches. Future phones will require an even greater number of these switches to implement hardware such as agile antennas. The ever increasing need for higher performance and lower power consumption have brought the RF PIN diode to the edge of its capabilities in these applications. RF micro-electromechanical (MEMS) switches can easily provide the required low insertion loss, low inter-modulation and low power consumption combination, but their reliability limits are not yet satisfactory to industry. In conjunction with Motorola Personal Communications Sector (PCS), PRL is undertaking a project to examine the possibility of using plasma in a completely novel type of RF switch. A basic concept of variable "plasma capacitors" constructed from DC commercial fluorescent tubes

has been analyzed up to 1.3 GHz. The four different configurations tested show some consistent behavior and a definite impedance change between the on and off states. A simple model reliant on RF sheath theory also shows some agreement.

*The authors would like to acknowledge the support of Motorola Personal Communications Sector (PCS)

QWP 33 Large-Area Surface Wave Excited N₂-Ar Overdense Plasma E. TATAROVA, F.M. DIAS, J. HENRIQUES, C.M. FERREIRA, *Centro de Física dos Plasmas, Instituto Superior Técnico, 1049-001 Lisboa, Portugal* A slot-antenna excited, large area surface wave (SW) plasma source operating in N₂-Ar mixtures is investigated. Surface waves propagating radially and axially along the interface between the plasma and a dielectric plate ($\epsilon_d=3.78$, $d=1$ cm) located at the top wall of a large diameter cylindrical camera ($R=11$ cm) are the energy source for the plasma. The waves form a resonant eigenmode satisfying the boundary conditions and the plasma "sticks" to some discrete density values which ensure that some of the resonant eigenmodes exactly appear at the excitation frequency (2.45 GHz). For this reason, we analyse an overdense plasma sustained by discrete pure surface modes, i.e. TM_{33} , TM_{62} , etc. A 2D theoretical model is developed. The plasma density at which a given mode appears and the electric field pattern in the $\gamma - \phi$ plane ($Z=\text{const}$) are calculated from Maxwell's equations and the wave dispersion equation. The values of the electric field intensity are determined on the basis of the self-consistently calculated maintaining electric field satisfying the electron density balance equation. The 2D distribution of the electron rate coefficients are obtained by solving the electron Boltzmann equation in the local approximation. Then the rate balance equations for the most important excited species are solved and their $\gamma - \phi$ distribution is obtained.

QWP 34 INDUCTIVELY COUPLED PLASMAS

QWP 35 2D spatial distribution of Ar metastables in front of biased wafer in an ICP for SiO₂ etching in CF₄/Ar T. DENDA, Y. MIYOSHI, T. OMI, T. GOTO, T. MAKABE, *Keio University at Yokohama, Japan* An inductively coupled plasma (ICP) has been widely used for metal and Poly-Si etching for ULSI circuits fabrication. The ICP with wafer biased by a low frequency voltage source with amplitude of several hundred volts for SiO₂ etching is still under development. In this work, we investigate the plasma structure in the processing room with a highly biased electrode in the ICP by using absorption CT[1] in addition to the emission CT[2] in pure Ar and CF₄(5%)/Ar. The bias electrode at 500 kHz is positioned at 125 mm from the plasma source driven by one-turn current coil at 13.56 MHz. A line-integrated laser absorption spectroscopy by using tunable diode laser is inverted by Abel transform in order to obtain the axisymmetric 2D density distribution of metastables, Ar(1s₅) and Ar(1s₃). Two absorption lines, 772.376nm for Ar(1s₅) → Ar(2p₇) and 772.421nm for Ar(1s₃) → Ar(2p₂) have been selected for this purpose. 2D distributions of Ar(1s₅) and Ar(1s₃) are shown and discussed as a function of low

frequency bias power in addition to other external plasma parameters. [1] M. Tadokoro, H. Hirata, N. Nakano, Z. Lj. Petrovic, and T. Makabe, *Phys. Rev. E* 58, 7823 (1998). [2] Y. Miyoshi, Z. Lj. Petrovic, and T. Makabe, *J. Phys. D: Appl. Phys.* 35, 454 (2002).

QWP 36 A mixed mode discharge to control the EEDF of a low temperature plasma: A diagnostic study RAMIN MADANI, IoP ROBERT CHERRY, *IoP Surface waves* travelling on and sustaining low pressure discharges have been investigated for over three decades. One attractive feature of the phenomenon is the relationship between the dispersion of the surface wave as it moves along a cylindrically bound plasma to the local plasma density. We have launched a surface wave discharge through the stray capacitances of a coil, which is simultaneously sustaining an inductive discharge. This has been devised to test the extent to which a surface wave can modify the EEDF. In particular a mixed-mode system is supporting a lower frequency "H" mode ($f_H < 100$ MHz) and a higher frequency surface wave mode ($f_{SW} > 200$ MHz). The geometry of the device favours double probe measurements. Tail measurements of the EEDF obtained from a double probe system will be evaluated with a series of numerically calculated EEDFs mapped for varying electron temperatures and ion densities. The effect of any substantial alterations to the EEDF can be reconstructed from the information obtained by a double probe. These will be compared with measured dispersion relationships and the plasma parameters defining the discharge.

QWP 37 Effects of nonlocal conductivity on EEDF for low pressure inductively coupled discharges: comparison between the actual EEDF and a Maxwellian BADRI RAMAMURTHI, DEMETRE J. ECONOMOU, *Plasma Processing Laboratory, Department of Chemical Engineering, University of Houston, Houston, TX 77204-4004* IGOR D. KAGANOVICH, *Plasma Physics Laboratory, Princeton University, Princeton, NJ 08543* A self-consistent model was developed to study the effect of non-local electron transport on power absorption, electron energy distribution function (EEDF), and plasma density profiles in a planar inductively coupled argon discharge at low pressures (< 10 mTorr). The RF electric field and current density profiles in the plasma were computed by a non-local electron conductivity model for inhomogeneous plasmas. The EEDF was calculated by a non-local approach. Computations were also done assuming a Maxwellian EEDF. When using a Maxwellian EEDF, the plasma density profiles are essentially identical, irrespective of the electron conductivity model used (local or non-local). With a Maxwellian EEDF, although the power deposition profiles are affected, the plasma density profiles depend only on the total power deposition. With the actual EEDF, both the power deposition profiles and the plasma density profiles are affected, depending on which electron conductivity model is used (local or non-local). The true EEDF predicts smaller electron densities compared to an assumed Maxwellian EEDF. Work supported by the NSF and the Princeton Plasma Physics Laboratory through a University Research Support Program.

QWP 38 Electron Density and Temperature in an Inductively Coupled Discharge in Hydrogen V.A. KADETOV, U. CZARNETZKI, *Institut for Plasma and Atomic Physics, Bochum University, 44780 Bochum, Germany* H. F. DOEBELE, *Institut for Experimental Physics, Essen University, 45117 Essen, Germany*

An inductively coupled discharge in hydrogen is operated in a modified GEC reference cell. The radial distribution of the electron density and temperature is measured by a Langmuir probe. The distribution function is well described by a Boltzmann distribution up to energies around 20 eV. This motivates a straightforward simulation of the discharge in the frame of a global model. In contrast to the standard procedure, a one-dimensional model is applied that includes also the ion inertia term. The analytical solution for the electron temperature is in good agreement with the measurements, if the correct neutral gas temperature is considered. TALIF measurements of the Doppler broadening in atomic hydrogen reveal gas temperatures up to 1100 K. The distribution of the axial electron density and plasma potential predicted by the model agrees also well with a comparison of the probe data in the bulk with values deduced from electric field and ion energy measurements close to the surface of a grounded electrode. Further, the power and pressure dependence of absolute values of the plasma density and the threshold for ICP operation is predicted correctly.

QWP 39 Current Nodes on Inductively Coupled Plasma Sources S. SRINIVASAN, L. PRATTI, L. OVERZET, M. GOECKNER, *The University of Texas at Dallas, P.O. Box 830688, EC33 Richardson TX 75083* The azimuthal symmetry of electron and ion densities in Inductively Coupled Plasmas (ICP) is a function of source geometry. Azimuthal uniformity of ions at the plane of the wafer depends on the azimuthal uniformity of the magnetic and electric fields of the ICP source. ICP sources are modeled as transmission lines when the length of the source becomes comparable to the wavelength used. The current and the voltage vary along the length of the ICP source and can even produce a current node along the source. In this poster, the feasibility of producing uniform magnetic and electric fields despite the presence of a current node on the source is studied. The three-dimensional ICP source geometry is modified to negate the effect of a current node. Comparisons between the modeled field profiles for various source designs and experimentally measured field profiles show partial agreement. The ion, electron density and electron temperature profiles derived from the spatial characterization of the inductively coupled plasma are consistent with the experimentally measured field profile. An improved model treats the ICP source as a three-dimensional transmission line system including interaction between the various loops of the coil. This material is based upon work supported by the State of Texas Advanced Technology Program under Grant No. 009741-0081-1999.

QWP 40 Experimental study of diffusive and collisional cooling of electrons in a pulsed inductively coupled plasma* MICHAEL HEBERT, UWE KORTSHAGEN, *University of Minnesota, Mechanical Engineering, Minneapolis, MN 55455* A cylindrical Langmuir probe has been used to obtain measurements of the temporal behavior of the electron distribution function in the afterglow of a low-pressure inductive discharge. For low pressures, the appearance of the measured electron distribution functions indicates that the loss of high energetic electrons to the wall of the discharge chamber is the main energy loss mechanism, where electron-heavy particle collisions play only a secondary role for the energy loss. While energetic electrons are rapidly lost to the walls, low energy electrons remain trapped within the ambipolar potential well, thus yielding a fast cooling of the electron distribution function. However, as the pressure is increased, the ion transport to the walls diminishes thus causing a reduction in the wall loss of electrons. This leads to a non-monotonous varia-

tion of the energy relaxation time this pressure. At low pressure when the electron wall loss is the main energy loss mechanism, the energy relaxation time increases with increasing pressure. At higher pressures, a transition to collisional energy relaxation is observed and the energy relaxation time decreases with increasing pressure.

*This work is supported by DOE through grant ER54554.

QWP 41 Energy flows in an inductively coupled plasma JAAP FEIJEN, CAROLE MAURICE, GERRIT KROESEN, *Eindhoven University of Technology* EPG TEAM In a planar-coil inductively coupled plasma, the plasma potential, the electron density and the electron energy distribution have been acquired with an RF compensated Langmuir probe. Ion velocities have been determined by Doppler shifted LIF. Ion energy distributions of ions arriving at the electrode have been determined with energy resolved mass spectroscopy. Furthermore, the efficiency of the coupling of the RF power from generator into plasma has been determined. Using all experimental data, we have calculated the several "destinations" of the RF power coupled into the plasma. About 19 % is lost before it enters the plasma. 16 % of the power actually ends up at the electrode, in kinetic ion energy. Another 10 % is also usable at the electrode: the potential energy of the ions (the ionisation energy, which might be used for chemical activity). The electrons carry away 15 % when they leave the plasma. The remaining 40 % is lost in the ion bombardment of the quartz window and ion losses at the outer radius of the discharge.

QWP 42 Ion and Radical Densities in Inductively Coupled C_4F_6 Plasmas ERIC BENCK, AMANDA GOYETTE, GUERMAN GOLUBIANTNIKOV, YICHENG WANG, JAMES OLTHOFF, *National Institute of Standards and Technology* Alternative fluorocarbon chemistries, such as hexafluoro-1,3-butadiene (C_4F_6) have been proposed as a means of reducing the global warming impact of perfluoro-compounds commonly used in the semiconductor industry for dielectric etch. Mass resolved, ion energy and sub-millimeter wave absorption spectroscopy measurements have been used to characterize inductively coupled C_4F_6 plasmas in the ICP-GEC Reference Cell Reactor. Ion and radical densities have been measured as a function of plasma power, pressure, C_4F_6/Ar ratio and flow rate.

QWP 43 MAGNETICALLY ENHANCED PLASMAS

QWP 44 A two dimensional modeling of an rf magnetron plasma for sputtering T. MINE, M. TAKADA, T. MAKABE, *Keio University at Yokohama, Japan* A magnetron discharge at low pressure is well-known tool for deposition of various kinds of thin films by using ion sputtering on a target. In previous papers, we have developed a hybrid model for a dc magnetron discharge for material sputtering[1]. In order to deposit dielectric films by using the physical mechanism of the ion sputtering of a dielectric target material, a radio frequency source will be required for sustaining the magnetron plasma. In this study, we present a two dimensional hybrid model, consisting of a particle model of elec-

trons and relaxation continuum model of massive ions for an rf magnetron plasma for sputtering. It is known that the electron shows a very complicated transport even in a uniform $E \times B$ field[2]. Under these circumstances, Monte Carlo simulation has a benefit of simplicity though it is time consuming. In this study we discuss the results of 2D plasma structure, I-V characteristics, and the ion energy distribution incident on the target, etc. Especially the incident ion energy distribution is one of the key parameters of physical sputtering and deposition. [1] E.Shidoji, E.Ando, and T.Makabe, *Plasma Sources Sci. Technol.* 8, 621(2001), E.Shidoji, H.Ohtake, N.Nakano, and T.Makabe, *Jpn. J. Appl. Phys.* 38, 2131(1999). [2] K.Ness and T.Makabe, *Phys.Rev.E* 62, 4083(2000), Z.Raspopovic, S.Sakadzic, Z.Lj.Petrovic, and T.Makabe, *J.Phys.D* 33, 1298(2000).

QWP 45 2-D experimental study of DC discharge parameters in the cylindrical magnetron J.F. BEHNKE, *Ernst-Moritz-Arndt University, Institute of Physics, Domstrasse 10a, D-17487 Greifswald, Germany* M. HOLIK, P. KUDRNA, O. BILYK, J. RUSZ, M. TICHÝ, *Charles University in Prague, Czech Republic* In this paper we present a study of the variations of plasma parameters in both the axial as well as in radial directions in the novel construction of cylindrical magnetron. Six evenly distributed coils create the axial magnetic field with the homogeneity 0.2 % over the whole discharge vessel length 300 mm (vessel diameter 58 mm). The system is equipped with three cylindrical Langmuir probes movable in radial direction, placed in ports located in between each couple of coils in distance 60 mm from each other. In order to measure the axial variations of the discharge current, one half of the cathode length is segmented into 14 segments, i.e. one segment has a length of about 10 mm. We present measurements of the axial distribution of the discharge current in argon at different pressures and magnetic fields. We demonstrate measurements of the radial variations of the electron density measured simultaneously by probes at three different axial positions.

QWP 46 Manipulating Sputtered Materials During Growth in Pulsed DC Magnetron Discharges C. MURATORE, *Advanced Coatings and Surface Engineering Laboratory, Colorado School of Mines* J.J. MOORE, *Advanced Coatings and Surface Engineering Laboratory, Colorado School of Mines* J.A. REES, *Hidden Analytical Ltd.** Time-averaged ion energy distributions and time-resolved floating potentials were measured for a range of duty cycles at electrodes immersed in a 60 kHz pulsed magnetron discharge. The time-averaged ion energy distributions respond to the voltage on the cathode during pulsing, and correlation of the data reveal the time-resolved ion energy distributions at surfaces in the discharge. From the measured data, time-resolved electron temperatures for both pulsed and DC discharges were calculated at times relative to pulse events, and found to be approximately constant at 3 eV. Electrically conductive titanium oxide (TiO) thin films were deposited in the characterized discharges. The structure and properties of the deposited films were measured using conventional techniques. Increased crystallographic texture, hardness, electrical conductivity and packing density were all observed as the incident ion energy was increased by manipulating the discharge pulse parameters.

*C.M is currently at the U.S. Naval Research Laboratory, Plasma Physics Division

QWP 47 Cylindrical Magnetron Discharge via Experiment and Modelling J.F. BEHNKE, *Ernst-Moritz-Arndt University, Institute of Physics, Domstrasse 10a, D-17487 Greifswald, Germany* YU.B. GOLUBOVSKII, I.A. POROKHOVA, *St. Petersburg State University, Russia* P. KUDRNA, M. TICHÝ, *Charles University in Prague, Czech Republic* Plasma in cylindrical magnetron discharge with all quantities varying radially and uniform axial magnetic field, is studied experimentally and theoretically by PIC, non-local kinetic and local kinetic models. Discharge conditions are Ar at pressure 4 Pa, magnetic field strength is 30 mT, currents 100-400 mA. Discharge length is 30 cm, radii of inner cathode and outer anode are 0.9 and 2.9 cm. The self-consistent descriptions of cylindrical magnetron in argon is obtained by three models with each of them giving spatial distributions of macroscopic parameters from cathode through the positive column to anode. Each model has its advantages in calculating the plasma parameters, and it is an objective of this study to demonstrate and discuss them through a comparison of the simulation results for the EDFs, radial profiles of particle densities, electric field and average energy of electrons with the results of experimental study.

QWP 48 Properties of Electromagnetic Waves in a Radio-Frequency Discharge Plasma Generated by Phased Helical Antennas GENTA SATO, WATARU OOHARA, RIKIZO HATAKEYAMA, *Department of Electronic Engineering, Tohoku University, Sendai 980-8579, Japan* Phased helical antennas consist of four one-turn helical antennas which are azimuthally spaced by 90° . The antennas are supplied with radio-frequency (RF) currents, each phase of which is sequentially shifted by 90° , providing the rotating RF electromagnetic-fields (400W, $f_{rf} = 14$ MHz) with the dominant mode number $|m| = 1$. An argon plasma is generated by the RF fields at a gas pressure of 0.5 mTorr in an axially uniform magnetic field ($B_0 < 200$ G). The plasma density depends on B_0 and drastically increases up to $2 \times 10^{11} \text{ cm}^{-3}$ for $B_0 \sim 20$ G when the RF fields rotate in the electron-diamagnetic direction. According to the measurement for various RF frequencies, this density increment is found to take place under the condition of $f_{ce}/f_{rf} \sim 4$, where f_{ce} is the electron cyclotron frequency. In this case it is observed that the electromagnetic wave with a unique spatial structure propagates in the downstream from the antenna region. The dispersion relation of the wave is consistent with that of TG wave calculated in the plasma column with a conducting boundary. The wave-amplitude dependence on B_0 is directly connected with the plasma density, indicating that the traveling wave stimulates the plasma generation.

QWP 49 Helicon plasmas with immersed antenna ANE AANESLAND,* CHRISTINE CHARLES, *Plasma Research Laboratory, Research School of Physical Science and Engineering, Australian National University, ACT 0200, Australia* ÅSHILD FREDRIKSEN, *Physics Department, University of Tromsø, N-9037 Tromsø, Norway* ROD BOSWELL, *Plasma Research Laboratory, Research School of Physical Science and Engineering, Australian National University, ACT 0200, Australia* In many plasma processing systems, the substrate is powered with the same RF frequency as the antenna which creates the plasma. Commonly, the phase between the two generators are controlled to ensure that beating and instabilities do not occur. These phenomena have been observed in a helicon reactor with a RF powered substrate where changing the phase between the helicon source

and the substrate changes the plasma density and the substrate bias. To more fully investigate the interaction, we have constructed a helicon source with a second antenna inserted through the source end plate and in contact with the plasma. Quite dramatic changes in all plasma parameters are observed as the power on the immersed antenna or the phase between the two antennas are changed. Under certain circumstances, low frequency instabilities are observed which perturb the plasma. It is expected that using electronegative gases will exacerbate the instability problem.

*Permanent address: Physics Department, University of Tromsø, N-9037 Tromsø, Norway

QWP 50 One Dimensional Simulation of LAPPS* GLENN JOYCE, RICHARD F. FERNSLER, *Naval Research Laboratory, Plasma Physics Division, Washington, DC 20375* We have developed a one-dimensional fluid simulation code for studies of the Large Area Plasma Processing System (LAPPS) at the Naval Research Laboratory. The code is time dependent, can be run in a quasi-neutral or electrostatic mode, solving Poissons equation and in the latter mode can resolve the plasma sheath. The code is multi-species, where the species are easily included by supplying the appropriate collision frequencies. The electron species is treated in the collision approximation in which inertial terms are neglected, but the ion equations include all inertial terms¹. The simulation direction is perpendicular to the electron beam used to produce the LAPPS plasma and to the beam-confining magnetic field. The effect of the magnetic field is represented by an enhanced electron diffusion coefficient. The electron beam is represented by a source of electrons in an interior region of the plasma. We present results for various gases and combinations of gases with parameters based on LAPPS experiments. We pay particular attention to the sheath-presheath interface and to the properties of ion flow at this interface. * Work supported by ONR 1. J.D. Huba, G. Joyce, and J.A. Fedder, JGR, 105, 23035, (2000)

QWP 51 Experiments on LAPPS Cathode Source Optimization and Development* DAVID BLACKWELL, *SFA, Inc., Landover, Maryland 20785* DONALD MURPHY, *Naval Research Laboratory, Plasma Physics Division, Washington, DC 20375* SCOTT WALTON, *SFA, Inc., Landover, Maryland 20785* DARRIN LEONHARDT, *Naval Research Laboratory, Plasma Physics Division, Washington, DC 20375* RICHARD FERNSLER, *Naval Research Laboratory, Plasma Physics Division, Washington, DC 20375* ROBERT MEGER, *Naval Research Laboratory, Plasma Physics Division, Washington, DC 20375* The Large Area Plasma Processing System at NRL has been demonstrated¹ to have great potential as a materials processing source. The low temperature, electron beam generated plasma allows a great deal of control over the plasma conditions while providing a wide surface area from which to draw ion and radical flux. The 1-4 keV electron beam is extracted with a high voltage grid from a hollow cathode glow discharge at pressures of 1-30 millitorr of argon or oxygen. Typical plasma densities are 10^{10} to 10^{13} cm^{-3} with electron temperatures of ≈ 0.5 eV and plasma potentials of $\approx 3-5$ volts. We will present results from experiments designed to further the progress on improving plasma uniformity and broadening the operating parameters. Spatial measure-

ments of the interior, hollow cathode and beam produced plasma will be correlated with cathode geometry, grid size, and operating conditions. Operation of a differentially pumped system for the use of more reactive process gases will be described.

*work supported by the Office of Naval Research

¹R.A. Meger et. al., *Phys. Plasmas* 8, 5, 2558 (2001)

QWP 52 Measurement of Ion Energy Ratio T_i/E_z Using PAD in Compact ECR and Helicon Ion Sources GON-HO KIM, Dept. of Applied Physics, Hanyang University-Ansan, Kyunggido, 425-791, Korea JUNG-HYUN CHO, BONG-CHUL JANG, HYUN-JONG YOO, Dept. of Nuclear Engineering, Hanyang University, Seoul, 122-791, Korea KYU-SUN CHUNG High-density plasma generated in a compact electron cyclotron resonance ion source (ECRIS) and a compact helicon plasma (CHEPIS) source was investigated. Especially, in this work, it is observed that the ratio of the perpendicular ion energy T_i to the parallel ion energy E_z . PAD(Pitch-angle diagnostic) method¹ is employed to measure T_i/E_z for various powers and pressures in those plasma sources. Driving frequencies 2.45GHz and 13.56Mhz are used for ECRIS and CHEPIS, respectively. Also the permanent magnets are employed to generate the waves and confine the plasma. Especially, Nagoya type $m=1$ antenna is wrapped in cylindrical quartz reactor of CHEPIS. Experiments were carried on He and Ar plasmas with operating pressure 1mtorr to 50mtorr and RF power $< 2000W$. Preliminary results that the ratio T_i/E_z increases as RF power increases drastically until 600W and it saturates for 600 1500W and then it slightly decreases for 1500 2000W for Ar, which powers are correspond to those powers of the mode transition as E-H and H-W. However, He data have totally different distribution. Further studies for ECRIS and CheIS will be presented.

¹S. W. Lam and N. Hershkovitz, A new ion pitch-angle diagnostic for magnetized plasmas, *Plasma Sources Sci. Technol.* 3. 40-48 (1994).

QWP 53 PLASMA BOUNDARIES, SHEATHS, PRESHEATHS II

QWP 54 Particle Simulation of a Sheath Instability in Electronegative Plasmas A. KONO, Nagoya University, Nagoya 464-8603, Japan In electronegative plasmas, the positive ion flow towards the wall (electrode) can reach the ion sound speed u_s in the presence of negative ions with α_s (negative-ion/electron density ratio) $> \sim 0.5$, so that $u_s < u_B$, where u_B is the usual Bohm speed $(kT_e/M)^{1/2}$. At that point, a potential step is formed, which repels negative ions, yielding positive space charge. However, with further acceleration of the positive ion flow, the positive ions are rarefied more rapidly than electrons as long as the flow speed is below u_B . With $\alpha_s < \sim 5$, the positive ions become even less dense than electrons before the flow speed reaches u_B , i.e., the space charge changes its polarity. Fluid model computations of

this situation predict the formation of spatial potential oscillations. However, any potential minima associated with the potential oscillations trap slow ions, which fill up potential wells; thus the stationary spatial potential oscillations are unphysical. A particle simulation of the corresponding phenomena suggests an instability caused by quasi-periodic trapping and de-trapping of slow ions. Simulation results for various positive ion collisionality and electron attachment rates will be presented.

QWP 55 Ion Acoustic Wave Dispersion Relation in Presheath EUNSUK KO, XU WANG, NOAH HERSHKOWITZ, Dept. of Engineering Physics, University of Wisconsin-Madison, Madison, WI 53706 A presheath provides a transition region between a plasma-wall sheath and bulk plasma. The generalized Bohms criterion expresses a plasma condition that must be satisfied at the presheath-sheath boundary. The propagation of ion acoustic waves in uniform plasma is well described by dispersion relations derived from ion fluid equations assuming Boltzmann electrons for stationary and uniformly drifting plasmas. However, since a density gradient exists in the presheath, the ion acoustic wave and the ion drift velocity will be affected. For multi-ion species, the ion acoustic wave dispersion relation is derived in the presheath including convective terms and frictional forces in the ion fluid equations. For both single and multi-ion species plasmas, the dispersion relation and the uniform medium dispersion relation are similar near the presheath-bulk plasma boundary because the density variation is very small, but the effect becomes important near the sheath-presheath boundary. The dispersion relation in multi-ion species plasma is complicated by the presence of the ion-ion beam instability. Each ion has a fast and a slow mode, and the interaction of these modes forms unstable modes. *Work Supported by US DOE grant DE-FG02-97ER 54437

QWP 56 The Measurement of Ion Drift Velocities in Presheath in Single and Two Ion Species Plasmas XU WANG, EUNSUK KO, GREG SEVERN, University of San Diego NOAH HERSHKOWITZ, Dept. of Engineering Physics, University of Wisconsin-Madison The presheath is a region of weak electric field that accelerates ions to satisfy the generalized Bohm criterion. The measurements were performed in multi-dipole plasmas with pure Ar and He-Ar. To measure ion drift velocities in the presheath, a technique by launching ion acoustic wave was developed [1]. The concentration of ion species in two ion species plasma was determined by measuring ion acoustic wave phase velocity and electron temperature in the bulk region [2]. The dispersion relation in the presheath for single ion species was verified by experiments with pure Ar plasma. Based on the dispersion relation in the presheath for multi-ion species plasma and phase velocity measurements in He-Ar plasma ($P_{Ar} \sim 0.1mTorr$, $P_{He} \sim 2.8mTorr$, $n_e \sim 1E9cm^{-3}$, $T_e < 2eV$), the relationship between Ar and He ion drift velocities was determined. Using Ar ion drift velocities from LIF data, the He ion drift velocities were determined from that relationship. *Work supported by US DOE grant DE-FG02-97ER54437 [1] A. M. Hala, Presheaths in two ion species plasma, Ph.D. Thesis (2000). [2] A. M. Hala and N. Hershkovitz, *Rev. Sci. Instrum.* 72, 2279 (2001).

QWP 57 How fast do ions fall into the sheath in a multiple ion species plasma?* GREG SEVERN, *Dept. of Physics, University of San Diego* NOAH HERSHKOWITZ, *Dept. of Engineering Physics, University of Wisconsin-Madison* XU WANG, *Dept. of Engineering Physics, University of Wisconsin-Madison* EUNSUK KO, *Dept. of Engineering Physics, University of Wisconsin-Madison* UW-MADISON, USD SHEATH COLLABORATION In a multiple ion species plasma, it is known that a given ion species reaching the sheath edge may satisfy the generalized Bohm criterion by attaining a speed anywhere along a continuum bounded by speeds much faster than and slower than the single species Bohm speed. We have attacked the problem experimentally using emissive probes and LIF, and have found evidence that ions do not enter the sheath traveling at their respective Bohm speeds. For the case of argon-helium plasmas created in a DC hot filament discharge with magnetic multi-dipole confinement (where the helium and argon ion densities are approximately equal, and the total neutral pressure is of order 1 mTorr) the data suggest that Ar II, upon reaching the sheath, significantly exceeds its own Bohm speed.

*Work supported by DOE grant no.DE-FG02-97ER54437 and NSF grant no. PHY9722658; G.D.S. gratefully acknowledges sabbatical support from the University of Wisconsin-Madison.

QWP 58 Multiterm Treatment and Monte Carlo Simulations of the Electron Kinetics in the Anode Region of Glow Discharge Plasmas DETLEF LOFFHAGEN, FLORIAN SIGENEGER, ROLF WINKLER, *Institut für Niedertemperatur-Plasmaphysik, 17489 Greifswald, Germany* The axial behavior of the electrons in the column-anode plasma region of low-pressure dc glow discharges has been investigated by solving the space-dependent electron Boltzmann equation in multiterm approximation. A recently developed method has been generalized and adopted to evaluate the influence of the anode fall and the accuracy reached by the simpler two-term treatment. In particular, boundary conditions for the multiterm treatment have been derived that take consistently account of a variable degree of electron absorption at the anode. The analysis of the spatial electron behavior shows that the two-term treatment of the kinetic equation can lead to considerable differences from the convergent behavior which is generally obtained by a six- to eight-term approximation of the Legendre polynomial expansion of the electron velocity distribution function. The deviations of the two-term results from the convergent ones depend sensitively on the parameters of the anode fall. They become more pronounced the stronger and more rapid the electric field in the anode fall region increases. The multiterm results are additionally confirmed by the excellent agreement with corresponding results obtained by Monte Carlo simulations.

QWP 59 Plasma diffusion into a picket-fence magnetic field in ARIS FELIPE SOBERON, *Dublin City University* RONAN FAULKNER, *Dublin City University* ALBERT R. ELLINGBOE, *Dublin City University* The formation and extraction of the negative ions of Hydrogen and Deuterium (H- & D-) are of interest for application to Fusion Neutral-Beam Heating and Next Generation Hadron Accelerators. The ARIS experiment has been designed to allow comparison with 2-D plasma simulation for understanding

and optimising the plasma chemistry for the volume production of H- and D-. The system consists of an inductively coupled rf source, a diffusion chamber, and an extraction region. The extraction region consists of a picket-fence magnet array, resulting in dramatically different electron temperatures than in the diffusion-chamber region. Electrostatic probes are used to measure changes in the plasma parameters as a function of source parameters and distance into the picket-fence magnetic field forming the extraction region. Emissive probes, double probes and floating probes yield plasma potential, ion density and hot electron temperature, and cold electron temperature, respectively. Work Supported by EURATOM

QWP 60 PLASMA DIAGNOSTICS II

QWP 61 Ion and neutral particle energies and flight times in mass spectrometric studies of processing plasmas I.D. NEALE, J.A. REES, T.H. RUSSELL, P.J. HATTON, Y. ARANDA GONZALVO, *Hidden Analytical Ltd, 420 Europa Boulevard, Warrington, WA5 7UN, U.K.* The transmission efficiency and time response of instruments employed to examine the ionic and neutral species sampled from processing plasmas are important factors in the design of diagnostic investigations for such plasmas. The time response of a Hidden EQP mass/energy analyser, for both ionic and neutral species sampled from a plasma reactor, has been measured in terms of the flight times of particles through the instrument and of the attainable time resolution. For the ionic species, a pulsed, thermal source of caesium ions generated ions of 5eV incident on the EQP's sampling orifice. The transit times of the ions through the analyser for various values of the instrument's operating parameters were found to be in good agreement with theoretical predictions. The sharpness of the edges of the ion pulses arriving at the instrument's channeltron detector was also examined. For the neutral species, a novel technique demonstrated that the EQP's ionisation source was capable of resolving neutral signals sampled from a pulsed plasma to better than 40 μ sec. The EQP was used in conjunction with a d.c. plasma cell to examine the energies of ions arriving at the cathode electrode when this was biased at around *300 volts at a gas pressure of 320 mTorr (160 < E/P < 200V/cm.Torr). Comparison of the data with an available theoretical model of the cathode sheath region indicated that the ion transmission of the EQP was linear over a range of more than 150eV.

QWP 62 Analysis of Ion Species in N₂ and O₂ inductively Coupled Plasma with Inert Gas Mixing K. H. BAI, D. S. LEE, H. Y. CHANG, *Korea Advanced Institute of Science and Technology* H. S. UHM, *Ajou University* We control the ion density ratio of [N⁺]/[N₂⁺] and investigate the relation between the ion ratio and the plasma parameters in inductively coupled plasma. We measure the electron energy distribution functions and the ion ratio in a N₂ / He,Ar,Xe mixture system as a function of mixing ratio. We can control the [N⁺]/[N₂⁺] ion ratio from 0.002 to 1.4, and the ion ratio is a strong function of the electron temperature. We can calculate the ion ratio using a simple model, and the obtained results agree well with the measured values in N₂ /

He, Ar, but there is a large discrepancy in the N_2/Xe discharge. The non-Maxwellian structure of the electron energy distribution functions may be the reason for the discrepancy. We measure the ion density ratio and plasma parameters in $O_2/He, Xe$ mixture system also. The relation between the ion density ratio of $[O^+]/[O_2^+]$ and plasma parameters shows different trend to that of $N_2/He, Xe$ mixture case.

QWP 63 Stationary Inverted Balmer and Lyman populations for a CW HI water-plasma laser RANDELL L. MILLS, *Black-Light Power, Inc.* PARESH CHANDRA RAY, ROBERT M. MAYO Stationary inverted H Balmer and Lyman populations were observed from a low pressure water-vapor microwave discharge plasma. The ionization and population of excited atomic hydrogen levels was attributed to energy provided by a catalytic resonance energy transfer between hydrogen atoms and molecular oxygen formed in the water plasma. The catalysis mechanism was supported by the observation of O^{2+} and H Balmer line broadening of 55 eV compared to 1 eV for hydrogen alone. The high hydrogen atom temperature with a relatively low electron temperature, $T_e = 2$ eV, exhibited characteristics of cold recombining plasmas. These conditions of a water plasma favored an inverted population in the lower levels. Thus, the catalysis of atomic hydrogen may pump a cw HI laser. From our results, laser oscillations are may be possible from (i) $n = 3, n = 4, n = 5, n = 6, n = 7$, and $n = 8$ to $n = 2$, (ii) $n = 4, n = 5, n = 6$, and $n = 7$ to $n = 3$ and (iii) $n = 5$ and $n = 6$ to $n = 4$. Lines of the Balmer series of $n = 5$, and $n = 6$ to $n = 2$ and the Paschen series of $n = 5$ to $n = 3$ were of particular importance because of the potential to design blue and 1.3 micron infrared lasers, respectively, which are ideal for many communications and microelectronics applications. At a microwave input power of $9W/cm^3$, a collisional radiative model showed that the hydrogen excited state population distribution was consistent with an $n = 1 \rightarrow 5, 6$ pumping power of an unprecedented $200W/cm^3$. High power hydrogen gas lasers are anticipated at wavelengths, over a broad spectral range from far infrared to violet which may be miniaturized to micron dimensions. Such a hydrogen laser represents the first new atomic gas laser in over a decade, and it may prove to be the most efficient, versatile, and useful of all. A further application is the direct generation of electrical power using photovoltaic conversion of the spontaneous or stimulated water vapor plasma emission.

QWP 64 Diagnostics of Stable and Transient Species in CF_4/H_2 Plasmas by Electron Attachment (EAMS)- and Appearance Potential Mass Spectrometry (APMS) VALENTINA KROUTILINA, MARTIN GEIGL, JURGEN MEICHSNER, HANS-ERICH WAGNER, *Institute of Physics, University of Greifswald, D-17489 Greifswald, Germany* LOW TEMPERATURE PLASMA PHYSICS TEAM Transient and stable species, produced from CF_4/H_2 gas mixtures (0-40 % H_2) have been investigated, comparing quite different non-thermal low pressure plasma conditions (50, 120 kHz, 13.56 MHz, parallel plate reactors, closed system). In particular, the temporally resolved synthesis of C_2F_6 , C_3F_8 and CHF_3 as well as the polymer film deposition has been examined. The calibration of the EAMS measurements allowed the estimation of the averaged C/F ratio in the volume and of the deposited layer. Additionally, APMS has been used to trace the time dependence of the CF_x radical density ($x=1-3$) and

higher order stable products C_xF_y ($x \leq 5$) which show the successive composition of long chains from the feeding gas. Therefore, APMS and EAMS give complementary information on stable and transient species in the plasmas under investigation.

QWP 65 Diagnostics of O Atoms in Inductively Coupled O_2 Plasma Employing Vacuum Ultraviolet Absorption Spectroscopy HISAO NAGAI, MASARU HORI, TOSHIO GOTO, *Department of Quantum Engineering, Nagoya University, Japan* MINEO HIRAMATSU, *Department of Electrical and Electronic Engineering, Meijo University, Japan* SEIGOU TAKASHIMA, *Nippon Laser & Electronics LAB., Japan* The compact measurement system for absolute densities of oxygen (O) atom has been developed employing a vacuum ultraviolet absorption spectroscopy (VUVAS) technique with a high-pressure micro-discharge hollow cathode lamp (MHCL) as a light source. The influences of self-absorption, emission line profiles of the MHCL, and the background absorption on determination of absolute O atom density were investigated. This system has been applied for measuring of absolute O atom densities in an inductively coupled O_2 plasma. O atom densities were estimated to be on the order of $4 \times 10^{11} - 4 \times 10^{12} cm^{-3}$, at an O_2 pressure ranging from 1.3 to 26.7 Pa. The behavior of O atom density measured using VUVAS technique was consistent with that obtained by actinometry technique using 844.6 nm and 777.2 nm. Moreover, the lifetime of O atom in the afterglow plasma has been investigated. The decay curves of the O atom density were fitted with exponential functions. The extinction process of O atom in the inductively coupled O_2 plasma is discussed.

QWP 66 Spectroscopic Analysis of Multi-Component Media A. IONIN, A. KOZLOV, A. KOTKOV, L. SELEZNEV, *P.N. Lebedev Physics Institute of Russian Academy of Sciences* S. IVANOV, *Institute of Laser Information Technologies of Russian Academy of Sciences* P.N. LEBEDEV PHYSICS INSTITUTE OF RUSSIAN ACADEMY OF SCIENCES COLLABORATION, INSTITUTE OF LASER INFORMATION TECHNOLOGIES OF RUSSIAN ACADEMY OF SCIENCES COLLABORATION The quantitative analysis of sensitivity and selectivity characteristics for spectroscopic gas and plasma analysis with different mid-infrared molecular lasers (HF, DF and first-overtone (FO) CO lasers) was carried out. The analysis demonstrated that FO CO laser due to its spectral properties is very perspective source of light for laser spectroscopy of multicomponent mixtures, for example, for detecting atmospheric pollutants when remote sensing of environment. The FO CO laser spectral range 2.5-4.2 microns overlaps the transparency window of the atmosphere in the wavelength range 3-4 microns and covers that of HF and DF lasers, with its ro-vibrational line spacing being several times less than that of those lasers. The FO CO laser spectral lines coincide with a large number of absorption lines belonging to numerous organic and non-organic substances which can be found both in the atmosphere and atmospheric plasma. The linear and nonlinear absorption of the FO CO laser by different gaseous substances was calculated and compared with the experimental data.

QWP 67 Pulsed Discharge Dissociation of Methane in Methane/Argon Mixtures MICHAEL BROWN, ROBERT FORELINES, *Innovative Scientific Solutions, Inc. Dayton, OH* BISWA GANGULY, *Air Force Research Laboratory, Wright-Patterson AFB* Pulsed DC discharges are generated (15 ns rise time, 2-4 kV peak voltage, 50-Hz rate) in variable-electrode-gap pyrex tubes between 30 and 100 Torr. After breakdown, a quasi

steady-state discharge (duration controlled by high-speed switch) characterized by a nearly constant voltage and current is achieved. In argon/methane mixtures at 90 Torr with a 200-ns pulse width, E/n climbs rapidly from 25 Td for pure Ar to 120 Td for 20% added CH_4 . With increasing CH_4 addition, E/n climbs slowly to 125 Td for 100% methane. At fixed pressure in 20% methane, the average E/n drops by 30% or more with a pulse width increase to 600 ns. In 100% methane time-averaged spatially-resolved (2-D) emission from H, CH and C_2 exhibit peak intensities near the cathode surface. With dilution by argon the peak emission intensities move toward the discharge midplane. For a 3-mm gap, the Ar emission peaks between 1.5 and 1.8 mm from the cathode while the dissociated species exhibit peak intensities closer to the cathode (0.6-1.2 mm). Both CH and C_2 appear vibrationally hot. In pure methane, the C_2 vibrational temperature (T_{vib}) rises above 10,000 K at 90 Torr. Peak T_{vib} is found closer to the cathode than peak emission intensities. With up to 80% Ar addition, peak T_{vib} drops to 7200 K and then rises to 7800 K with addition to 95%. High internal energy deposition into molecular excited states via direct electron impact dissociation has implications for plasma-assisted combustion.

QWP 68 Diagnostics of Surface Wave Nitrogen Discharge Generated by Slot Antenna Plasma Source REO TOYOYOSHI, TAKESHI SAKAMOTO, HARUAKI MATSUURA, HIROSHI AKATSUKA, *Research Laboratory for Nuclear Reactors, Tokyo Institute of Technology* We generated nitrogen plasma, introducing microwave power into a vacuum chamber by a slot antenna through a quartz window. The plasma discharge was sufficiently stable and generated continuously. We set the microwave power at 600 W with the discharge pressure about 0.3 – 1.0 Torr, feeding pure nitrogen gas. We measured intensity of emission spectrum of second positive system ($\text{C}^3\Pi_u - \text{B}^3\Pi_g$) of nitrogen molecule, at the center of the circular quartz window by a monochromator calibrated absolutely. Population densities of the vibrationally excited levels of the C state were measured, and we obtained its vibrational temperature. In addition, we numerically calculated the overall emission spectra by taking the overlaps of the rotational spectra into account. Consequently, we obtained the rotational temperature by comparing the calculated spectra with the experimental ones. As a result, it was found that the vibrational temperature was about 0.67 – 0.86 eV under the discharge pressure 0.3 – 1.0 Torr, and that it decreased as the discharge pressure increased. On the other hand, the rotational temperature was found to be 0.13 – 0.14 eV, which was almost constant irrespective of the discharge pressure.

QWP 69 Gas Temperature in Low Pressure Discharges by Laser Absorption Spectroscopy PHIL MOSKOWITZ, *Osrsm Sylvania, Beverly, MA 01915* The gas temperature in low pressure (<3 Torr) Ar and low pressure (<0.1 Torr) Hg discharges was measured using the spectral width of Doppler broadened absorption lines. Either a CW diode or dye laser was tuned thru the transition (810.3nm in Ar, 435.8nm in Hg), with the laser beam traversing a diameter of the 50mm diameter cylindrical glass discharge chambers. In these low pressure discharges, the neutral atoms and ions are not in equilibrium with the electrons, and the rates for collisional energy transfer between the two groups depends on the electron density and the electron energy distribution. In general, the atoms thermal velocity can be ten to a hundred times smaller (500 m/s for argon) than the electron's (20,000 m/s for a 1eV electron). This translates into atom temperatures of

several hundred °C. Knowledge of the gas temperature can serve as a check on the energy balance of the discharge, and data are compared with collisional-radiative discharge models currently under development. Estimates of electron density using these data and independent knowledge of the electron temperature are compared with Langmuir probe and microwave interferometer data.¹

¹R.C. Garner and R.B. Piejak, 2002, The 29th Int'l Conf. on Plasma Science, Banff, Alberta, Canada, paper 5P34.

QWP 70 Time Resolved Rotational Temperature Measurements of N_2 and N_2^+ in a Pulsed ICP* C. A. DEJOSEPH, JR., *Air Force Research Laboratory, Wright-Patterson AFB, OH* WEI GUO, *Innovative Scientific Solutions, Inc., Dayton, OH* JEFFRY HEGGEMEIER, *Dept. of Electrical Engineering, Univ. of Minnesota* A planar inductively coupled plasma (ICP) source is operated at 13.56MHz with 100% power modulation of the rf supply. Repetition rate and duty cycle are variable but typical values are 1KHz and 25%. A half-meter spectrometer with a gated, intensified CCD array is used to acquire time resolved emission spectra from the $\text{N}_2(\text{C-B})$ and the $\text{N}_2^+(\text{B-X})$ band systems at pressures of 10-20 mTorr in pure N_2 . The limited spectral resolution of the system (0.1 nm) and the complexity of the emission prevent using "Boltzmann plots" to obtain rotational temperatures, so a computed spectrum is least-squares fit to the measured band contours. The computed spectrum is a detailed line-by-line calculation convolved with the spectrometer instrumental line shape function. Spectra containing overlapping bands from both systems can be fit simultaneously with different temperatures assigned to each system. Rotational temperatures obtained for each band system at gate widths of 0.5 μs and gate delays over the time span of the rf pulse will be presented. These data will be compared with time resolved rf power, complex impedance, and Langmuir probe measurements.

*This work supported by Air Force Office of Scientific Research.

QWP 71 LASER MEDIA AND KINETICS

QWP 72 Plasma Composition of an Electrical Discharge in SF_6 Gas and $\text{SF}_6/\text{C}_n\text{H}_m$ Mixtures SERGUEI GORTCHAKOV, *Institut für Niedertemperatur-Plasmaphysik, 17489 Greifswald, Germany* YURI BYCHKOV, ARKADY YASTREMSKY, *Institute of High Current Electronics, 634055 Tomsk, Russia* Electrical discharges in SF_6 and its mixtures are mainly used as an active medium of pulsed chemical HF lasers. Despite of the progress in development of these lasers, some physical phenomena occurring in the discharge plasma are studied insufficiently. Investigations of e-beam pumped systems have demonstrated an effect of e-beam cutoff caused by the decrease of the plasma conductivity due to accumulation of negative charge carriers through the conversion of thermal electrons into the SF_n^- ions in attachment processes. Experimentally detected effects in discharge excited systems—unipolarity of the discharge current, high value of the residual voltage, and peculiarities of the discharge contraction process—

indicate that the growth of discharge current density accelerate such conversion. As a result the density of negative ions is higher than that of the electrons. In order to investigate the dynamics of charge carriers production and loss in discharge excited systems a self-consistent numerical model has been developed. Results of simulations of a homogeneous and an inhomogeneous discharge in $SF_6/(C_2H_6, C_6H_{14})$ and a comparison with experimental data are presented and discussed.

QWP 73 LIGHT SOURCES II

QWP 74 Radial variations of the plasma properties in a low-pressure Hg-Ar discharge GEORGE PETROV, *Berkeley Scholars, Inc., P.O.Box 852, Springfield, VA 22150* JOHN GIULIANI, *Plasma Physics Division, Naval Research Laboratory, Washington, DC, 20375* Mercury-rare gas discharge at low mercury pressure and moderate argon pressure has been modeled. The model is based on a 1D Boltzmann code selfconsistently coupled to equations for excited species and ions in a cylindrical geometry. The results describe the radial structure of the discharge, including the emission of 254 nm and 185 nm UV radiation. Summarizing the results of wide-range variations of external parameters such as Hg pressure and discharge current, we conclude that (i) the electron energy distribution function (EEDF) is strongly nonlocal (former models based on the local EEDF do not account for radial variations); (ii) the excitation and ionization rates peak near the center and the excited states densities deviate from Bessel profile, particularly those for the resonance and highly excited states and (iii) there is a substantial power transfer from one part of the discharge to another due to electron thermal flux. Comparison with existing experimental data demonstrate agreement with global properties such as power absorption per unit length and UV radiation, but the species population are calculated to be more centrally peaked than the limited data indicate.

QWP 75 Species Distributions in a Ceramic Rare-Earth Metal-Halide Lamp Using X-ray Induced Fluorescence*

JOHN J. CURRY, *National Institute of Standards and Technology, Gaithersburg, MD 20899* HELMAR G. ADLER, *Osram Sylva, Beverly, MA 01915* We have used x-ray induced fluorescence to determine the spatial distributions of elemental components in a ceramic metal-halide arc lamp dosed with DyI_3 and CsI . The distribution of Hg, in combination with optically obtained wall temperatures, has been used to determine the absolute gas temperature distribution in the arc. We have used our experimentally determined elemental densities and gas temperatures to derive atomic, ionic, and molecular species distributions based on thermo-chemical data from the literature.

*A portion of this work was performed while JJC was with the Physics Department, University of Wisconsin. Work at the University of Wisconsin was supported by OSRAM SYLVANIA.

QWP 76 Microwave Discharge Characteristics of Plasma Lighting System BYEONG-JU PARK, JOON-SIK CHOI, HYOSIK JEON, JI-YOUNG LEE, HYUN-JUNG KIM, YONG-SEOG JEON, *LG Electronics Inc.* PLS (plasma lighting system) is an electrode-less light source to provide visible light of continuous spectrum with high power efficiency. The light source comprises a bulb containing a plasma forming medium. When the bulb is placed in a microwave energy field, the field ionizes buffer gas within the bulb. A low pressure plasma discharge forms within the bulb, heating the bulb wall, vaporizing materials such as sulfur within the bulb to generate light. The goal of our experiment is to achieve higher light-conversion efficiency. For this work, we studied experimentally the microwave discharge characteristics in the PLS.

QWP 77 UV radiation sources operating in an abnormal microdischarge regime S.A. STAROSTIN, S.V. MITKO, P.J.M. PETERS, K.J. BOLLER, *Chair of Laser Physics, University of Twente, P.O.Box 217, 7500 AE Enschede, The Netherlands* YU.B. UDALOV, *NCLR B.V., P.O.Box 2662, 7500 CR Enschede, The Netherlands* Recently we proposed a new design approach for microdischarge plasma sources and microdischarge arrays [1]. The major improvement comes from the fact that the ceramic dielectric layer is sintered directly on the metal cathode. The discharge channels are drilled in the dielectric layer mechanically or by laser. This design approach excludes the undesirable cathode spot spread, which usually occurs if dielectric is mechanically pressed on the cathode surface. Another advantage is a possibility of efficient cooling. The electrical characteristics of a single microdischarge and microdischarge array operating in abnormal regime were investigated in different gas mixtures (He, Ar, Xe, He-Ar-Xe, He-Xe-HCl) at different gas pressures and configurations of the discharge set-up. The studied set-up allows to achieve discharge voltages up to 2kV in continuous wave DC mode at gas pressures of 100-200 mbar in He or He-Xe gas mixtures. The obtained results indicate that this kind of discharge can be considered as a low-energy electron-beam source. It can be used for efficient pumping of gas lasers (for instance atomic Xe) or for large area planar VUV light sources based on excimers with relatively high excitation threshold (for instance He_2 or Ne_2 dimers).
1. RU.Patent N° 2172573

QWP 78 Study of Far Field Surface Irradiance Distributions by Nonuniform Ultraviolet (UV) Sources

MARK RUCKMAN, BORIS GELLER, MIKE AROUTUNOV, PEDRO LEZCANO, ED DAVIS, MIODRAG CEKIC, *Fusion UV Systems, Gaithersburg, MD 20878* There is renewed interest in applying high power microwave driven Hg and metal halide-filled Ar plasma sources for the UV treatment of 3D objects in the far field. Irradiance and absorbed energy are critical factors controlling the treatment process. However, the radiant flux from the plasma is nonuniform, a function of the atomic emission line and a function of microwave power. A scanning radiometer was used to map the far field irradiance over a 4 m^2 area. The microwave power and distance were varied. An imaging spectrophotometer was used to acquire radiant flux distributions for selected Hg and metal emission lines as a function of position along the bulb axis. The same spectrophotometer was used to analyze the spectra of the lamps under various operating conditions. Examination of the lamp spectra indicated changes in the plasma chemistry, density and temperature as a function of micro-

wave power. Differences in the far field irradiance patterns are seen between Hg and metal halide-filled bulbs and for metal halide-filled bulbs operated at different power levels.

QWP 79 Modelling and experimental characterisation of electrical breakdown in discharge lamps WOUTER BROK, TUE JAN VAN DIJK, TUE MAXIME GENDRE, TUE HUUB VAN DEN NIEUWENHUIZEN, CDL TED VOS,* MARCO HAVERLAG, CDL JOOST VAN DER MULLEN, TUE GERRIT KROESEN, TUE TUE: EINDHOVEN UNIVERSITY OF TECHNOLOGY COLLABORATION, CDL: PHILIPS CENTRAL DEVELOPMENT LIGHTING COLLABORATION A 2-D fluid model, which has originally been developed for microdischarges, has been used to simulate the electrical breakdown in tubular discharge lamps (length: 10 cm, inner diameter: 10 mm) with heated electrodes. The emission of the lamp is imaged on a fast, gateable, CCD camera. The experiments have been done by gating the camera briefly after an adjustable delay which follows the voltage step which is applied to the electrode. In order to increase the signal/noise ratio, several voltage steps are integrated before the delay is modified. By scanning the delay, a 2-D film of the plasma emission during the breakdown can be recorded. This emission can be compared to the ionisation rate, which is predicted by the model. During the forward strike (cathode to anode), the models and the experiments agree very well. During the following backward strike (anode to cathode), the agreement is less good, which is probably due to non-Maxwellian electron energy distributions.

*CDL

QWP 80 Excimer Emission from Argon Microhollow Cathode Discharges* MOHAMED MOSELHY, KARL H. SCHOENBACH, *Physical Electronics Research Institute, Old Dominion University* Excimer emission from direct current microhollow cathode discharges had been studied for rare gases and mixtures of rare gases and halides as working gases [1]. In static xenon, the dc efficiency was measured as 6%-9%. In static argon, however, the efficiency is only on the order of 1%. This relatively low value was found to be due to excimer quenching processes caused by impurities. By flowing the argon, rather than operating under static conditions we could increase the efficiency to 6%. Applying a 10 ns pulse of 600 V to the DC discharge in argon resulted in an increased intensity by a factor of six. The decay time for argon excimer emission was found to be 500 ns, indicating that quenching processes even with purging of the discharge chamber are still more effective by a factor of six in depopulating the excimer level than excimer radiation. The major quenching effect is based on resonant energy transfer from the argon excimer to atomic oxygen [2]. The addition of small amounts of oxygen allowed us therefore to convert the argon excimer emission centered at 128 nm into narrowband emission at 130.4 nm (oxygen triplet) with an optical power of up to 13 mW. This material was supported by NSF (CTS-0078618). [1] Karl H. Schoenbach, Ahmed El-Habachi, Mohamed M. Moselhy, Wenhui Shi, and Robert H. Stark, *Physics of Plasmas* 7, 2186 (2000). [2] M. Moselhy, R.H. Stark, K.H. Schoenbach, and U. Kogelschatz, *Appl. Phys. Lett.* 78, 880 (2001).

QWP 81 HIGH-PRESSURE NONTHERMAL PLASMAS II

QWP 82 Radio frequency atmospheric pressure plasma in Argon* NAVIN MUTHUSWAMI, *Electrical Engineering, Southern Illinois University* BIJAN PASHAIE, *Southeast Missouri University* SHIRSHAK DHALI, *Electrical Engineering, Southern Illinois University* Experimental results from a dielectric-barrier type discharge driven by RF are discussed. The discharge is produced under ambient conditions. The discharge produces an afterglow in Argon and Argon mixtures with oxygen and hydrogen. Although the discharge is easier to strike in Helium, the afterglow does not persist in the ambient. By increasing the Argon gas flow and power input, the afterglow can be extended further in the atmosphere. The long lived species of argon can be used to carry out plasma chemical reactions in the ambient. These discharges have the potential for industrial application. Results from plasma treatment of steel surfaces prior to coating will be discussed.

*Supported by the National Science Foundation

QWP 83 Small scale micro-discharge in Xe dielectric barrier discharge HARUAKI AKASHI, *Dept. of Applied Physics, National Defense Academy of Japan* AKINORI ODA, *Dept. of Systems Eng., Nagoya Institute of Technology* HARUMI ENDO, *Dept. of Applied Physics, National Defense Academy of Japan* YOSUKE SAKAI, *Dept. of Electronic Material Eng., Hokkaido University* Small scale micro-discharges in a Xe dielectric barrier discharge (DBD) has been analyzed using one dimensional fluid model. Fast rise rectangular ac voltage is applied to the discharge gap in high pressure condition. As a result, extremely, asymmetric micro-discharges were obtained in first and second half of the cycle. The electron density is also obtained asymmetric in a wide gap (1cm) discharge, but it is slightly asymmetric. In a narrow gap (0.1cm) DBD, to obtain filamentary discharge, high applied voltage is required. Then, electron density near the powered electrode increases significantly, when the voltage of the powered electrode was changed from positive to negative. Accumulated charges on the dielectrics also influenced micro-discharge's asymmetry in significant. In the first half cycle, electron density stayed low in the gap. In the second half of the cycle, the maximum value of electron density is about 20 times higher than that in wide gap case applying about the same amplitude of voltage in narrow gap case. The electron density is about twice higher in the bulk region than that in a wide gap. Similar to electron density, about twice higher excimer density is obtained in bulk region, and about 20 times higher in maximum value in the second half of the cycle. However, in the first half of cycle, excimer density in the bulk region is obtained in about the same value as in wide gap case.

QWP 84 PSPICE SIMULATION OF ONE ATMOSPHERE UNIFORM GLOW DISCHARGE PLASMA REACTOR SYSTEMS* ZHIYU CHEN, *UT Plasma Sciences Laboratory, University of Tennessee* J. REECE ROTH, *UT Plasma Sciences Laboratory, University of Tennessee* PLASMA SCIENCES LABORATORY COLLABORATION We have used the PSpice software to provide a comprehensive simulation of the electrical characteristics of a One Atmosphere Uniform Glow Discharge

Plasma (OAUGDP) reactor system, including the power supply, the impedance matching network, and the plasma reactor. The OAUGDP reactor consists of two parallel electrode plates with a small gap between them. At least one electrode is covered with a dielectric plate, which can be modeled as a capacitor, as can the gap containing the plasma. The plasma discharge itself is modeled as a voltage-controlled current source that is switched on as long as the voltage across the gap exceeds the breakdown voltage. The current source and its output current follow a power law, characteristic of the voltage-current behavior of a normal glow discharge. Simulation results agree well with the experimental data. It has been found that at different plasma operating conditions, the discharge current of OAUGDP is described by different power laws, and the exponent in the power law affects the shape of the modeled discharge current waveform.

*Supported in part by AFOSR contract AF F49620-01-1-0425 (Roth)

QWP 85 Determination of NO₂ production by a DBD discharge in air by means of TDLAS F. FRESNET, F. JORAND, S. PASQUIERS, A. ROUSSEAU, *LPGP, Univ. Paris-Sud / CNRS, 91405 Orsay, France* J. RÖPCKE, *Institute of Low Temperature Plasma Physic, 17489 Greifswald, Germany* It has been already demonstrated that dielectric barrier discharges (DBD) are well suited for flue gas cleaning, in particular removal of NO in air at atmospheric pressure. However NO can be also produced by the discharge, at a concentration depending on parameters such as the gas temperature, the frequency of the electrical excitation pulse, the energy density deposited in the plasma per pulse. In many cases, NO is mainly converted in NO₂ owing to oxidation reactions with ozone. We present absolute measurement of the NO₂ concentration at the exit of a DBD reactor, using the TDLAS technique. Three NO₂ lines around 1626 cm⁻¹ are used for absorption measurements, and the minimum concentration which can be measured with the laser device is 50 ppb. The DBD is produced by a voltage pulse (20-40 kV) between two plane electrodes, one of them recovered by a glass plate, at a repetition frequency up to 200 Hz. The discharge volume is 6.6 cm³ and the maximum air flux is 45 cm³/sec at ambient temperature. Influence of the pulse frequency, of the energy per pulse, of the air flux, and of the water vapor concentration in air on the NO₂ production are reported and discussed.

QWP 86 Spectroscopic investigation of dielectric barrier discharges in nitrogen, helium and neon HANS-ERICH WAGNER, *Institute of Physics, University of Greifswald, Domstrasse 10a, D-17493 Greifswald, Germany* RONNY BRANDENBURG, *Institute of Physics, University of Greifswald* KIRILL V. KOZLOV, *Moscow State University, Department of Chemistry, Russia* NICOLAS GHERARDI, *Labaratoire de Genie Electrique Toulouse, France* PETER MICHEL, *Institute of Physics, University of Greifswald* CATHERINE KHAMPAN, *CPPIA Toulouse, France* FRANÇOISE MASSINES, *Labaratoire de Genie Electrique Toulouse, France* DAVID TRUNEC, *Department. of Physical Electronics, University of Brno, Czech Republik* Dielectric barrier discharges can be operated in a diffuse (glow-like) mode at atmospheric pressure in nitrogen, helium and neon, provided that the feeding sinusoidal voltage is within the kHz range. These homogeneous discharges have been investigated by spatio-temporally resolved emission spectroscopy. The analysis of experimental data including their comparison with the corresponding results of numerical modelling enables to clarify the mechanisms

of discharge development. These mechanisms appear to be essentially different for the cases of noble gases and nitrogen. For example in nitrogen the maximum of light intensity is located at the anode, while in helium and neon a cathode directed propagation of a luminosity wave is observed.

QWP 87 Optical and electrical measurements of a highly asymmetric dielectric barrier discharge for flow control on aerodynamic surfaces C. L. ENLOE, *Department of Physics, USAF Academy* T. E. McLAUGHLIN, R. D. VANDYKEN, *Department of Aeronautics, USAF Academy* A dielectric barrier discharge using a highly asymmetric electrode configuration and a single dielectric barrier is a candidate for no-moving-parts flow control on aerodynamic surfaces, since the plasma in this configuration has been shown to impart significant momentum to the surrounding air. A chief concern in understanding this effect is the mechanism for the momentum transfer. We present optical and electrical measurements which indicate that there is a substantial difference in the spatial structure of the plasma between the different halves of the AC discharge cycle for a number of waveforms. We show that, to lowest order, the momentum transfer is proportional to the plasma density, supporting an interaction mechanism via the discharge current directly, rather than through an electric field interaction with the bulk plasma, as some have suggested.

QWP 88 Energy regeneration from vibrationally excited methane in catalyst enhanced barrier discharges TOMOHIRO NOZAKI, NAHOKO MUTO, SHIGERU KADO, KEN OKAZAKI, *Department of Mechanical and Control Engineering, Tokyo Institute of Technology* Vibrationally excited species are the most abundant in methane-fed barrier discharges due to relatively low electron temperatures (≈ 5 eV). In the most cases, those excited energy is wasted as heat due to low reactivity. On the other hand, vibrationally excited methane show high-reactivity on a specific transition metal catalyst to dissociation. And we investigated energy regeneration from vibrationally excited methane in catalyst enhanced barrier discharges. The coaxial barrier discharge reactor packed with pellets of either SiO₂ or 3wt%Ni/SiO₂ was used for this purpose. Methane and water-vapor mixture was fed into the reactor at 200, 400, 600 degC. Catalyst could not activated at 200 degC, so plasma reaction (main products: C₂H₆, C₃H₈) become dominant. At 600 degC catalyst reaction was dominant, so main products were CO₂ and H₂. Most significant plasma and catalyst interaction was observed at 400 degC. Under this condition, methane dissociation by plasma and catalyst was expected.

QWP 89 Calculated ion and neutral energy flux distributions to the surface in plasma display panel cells in Xe/Ne mixtures D. PISCITELLI, I. REVEL, L.C. PITCHFORD, J.-P. BOEUF, *CPAT-CNRS, Univ. P. Sabatier, Toulouse, France* The purpose of this work is to evaluate the influence of different operating conditions on the sputtering rate of the MgO layer covering the dielectric surfaces in Plasma Display Panels (PDP's) in Xe/Ne mixtures. Sputtering of the MgO layer, caused by impacting ions and fast neutrals, is a lifetime limiting factor in PDP's. We use a one-dimensional electrical model to determine the electric field and ionization source term as functions of position and time during one discharge pulse in steady-state operation. This information is then input to a Monte Carlo simulation, from which we determine the time-integrated energy distributions of the fluxes of the heavy

particles to the surface. From these results and an estimate of the sputtering yields of MgO, we predict that the lifetime of the MgO layer can be increased by increasing the xenon concentration in the mixture up to a maximum near 20% Xe. The effect of other parameters (gas pressure, operating voltage, dielectric capacitance) has also been evaluated.

QWP 90 BIOLOGICAL APPLICATIONS OF PLASMAS

QWP 91 Surface Investigation of Bone Tissue Treated with Non-thermal Plasmas J.-C. CIGAL, C.Y.M. MAURICE, E. WAGENAARS, L.J. VAN IJZENDOORN, A.H.F.M. BAEDE, E. STOFFELS, *Department of Physics, Eindhoven University of Technology, 5600 MB Eindhoven, The Netherlands* R. HUISKES, *Department of Biomedical Engineering, Eindhoven University of Technology, 5600 MB Eindhoven, The Netherlands* G.M.W. KROESEN, *Department of Physics, Eindhoven University of Technology, 5600 MB Eindhoven, The Netherlands* Plasma treatment of bio-materials is a technique directly derived from material surface processing. In future it may lead to a plasma-based cure for various skin and bone diseases. Non-thermal atmospheric plasmas for medical treatment have been developed. In this work we use a low-pressure discharge as a model case to study plasma interactions with bone tissue. The samples have been exposed to the plasma, using different gases (argon, krypton, helium, and oxygen in mixture) and analyzed using infrared spectroscopic ellipsometry. This technique gives accurate information on the chemical composition of the surface of the tissue. Results have been compared with EDX, environmental scanning electron microscopy (ESEM), and nano-indentation. We have also performed some ion beam diagnostics like RBS and ERDA. These complementary experiments allow us to determine the elemental composition of the bone tissue. The particular effects of plasma treatment on the tissue can be related to the plasma parameters.

QWP 92 Interactions of the plasma needle with cells in culture E. STOFFELS, *Department of Physics, Eindhoven University of Technology, 5600 MB Eindhoven, The Netherlands* J.L.V. BROERS, *Department of Molecular Cell Biology, University of Maastricht, The Netherlands* S. KUNTS, *Optical Radiation Laboratory, High Current Electronics Institute, 634055 Tomsk, Russia* R.A.A. CORNELIS, V. CAUBET, F.C.S. RAMAEKERS, *Department of Molecular Cell Biology, University of Maastricht, The Netherlands* A non-thermal atmospheric plasma source (plasma needle) has been developed. This plasma operates at room temperature, low voltages and power levels, so it can be applied for fine treatment of organic material. In this work the impact of the plasma needle on living cells is explored. For this purpose CHO-K1 (Chinese hamster ovary) cells in culture have been plasma-treated and their responses have been recorded by means of propidium iodide staining. Plasma treatment at low to intermediate power levels leads to damage of the DNA in the cell nucleus, which causes cell death. Characteristic features are high precision of plasma action (influenced cells are strictly localized) and induction of cell death without destroying the cell integrity. Possibilities of using plasma treatment for removal of unwanted cells (e.g. cancer cells) will be investigated.

QWP 93 Interaction of a plasma with bone tissue JEAN-CHARLES CIGAL, TUE ERIK WAGENAARS, TUE LOEK BAEDE, TUE CAROLE MAURICE, TUE LEO VAN IJZENDOORN, TUE RAINER GROETZSCHEL, FZR WOLFHARD MOELLER, FZR GERRIT KROESEN, TUE TUE: EINDHOVEN UNIVERSITY OF TECHNOLOGY COLLABORATION, FZR: FORSCHUNGSZENTRUM ROSSENDORF, DRESDEN COLLABORATION An inductively coupled plasma has been used to treat bone surfaces. This discharge geometry has been chosen because it offers independent control of the energy and the flux of the ions bombarding the surface. The long-term goal of this research is to investigate the perspective for plasma-based medical treatments. The bone surface has been characterised with spectroscopic infrared ellipsometry, RBS and ERDA. The hardness and elasticity modulus have been determined with nano-indentation. The experimental data shows that the penetration depth of the plasma treatment is a few hundred nanometers. The organic compounds (in e.g. the collagen) are most strongly affected. There is a good correlation between the infrared behavior and the elemental analysis techniques. An analysis of all data will be presented.

SESSION RR1: INSTABILITIES

Thursday morning, 17 October 2002; North Forum, Millennium Hotel at 8:00; M. M. Turner, Dublin City University, Ireland, presiding

Invited Papers

8:00

RR1 1 Instabilities in inductive discharges in reactive gases.

PASCAL CHABERT, *Laboratoire de Physique et Technologie des Plasmas, Ecole Polytechnique, France*

High-density inductively coupled plasmas (ICP) are routinely used for etching in the microelectronics industry. Since there is a substantial voltage across the non-resonant inductive coil, a fraction of the discharge power is deposited capacitively. The real inductive discharge can therefore exist in two different modes: the capacitive mode (E mode), for low power, and the inductive mode (H mode), for high power. As the power is increased, transitions from capacitive to inductive modes (E-H transitions) are observed. Tuszewski (Journal of Applied Physics, 1996) found that when operating with reactive gases containing negative ions the transition can be unstable, and a wide range of powers exist where the discharge oscillates between higher and lower electron density states. Later, Lieberman and co-workers (Lieberman et al., Applied Physics Letters 1999, and Chabert et al. Plasma Sources Sci. and Technol. 2001) proposed a model of this instability, based on particle and energy balance, showing the crucial role of negative ions in the instability process. This paper will present recent experimental and theoretical work in this area. Oscillations in the unsaturated radical (CF and CF₂ in a CF₄ inductive discharge) concentrations were measured during the instability by time-resolved laser induced fluorescence, showing that neutral species dynamics can be significant. On the theoretical side, conditions for the stability of inductive discharges with electronegative gases were derived from the model.

Contributed Papers

8:30

RR1 2 Characterization of Instabilities in Inductively Coupled Plasmas*

A.M. MARAKHTANOV, A.J. LICHTENBERG, M.A. LIEBERMAN, *Department of EECS, University of California, Berkeley, CA 94720* M. TUSZEWSKI, *Los Alamos National Laboratory, Los Alamos, NM 87545* P. CHABERT, *LPTP, Ecole Polytechnique, Palaiseau, France 91128* We present new studies of plasma instabilities in inductive discharges using SF₆ and Ar/SF₆ gases. Instabilities occur in transition from capacitive to inductive mode of the discharge [1]. The capacitive coupling plays a crucial role in the instability process. A variable electrostatic (Faraday) shield has been used to control the capacitive coupling from the excitation coil to the plasma. An increase of the shielded area reduces the capacitive coupling and leads to the reduction of stable capacitive and unstable regions of the discharge. The plasma instability disappears when the shielded area exceeds 65% of the total area of the coil. A global model of instability gives slightly higher value of 85% for instability suppression with the same discharge conditions (Ar/SF₆ 1:1, 5 mTorr). The variations of plasma parameters have been explored for Ar/SF₆ gas pressures between 5 and 40 mTorr. Space and time variations of plasma density have been observed at higher pressures during the instability. The instability decays toward the center of the chamber more rapidly as the gas pressure increases. Weaker plasma instabilities have been also observed in pure inductive discharges for an Ar/SF₆ gas pressure above 20 mTorr. This weaker instability, not related to the E-H transition, is probably an attachment instability. Measurements of the chemical composition of the plasma have allowed improvements in the instability model. [1] P. Chabert, A.J. Lichtenberg, M.A. Lieberman, and A.M. Marakhtanov, Plasma Sources Sci. Technol. 10, 478 (2001).

*Work supported by the State of California UC-SMART Program under Contract 97-01

8:45

RR1 3 Instabilities in a Dielectric Barrier Discharge at Atmospheric Pressure

EUGEN ALDEA, *Eindhoven University of Technology, Dept of Applied Physics* C.P.G. SCHRAUWEN, *TNO TPD, Division Models and Processes* M.C.M. VAN DE SANDEN, *Eindhoven University of Technology, Dept of Applied Physics* Due to their enormous potential for cost-efficient industrial applications, atmospheric low temperature (300-500 K) plasmas generated in dielectric barrier configuration received large attention in recent years. The generation of homogeneous plasma at atmospheric pressure is assumed to be related to the gas pre-breakdown pre-ionisation by metastable-metastable collisions, but there are not yet unambiguous experimental evidences of a significant pre-ionization due to this mechanism. In this paper the work was focussed on the investigation of the role of metastables in the excitation or ionisation processes in a atmospheric plasma generated in Ar, nitrogen and air between two electrodes (electrode gap 0.3-5 mm) covered by a dielectric mounted in a gas tight cabinet. The importance of metastables is evaluated on basis of the plasma rovibrational and excitation temperatures derived from the optical emission spectroscopic data, and on the study of the correlation between temporal dependence of the plasma emission and of the current pulse. It is demonstrated that metastable-metastable collisions cannot be responsible for a significant pre-ionization and that other factors are playing a key role in plasma stability.

9:00

RR1 4 Light emission and charged particle modulations in an inductively coupled Ar/Cl₂ discharge

C.S. CORR, P.G. STEEN, W.G. GRAHAM, *Queens University Belfast* A number of authors, including ourselves, have reported modulation of the light intensity and electrostatic probe measurements in inductively coupled discharges operating with electronegative gases. In our inductively coupled discharge in pure Cl₂, when optimally matched, we find no evidence for these modulations over a broad range of operating conditions. Modulations are observed when argon is introduced. In fact the frequency and amplitude of the modulations are sensitive

to the operating pressure, argon fraction and input power. We find that the addition of argon to a chlorine discharge leads to an increase in electron density and decrease in the negative ion fraction. When operating in Ar/Cl₂ mixtures where the modulations are observed the negative ion percentage is about 50 %. Under the

same operating conditions the negative ion percentage can reach values of 80 % in pure Cl₂ while the total negative ion density remained in the order of $1.5 \times 10^{10} \text{ cm}^{-3}$. Time-resolved measurements confirm that the modulations in the negative ion densities, charged particle densities and light emission are correlated.

SESSION RR2: COLLISIONS WITH COMPLEX TARGETS

Thursday morning, 17 October 2002; Center Forum, Millennium Hotel at 8:00; Carl Winstead, California Institute of Technology, presiding

Invited Papers

8:00

RR2 1 Electron Momentum Spectroscopy and Density Functional Theory Studies into Complex Organic Molecules.

MICHAEL BRUNGER,* *SoCPES, Flinders University of SA, GPO Box 2100, Adelaide, SA 5001 Australia*

We report on results from our High-Resolution Electron Momentum Spectroscopy (HREMS) studies and Density Functional Theory (DFT) calculations into the complete valence electronic structures of norbornadiene (C₇H₈), norbornene (C₇H₁₀) and 2,6-stelladione (C₈H₈O₂). Representative examples of our measured and calculated momentum distributions (MDs), and a comparison between them, for each of the molecules we studied are presented. In addition, some of the important physico-chemical properties of both norbornadiene and norbornene, that we derived from these studies, are also presented and discussed. These latter results are compared against corresponding values from independent measurements and calculations.

*Other contributors: Kate Nixon, Laurence Campbell, Heather Mackenzie-Ross, Feng Wang, Bill Appelbe, Rolf Gleiter, David Winkler.

8:30

RR2 2 Electron Scattering with Complex Targets: Gas-Phase Similarities vs. Interference and Many Body Effects.

THOMAS ORLANDO,* *School of Chemistry and Biochemistry and School of Physics, Georgia Institute of Technology, Atlanta, GA 30332*

The physics and chemistry associated with desorption induced by electronic transitions, particularly electron stimulated desorption (ESD), is the basis for electron-beam induced processes in materials growth and etching, lithography, and hot-electron induced defects in devices. We have recently demonstrated experimentally and theoretically that total ESD yield of Cl⁺ from Cl-terminated Si(111) is a function of incident electron-beam direction. We refer to this phenomena as Diffraction in Electron Stimulated Desorption (DESD). The fine-structure in the desorption yields is due to quantum-mechanical scattering and interference of the incident electron to form a surface standing wave in the initial state of the desorption process. This electron standing wave exhibits spatially localized maxima and minima in the electron density. Whether a particular site or domain on a surface experiences a maximum or a minimum depends on i) the electron energy (wavelength), ii) the electron direction of incidence and iii) the arrangement of nearest-neighbor atoms. Since the probability of desorption is proportional to the incident electron density at the site of the "absorbers," the total desorption yield depends upon the local atomic structure and the k-vector of the incident wave. The importance of these many body elastic interference processes and surface localized inelastic scattering events to desorption and nanopatterning will be discussed.

*In collaboration with M. T. Seiger (INTEL) and G. Schenter (PNNL).

Contributed Papers

9:00

RR2 3 Electron Collisions with C₂H₄, C₂F₄ and c-C₄F₈: Elastic Scattering and Vibrational Excitation RADMILA PANAJOTOVIC, MILICA JELISAVCIC, JULIAN LOWER, STEPHEN BUCKMAN, *Australian National University, Canberra* MASASHI KITAJIMA, HIROSHI TANAKA, *Sophia University, Tokyo* We have carried out independent measurements in our two laboratories of low energy (1-100 eV) electron scattering from ethylene, tetrafluoroethylene and perfluorocyclobutane. The main

motivation for the measurements in the fluorinated molecules are their applications in plasma processing, whilst for ethylene, it is interesting to compare the cross sections with a body of contemporary scattering calculations and previous experimental results and also to contrast the results with those for the fully fluorinated molecule. The experimental results consist of absolute differential and integral cross sections for elastic scattering and vibrational excitation. The absolute scale in each case has been established by the use of the relative flow technique with the helium elastic cross sections as the reference standard. Where possible, the results are compared with recent calculations.

9:15

RR2 4 Proton Transfer Reaction Rate Coefficients Measured for H_3O^+ Reactions with Alkene Molecules G. BROOKE IV, S. POPOVIĆ, L. VUŠKOVIC, *Department of Physics, Old Dominion U., Norfolk, VA 23529* We have measured at 300 K the gas phase proton transfer rate coefficient between the hydronium ion (H_3O^+) and the alkene molecules: ethene (C_2H_4), propene (C_3H_6), and 1-butene (C_4H_8). The measurements were performed using a flow tube apparatus employing an Asmussen-type microwave cavity discharge ion source.¹ With water vapor as the discharge gas, we have obtained H_3O^+ count rates as high as 10^4 counts per second at buffer gas velocities as low as 20 m/s. In addition, H_3O^+ is the predominant ion produced in the source, so

additional filtering is not required for the measurements where H_3O^+ is used as our proton donor. Experimental results were compared with collision rates calculated using ADO theory.² Propene and 1-butene have proton affinities (PA) larger than water so the reaction rates are approximately equal to the collision rates. However, the PA of ethene is lower than water, so the measured reaction rate is smaller than the collision rate. We will present the results of the reaction rate coefficient measurements and their comparison with the calculated collision rates.

¹J. Asmussen, R. Mallavarpu, J. R. Hamann, and H. C. Park, Proc. IEEE **62** 109 (1974).

²T. Su and M. T. Bowers, Int. J. Mass Spectrom. Ion Phys. **12** 347 (1973).

SESSION SR1: PLASMAS FOR NANOSTRUCTURED MATERIALS

Thursday morning, 17 October 2002; North Forum, Millennium Hotel at 10:00; Anna Fontcuberta i Morral, California Institute of Technology, presiding

Invited Papers

10:00

SR1 1 Synthesis and Electron Field-Emission of 1-D Carbon-Related Nanostructured Materials.*

HAN C. SHIH,[†] *Department of Materials Science and Engineering, National Tsing Hua University, Hsinchu, Taiwan 300, R.O.C.*

Carbon nanotubes, a new stable form of carbon that was first identified in 1991 [1], are fullerene-related structures which consist of graphitic cylinders closed at either end with caps containing pentagonal rings. Although carbon nanotube structures are closely related to graphite, the curvature, symmetry and small size induce marked deviations from the graphitic behavior. Various methods have been used to produce carbon nanotubes, e.g., arc-discharge, laser-vaporization, catalytic chemical vapor deposition, but too many impurities also be produced, such as fullerenes, carbon nanoparticles and amorphous carbons. The microwave plasma enhanced chemical vapor deposition (MPECVD) system has been used to grow carbon nanotubes in this work and other 1-D carbon-related nanostructured materials was synthesized by the electron cyclotron resonance (ECR) plasma system. Plasma is generated by microwave excitation at 2.45 GHz by a magnetron passes through a waveguide and fed perpendicularly through a quartz dome into an 875 G magnetic field generated by the coils surrounding the resonance volume that creates the ECR condition. The deposition chamber was pumped down to the base pressure of 6.7×10^{-4} Pa (5×10^{-6} Torr) with a turbomolecular pump for ECR-plasma and subatmospheric pressures for MPECVD by a rotary mechanical pump. Well-aligned carbon-related nanostructures have been synthesized in nanoporous alumina or silicon with a uniform diameter of 30-100 nm by microwave excited plasma of CH_4 , C_2H_2 , N_2 , H_2 and Ar precursors. Nickel nanowires not only serve as catalysts to decompose hydrocarbons to form nanostructures but also function as an electrical conductor for other advanced applications. A negative dc bias is always applied to the substrate to promote the flow of ion fluxes through the nanochannels of the template materials that facilitate the physical adsorption and subsequent chemical absorption in the formation of carbon- and carbon-nitride nanotubes[2]. The electron field emission characteristics of the 1-D carbon-related nanostructures were measured by the conventional diode method at an ambient pressure of 1.3×10^{-3} Pa (10^{-5} Torr). The films (1×1 -cm²) were separated from the anode by ITO (indium tin oxide) coated glass, where a glass fiber spacer was maintained at 150 μ m from the cathode. The current density and electric field characteristics were measured using a Keithley 237 electrometer. A range of onset electron emission field from 3.5 to 1.5 V/ μ m and an emission current density up to 1 mA/cm² at 3V/ μ m have been achieved in this study, apparently superior to other carbon-based electron field emitters[3]. The results were reproducible over a period of weeks and the nanotubes did not degrade physically when exposing to a humid air of RH 90 using the Fowler-Nordheim model, $I = aV^2 \exp(-b\Phi_e^{3/2}/V)$, where a and b are constants. The turn-on voltage was estimated as the voltage deviating from $\ln(I/V^2) - 1/V$ curve. The effective work function ($\Phi_e = \Phi/\beta$) of the arrayed carbon nanotubes was calculated from the slope of the Fowler-Nordheim plot, where the value of β , the field enhancement factor, was found to be 1517. This value increased to 3357 when nitrogen was doped, but decreased to 974 when boron was doped. The incorporation of nitrogen or boron into the carbon network apparently changes the original nanostructure and the chemical bonding. The structural and compositional modification by the incorporation of nitrogen, boron, or hydrogen into the 1-D carbon-related nanostructured materials were analyzed by FTIR, XPS, Raman spectroscopy, and FE-SEM. Various forms in connection with 1-D nanostructured materials applicable to the NEMS, e.g., nanowelding of

nanotubes[4], tubes on tube, open-end nanotubes and coils of nanofiber and nanotubes have been produced in this research depending on the plasma chemistry, catalytic effect and the design of template. [1]. S. Iijima, *Nature* 354, 56 (1991). [2]. S. L. Sung, S. H. Tsai, C. H. Tseng, X. W. Liu, and H. C. Shih, *Appl. Phys. Lett.* 74, 197 (1999). [3]. S. H. Tsai, C. W. Chao, C. L. Lee, and H. C. Shih, *Appl. Phys. Lett.* 74, 3462 (1999). [4]. S. H. Tsai, C. T. Shiu, W. J. Jong, and H. C. Shih, *Carbon* 38, 1879 (2000).

*Field emission, MPECVD, ECR-plasma, Carbon-related nanostructures.

†Professor.

10:30

SR1 2 Creation of Novel Structured Carbon Nanotubes Using Different-Polarity Ion Plasmas.

RIKIZO HATAKEYAMA, *Department of Electronic Engineering, Tohoku University, Sendai 980-8579, Japan*

Since electronic properties of single-walled carbon nanotubes (SWNTs) are expected to be controlled by the accommodation of foreign atoms or molecules, researches on their encapsulation within the SWNTs have been attracting a great deal of attention. Especially, the recent report has presented the possibility of nano-scale rectifying device for the case of intercalation of a (alkali metal / halogen element) junction inside the SWNTs. For this reason, we attempt to perform an original approach of ion irradiation using different-polarity ion plasmas, where various kinds of atoms, molecules or their combinations can be selectively encapsulated within carbon nanotubes. We have already reported the successful formation of the SWNTs encapsulating fullerenes [1] using an alkali-fullerene plasma system. On the basis of this previous work, we here demonstrate the validity of a method of alternative Cs/C₆₀ ions irradiation to SWNTs, which realizes the encapsulation of a Cs/C₆₀ junction inside the SWNT. When DC bias voltages (ϕ_{ap}) are applied to the substrate covered with the SWNTs in the Cs⁺ - C₆₀⁻ plasma, positively- and negatively-charged particles are substantially accelerated by plasma sheaths in front of the substrate for $\phi_{ap} < 0$ and $\phi_{ap} > 0$ with respect to the plasma potential, respectively. As a result of the bias application with instantaneous polarity change between positive and negative values, a junction of electron-donor Cs atoms on one side and electron-acceptor C₆₀ molecules on the other is amazingly realized inside the SWNT. It is very important to note that we have for the first time verified the existence of eCs/C₆₀f junction-structure encapsulated SWNT, which is created successfully by the alternative bias application in the different-polarity ion plasma. Although some problems remain to be resolved as to actual nano-devices, our result gives a high feasibility of the application of this novel-type nano material. [1] G. -H. Jeong et al., *Appl. Phys. Lett.*, 2001, 79, 4213. The author would like to thank K. Tohji, Y. Kawazoe, T. Hirata, and G. -H. Jeong for their collaborations. This work is supported by a Grant-in-Aid for Scientific Research from the Ministry of Education, Culture, Sports, and Technology, Japan.

Contributed Papers

11:00

SR1 3 Controlled growth of aligned carbon nanotube using pulsed glow barrier discharge

TOMOHIRO NOZAKI, YOSHITO KIMURA, KEN OKAZAKI, *Department of Mechanical and Control Engineering, Tokyo Institute of Technology* We first achieved a catalytic growth of aligned carbon nanotube (CNT) using atmospheric pressure pulsed glow barrier discharge combined with DC bias (1000 V). Aligned CNT can grow with the directional electric field, and this is a big challenge in barrier discharges since dielectric barrier does not allow DC bias and forces to use AC voltage to maintain stable plasma conditions. To overcome this, we developed a power source generating Gaussian-shape pulses at 20 kpps with 4% duty, and DC bias was applied to the GND electrode where Ni-, Fe-coated substrate existed. With positive pulse, i.e. substrate was the cathode, random growth of CNT was observed at about 10^9 cm^{-2} . Growth rate significantly reduced when applied negative pulse; Negative glow formation near substrate is essential for sufficient supply of radical species to the catalyst. If -DC was biased, aligned CNT with 20 nm was synthesized because negative bias enhanced negative glow formation. Interestingly, 2 to 3 CNTs stuck each other with +DC bias, resulting in 50-70 nm and non-aligned CNT. Atmospheric pressure glow barrier discharges can be highly controlled and be a potential alternative to vacuum plasmas for CVD, micro-scale, nano-scale fabrication.

11:15

SR1 4 Preparation of Nanostructured Amorphous Carbon Films by Plasma-Assisted Pulsed Laser Deposition and Their Field Emission Property*

Y. SUDA, Y. SUGANUMA, Y. SAKAI, *Hokkaido University, Sapporo, 060-8628, Japan* Amorphous carbon film is expected to be good electron emission material, which is attributed to its low electron affinity. Since electron emission occurs from grain boundaries on the film surface, nanostructured film surface is expected to improve the field emission property. We have presented that plasma-assisted pulsed laser deposition is effective for preparation of nanometer size amorphous carbon particles.¹ In this report, we will present the correlation between the film surface structure and electron emission property. ArF excimer laser (fluence: 2.1 J/cm²; wavelength: 193 nm; deposition time: 60 min) is used as a light source, and a target material is sintered graphite. RF plasma is generated in a helical coil installed between the substrate and the target. Ar pressure is varied from 0.13 to 13 Pa. The surface morphology is examined by scanning electron microscopy and atomic force microscopy. The field emission property is evaluated by measuring the current between parallel plate electrodes installed in vacuum chamber.

*Work in part supported by the Inamori Foundation.

¹Y. Suda, *Thin Solid Films*, in press

11:30

SR1 5 Chemical Vapor Deposition of Superhard Nanocomposites in a Triple Torch Plasma Reactor*

NICOLE WAGNER, *University of Minnesota* DIETMAR BENDIX, *University of Minnesota* JOACHIM HEBERLEIN, *University of Minnesota* A triple torch thermal plasma reactor has been used to synthesize superhard nano-structured Si-N-C composite films on molybdenum

substrates at pressures between 30-100 kPa. Vaporized silicon tetrachloride and gaseous acetylene precursors were alternated to deposit silicon nitride and silicon nitride/carbide layers. An Ar-N₂ thermal plasma plume was used to provide dissociated nitrogen to the reactive multi-phase precursors. Both precursors were pre-heated before entering the reactive plasma plume. The experimental set-up was designed to vaporize and safely deliver the silicon tetrachloride to the reaction zone. The composition, surface morphology and crystal structures of the composite films were determined by FTIR, SEM and XRD.

*This work is funded by the Department of Energy.

11:45

SR1 6 Hypersonic Plasma Particle Deposition of Nanostructured Films and Patterns A. GIDWANI, S. GIRSHICK, J. HEBERLEIN, P. McMURRY, W. GERBERICH, B. CARTER, B.

NELSON, R. MUKHERJEE, T. RENAULT, W. MOOK, C. PERREY, X. WANG, *University of Minnesota* Nanostructured materials are attractive candidates for advanced friction- and wear-resistant coatings. We have developed a one-step method of producing and depositing nanoparticles using a plasma expansion process. In this process, vapor phase reactants are injected into a thermal plasma, which is then expanded to a low pressure through a cooled ceramic nozzle. The rapid cooling drives supersaturation of reactant vapors and subsequent nucleation of nanoparticles. These nanoparticles are deposited onto substrates located downstream in either of the following two ways to form films and micropatterns. In the first method, the nanoparticles are deposited by hypersonic impaction onto a substrate placed 20 mm downstream of the nozzle to form a dense coating. In the second process, the nanoparticles are collimated into a tight beam ($\sim 50 \mu\text{m}$) using an aerodynamic lens assembly and deposited by inertial impaction onto a translating substrate to form micropatterns with feature sizes down to a few tens of microns.

SESSION SR2: NEAR THRESHOLD PROCESSES

Thursday morning, 17 October 2002; Center Forum, Millennium Hotel at 10:00; Chris Dateo, Eloret Corporation, presiding

Invited Papers

10:00

SR2 1 Vibrational excitation and associative detachment at low energies.

MICHAEL ALLAN, *Department of Chemistry, University of Fribourg, Switzerland*

The talk will be on threshold peaks and near threshold structures in electron-molecule scattering and in associative electron detachment (AD), $\text{H} + \text{X}^- (\text{E}_{\text{coll}}) \rightarrow \text{HX}(v, J) + e^-(\epsilon)$, for $\text{X} = \text{Cl}$ and Br . The performance of an electron spectrometer with hemispherical analyzers has been improved both in terms of low-energy capacity and in terms of resolution. A new instrument has been constructed to measure the energy spectra of electrons from AD. More details on known threshold peaks and structures could be observed, and new structures were discovered in HF, HCl, HBr HI and CH₃I. Nonlocal resonance theory of Domcke, Horáček and Čížek succeeded in describing all the structures in hydrogen halides. It also predicted pronounced structures due to interchannel coupling in associative electron detachment. These structures were confirmed by experiment. Pronounced selectivity was observed in the excitation of Fermi-coupled vibrations near threshold in CO₂, at energies where cross section enhancement is attributed to a virtual state. Recently narrow structures turning gradually into boomerang oscillations were discovered even in the virtual state region of CO₂, in the excitation of certain higher-lying Fermi-coupled vibrations. Sharp structures were observed in CS₂.

10:30

SR2 2 Almost bound states of heavy negative alkali ions.

UWE THUMM,* *Dept. of Physics, Kansas State University, Manhattan, KS 66506*

Based on the Dirac R-matrix method [1], a relativistic generalization of the effective range theory [2], and a boundary-corrected Pauli equation (PE) approach [3], I will discuss the spectra of Rb⁻, Cs⁻, and Fr⁻ anions in electron scattering [4] and photodetachment [3]. For incident electron energies below 2.8 eV, our calculated angle-differential, momentum-transfer, and total scattering cross sections predict the same ³P^{o,e}, ³F^o, and ¹P^o resonances for all three anions. Our $J^{\Pi} = 1^+$ partial cross sections show pronounced Ramsauer-Townsend minima at 41/46/32 meV for Rb/Cs/Fr which are caused by the large atomic polarizabilities and are related to ³S^e virtual states [2]. I will discuss relativistic effects in the resonance profiles and review our spin-flip and spin-exchange cross sections for slow e⁻ + Rb, Cs, and Fr collisions in comparison with experimental data. By integrating the PE using an effective potential that is adjusted to reproduce scattering phase shifts provided by exact Dirac R-matrix scattering calculations [4], we calculated angle-differential and total photodetachment (PD) cross sections [3]. In order to avoid an unphysical singularity of the standard PE, we formulated an appropriate boundary condition near the nucleus based on the exact solution of the Dirac equation for a

Coulomb potential. Our $^3P_1^o$ resonance contribution to the PD cross section of Cs^- agrees (in position and width) with recent experiments [5]. [1] U. Thumm and D.W. Norcross, *Phys.Rev.A* 45, 6349 (1992). [2] C. Bahrim, U.Thumm, and I.I. Fabrikant, *J. Phys. B* 34, L195 (2001). [3] C. Bahrim, I.I. Fabrikant, and U. Thumm, *Phys.Rev.Lett.* 87, 123003 (2001). [4] C. Bahrim, U. Thumm, and I.I. Fabrikant, *Phys.Rev. A* 63, 042710 (2001); *Phys.Rev. A* 64, 022716 (2001). [5] M. Scheer et al., *Phys.Rev.Lett.*80, 684 (1998).

*In collaboration with Cristian Bahrim (Lamar University) and Ilya I. Fabrikant (University of Nebraska, Lincoln) and supported by the Office of Fusion Energy, US DOE.

Contributed Papers

11:00

SR2 3 Near-threshold electron-impact excitation of xenon* A. N. GRUM-GRZHIMAILO,[†] Drake University K. BARTSCHAT,[‡] *ITAMP, Harvard Smithsonian Center for Astrophysics* Near-threshold electron-impact excitation is often dominated by contributions from one or just a few partial-wave symmetries. Consequently, negative-ion resonances may become the prominent features. Following up on previous *R*-matrix (close-coupling) calculations for the angle-integrated excitation cross sections and the Stokes parameters of the light emitted from the $np^5(n+1)s$ states in noble gases [1,2], we have performed new calculations for e-Xe collisions [3]. We extend the discussion from angle-integrated to angle-differential cross sections and investigate the effect of near-threshold resonance structures for selected scattering angles. The results will be compared with the available experimental data. [1] V. Zeman and K. Bartschat (1997), *J. Phys. B* 30, 4609. [2] V. Zeman et al. (1998), *Phys. Rev. A* 58, 1275. [3] A.N. Grum-Grzhimailo and K. Bartschat (2002), submitted to *J. Phys. B*.

*Work supported by the NSF and NATO.

[†]permanent address: Moscow State University

[‡]permanent address: Drake University

11:15

SR2 4 Positron Scattering from Noble Gas Atoms* J.P. MARLER, J.P. SULLIVAN*, S.J. BUCKMAN**, C.M. SURKO, *Dept. of Physics, University of California, San Diego* This talk will discuss recent experiments using a high-resolution, trap-based positron beam to study positron scattering from noble gas atoms. The experiments exploit the properties of positron orbits in a magnetic field, using two distinct regions of field strength to resolve inelastic scattering processes. [1-3] Recent measurements of the cross sections for state-resolved electronic excitation, ionization, and positronium formation for argon and xenon will be presented. These measurements will be compared with theoretical predictions and the results of previous experiments, where available. ⁺This work is supported by NSF and ONR. [1] S. J. Gilbert et al., *Phys. Rev. Lett.* 82, 5032 (1999) [2] J. P. Sullivan, et al., *Phys. Rev. Lett.* 86, 1494 (2001) [3] J. P. Sullivan et al., *Phys. Rev. Lett.* 87, 073203 (2001) *Present Address: Photon Factory, KEK, Tsukuba, Japan ** Present Address: Research School of Physical Sciences, Australian National University, Canberra, A.C.T., Australia

11:30

SR2 5 Dependence of optical emission cross sections on target gas pressure and its utilization for studying electron-atom and atom-atom collisions* JOHN B. BOFFARD, CHUN C. LIN, M. D. STEWART, *University of Wisconsin-Madison* In the measurement of electron-impact optical-emission cross sections, one often observes a dependence of the cross section on the target gas pressure. While these pressure effects are usually an unwelcome nuisance in measuring electron-atom collision cross sections, we have exploited these effects to measure additional electron-atom and atom-atom collision cross sections. The nearly complete radiation trapping of resonance radiation at high target gas pressures has allowed us to measure electron-atom cross sections for high lying resonant levels of numerous heavy rare gases.¹ Excitation transfer from an atom in level-*i* (excited by an electron-atom collision event) to another level-*j* (due to a collision with another atom) leads to a pressure dependence in the optical emissions out of level-*j* that can be used to deduce the atom-atom collision transfer cross section.²

*This work supported by the Air Force Office of Scientific Research and the National Science Foundation.

¹M. D. Stewart, Jr., et al., *Phys. Rev. A* 65, 032704 (2002).

²J. B. Boffard, et al., *Phys. Rev. A* 65, 062701 (2002).

11:45

SR2 6 Use of FFT Methods in Electron Scattering with Exchange* MERLE E. RILEY, *Sandia National Labs* A. BURKE RITCHIE, *Lawrence Livermore National Lab* Fully numerical (i.e. grid or lattice in 3D) solutions for electron scattering have usually been done by time-dependent solutions for electron wave packet evolution. The wave packet is necessary to localize the continuum particle within the computational zone. In this work we show that the scattering of electrons can be simulated by solution of the integral Lippmann-Schwinger equation incorporating boundary conditions via the Green's function. The use of Fast Fourier Transform (FFT) methods enables the computation to be done in an $N \log(N)$ operation count where *N* is the total number of points used to represent the 3D scattering wave function. We will present results for the e+H singlet and triplet scattering problems in the static-plus-exchange approximation. The integral equation for the static-plus-exchange theory is solved by a variant of the iterative approach with almost global success in convergence from low to high energy. Some problems remain in the triplet convergence near $k=1$ (a.u.), but the overall computational speed and accuracy is quite good. The solutions are shown to converge to the static-plus-exchange partial wave results.

*Work supported by US DoE at Sandia Labs under contract DE-AC04-94-AL85000

SESSION TR1: PLASMA DIAGNOSTICS: ELECTRICAL AND OPTICAL

Thursday afternoon, 17 October 2002

North Forum, Millennium Hotel at 13:30

Mark Bowden, Eindhoven University of Technology, presiding

13:30

TR1 1 Structure of the ion wakefield potential surrounding objects immersed in a plasma G.A. HEBNER, M.E. RILEY, *Sandia National Laboratories* Ion flow past a isolated, negatively charged structure such as a Langmuir probe tip or a dust particle immersed in a charge neutral plasma can result in ion focusing and creation of a positive space charge region downstream from the object. The structure and magnitude of the positive space charge region is a sensitive function of the bulk plasma parameters, the sheath that forms around the object, the sheath associated with the driven electrode and the charge on the object. We present measurements of the absolute magnitude and shape of the ion wakefield potential derived from extremely low-energy, head-on collisions between micron diameter dust particles levitated in a weak rf driven plasma. Over a range of particle spacing, there exists an attractive interaction between the two negatively charged dust particles due to the positive space charge region. The magnitude of the attractive and repulsive particle-particle interactions is found to be on the order of 10^{-14} N. A model for the particle-particle interaction potential that includes the attractive potential has been developed and is in good agreement with experimental data. This work was performed at Sandia National Laboratories and supported by DoE Office of Science and the United States Department of Energy (DE-AC04-94AL85000).

13:45

TR1 2 Two-dimensional Spatial Distributions of Ion Flux Impinging on the Wafer Surface in Discharges Maintained in Inductively Coupled Plasma Etching Reactors TAE WON KIM, *University of California, Santa Barbara* ERAY S. AYDIL, *University of California, Santa Barbara* A two-dimensional array of planar Langmuir probes manufactured on a 200 mm diameter silicon wafer was used to measure the radial and azimuthal variation of ion flux impinging on the wafer surface in various mixtures of electropositive (Ar) and electronegative gas discharges (SF_6 , Cl_2) maintained in an inductively coupled plasma etching reactor with a planar spiral coil. The spatial variation of ion flux in an electropositive discharge is radially symmetric and peaks at the center of the wafer, whereas the spatial distribution of ion flux in an electronegative discharge has a flattened or hollow profile depending on the plasma conditions. In conjunction with the experiments, we developed a two-dimensional finite element fluid model to provide a framework within which the spatial variation of ion flux in gas mixtures can be understood. This simple model captures the change in the ion flux uniformity in a variety of discharge mixtures though dimensionless ratios of various length and time scales. Ion flux uniformity in Cl_2 , He, Ar, HBr, O_2 , and SF_6 discharges and their binary mixtures will be discussed.

14:00

TR1 3 Frequency effects in a RF capacitive discharge in hydrogen SEBASTIEN DINE, VALERIY LISOVSKIY, JACQUES JOLLY, JEAN GUILLON, *Laboratoire LPTP, Ecole Polytechnique, France* Capacitive radio-frequency discharges working above the conventional 13.56 MHz frequency have been found to increase deposition and etching rates and may be attractive for the deposition of microcrystalline silicon. To quantify the benefit of VHF, we measured DC bias, plasma potential and plasma density with cylindrical and planar Langmuir probes. Measurements were made in a slightly asymmetric parallel plate discharge ($A_{\text{ground}}/A_{\text{rf}} \sim 2$) in the 13.56 MHz - 100 MHz frequency range with hydrogen pressure between 0.1 torr and 0.5 torr. The diameter of electrodes is 12 cm and the inter-electrode distance is 3 cm. The power dissipated in the discharge and the plasma impedance were determined from voltage and current probes measurements, and with a bi-directional coupler placed between the matching box and the reactor. For an accurate phase difference measurement, a wide bandwidth (300 kHz - 6 GHz) vector network analyser was used.

14:15

TR1 4 Monitoring Sheath Voltages and Ion Energies in High-Density Plasmas using RF Current and Voltage Measurements MARK SOBOLEWSKI, *N.I.S.T.* Energetic ion bombardment plays an important role in plasma processing. To obtain optimal results, ion bombardment energies must be carefully controlled. However, measuring ion energy distributions in situ, at a wafer surface during plasma processing, is difficult or impossible. A method for indirectly monitoring ion bombardment energies would thus be useful. Accurate ion energy distributions can be calculated by models of plasma sheaths if one knows the sheath voltage, the electron temperature, and the total ion flux. These parameters are in turn related to radio-frequency (rf) current and voltage signals that can be measured outside a plasma reactor, without perturbing the plasma or the process. In this study, three different model-based methods for using rf measurements to determine sheath voltages and ion energies have been developed and tested. Tests were performed in argon and CF_4 discharges at 10 mTorr, in an inductively coupled, high-density plasma reactor. All the methods were able to successfully detect changes in sheath voltages and to infer the effect of these changes on ion energy distributions.

14:30

TR1 5 Collisional theory for cylindrical Langmuir probes ZOLTAN STERNOVSKY, *Department of Physics, University of Colorado, Boulder, CO 80309-0390* SCOTT ROBERTSON, *Department of Physics, University of Colorado, Boulder, CO 80309-0390* MARTIN LAMPE, *Plasma Physics Division, Naval Research Laboratory, Washington, D.C. 20375-5346* A theory for cylindrical Langmuir probes including charge exchange collisions is presented. Charge exchange creates low energy ions inside the probe sheath that may become trapped. These trapped ions have greater probability to fall into the probe, thus increasing the probe ion current. The charge exchange current is modeled as the rate of these collisions integrated over the probe sheath weighted by the capture probability. The charge exchange rate is enhanced in the inner sheath due to ion acceleration. The validity of the model is verified experimentally with a simple set-up. Low temperature Ar plasma is created with a hot cathode discharge. The plasma density is determined from a microwave resonant method and varies from $0.6\text{E}7$ to $3\text{E}7$ cm⁻³. The charge exchange currents are ob-

tained by subtracting the theoretical OML current from the measured net ion current and are typically larger than the OML current. The charge exchange current varies nearly linearly with probe bias and increases with neutral gas pressure.

14:45

TR1 6 Phase resolved emission spectroscopy of RF discharges: A powerful novel diagnostic tool T. GANS, *Plasma Research Laboratory, Dublin City University, Ireland* V. SCHULZ-VON DER GATHEN, H.F. DÖBELE, *Institut f. Laser- und Plasma-physik, Universität Essen, 45117 Essen, Germany* A novel optical emission spectroscopic technique for capacitively and inductively coupled RF discharges has been developed and applied to hydro-

gen plasmas. This technique is based on the phase and space resolved investigation of the population dynamics of excited states. It allows - in combination with an analytical model - quantitative measurements of: a) Lifetimes and quenching coefficients; b) Temporally and spatially resolved electron densities and EE-DF's of energetic electrons (>12eV), especially in the sheath region; c) The degree of dissociation; d) The dynamics of rotational distributions, with relevance for gas temperature measurements. The model takes into account: electron impact excitation, heavy particle collisional excitation, radiationless collisional de-excitation (quenching), radiation trapping and cascading processes from higher electronic states. This work was supported by the DFG in the frame of SFB 191.

SESSION TR2: RECOMBINATION AND DISSOCIATION

Thursday afternoon, 17 October 2002; Center Forum, Millennium Hotel at 13:30; Ann E. Orel, University of California, Davis, presiding

Invited Papers

13:30

TR2 1 Jahn-Teller coupling and Rotational Excitation in the Dissociative Recombination of H_3^+ .*

CHRIS H. GREENE, *Department of Physics and JILA, University of Colorado*
V. KOKOULINE, *Department of Physics and JILA, University of Colorado*

When a low-energy electron collides with the simplest triatomic ion H_3^+ , it can destroy the molecule through the process of dissociative recombination (DR), which forms either $H_2 + H$ or else $H + H + H$. Limited dimensionality (2D) models of this process have not been able to obtain recombination rates anywhere near as fast as the rates measured in storage ring experiments.¹ A recent study² provided evidence that the mechanism controlling the unexpectedly fast DR rate of H_3^+ is the Jahn-Teller symmetry-distortion effect. The incorporation of Jahn-Teller effects into dissociative recombination theory will be described in this talk. I will also describe our recent progress toward implementing a full-scale calculation for H_3^+ that includes fully quantized rotational dynamics of the ion.

*This work was supported in part by the National Science Foundation.

¹G. Sundström, *et al.*, *Science* **263**, 785 (1994).

²V. Kokoouline, C. H. Greene, and B. D. Esry, *Nature* **412**, 891 (2001).

14:00

TR2 2 Ionic fragment production in dissociative electron-molecular ion collisions.

NADA DJURIC,* *JILA, University of Colorado, Boulder*

During the past several years we have been studying cross sections for dissociative electron-molecular ion collisions. The presence of molecular ions in the edge plasmas of fusion reactors as well as in the dark and diffuse molecular clouds and the importance of reactions of molecular ions in plasma generators for etching and for deposition have stimulated such investigations. We are using two different experimental approaches for these studies. In JILA we are detecting light fragment ions from dissociation (dissociative excitation and dissociative ionization) of heteronuclear molecular ions. In GRYPING experiments neutral fragments from dissociative recombination and dissociative excitation have been recorded, while detection of negatively charged fragments have been used for resonant ion pair formation studies. We will discuss the techniques and present selection of our results at the meeting. *This work was supported in part by the Office of Fusion Energy of the U. S. Department of Energy under Contract No. DE-A102-95ER54293 with the National Institute of Standards and Technology

*Work performed with G. H. Dunn, JILA and GRYPING team, Stockholm University.

Contributed Papers

14:30

TR2 3 Dissociative ionization of benzene by electron impact
WINIFRED HUO, *NASA Ames Research Center* CHRISTOPHER DATEO, *Eloret Corporation* We report a theoretical study of the dissociative ionization (DI) of benzene from the low-lying ionization channels. Our approach makes use of the fact that electron motion is much faster than nuclear motion and DI is treated as a two-step process. The first step is electron-impact ionization resulting in an ion with the same nuclear geometry as the neutral molecule. In the second step the nuclei relax from the initial geometry and undergo unimolecular dissociation. For the ionization process we use the improved binary-encounter dipole (iBED) model.¹ For the unimolecular dissociation step, we study the steepest descent reaction path to the minimum of the ion potential energy surface. The path is used to analyze the probability of unimolecular dissociation and to determine the product distributions. Our analysis of the dissociation products and the thresholds of their productions are compared with the recent dissociative photoionization measurements of Feng et al.² The partial optical oscillator strengths from Feng et al. are then used in the iBED cross section calculations.

¹W.M. Huo, *Phys. Rev. A* **64** 042719-1 (2001)

²R. Feng, G. Cooper, C.E. Brion, *J. Electron Spectrosc. Relat. Phenom.* **123** 211 (2002)

14:45

TR2 4 Nitrogen Dissociation in N₂-Ar Microwave Plasmas
J. HENRIQUES, E. TATAROVA, C.M. FERREIRA, *Centro de Física das Plasmas, Instituto Superior Técnico, 1049-001 Lisboa, Portugal* Microwave N₂-Ar discharges driven by a traveling surface wave (SW) attract attention due to their advantageous properties for plasma processing technologies, in particular for nitriding surfaces. Nitrogen atoms are the most important precursors in gas discharge nitriding and the study of their production and loss mechanisms is of fundamental importance. The kinetics of dissociation of N₂ in N₂-Ar microwave plasmas was investigated as a function of the spatial position, mixture composition and pressure. A theoretical model¹ was developed for the following situation: an azimuthally symmetric SW ($TM_{00}, \omega/2\pi = 2.45$ GHz) propagates and sustains an N₂-Ar plasma column in a dielectric tube ($a=0.75$ cm, $\epsilon_d=3.78$) surrounded by a metal screen ($R=2.5$ cm). The model accounts in a self-consistent way for the electron and heavy particle kinetics, gas thermal balance and wave electrodynamics. It is demonstrated that charge transfer $Ar^+ + N_2 \rightarrow N_2^+ + Ar$ followed by dissociative recombination $e + N_2^+ \rightarrow N(^4S) + N(^4S)$ increases the dissociation degree of nitrogen at high Ar fractional percentage in the mixture. The predictions are validated by optical emission spectroscopy².

¹J. Henriques, E. Tatarova, V. Guerra and C.M. Ferreira, *J. Appl. Phys.* **91** 5622 (2002).

²J. Henriques, E. Tatarova, F.M. Dias and C.M. Ferreira, *J. Appl. Phys.* **91** 5632 (2002).

SESSION UR1: INDUCTIVELY COUPLED PLASMAS AND PLASMA SOURCES

Thursday afternoon, 17 October 2002

North Forum, Millennium Hotel at 15:30

L. Overzet, University of Texas at Dallas, presiding

15:30

UR1 1 Numerical simulation of collisionless heating in an inductively-coupled plasma reactor
M. SHIOZAWA, K. NANBU, *Institute of Fluid Science, Tohoku University, Japan* The effect of collisionless heating on inductive chlorine discharges is examined using particle modeling. Electromagnetic fields in plasma are obtained using two kinds of plasma current, i.e., cold plasma current given by Ohm's law and warm plasma current sampled from the motions of electrons. The results for the warm plasma current include the effect of both collisionless heating and ohmic heating. Electric field, power deposition, electron density, and electron energy distribution function (EEDF) are obtained at gas pressures of 0.5, 1.0, and 2.0 Pa. The electron density and power deposition for the warm plasma current are larger than those for the cold plasma current; at 0.5 Pa, the power deposition for the warm plasma current is twice as large as that for the cold plasma current. The difference of the power deposition between cold and warm plasmas is ascribable to the difference of the phase difference between the electric field and current density.

15:45

UR1 2 Modeling of inductively coupled CHF₃/Ar plasma mixture
DEEPAK BOSE, *Eloret Corp.* T. R. GOVINDAN, *NASA Ames Research Center, Moffett Field, CA 94035* M. MEYYAPPAN, *NASA Ames Research Center, Moffett Field, CA 94035* Fluorocarbon plasmas are used widely for etching of silicon dioxide and other silicon compounds. Most modeling studies of fluorocarbon discharges in the literature have focused on CF₄ discharges. Modeling of CHF₃ plasmas in the literature is limited due to significant uncertainties in the reaction mechanism leading to dissociation and ionization into a large array of neutral radicals and ions. Only a small fraction of these possible reaction steps have been characterized experimentally or via ab initio studies. In this work we will present 2d ICP modeling results at low pressures (10-50 mTorr) based on currently available data. In an attempt to reduce some of the uncertainty in the reaction mechanism, we will compare the modeling results with available mass spectrometric and langmuir probe data in the literature. Apart from bulk plasma properties, we will compare relative ion fluxes into the wafer in order to assess the validity of predicted radical and ion concentrations in the discharge.

16:00

UR1 3 Characterization of Radio-Frequency Oxygen Plasmas in the GEC cell
M.V.V.S. RAO, *ELORET* S.P. SHARMA, A.A. BOLSHAKOV,* B.A. CRUDEN, *ELORET* M. MEYYAPPAN, *NASA Ames Research center* Oxygen plasmas generated in the gaseous electronics reference (GEC) cell, in which the 13.56 MHz radio-frequency (RF) power is coupled through a planar spiral induction coil, were studied by using Langmuir probe, mass spectrometry, and electrical measurements. The data were collected in the pressure range of 25-300 mTorr at RF powers 150-300 W. The electron energy probability function exhibits non-Maxwellian behavior at all conditions and two-temperature behavior at pressures above 100 mTorr. At pressures below 50 mTorr the mean ion

energies (E_i) are less than 20 eV, decrease with pressure and are nearly independent of power, which is a typical signature of inductively coupled plasma. Above 50 mTorr, however, E_i increases steeply with pressure and decreases with increasing power, indicating a significant stray capacitive coupling giving a large voltage drop across the sheath. Ion energy data is consistent with the plasma potential and electron temperature, and, similarly, the ion flux with electron and ion number densities and with the emission data¹ of O, O₂, O⁺, and O₂⁺ species.

*NRC/NASA Senior Research Associate

¹S. P. Sharma et al. at this conference

16:15

UR1 4 Inductive to Capacitive Mode-Transition of an RF-Discharge Investigated by Phase-Resolved Emission Spectroscopy V.A. KADETOV, U. CZARNETZKI, *Institut for Plasma and Atomic Physics, Bochum University, 44780 Bochum, Germany* H. F. DOEBELE, *Institut for Experimental Physics, Essen University, 45117 Essen, Germany* In RF discharges, the high energy part of the electron distribution function is modulated with the RF frequency in a characteristic way which depends on the mode of operation. This modulation is observed by the phase and space resolved emission at Balmer- α in a hydrogen discharge in a modified GEC reference cell. Regardless of the intensity amplitude, one can distinguish between capacitive and inductive operation by the temporal structure of the emission: One maximum in case of the capacitive mode and two maxima in case of the inductive mode. The transition between the modes is investigated as a function of power and pressure and compared with ion energy spectra. The technique is particularly useful in case of pulsed operation for the investigation of the transient ignition phase. It is shown that the discharge ignites capacitively and switches gradually to the inductive mode after a few hundred RF cycles.

16:30

UR1 5 Effects of Electron Current on Collisional Interactions in ICP Reactors CHONG H. CHANG, *Los Alamos National Laboratory, Los Alamos, NM 87544* DEEPAK BOSE, *Eloret, NASA Ames Research Center, Moffett Field, CA 94035* In continuum modeling of low pressure plasma discharges, electron collisional interaction terms are modeled using collision frequencies based on electron temperature. However, this becomes inaccurate in ICP reactors where the directed azimuthal electron velocity can become comparable to the electron thermal velocity, significantly altering electron transport properties and the azimuthal current and electric field relationship. By retaining the directed relative velocities in the collision integrals for multi-temperature mixtures, we have derived necessary corrections for plasma conductivity. Computational results of an argon discharge (10 mTorr) show that these corrections result in increased collision frequencies, leading to increased total power deposition of about 10 % at 500 W in a 300 mm TCP reactor, for a constant inductive coil current. This increase is expected to be significant at high powers and low pressures. A correction of electrical conductivity also results in significant changes in both electric field and current density in the azimuthal direction.

16:45

UR1 6 Experimental Characterization of a Time-Modulated Inductively-Coupled Discharge* K.C. LEOU, T.L. LIN, C.H. CHENG, G.S. CHEN, G.W. YEN, *National Tsing Hua University, Hsinchu, Taiwan* PLASMA PROCESSING GROUP COLLABORATION The basic properties of a time modulated low pressure inductively-coupled plasma has been characterized by using various diagnostic tools, including a RF impedance meter, a Langmuir probe, a 36 GHz interferometer and optical emission spectroscopy. These tools have been modified from conventional ones to measure time resolved properties of the discharge. In addition to plasma density, plasma potential and electron temperature, the Langmuir probe has also been used to extract the electron energy probability function (EPPF) of the plasma. Measurement results show that high energy (roughly $E > 10$ eV) electrons are lost quickly after the driving RF power is turned off. The low energy part of the electrons remains nearly unchanged during the entire off period. The electron temperature thus drops quickly while plasma density changes little during RF off period as observed in other studies. Spatial-temporal behaviors of plasma density have also been measured. The radial distribution of plasma density only change slightly at different times of the RF on or off periods although the overall plasma density varies significantly. The electric properties of the discharge was measured by a home made impedance meter which detects the time varying amplitude and phase of the RF voltage and current, and thus net input RF power and complex impedance of the discharge. For different waveforms of modulation, such as square, triangular, sinusoidal and trapezoidal, impedance meter measurements show that, when the RF power is turned on, there is always a transient surge of RF voltage and current on the inductive coil, thus the net input power into the plasma. The temporal profiles of electric properties, however, do not vary significantly for different types of modulations. Comparison of probe and impedance meter measurements to interferometer and OES measurements will also be presented.

*Work Supported by the grant NSC 89-2212-E007-070

17:00

UR1 7 Effect of non-local electron conductivity on power absorption and plasma density profiles for low pressure inductively coupled discharges* BADRI RAMAMURTHI, *University of Houston* DEMETRE ECONOMOU, *University of Houston* IGOR KAGANOVICH, *Princeton Plasma Physics Laboratory* A self-consistent model was developed to study the effect of non-local electron transport on power absorption, electron energy distribution function (EEDF), and plasma density profiles in a planar inductively coupled argon discharge at low pressures (< 10 mTorr). The RF electric field and current density profiles in the plasma were computed by a non-local electron conductivity model for inhomogeneous plasmas. Computations were also performed assuming a local electron conductivity model (Ohm's law). As power increases, the electron density also increases and the EEDF deviates less from a Maxwellian, due to electron-electron collisions. The effective electron temperature decreases with increasing power. The combined effect of electron density and effective temperature variation with power makes the discharge behave non-locally for low and high powers. For intermediate values of power, however, the discharge approaches local behavior, in the

sense that the plasma density profiles are quite similar irrespective of the electron conductivity model (local or non-local) used. Finally, results on the EEDFs and RF field and current density profiles are compared with available experimental data.

*Work supported by the NSF and the Princeton Plasma Physics Lab (PPPL) through a University Research Support Program.

17:15

UR1 8 Characteristics of Magnetically Enhanced Capacitively Coupled Discharges* ALEX VASENKOV, MARK J. KUSHNER, *University of Illinois/Urbana-Champaign* Magnetically Enhanced Reactive Ion Etching (MERIE) discharges are used for a variety of plasma etching processes for microelectronics fabrication, and for dielectric etching in particular. Typical plasma

sources use parallel plate electrodes with a static magnetic field applied parallel to the electrodes with a pattern that may rotate in the (r, θ) plane. We report on a computational investigation of MERIE plasma sources sustained in 10s mTorr of Ar and Ar/fluorocarbon gas mixtures having applied magnetic fields of up to 100s G. The modeling platform is the Hybrid Plasma Equipment Model with improved algorithms to address large magnetic fields. We found that in addition to an increase in ion density and decrease in dc bias due to confinement by the magnetic field, the uniformity of the ion flux to the substrate could also be optimized by judicious choice of magnetic field profile.

*Work was supported by CFD Research Corp, Sematech, Semiconductor Research Corp. and the National Science Foundation (CTS99-74962).

SESSION UR2: ATMOSPHERIC PRESSURE NONTHERMAL PLASMAS I

Thursday afternoon, 17 October 2002; Center Forum, Millennium Hotel at 15:30; J. Davidson, University of Minnesota, presiding

Invited Papers

15:30

UR2 1 Spatio-temporally resolved diagnostics of the barrier discharge by cross-correlation spectroscopy in air at atmospheric pressure.

HANS-ERICH WAGNER, *Institute of Physics, University of Greifswald, Domstrasse 10a, D-17489 Greifswald, Germany*

The technique of spatially resolved cross-correlation spectroscopy (CCS) is used to carry out diagnostic measurements of the barrier discharge (BD) in air at atmospheric pressure.¹² Quantitative estimates for the electric field strength $E(x, t)$ and for relative electron density $n_e(x, t)/n_{e, max}$ are derived from the experimentally determined spatio-temporal distributions of the luminosity for the spectral bands of the 00 transitions of the second positive system of $N_2(\lambda = 337.1nm)$ and the first negative system of $N_2^+(\lambda = 391.5nm)$. All the measurements and calculations have been performed for a BD with the symmetrical electrode arrangement (glass glass), discharge gap width of 1.2mm, in flowing synthetic air (80% N_2 + 20% O_2) at atmospheric pressure. It is shown that the streamer starts directly from the surface of the anode and crosses the gap with an increasing velocity that reaches $10^6 m/s$. The reduced electric field of the streamer grows from $120Td$ at the anode to $240Td$ at the cathode, respectively. The influence of the spatio-temporal structure of the discharge on the chemical kinetics of ozone synthesis is studied within the frame of the kinetic model based on the results of spatially resolved CCS measurements. It is demonstrated that the properties of the plasma in the region near the anode (where the electric field is lower but electron density is higher than near the cathode), favor dissociation of molecular oxygen by direct electron impact. In the case of the excitation of triplet nitrogen states, the contributions of both regions to this process appear to be comparable.

¹Kozlov K V, Wagner H-E, Brandenburg R, Michel P 2001 J. Phys. D: Appl. Phys. 34 3164-3176.

²Kozlov K V, Dobryakov V V, Monyakin A P, Samoilovich V G, Shepeliuk O S, and Wagner H-E, Brandenburg R, Michel P 2002 in: Selected Research Papers on Spectroscopy of Nonequilibrium Plasma at Elevated Pressures, Vladimir N. Ochkin, Editor, Proceedings of SPIE vol. 4460, 165-176 Washington (USA).

Contributed Papers

16:00

UR2 2 Modeling of Discharge Dynamics in Radio Frequency Plasma Display Panels* SATOSHI UCHIDA, FUMIYOSHI TOCHIKUBO, TSUNEO WATANABE, *Tokyo Metropolitan University* The discharge characteristics of radio frequency plasma display panels (RF-PDP) were investigated using a one dimensional fluid model with the electron energy conservation equation. In the present analysis, the addressing and sustaining voltages (V_a

and V_s) are 200 V and 85 V, respectively. When the driving frequency f was tuned to 50 MHz at the gas pressure $p = 100$ Torr with the gap length $d = 0.075$ cm, 72 % of the input power was injected into electrons. Since the excitation of Xe was promoted, the radiation efficiency of ultraviolet light became as high as 42 %. Under the condition of constant pd and fd , the discharge continued stably. The spatio-temporal distributions of electron density showed similar pattern for different f . With respect to the influence of wall charge on the discharge characteristics, the wall voltage V_w increased with the wall charge density n_{qw} in the addressing period. Then V_w contributed to trigger the onset discharge. However,

this memory effect, which is an essential phenomenon to driving of the conventional PDP, disappeared during the sustaining period because of significant decrease of n_{qw} . This result suggests that the switch of V_s to a lower value is required to erase the discharge in RF-PDP.

*Work in part supported by Grant-in-Aid for Scientific Research of Japan Society for the Promotion of Science.

16:15

UR2 3 Experimental and numerical study of an atmospheric pressure glow discharge in helium LORENZO MANGOLINI, PENG ZHANG, CURTIS ANDERSON, UWE KORTSHAGEN, JOACHIM HEBERLEIN, *University of Minnesota, Mechanical Engineering, Minneapolis, MN, USA* Atmospheric pressure glow discharges in helium have been reported to produce radially uniform plasmas and to show one single current pulse per half cycle of the AC high voltage [1]. However, in other studies the appearance of multiple periodic peaks per half cycle has been reported as well. Different interpretations have been given for this effect ranging from the oscillation of the cathode sheath [2] to multiple successive breakdowns [3]. We have performed studies with different dielectrics to investigate their effect on the discharge behavior: two circular 4 cm diameter electrodes have been covered with (1) 1.7 mm thick glass plates ($\epsilon_r = 4.6$) and with (2) 0.635 mm thick alumina plates ($\epsilon_r = 9$). At a gap of 5 mm, multiple current peaks were observed with both configurations. Time resolved measurements of the emission intensity using a gated intensified CCD camera were performed, both in axial and radial direction. These indicate that the first current pulse is produced by a radially propagating ionization front, while later peaks are related to breakdowns at the electrode edges. With 0.635 mm thick alumina plates we could observe the appearance of a strong cathode fall in front of the momentary cathode, together with a Faraday dark space and a positive column that extended for a length of 2-3 mm. A two-dimensional fluid model has been realized to study the glow discharge behavior. The numerical result is qualitatively in good agreement with the observed structure of the discharge. The model reproduces the radial propagation of the ionization wave. This work is supported by the Department of Energy under grant DE-FG02-00ER54583. [1] Massines F., Rabehi A., Decomps P., Gadri R.B., Segur P., and Mayoux C., *J.Appl.Phys.* 83, 2950-2957 (1998). [2] Akishev Y.S., Dem'yanov A., Karal'nik V.B., Trushkin N.I., and Pan'kin M.V., *Proc. Of XXIV ICPIG, Poland*, July 11-16, 137-138, (1999). [3] Mangolini L., Orlov K., Kortshagen U., Heberlein J., and Kogelschatz U., *Appl.Phys.Lett.*80, 1723 (2002).

16:30

UR2 4 Al Surface Cleaning Using a Capillary Plasma Electrode Discharge (CPED) Plasma L. MOSKWINSKI, *Stevens Institute of Technology, Hoboken, NJ* P.J. PICATTO, S. BABKOMALYI, R. CROWE, *Plasamsol Corporation, Hoboken, NJ* N. ABRAMZON, *Stevens Institute of Technology and Plasmasol Corporation, Hoboken, NJ* C. CHRISTODOULATOS, K. BECKER, *Stevens Institute of Technology* The cleaning of metal surfaces such as Al (or stainless steel) both during manufacturing and prior to their use in specific applications has been a significant challenge for industry. We investigate the interaction of a novel capillary plasma electrode discharge (CPED) plasma operating in atmospheric-pressure ambient air with contaminated Al surfaces. We have established a protocol to deposit uniform oil films of a desired thickness on Al substrates, expose the contaminated Al substrate to the plasma under controlled operating conditions in

terms of power, plasma density, residence time, feed gas composition, etc., and analyze the plasma-treated sample using a variety of surface analysis techniques as well as the volatile by-products of the plasma treatment. Hydrocarbon removal rates of essentially 100% have been achieved for residence times of only a few seconds. Work supported by the NSF.

16:45

UR2 5 One-Dimensional Spatiotemporal Pattern Formation in a Novel Dielectric-Barrier Discharge System* MASON KLEIN, *Harvard University* MATTHEW WALHOUT, *Calvin College* In a novel dielectric-barrier discharge system at atmospheric pressure, discharge filaments fire between diametrically opposite sides of a narrow glass tube and stabilize at regular intervals along the tubes length. Various one-dimensional, periodic patterns are observed, as well as disordered states. Measurements of charge transfer show that for each spatial pattern, a number of distinct discharge stages occur during each voltage half-cycle. Time-resolved images, obtained with a makeshift streak camera, reveal a variety of spatial and temporal structures. These experiments and preliminary modeling efforts will be discussed.

*Research supported by Calvin College and NSF Grant 9876679.

17:00

UR2 6 Molecular dissociation and rotational temperature measurements in a short pulse dielectric barrier discharge P. BLETZINGER, *ISSI, Dayton OH 45440* B. N. GANGULY, *Air Force Research Laboratory, WPAFB OH 45433* Measurements were made in a dielectric barrier (DB) discharge, excited by a 3 to 30 kHz repetition rate, 20 to 40 kW peak power, 20 nsec FWHM voltage pulse; gas mixtures were Ar+N₂ and Ar+O₂ up to 200 Torr pressure in a 1 cm diameter Pyrex discharge tube with external electrodes. The electrical power coupling efficiencies as functions of pressure and gas mixtures were correlated with the collisional quenching corrected emission intensities of 750 and 641 nm argon lines, and also the band head intensity ratios of N₂ C-B (0,2) with the N₂⁺ B-X (0,0) lines. The gas pressure and gas mixture dependent relative dissociation efficiencies of O₂ were monitored from the emission intensity ratios of the 777 nm atomic oxygen line with the 750 and 641 nm argon lines; O atom emission intensity increased 40 percent faster with increasing voltage, 6 to 12 kV, and power than the Ar emission. The repetition rate and pressure dependent gas temperature rise was measured from the N₂⁺ B-X (0,0) emission band. For this short pulsed DB discharge, the two step excitation does not contribute to the N₂⁺ B state population, therefore, it provides an accurate measurement of the N₂ ground state temperature. Rotational temperatures measured at 10 kHz rep rate with 12 kV applied voltage increased from 530 K at 15 Torr to 620 K at 200 Torr; also a 1:5 dilution ratio of N₂ in Ar decreased temperature by 80 K.

17:15

UR2 7 Studies of a low power atmospheric pressure discharge with flowing He[#] K.R. STALDER, *Stalder Technologies and Research* A.H. EL-ASTAL, *Al-Aqsa University, Gaza*, P.G. STEEN, *Queens University Belfast, UK* W.G. GRAHAM, *Queens University Belfast, UK* T. MORROW, *Queens University Belfast, UK* The mechanisms that create and sustain atmospheric pressure glow discharges (APGD) are still the subject of debate. Here electrical, optical and laser-aided diagnostic techniques are used to characterise a low power atmospheric pressure discharge, operating in air with helium gas flowing through the inter-electrode

space. The discharge is created between two copper covered glass plates, separated by 2.6 mm. The outputs of a variable frequency voltage supply are attached to each electrode. At driving frequencies of about 25 kHz what appears visually to be a spatially and temporally uniform glow discharge is established at pk-pk voltages above 180 V. This mode is characterised by discrete current draw, persisting for 2 microsec., twice during the voltage period. The visible spectra are dominated by emission from N₂ and N₂⁺ with some evidence of He emission lines. These results are consistent with other results [1]. Preliminary analysis of the N₂ second positive series indicates rotational temperatures 400 K and vibrational temperatures 3000 K. Preliminary absorption measurements indicate densities of the triplet and singlet metastable states of Helium are less than 3×10^9 atoms cm⁻³ and no evidence of long lived nitrogen species. [1] F. Massine et al. J. Appl. Phys. 83, 3411-3420 (1998) *Supported by UK EPSRC

17:30

UR2 8 Dielectric Barrier Discharges in Helium at Atmospheric Pressure: Experiments and Model in the Needle-Plane Geometry ION RADU, *Department of Engineering Physics, Ecole Polytechnique, Montreal, QC H3C 3A7, Canada* RAYMOND BARTNIKAS, *Hydro Quebec Research Institute, Varennes, QC J3X 1S1, Canada* MICHAEL WERTHEIMER, *Department of Engineering Physics, Ecole Polytechnique, Montreal, QC H3C 3A7, Canada* We present an experimental and theoretical modeling study of "dielectric barrier discharges" (DBD) at atmospheric pressure in a needle-plane configuration. Synchronous, Ultra High Speed Imaging (UHSI, using a Princeton Instruments PI-MAX 512RB Digital ICCD Camera System) and real-time dual detection (optical-electrical) diagnostics have been carried out in a flow

of He. A phase-resolved synchronizing circuit was used to trigger the ICCD cameras shutter for durations varying from 2 ns up to 100 ns. All diagnostics, including the PI-MAX images, could be precisely synchronized and processed on a PC computer. The high voltage electrode was a steel needle with a sharp point of precisely-machined radius, while a thin (1.6 mm) ceramic (Al₂O₃) plate with a metallized bottom surface was used as the ground electrode. Three different situations have been studied, namely (i) the bare Al₂O₃, and with an ultra-thin coatings of (ii) graphite (a semiconductor) or (iii) metal, the latter two at floating potential. The purpose of these experiments was to investigate possible effects of surface charging on the discharge behavior [1]. The axial [y(t)] and radial [x(t)] time evolutions of the discharge have been measured by UHSI, plotted, and found to differ very significantly among cases (i) to (iii). In the needle-plane configuration (like in the plane-plane case), the DBD is characterized by a single pulse per half-period of the applied voltage. A two-dimensional model of the needle-plane discharge, based upon the continuity equations for electrons, ions, excited particles, and the Poisson equation, is developed; it assumes a low degree of ionization, so that the transport coefficients of the gas are uniquely determined by the local electric field [2]. In order to determine the electric field and the electrical potential in the (hyperboloidal) needle-plane geometry, the finite element method is used. We have found excellent agreement between measured and calculated [y(t)] and [x(t)] data, indicating that surface charge density and -distribution greatly influence the discharge events while they evolve across the gap space. [1] Nikonov V., Bartnikas R., and Wertheimer M.R., IEEE Trans. Plasma Sci. 29 (2001) 866. [2] Novak J.P., and Bartnikas R., J. Appl. Phys. 62 (1987) 3605.

SESSION WF1: PLASMA SURFACE INTERACTIONS

Friday morning, 18 October 2002; North Forum, Millennium Hotel at 8:00; Jim Olthoff, National Institute of Standards and Technology, presiding

Invited Papers

8:00

WF1 1 Beam Study of Si and SiO₂ Etching Reactions by Energetic Fluorocarbon Radicals.

HIROTAKE TOYODA,* *Department of Electrical Engineering, Nagoya University*

Highly-selective high-aspect-ratio etching of SiO₂/Si is an indispensable key issue in the next generation ULSI manufacturing processes. To achieve such etching performance, precise control of fluorocarbon plasmas based on deep understanding of radical reactions on SiO₂ and Si surfaces is required. Besides complex real experiments in etching reactors, well-defined beam experiments in ultra-high vacuum are powerful for basic study of surface reactions. This paper reports elementary surface processes found in a beam device. The device was specially designed so as to enable in situ measurements of both etching products and etched surfaces. Namely, a mass-selected single species of ionic radical CF_x⁺ (x=2, 3) and F⁺ is incident on a clean Si or SiO₂ surface at a controlled energy from 50 to 400 eV. Desorption of neutral species such as CF_x, CO and SiF_x from the surface is monitored by a quadrupole mass spectrometer, while in situ X-ray photoelectron spectroscopy (XPS) analysis reveals a time evolution of atomic composition of surface layer during etching. In the case of Si surface experiment, a stationary surface layer of 2-3 nm in thickness is formed on the Si substrate during etching, along with saturation of CF₂ radical desorption, when the CF₃⁺ irradiation at 400 eV exceeds 3x10¹⁶ cm⁻². A mass balance between the incident and desorbed C atoms seems to support the observations. In the case of SiO₂ experiment, however, a C-containing surface layer is not recognized on a top surface of SiO₂ under etching by CF₃⁺ irradiation at 400 eV. Furthermore, less CF₂ desorption and more SiF_x desorption at the same incident energies of CF₃⁺ are observed in comparison to the Si surface. An increase in the incident energy enhances the SiO₂ etch rate along with a decrease of CF₂ desorption. These observations suggest that the incident C atoms are mainly consumed for CO formation rather than CF₂ formation in the SiO₂ etching. More results on the incident energy dependence, other neutral species desorbed from surfaces, and the CF₂⁺ and F⁺ incidence experiment will also be presented.

*In collaboration with Hideo Sugai.

Contributed Papers

8:30

WF1 2 Plasma molding over surface topography and resulting ion/fast-neutral distribution functions*

DEMETRE ECONOMOU, *University of Houston* DOOSIK KIM, *University of Houston* Plasma molding over surface topography finds applications in MEMS microfabrication, neutral beam sources, plasma extraction through grids, and plasma contact with internal reactor parts (e.g., wafer chuck edge). The flux, energy and angular distributions of ions incident on the substrate are of primary importance in these applications. These quantities depend critically on the shape of the meniscus (plasma-sheath boundary) formed over the surface topography. A two-dimensional fluid/Monte Carlo simulation model was developed to study plasma "molding" over surface topography. The radio frequency (RF) sheath potential evolution, and ion density and flux profiles over the surface were predicted with a self-consistent fluid simulation. The trajectories of ions and energetic neutrals (resulting by ion neutralization on surfaces or charge exchange collisions in the gas phase) were then followed with a Monte Carlo simulation. Ion flow and energy and angular distributions of ions and energetic neutrals bombarding an otherwise planar surface with a step will be reported. The step height was comparable to the sheath thickness for the RF high density plasma considered. As one approaches the step sidewall, the ion flux decreases, the ion energy distribution narrows, and the ion impact angle increases drastically. The ion impact angle at the foot of the

step scales with the ratio of sheath thickness to step height. The energetic neutral flux is found to be comparable to the ion flux on the horizontal surface near the step sidewall. Simulation results are in good agreement with experimental data, taken at Sandia National Labs.

*Work supported by the National Science Foundation and Sandia National Laboratories.

8:45

WF1 3 Electron Transfer and Emission in Highly Charged Ion-Surface Interactions

UWE THUMM, *Dept. of Physics, Kansas State University, Manhattan, KS 66502* JENS DUCREE, *University of Freiburg, Germany* This talk will address interactions of slow highly charged ions with metal and insulator surfaces, leading to the formation of unstable, multiply excited projectiles. We have simulated the formation and decay of such hollow ions on the basis of a refined classical over-barrier model. These simulations include the full trajectory of the projectile and allow for the simultaneous evaluation of projectile kinetic energy gains, final charge-state distributions, and emitted Auger electron yields. Duce et al., *Phys. Rev. A* **60**, 3029 (1999). Bahrim et al., *NIM B* **164**, 614 (2000).

9:00

WF1 4 The effect of ion energy upon the chemical structure of triglyme and E2OV plasma polymerised films

DAVID BARTON, *University of Sheffield, UK* STUART FRASER, *University of Sheffield, UK* ROBERT D. SHORT, *University of Sheffield, UK* JAMES W. BRADLEY, *umist, UK* Using energy resolving plasma mass spectrometry, QCM deposition rate monitoring and XPS samples, we have studied the effect of ion energy upon derived

polymer film properties. The polymers are produced in a 13.56MHz RF plasma reactor, at a pressure of 50mTorr, and a generator output of 5W. The films are deposited onto a specially designed substrate, behind which are placed the diagnostics. By applying an RF bias to the substrate, which is phase and amplitude matched to the RF potentials in the plasma, we can manipulate the ion energy between set limits. These limits are the time average potential differences V_p - V_{sb} , down to the DC minimum of V_p - V_f . The subscripts refer to the plasma (p), self bias (sb) and floating (f) potentials respectively. An important feature of this technique is that the bulk plasma is undisturbed, so that ion energy is the only parameter under investigation. Using the monomers triglyme and E20V, chosen for their biological anti-fouling properties, we demonstrate the ability to manipulate film properties by selective control of plasma ion energies.

9:15

WF1 5 Characterization of a modified Gaseous Electronics Conference (mGEC) Reference Cell and the effects of wall material ERIC A. JOSEPH, BAOSUO ZHOU, YONGHUA LIU, LAWRENCE J. OVERZET, MATTHEW J. GOECKNER, *University of Texas at Dallas* Gas-phase plasma properties such as density, neutral temperature, and partial pressure are studied for inductively coupled CF₄ discharges in a modified inductively coupled GEC reference cell using in-situ Fourier Transform Infrared (FTIR) spectroscopy. The influence of plasma-wall interactions, for a variety of wall materials including aluminum and silicon, is determined by measuring etch and deposition rates with in-situ spectroscopic ellipsometry. A comparison between the mGEC reference cell and a standard stainless steel inductively coupled GEC reference cell will also be presented. This work is supported by a grant from NSF / DOE, CTS-0078669.

SESSION WF2: NONEQUILIBRIUM LIGHT SOURCES

Friday morning, 18 October 2002

Center Forum, Millennium Hotel at 8:00

D. Smith, University of Wisconsin, presiding

8:00

WF2 1 Self-Consistent Description of a He-Xe Low-Pressure Plasma for Lighting Purpose DIRK UHRLANDT, SERGUEI GORTCHAKOV, RENÉ BUSSIAHN, HARTMUT LANGE, *Institut für Niedertemperatur-Plasmaphysik, 17489 Greifswald, Germany* Glow discharges in rare-gas mixtures including xenon are favoured candidates for the design of mercury-free low-pressure VUV radiation and light sources. Optimal operation conditions with respect to the radiation efficiency can be evaluated by an appropriate self-consistent analysis of the column plasma of such glows. A comprehensive model of the cylindrical dc column plasma in helium-xenon mixtures is presented. The model is based on a recently developed hybrid method and comprises a spatially resolved kinetic treatment of the plasma electrons, a detailed balance description of the excited states in xenon as well as a self-consistent determination of the axial heating field and the radial space-charge field. First results of the model are compared with probe and spectroscopic measurements and a sufficiently well agreement has been obtained. The reliability of the applied collision-radiative model of xenon and the choice of the cross

sections of collision processes between electrons and excited atoms is critically evaluated. It has been found that a change of these cross sections within their range of uncertainty has a considerable impact on the results for the electric field and the densities of excited states.

8:15

WF2 2 Novel Inductively Coupled Plasma Source ANDREW RYBIN, *Dublin City University* ALBERT R. ELLINGBOE, *Plasma Research Laboratory, Dublin City University* Novel Inductively Coupled Plasma Source A novel high-pressure, high-power-density-compatible plasma source is investigated. Possible applications include high brightness lightning, effluent abatement and chemical activation for downstream use. The systems comprises an inductively coupled rf antenna and plasma. The plasma housing chamber and plasma act as a secondary windings to the antenna. The design features auto-self-correction to give high voltage operation to attain breakdown (E-mode), and low voltage operation once a high density plasma is formed (H-mode). Electrical parameters (antenna current, voltage, plasma current, chamber voltage, light emission, rf-magnetic-field, etc.) are collected during a power ramp, enabling identification of the E-mode and H-mode power coupling regimes. At sufficiently high power density, the H-mode enters a new regime in which the power coupling between the antenna and plasma increases dramatically. This results in antenna current and voltage dropping with increasing rf power; plasma current, however, continues to increase. Work Supported by EURATOM

8:30

WF2 3 Consequences of Radiation Trapping on Electron Energy Distributions in Low Pressure Inductively Coupled Hg-Ar Discharges* KAPIL RAJARAMAN, ALEX VASENKOV, MARK J. KUSHNER, *University of Illinois/Urbana-Champaign* Inductively coupled Hg/Ar discharges operating at low pressures (100s of mTorr) are finding increasing use as long-life electrodeless lamps. Resonance radiation trapping is an important component of the energy balance in the positive column of these lamps, affecting both the magnitude and spatial distribution of excited species. These excited states then feedback to the electron swarm through collisional processes. In this paper, we discuss the consequences of radiation trapping on the electron energy distribution (EED) throughout the plasma. This computational study was performed with a 2-dimensional plasma chemistry model containing a radiation transport module and a kinetic description of electron transport. Radiation trapping leads to a higher Hg* densities which, in turn, produces larger rates of superelastic collisions. As a result, we observe a significant modification in the tail of the EED under conditions where radiation trapping is important. Results from a parametric study of the behavior of EEDs as a function of pressure, mole fraction of Hg and power deposition will be discussed, as will the consequences of electron-electron collisions on the EEDs.

*Work supported by EPRI, Osram-Sylvania and the National Science Foundation (CTS99-74962).

8:45

WF2 4 Experimental and numerical studies on Xe²⁺ VUV emission in fast electric discharge afterglow DENNIS LO, *Physics Department, The Chinese University of Hong Kong* CHENG SHANGGUAN, *Shanghai Institute of Optics and Fine Mechanics, Academia Sinica* IGOR KOCHETOV, ANATOLY NAPARTOVICH,* *State Science Center Troitsk Institute for Innovation and Thermonuclear Research* HONG KONG COLLABORATION, SHANGHAI COLLABORATION, TROITSK TEAM Optical and electrical properties of a fast (50 ns) high-pressure discharge in pure Xe and Xe-Ne mixtures were studied experimentally and simulated numerically. Afterglow VUV emission was revealed lasting for a few microseconds. Its duration depended on gas pressure and Xe content. Observations of VUV emission intensity across the discharge aperture demonstrated a good uniformity with sizes 4.5x 2 mm². The length of the discharge was 42 cm. Operation of the discharge was limited in gas pressure by development of instability. The highest pressure for stable discharge run was 0.55 bar for pure Xe and 5 bar for xenon-lean mixture. A detailed kinetic model of discharge plasma was developed, which calculated self-consistently electron energy distribution function and excited states including excimer population dynamics. VUV emission dynamics observed experimentally can be explained theoretically only in a model with an essentially increased number of electronic states taken into account. Calculated discharge voltage history and VUV emission dynamics agree satisfactory with measurements.

*Corresponding author

9:00

WF2 5 Kinetic Processes in Active Medium of Carbon Monoxide Laser Operating on High Vibrational Transitions* A. IONIN, A. KOTKOV, Y.U. KLIMACHEV, L. SELEZNEV, D. SINITSYN, *P.N. Lebedev Physics Institute of Russian Academy of Sciences* A. KURNOSOV, A. NAPARTOVICH, S. SHNYREV, *Troitsk Institute for Innovation and Fusion Research* G. HAGER, J. McCORD, *Air Force Research Lab, Kirtland AFB* P.N. LEBEDEV PHYSICS INSTITUTE OF RUSSIAN ACADEMY OF SCIENCES COLLABORATION,[†] TROITSK INSTITUTE FOR INNOVATION AND FUSION RESEARCH COLLABORATION,[‡] AIR FORCE RESEARCH LAB, KIRTLAND AFB COLLABORATION[§] Kinetic processes on highly excited vibrational levels of CO molecules pumped by pulsed electron beam sustained discharge are discussed. Temporal behavior of small signal gain (SSG) in active medium of pulsed single-line fundamental band CO laser operating up to 18- > 17 vibrational band has been studied both theoretically and experimentally with master oscillator power amplifier system. The SSG of pulsed single-line first-overtone CO laser operating on highly excited vibrational transitions from 20- > 18 up to 38- > 36 has been also studied both experimentally and theoretically. It is demonstrated that multiquantum vibrational-vibrational (V-V) exchange and asymmetric V-V exchange should be taken into consideration when analyzing population formation on high vibrational levels.

*The research was supported by Russian Federal Program The Integration of Higher Education and Basic Research (B0049), Russian Foundation of Basic Research (grant #02-02-17452) and International Scientific Technical Center (Project 2415P).

[†]53, Leninsky prosp., 117924, Moscow, Russia, Fax: (095) 132-0425

[‡]TRINITY, Troitsk, Moscow region, Russia

[§]Albuquerque, NM, USA

9:15

WF2 6 RF excited Microgap Discharge in He-Xe-HCl gas mixture Y.B. UDALOV, *NCLR B.V. P.O.Box 2662 7500 CR Enschede, The Netherlands* M.C.R. HOOGEVEEN, *Saxxon High Technical School, Enschede, The Netherlands* S.A. STAROSTIN, S.V. MITKO, P.J.M. PETERS, K.J. BOLLER, *Chair of Laser Physics, University of Twente, P.O.Box 217, 7500 AE Enschede, The Netherlands* A.V. DEMYANOV, *State Science Center Troitsk Institute for Innovation and Fusion Research, 142092 Troitsk, Moscow region, Russia* The design of (quasi-) continuous wave excimer lasers remains an ambitious goal for many years. Several approaches are thought to be suitable for that. It was demonstrated recently that in microdischarges the pumping with a very high specific CW power deposition (tens or hundreds kW/cm³) produces at atmospheric pressure non-thermal plasmas. Still the manufacturing of a sufficiently long array of microdischarges represents a major technical problem. We show that transverse RF sustained discharges at supra-atmospheric pressures can be considered as a serious alternative for the above mentioned technique. In this work we studied the properties of the RF discharge in He-Xe-HCl (1000:10:1) gas mixture for the gas pressures up to 1.4 bar. RF driven discharges in a frequency range of $f = 60\text{--}200$ MHz were successfully applied for the excitation of fairly long and homogeneous discharges (up to 37 cm). The inter-electrode distance of 160 mm was needed to run stable discharges at pressures of 1.4 bar. Fluorescence signal at 308 nm was measured for different input powers, gas pressures and electrode gaps. The estimated gain value is comparable with those obtained by microdischarge excitation. The experimental data are in a good agreement with the numeric results of the simulation based on our fluid model of the RF discharge. Prospects for further improvement of the design of quasi-CW excimer lasers are discussed.

SESSION XF1: PLASMAS FOR NANOSTRUCTURES AND DUSTY PLASMAS

Friday morning, 18 October 2002

North Forum, Millennium Hotel at 10:00

Steven Girshick, University of Minnesota, presiding

10:00

XF1 1 Radiation pressure and gas drag forces on a melamine-formaldehyde microsphere in a dusty plasma BIN LIU, JOHN GOREE, VLADIMIR NOSENKO, *Department of Physics and Astronomy, The University of Iowa, Iowa City, IA52242, USA* LAIFA BOUFENDI, *Laboratoire GREMI, Universite d'Orleans, 45067 Orleans, Cedex 02, France* A dusty plasma is an ionized gas containing small particles of solid matter. The particle can experience numerous forces in plasma. We measured the radiation pressure and gas drag forces acting on a single melamine-formaldehyde (MF) microsphere immersed in an Ar plasma produced by a capacitively-coupled parallel-plate rf electrode discharge. We verified that both forces are proportional to the particle cross-section area. We report quantitatively results for the coefficient for both forces. We also verified that the horizontal confining potential has a parabolic shape with a characteristic frequency that matches the frequency of random particle motion, as measured by the velocity autocorrelation function in the absence of any radiation pressure. Work at Iowa was supported by NASA and DOE.

10:15

XF1 2 Dispersion relations of compressional waves in a plasma crystal determined from a wakefield* V. NOSENKO, J. GOREE, *Dept. of Physics & Astronomy, The University of Iowa* D. H. E. DUBIN, *Dept. of Physics, UCSD* A plasma crystal is a strongly-coupled dusty plasma, where charged micron-size particles of solid matter arrange themselves in a pattern like a crystalline lattice. In the laboratory, a 2D triangular lattice with hexagonal symmetry can be formed by levitating a monolayer of particles in the sheath of a gas discharge plasma. It sustains two modes of in-plane motion: compressional and shear. We excited these waves with a moving spot of a high-intensity laser beam. Phase mixing of the various excited waves gives rise to constructive and destructive interference. The resulting interference pattern is termed a phonon wake, in analogy to a ship's wake. In the experiment we measure the velocity of all particles. A single snapshot of the wake's amplitude can be used to generate the entire dispersion relation, i.e., the wave's frequency ω vs. wavenumber k , for the compressional wave. The result is compared to a theoretical dispersion relation for a Yukawa triangular lattice, and good agreement is found.

*Work supported by NASA, NSF, DOE, ONR

10:30

XF1 3 Dusty Silane Plasmas WINFRED STOFFELS, JEROME REMY, MIKHAIL SOROKINE, CHARLOTTE GROOTHUIS, GERRIT KROESEN, *Eindhoven University of Technology, Department of Physics, P.O. Box 513, 5600 MB Eindhoven, The Netherlands* A low pressure capacitively coupled radio frequency discharge using 5% silane in argon is studied. Special emphasis is put on the initial stages of dust formation immediately after ignition of the discharge. The particle polymerisation process as well as the particle plasma interaction are studied. The latter is evident in changing electrical characteristics of the discharge outside (current and voltage) as well as inside (plasma density) the plasma. Several diagnostic techniques will be combined to obtain a complete picture. Diagnostics which currently are under development are: infrared cavity ringdown spectroscopy to determine chemical characteristics; fast measurement of voltage and current of the driving rf frequency and its higher harmonics; microwave resonance for electron density determination and laser induced photodetachment for ion density and particle charge.

10:45

XF1 4 Gas Temperature and Carrier Gas effects on nanoparticle formation in silane plasmas* UPENDRA BHANDARKAR, *University of Minnesota, Department of Mechanical Engineering* UWE KORTSHAGEN, *University of Minnesota, Department of Mechanical Engineering* STEVEN GIRSHICK, *University of Minnesota, Department of Mechanical Engineering* The improvement in the electronic properties of thin silicon films deposited under plasma conditions that favor particle formation has spurred further research interest in the particle properties as well as the pathways leading to particle formation. We have been carrying out simulations to study particle generation in silane processing plasmas used in such deposition processes. Our zero-dimensional model solves for gas and surface chemistry, particle growth due to coagulation and surface growth, particle charging and plasma properties. We have been studying the effect of gas temperature and carrier gas that has been found to influence the particle nucleation time in experiments. At present our simulations suggest that these effects may primarily be caused by diffusion. An increase in the gas temperature or a lighter carrier gas speed up

the diffusion of clusters and newly formed "nuclei." A decrease in the initial nuclei population has further effects in slowing down growth due to coagulation. This could have important implications in devising methods to control the particle growth in plasmas. We will present results obtained from these calculations that also include the effect of gas pressure and input power.

*This work was supported by NSF (grant ECS 9731568) and the Minnesota Supercomputer Institute.

11:00

XF1 5 Synthesis of Crystalline Monodisperse Silicon Nanoparticles in an Inductively Coupled Silane Plasma AMEYA BAPAT, UWE KORTSHAGEN, *Mechanical Engineering, University of Minnesota, Minneapolis, MN 55455* STEPHEN CAMPBELL, *Electrical and Computer Engineering, University of Minnesota, Minneapolis, MN 55455* Amorphous silicon has been used for a wide variety of electronic applications including thin film transistors and energy conversion devices. Since these devices suffer greatly from defect scattering and recombination, a method for depositing crystalline silicon would be highly desirable, especially if crystalline material can be deposited on low temperature substrates such as plastics. Our work aims at the synthesis of mono-disperse, single or polycrystalline silicon nanoparticles and their deposition on various substrates to be used for different applications. For our studies, we have used an inductively coupled silane plasma to create these nanoparticles. We run the plasma at pressures of 500-700 mTorr in 5% silane diluted in helium and argon, with power input in range of 100-150W. In this setup we are able to produce nearly monodisperse, crystalline nanoparticles in size ranges of 40-80 nm. Crystallinity is inferred from diffraction patterns and the cubic shape of some of the nanoparticles. This is likely due to the elevated gas temperature in this high power density discharge. We are now looking at improving the size control of particles with varying plasma conditions and the better control of the process of deposition of these particles on substrates. This work is supported by NSF through grant CTS-9876224.

11:15

XF1 6 Experimental Investigation of Nanosized Silicon Particle Formation in an Inductively Coupled Plasma System Z. SHEN, S.A. CAMPBELL, *Dept of Electrical and Computer Eng.* T. KIM, U. KORTSHAGEN, P.H. McMURRY, *Dept of Mechanical Eng., University of Minnesota* To understand the mechanisms of nanoparticle formation and its potential applications, we have investigated silicon particles formed in various gasses in an inductively coupled plasma (ICP) system and have measured their structural properties by electron microscopy. Particle generation in pure SiH₄, SiH₄/H₂, SiH₄/He, and SiH₄/Ar are reported. ICP silane plasmas are shown to be a rich source of nanoparticles. Three regimes are mapped out from our experiments: a no particle domain which is generally seen at the lowest pressures, a polydisperse and agglomerated domain which is seen at the highest pressures, and an monodisperse domain at intermediate pressures. Conditions that generate these nonagglomerated, extremely monodisperse silicon particles are emphasized. It is theorized that the rich charge concentrations seen in an ICP allows this unique production of these nanoparticles at high concentrations. Particle size can be controlled from 15 to 100 nm and is determined by the plasma on-time. In a pure silane plasma, there are two well-defined monodisperse particle growth phases were observed corresponding to weak and strongly pressure dependences. In the regime with weak pressure dependence particle growth may due

primarily to coagulation, while in the second phase particle growth is attributed primarily to surface deposition. For H₂ dilutions less than 92 pressure. However, particle growth decreases steadily when the H₂ dilution increases further. It is shown in the TEM images, however, that the particles change from compact to a looser structure. Under a very higher dilution ratio, polycrystalline particles are obtained. Ar and He dilution played a different role in the particle formation. Polydisperse and agglomerated particles are easily collected on the TEM grids under various experiment conditions.

11:30

XF1 7 MONITORING AND CONTROL OF THE FORMATION OF SILICON NANOPARTICLES IN RF PLASMAS FOR THE OPTIMIZATION OF THE QUALITY OF NANOSTRUCTURED SILICON FILMS ANNA FONTCUBERTA I MORRAL, 128-95 J. Watson Laboratories, California Institute of Technology, Pasadena, CA 91125 FREDERIC GRANGEON, PERE ROCA I CABARROCAS, LPICM, Ecole Polytechnique, 91128 Palaiseau Cedex, France The spectacular development of the nanosciences has lead in a high interest in nanostructured materials. Among all the techniques used for their fabrication, plasma processing offers the possibility of depositing areas up to $\sim 1\text{m}^2$ and deposition rates up to 10nm/s. In this paper, we focus on nanometer size silicon nanoparticles, which opens the possibility of fabricating optoelectronic devices such as non volatile memories or light emitting devices, but also open the possibility of obtaining nanostructured silicon materials, which have new properties. We will first present high resolution transmission electron micrographs of the material obtained under conditions where silicon nanoparticles are produced. Then, we will show how the contribution of the nanoparticles to the deposition are associated with an enhancement of the electronic properties of the material. This has motivated the study of the gas phase nucleation of the particles in order to maximize their contribution. For that purpose, we have

set up an in situ Cavity Ring Down experiment, which measures absorption coefficients of the gas phase between 10^{-6} and 10^{-9}cm^{-1} , just at the right range to detect and quantify silicon nanoparticles at the concentrations. We have found concentrations of $10^9\text{particles/cm}^3$ in our usual discharge conditions and tuned them in order to optimize the concentration of nanoparticles one order of magnitude, just before their coagulation in the gas phase, which has lead into an optimization of the material. Effects of the thermophoretic force on the transport of the nanoparticles, will also be presented. We will show how if thermal gradients in the chamber are high enough, the flow of the nanoparticles can be opposite to the gas drag.

11:45

XF1 8 Size-Dependent Kinetics of Deposition on Particles in a Dusty Plasma Chemical Vapor Deposition Reactor* JIN CAO, THEMIS MATSOUKAS, Department of Chemical Engineering, The Pennsylvania State University, University Park, PA 16802 We study the size-dependent kinetics of nanoscale film deposition of 2-propanol plasma polymer on silica particles of 4 sizes suspended as a dusty plasma in an RF discharge. The film growth rate increases markedly with the particle size. A kinetic model of the deposition process is presented. The model shows that the size dependence of film growth rate results from changes in the electron density and electron temperature in dusty plasmas loaded with different-sized particles. A closer examination reveals that electron density is the major factor influencing the film growth rate. The particle size distribution broadens with deposition, the rate of which is also size dependent. Experiments suggested the broadening of the size distribution to be a result of the gradient in the plasma. A model is presented that allows the size dependence of plasma non-uniformity to be extracted from the evolution of the particle size distribution. It is found that the plasma becomes increasingly less uniform with smaller particle sizes.

*work supported by NSF and DuPont

SESSION XF2: ATMOSPHERIC PRESSURE NONTHERMAL PLASMAS II

Friday morning, 18 October 2002; Center Forum, Millennium Hotel at 10:00; J. Behnke, University of Greifswald, presiding

Invited Papers

10:00

XF2 1 Plasma-Catalytic Processes in Non-Thermal Atmospheric Pressure Discharges.

ALEXANDER FRIDMAN, University of Illinois at Chicago

Plasma-catalytic processes combine actually two groups of chemical processes, which can be effectively organized using different types of electric discharges. The first group of plasma-catalytic processes include direct physical combination of discharge plasma or plasma-chemical products with active catalysts. Such hybrid processes were successfully applied, in particular, in automotive exhaust gas treatment, in hydrogen / syngas production from heavy hydrocarbons, and in air purification from volatile organic compounds (VOC). The second group of plasma-catalytic processes applies plasma as the catalyst, or instead of conventional catalyst—to stimulate chemical processes. In this case, plasma is not supposed to be used as a source of energy, but only as the stimulator of chemical processes. For example, plasma-catalytic organization of natural gas conversion into syngas permits to use only 10% of energy input from plasma, while the rest comes in form of low temperature heat. Both these two types of plasma-catalytic processes are going to be discussed in this presentation as well as general approach to the hybrid plasma systems and their applications.

10:30

XF2 2 Spectroscopic Characterization of Atmospheric Pressure Glow Plasma.KEN OKAZAKI,* *Department of Mechanical and Control Engineering, Tokyo Institute of Technology*

The thermal structure of methane-fed dielectric barrier discharge (DBD) and atmospheric pressure glow discharge (APG) has been investigated in terms of time-averaged gas temperature profile between two parallel-plate electrodes separated by 1.0 mm. Emission spectroscopy of rotational band of CH ((0,0) 431 nm) was performed for this purpose. DBD and APG was activated by 10 kHz with 2% duty cycle pulsed voltage in order to minimize average gas temperature increase. In DBD, temperature increase of a single microdischarge, on a time average, reached 200 K. It suddenly decreased below 100 K associated with the dark space formation near dielectric barrier. Also, gas temperature in the surface discharge was fairly low because emission in these regions was limited within the initial stages of propagation, whereas energy deposition would continue until microdischarge extinction; Rotational temperature seemed to estimate far below the actual gas temperature in these regions. In APG, gas temperature was uniformly increased by positive column formation. In addition, remarkable temperature increase due to negative glow formation was obtained only near the metallic electrode. In the practical interest, we also investigated net temperature increase with high frequency operations (AC 80 kHz), which depends on not only plasma properties, but also various engineering factors such as flow field, external cooling conditions, and total input power. In DBD, gas temperature in the middle of gas gap was significantly increased with input power due to poor cooling conditions. In APG, on the contrary, gas temperature near electrodes was significantly increased associated with negative glow formation.

*Tomohiro Nozaki.

Contributed Papers

11:00

XF2 3 NO₂ production in a high pressure pulsed microwave discharge designed for VOC removal

A. ROUSSEAU, A. DAN-TIER, A. MECHTCHANOV, *LPGP, bat 210 Univ. Paris-Sud / CNRS, 91405 Orsay, France* J. ROEPCKE, *Institute of Low Temperature Plasma Physic, 17489 Greifswald, Germany* Y. GOLUBOVSKI, Y. IONIKH, I. POROKHOVA, *Faculty of Physics, Univ. St. Petersburg, Russia* Non thermal pulsed microwave discharges represent an alternative to Dielectric Barrier Discharges for the removal of atmospheric pollutants. However, due to the relatively high peak power density injected in the plasma and to the high chemical efficiency of such a microwave plasma source, toxic nitrogen oxides may also be generated as undesirable by-products. Tuneable diode laser absorption spectroscopy (TDLAS) is used for highly sensitive and non intrusive diagnostic of undesirable NO₂ produced by the discharge itself. The influence of the pulsed discharge parameters (pressure, peak power, pulse duration and frequency) on the generation of NO₂ production is studied. It is showed that NO₂ density increases monotonously with the injected mean energy and the use of short pulses is a mean to limit its production. The time resolved measurements of the gas temperature are performed which shows that the heating of the gas occurs within 0.1ms. Finally, efficiency of such a discharge for VOC removal is studied.

11:15

XF2 4 High-Pressure Air Constituent Plasmas*

KAMRAN AKHTAR, JOHN E. SCHARER, SHANE M. TYSK, BEN O. WHITE, C. MARK DENNING, ENNY KHO, *Electrical and Computer Engineering Department, UW-Madison* High-Pressure air plasmas are finding increasing application in plasma processing industry as plasma reactors, light sources, and biological decontaminants. One of the major issues particular to such plasma is the high radio-frequency power required to initiate and sustain the discharge. However, once the gas breakdown has occurred and the discharge is initiated, radio frequency power can be more efficiently absorbed by the plasma through inductive coupling of the wave fields. Mixing noble gasses with the air constituents and improving the gas flow can also reduce power requirements. A

high-density $10^{12} - 10^{14} \text{cm}^{-3}$, large volume plasma of air constituents (N₂, O₂, Air, and Argon mixtures) is created by either laser (300 mJ for 20(±) ns half-pulse width) preionization of an organic gas (2-6 mTorr) seeded in a high-pressure gas (760 Torr); or by high power (1-25 kW) pulsed rf sources in gas mixtures. The effect of gas flow on the discharge characteristics will be presented. A multi-turn helical antenna is used to couple rf power through a capacitive matching network. A 105 GHz interferometer is employed to obtain plasma density in the presence of high collisionality utilizing phase shift and amplitude attenuation. A Boltzmann plot of the emission spectrum is used to calculate the excitation temperature. Network analyzer measurements of the antenna impedance provide an ANTENNA-II code predicted density estimate

*This work is supported by AFOSR Grants (F49620-00-1-0181).

11:30

XF2 5 Air Chemistry and Power to Sustain Air Plasma Generated by Electron-Beam Excitation*

ROBERT VIDMAR, *University of Nevada, Reno* KENNETH STALDER, *Stalder Technologies and Research* Computations of electron density decay using a kinetic model with an improved data set of rate coefficients for air constituents are discussed. The model includes the effects of an electric field, which increases plasma lifetime, principally by elevating the electron temperature which in turn, reduces attachment, enhances formation of metastable singlet delta oxygen molecules, enhances electron detachment from negative oxygen molecules, and increases ionization. The power to sustain a given level of plasma density is reduced by an electric field, and the associated ohmic heating of this nonequilibrium plasma model is quantified. Vibrational excitation of nitrogen and oxygen and their effects on plasma power budgets will be discussed.

*This material is based on research sponsored by the Air Force Research Laboratory, under agreement number F49620-01-1-0414.

11:45

XF2 6 Model of Ozone Production in the DC Corona Discharge JUNHONG CHEN, JANE DAVIDSON, *University of Minnesota* A comprehensive numerical model of ozone production in clean, dry air by DC corona discharges is presented. This model combines a first-principle corona plasma model with a chemistry and 2-D transport model to obtain the distributions of ozone and other gaseous products in the neighborhood of a corona discharge wire. Electron number density distribution is obtained by solving the continuity equations for electrons and ions and the simplified Maxwell's equation. The non-Maxwellian electron energy distribution is solved from the Boltzmann equation. The chemical kinetics of ozone formation and destruction are based on recent atmospheric chemistry models taking into account the contributions of excited molecules. The transport model includes the conservation equations for total mass, momentum, energy and the mass of individual species and is solved using FLUENT. The predicted ozone production rate agrees well with experimental data. Excited molecules contribute more than 80 percent of the total ozone produced. The effects of discharge polarity, current, wire radius, air temperature, and air velocity (residence time) on the production of ozone are discussed.

SESSION YF1: PLASMA DIAGNOSTICS: OPTICAL EMISSION

Friday afternoon, 18 October 2002

North Forum, Millennium Hotel at 13:30

V. Schulz-von der Gathen, University of Essen, presiding

13:30

YF1 1 Analysis of Emission data from Oxygen Plasmas SURENDRA SHARMA, A.A. BOLSHAKOV,* M.V.V.S. RAO, ELORET B.A. CRUDEN, ELORET M. MEYYAPPAN, *NASA Ames Research center* Optical emission spectra in the UV-visible (200-900 nm) and IR (1000-1300 nm) range from a RF (13.56 MHz) driven oxygen plasma are analyzed and the results are compared with the mass spectrometer and Langmuir probe data.² The experiments were conducted in a GEC cell equipped with a planar induction coil at 165, 248 and 330 W of input RF power and at several pressures in the 50-300 mTorr. 1% Ar was added as a tracer gas to the plasma for the measurements of atomic oxygen number densities using the intensity ratios of argon and oxygen lines and published excitation and relaxation data. At higher power and lower pressure the plasma exhibits characteristics of inductive coupling.² The emission spectra under these conditions is dominated by atomic lines with insignificant contribution from the O⁺ lines. As the pressure is increased the plasma undergoes a mode change and begins to exhibit characteristics of capacitive coupling.² The emission from atomic lines decrease more than one order of magnitude and from O⁺ lines increase becoming comparable to O₂⁺ emission band system. Along with the estimates of atomic oxygen number density, the emission data is analyzed to estimate the electron temperature and compared with the Langmuir probe data. A global model with Langmuir probe data¹ as input is used to highlight some relevant chemical kinetics features of the mode transition phenomena.

*NRC/NASA Senior Research Associate

¹M.V.V.S. Rao et al at this conference

13:45

YF1 2 Spectral line deconvolution GEORGE PETROV, *Berkeley Scholars, Inc.* The spectral line profile $z(\omega)$, passing through a measuring device with instrumental function $A(\omega)$, is recorded experimentally as $u(\omega)$. This device, for example, a Fabry-Perot Interferometer, distorts the spectral line profile and the experimentally measured one is a convolution of the real profile and the instrumental function. Restoring the line profile is a formidable problem, since it is strongly affected by numerical instabilities. Small changes in $u(\omega)$ (due to noise etc.) cause huge deviations in the solution $z(\omega)$. The problem is tackled by using the Tikhonov regularization method, which allows a smooth and stable solution to be obtained. This approach is particularly useful for "noisy" experimental data. An interactive user friendly object oriented code for spectral line deconvolution is developed. The program runs under Windows. It has build in graphical capabilities and visually displays the instrumental function, measured and deconvoluted spectral line profiles. A visual demo program located at www.geocities.com/gm_petrov/index.html can be downloaded for free.

14:00

YF1 3 Characterization of BCl₃/N₂ Plasmas KAREN J. NORDHEDEN, JOANNE SIA, *Plasma Research Laboratory, Chemical & Petroleum Engineering, University of Kansas* The effect of the addition of N₂ to BCl₃ plasmas has been investigated for the reactive ion etching of GaAs. The experimental results showed that the etch rate of GaAs increased from 80 Å/min in pure BCl₃ to over 1000 Å/min in a 40:60 BCl₃:N₂ mixture (15 mTorr, 50 W, 20 sccm). Optical emission spectroscopy, quadrupole mass spectrometry, and microwave measurements were used to study the effects of N₂ percentage on the plasma characteristics. The optical emission intensities of both molecular and atomic chlorine were observed to increase near 30% N₂, and an argon tracer indicated a large increase in argon emission as a function of increasing N₂ percentage. Microwave measurements indicated that the average electron density increased slightly up to 80% nitrogen and then increased more rapidly. Mass spectrometric analysis of the plasmas showed that both the dissociation of BCl₃ and the production of molecular chlorine were significantly enhanced with increasing N₂ percentage. It is believed that either an increase in the electron temperature as a result of electron attachment heating, or energy transfer from N₂ metastables (or a combination thereof), is responsible for the enhanced production of etch species.

14:15

YF1 4 Investigation of collisional mixing between Ar(4s[3/2]_{1,2}^o) and Ar(4s'[1/2]_{0,1}^o) Ar using optical-optical double resonance spectroscopy* MARIA-ANTOANETA BRATESCU, YOSUKE SAKAI, YASUNAO YOSHIZAKI, *Hokkaido University, Sapporo 060-8628, Japan* We investigated the collisional mixing between Ar(4s[3/2]_{1,2}^o) and Ar(4s'[1/2]_{0,1}^o) using optical-optical double resonance (OODR) absorption spectroscopy. As a preliminary result, saturated Ar(4p'[1/2]₁) population was obtained with a diode laser beam of a wavelength of 772.6 nm for the resonant transition from 4s'[1/2]₀^o to 4p'[1/2]₁. The laser beam intensity was modulated. The second laser beam with a wavelength of 826.7 nm corresponding to a transition from 4s'[1/2]₀^o to 4p'[1/2]₁ levels propagates in opposite direction against, overlapping the first laser beam through the discharge. The detected signal for 826.7nm is a Doppler free absorption line, depending on the population of the 4s'[1/2]_{0,1}^o level. The maximum OODR signal was obtained at 5 Torr to be 10⁹ cm⁻³ on the

$4s'[1/2]_0^o$ level and 10^{10} cm^{-3} on the $4s'[1/2]_0^o$ level. The discharge operated in pulsed regime with a high voltage switch. The discharge current was controlled with change of time duration (from 100 ns to ms) and voltage amplitude (from 2 kV to 10 kV) of a power source, and Ar gas pressure. Using the temporal absorption signals the diffusion constant and the two-body and three-body rates were analyzed for various pressures.

*This work was supported in part by Japan Grant-in-Aid for Scientific Research no.14550407

14:30

YF1 5 Multidimensional modeling of Trichel pulses in negative point-to-plane corona in air YURI AKISHEV, IGOR KOCHETOV, ALEXANDER LOBOIKO, ANATOLY NAPARTOVICH,* *State Science Center Troitsk Institute for Innovation and Fusion Research* It is known that an electric current in a negative corona for pin-to-plane configuration in a wide range of parameters has a form of periodic pulses, which are called Trichel pulses. In this paper results of comprehensive numerical simulations of pulses evolution for a corona with axial symmetry are reported for a cathode in a form of a needle with hemispherical cap in dry air at atmospheric pressure. Calculations demonstrated that current oscillations became perfect regular after about 25 pulses. Space-time evolution of electric field and charged species densities within one cycle of regular oscillations is described in detail. In contrast to simplified 1.5-D model predicting two-peak shape of Trichel pulse, the exact 3-D model predicts single-peaked pulses when ion induced secondary emission processes are included, and photo-emission is neglected. On the anode surface, radial profiles of electric field and ion and electron current components averaged over one cycle were calculated and compared with the experiments. Variations of individual current pulse amplitude and shape with discharge voltage growth are studied, too.

*Corresponding

14:45

YF1 6 Pin-plane negative corona radial structure evolution under corona-glow discharge-spark transition YURI AKISHEV, TRINITI, *Troitsk, Moscow region, 142190, Russia* ANATOLY NAPARTOVICH, TRINITI, *Troitsk, Moscow region, 142190, Russia* NIKOLAY TRUSHKIN, TRINITI, *Troitsk, Moscow region, 142190, Russia* It is widely believed that negative pin-plane corona in atmospheric pressure air is followed necessarily by spark with an increase in the corona current. We revealed an existence of an intermediate current mode located between well-known regimes (corona and spark) of discharge in pin-plane gap. This current mode named as glow discharge can be observed clearly if the relevant care like blowing of inter-electrode gap being taken to stabilize this regime. Coronaglow discharge transi-

tion is attended with appearance of an intensive light emission from the drift region of corona. An effective diameter of the luminosity radial profile grows with an increase in the corona current. In contrast, the effective diameter of a corona current channel decreases with discharge current. An anode region of glow discharge is unstable and shrinks to a small current spot, which provokes the glow discharge-spark transition. Therefore, in order to understand adequately the mechanism of the coronaspark transition, it is necessary to take into account the physical properties of glow discharge that is the intermediate stage of this transition. Experimental data on evolution of the current and light emission radial distribution under coronaglow discharge-spark will be presented in this report.

15:00

YF1 7 IONIZATION AT THE NOBLE GASES ION-ATOM COLLISIONS IN THE 1-7 KeV ENERGY RANGE BORIS KIKIANI, *Tbilisi state University, Professor* MARIKA CHITALADZE, *Tbilisi state University, laboratory assistant* JOSIF JAPARIDZE, *Tbilisi state University, laboratory assistant* NANA KAVLASHVILI, *Lecturer* RESEARCH LABORATORY OF ATOMIC AND MOLECULAR PHYSICS OF TBILISI STATE UNIVERSITY The absolute total cross sections for production of free electrons, all positive show target gas ions and partial cross sections for production of double charged slow target gas ions at these collisions have been measured. The measurements were carried out by improved transfers electric field ("condenser") and magnetic mass-analyzer methods[1]. It was shown that in the investigated energy range practically there are now slow ions with charged state more than two. Control experiments have been shown that process of electron's liberation from fast particles ("stripping" process) is unlikely in the investigated energy range. Therefore, one can suppose that total cross sections for productions of free electrons are equal to the total cross sections of ionization of the target gas atoms. For symmetrical pairs of colliding particles ($\text{He} + \text{He}$, $\text{Ne} + \text{Ne}$, etc) and for pairs $\text{He} + \text{Ne}$, $\text{Ar} + \text{Kr}$ and $\text{Kr} + \text{Xe}$ values of partial cross-sections are negligible. In the cases of $\text{He} + \text{Kr}$ and $\text{He} + \text{Xe}$ pairs value of these partial cross sections increases with colliding energy and reaches about three percent at the energy 4keV. However, in the cases of $\text{He} + \text{Ar}$, $\text{Na} + \text{Ar}$, Kr , Xe the values of relative portion of the double charged ions in the total amount of slow positive ions are significant (for example in $\text{He} + \text{Ar}$ collision at the energy of 4keV this portion is about 20-25 percent). Analyzes of the correlation diagrams of the diabetics terms of colliding particles system (MS) [2] show that the electron capture processes are accompanying by simultaneous excitation of auto-ionization states of target gas ions. The decay of these states are responsible for realize of double ionization process of the target gas atoms. 1. B. Kikiani, R.Lomsadze, N. Mosulishvili, *Proceedings of Tbilisi State University, Physics*, 34, 114, 1999; 2 M. Barat, W.Lichten, *Phys. Rev.*, A6, 211, 1972.

SESSION YF2: PLASMA PROPULSION AND PLASMA AERODYNAMICS

Friday afternoon, 18 October 2002; Center Forum, Millennium Hotel at 13:30; Rod Boswell, Australian National University, Canberra, presiding

Invited Papers

13:30

YF2 1 Insights on Physics of closed drift plasma thrusters by using externally driven and very fast current interruptions.

ANDRÉ BOUCHOULE,* GREMI, Université d'Orléans

Closed electron drift plasma thrusters, also known as Hall Thrusters or SPT (Stationary Plasma Thrusters) are magnetized discharges where the ion acceleration is provided in the plasma itself by the magnetic barrier restricting electron transport. After their developments and their demonstrations on satellites for orbit control these thrusters appear as very attractive ones in the space technology market. Simultaneously, significant research programs are developed in order to improve the knowledge on the complex physics involved in such devices and to improve simultaneously 2D or 3D simulation codes. Such a program involving academic research teams, agencies and industry is developed in France, in the frame of a coordinated program. GDR N. The experimental research was achieved on diagnostic equipped thrusters, similar to industrial ones. These thrusters are operated in the national research facility PIVOINE, installed in Orlans. The discharge of Hall thrusters is well known as sensitive to fluctuations or oscillations in the few tens kHz range and the physical phenomena connected to these regimes have been widely investigated. Externally driven current interruptions, with very fast ON-OFF transitions (0.15 s), have been shown as a convenient way for obtaining new data on thrusters physics, in connection with time resolved diagnostics like OES, LIF, electron Hall current probe and RFA. Experimental results evidence some details on excitation / ionization (single and multiply charged Xe ions) phenomena and lead to new inputs on electron transport phenomena in the magnetized discharge channel. New experimental insights on microinstabilities will be also be discussed in relation with simulations developed by using PIC codes.

*In collaboration with Mathieu Prioul, GREMI, Université d'Orléans; Jean-Claude Adam, Anne Héron, CPTH, Ecole Polytechnique; Jean-Pierre Boeuf, Laurent Garrigues, CPAT, Université de Toulouse; Daniel Pagnon, Michel Touzeau, LPGP, Université Paris-Sud Orsay.

Contributed Papers

14:00

YF2 2 Performance and Plasma Characteristics of Hall-Effect Thrusters

HIROKAZU TAHARA, Graduate School of Engineering Science, Osaka University TAKAO YOSHIKAWA, Graduate School of Engineering Science, Osaka University Low-power Hall thruster performance was investigated using THT-series Hall thrusters. The THT-III-A thruster could be stably operated in a wide range of magnetic field strength. A high thrust efficiency was achieved with a low discharge current and a high thrust for an optimum magnetic field strength regardless of discharge voltage at a constant mass flow rate. As a result, both the thrust and the specific impulse ranged from 10 to 70 mN and from 1200 to 2300 sec, respectively, at discharge voltages of 200-500 V with mass flow rates of 1-3 mg/s in a wide input power range of 250-1800 W. The thrust efficiency ranged from 30 to 45 %. Furthermore, one-dimensional flowfield calculation was made to understand the inner physical phenomena. Both ionization and plasma acceleration were found to efficiently occur in a thin region with a few mm thick near the acceleration channel exit. The calculated results roughly agreed with the experimental ones.

14:15

YF2 3 A Study of Novel Designs for Plasma Thrusters

ORSON SUTHERLAND, Plasma Research Laboratory, Research School Of Physical Sciences and Engineering, Australian National University, Canberra, Australia MICHAEL IRZYK, Plasma Research Laboratory, Research School Of Physical Sciences and Engineering, Australian National University, Canberra, Australia

CHRISTINE CHARLES, Plasma Research Laboratory, Research School Of Physical Sciences and Engineering, Australian National University, Canberra, Australia JOHN KELLER, Plasma Research Laboratory, Research School Of Physical Sciences and Engineering, Australian National University, Canberra, Australia ROD BOSWELL, Plasma Research Laboratory, Research School Of Physical Sciences and Engineering, Australian National University, Canberra, Australia An important aspect in the design of plasma thruster's for near and deep space environments, where resources are limited, is to maximise specific impulse, as this quantity is directly related to efficiency and maximum velocity. Typically plasma thrusters are designed and operated as high energy ion sources where heavy ions are ejected at high velocity to provide thrust. There is also a strong dependence on reliability. We have been carrying out experiments on several devices for this purpose. A high density Helicon source will be presented as well as two different extractor designs. The first is based around a typical three electrode extractor system, whilst the second makes use of a double layer to accelerate ions to high energies. Analytical and PIC style codes were used in the study as well as a broad range of experimental diagnostics, including langmuir probes, an energy analyser and an emittance counter. A major focus of the work on the three electrode extractor system was the beam formation mechanism, in particular the effects of electrode geometry on the plasma boundary and extractor induced aberrations. A direct comparison between experimental results based on beam measurements, electrode currents and computer simulation will be presented showing that the simulations are actually surprisingly accurate. The properties of divergent, convergent and adapted beams will be discussed as well as how they are obtained.

14:30

YF2 4 Subsonic Plasma Aerodynamics using Lorentzian Momentum Transfer in Atmospheric Normal Glow Discharge Plasmas* J. REECE ROTH, HOJUNG SIN, RAJA CHANDRA MOHAN MADHAN, *University of Tennessee* UT PLASMA SCIENCES LABORATORY COLLABORATION The recent development of the One Atmosphere Uniform Glow Discharge Plasma (OAUGDP) has made it possible to cover large areas, including the wings and fuselage of aircraft, with a thin layer of plasma at low energy cost. The Lorentzian collisions between the ions and neutral gas in the plasma layer couple the electric field and the neutral gas in this layer. The coupling is strong enough at one atmosphere to accelerate the boundary layer flow. One EHD flow acceleration method is based on paraelectric EHD effects, the electrostatic analog of paramagnetism, in which a plasma is accelerated toward increasing electric field gradients, while dragging the neutral gas with it. By using paraelectric effects to add momentum to the flow, we have recently achieved improved flow attachment and increased stall angles in airfoils for external aerodynamic applications. In a second approach, peristaltic flow acceleration, we have used a polyphase power supply to excite the OAUGDP at progressive voltage phase angles on successive linear electrode strips. This excitation produces a traveling wave analogous to the

moving lights on a theatre marquee, which accelerates the ions and neutral gas to velocities of aerodynamic interest.

*Supported in part by AFOSR contract AF F49620-01-10425 (Roth)

14:45

YF2 5 Plasma density and floating potential in the beam plasma with and without magnetic focussing SVETLANA RADOVANOVA, *Varian Semiconductor Equipment Associates, 35 Dory Road, Gloucester, MA 01930* An experimental study of the plasma downstream from an ion beam extraction system is presented. The extraction system is optimized to produce a broad boron beam at relatively low energies 5-20 keV. All ions are accelerated and are traveling with small angles relative to the z direction. Inelastic collisions between beam ions and the background gas form the beam plasma. The behavior of this plasma with and without magnetic focussing was experimentally studied and the potential at the beam edge was measured. The Langmuir probe was positioned downstream 20inch from the extraction region perpendicular to the z direction. The probe was oriented both normal and parallel to the magnetic field. The magnetic field effects on the local floating potential were evaluated. Beam potential as a function of beam energy and species agrees well with theory.(1) A simple model is used to reflect this picture. Calculated potential distributions were compared with the experimental data. 1. Holmes A.J.T. Phys.Rev A 19,(1979) 389.

- A**
 Aanesland, Ane **QWP 49**
 Abada, Hana **NW1 3**
 Abdel-Rahman, M. **GTP 51**
 Abramzon, N. **UR2 4**
 Achete, Carlos A. **GTP 18**
 Adibzadeh, Mehrdad
QWP 6
 Adler, Helmar G. **NW2 3**,
QWP 76
 Akashi, Haruaki **QWP 83**
 Akatsuka, Hiroshi **GTP 25**,
QWP 68
 Akhtar, Kamran **XF2 4**
 Akishev, Yuri **YF1 5**,
YF1 6
 Aldea, Eugen **RR1 3**
 Allan, Michael **SR2 1**
 Alves, L.L. **GTP 46**
 Anderson, Curtis **UR2 3**
 Arnold, S.T. **GTP 10**
 Aroutunov, Mike **QWP 79**
 Arslanbekov, Robert
GTP 79
 Aydil, Eray S. **TR1 2**
- B**
 Babko-Malyi, S. **UR2 4**
 Baede, A.H.F.M. **QWP 91**
 Baede, Loek **QWP 93**
 Bahrim, C. **GTP 8**, **GTP 9**
 Bai, K.H. **QWP 62**
 Bai, Kuenhee **GTP 30**
 Bano, Gregory **GTP 63**
 Bapat, Ameya **XF1 5**
 Barron, C.C. **HT1 5**
 Barroy, Pierre **GTP 53**
 Bartnikas, Raymond **UR2 8**
 Barton, David **WF1 4**
 Bartschat, K. **ET2 3**,
GTP 7, **SR2 3**
 Bastiaens, Bert **QWP 26**
 Basurto, E. **QWP 22**
 Becker, K. **QWP 9**,
QWP 10, **UR2 4**
 Behnke, J.F. **GTP 27**,
GTP 77, **GTP 77**,
GTP 78, **GTP 78**,
QWP 45, **QWP 47**
 Benck, Eric **NW1 1**,
QWP 42
 Bendix, Dietmar **SR1 5**
 Benilov, M.S. **FT2 5**,
NW2 4
 Bernardi, D. **FT2 7**
 Bhandarkar, Upendra
XF1 4
 Bhoj, Ananth **GTP 67**
 Bilyk, O. **QWP 45**
- Blackwell, David **GTP 54**,
QWP 51
 Bletzinger, P. **UR2 6**
 Boeuf, J.-P. **QWP 89**
 Boffard, John B. **SR2 5**
 Boller, K.J. **QWP 78**,
WF2 6
 Boller, Klaus **QWP 26**
 Bol'shakov, A.A. **HT2 4**
 Bolshakov, A.A. **UR1 3**,
YF1 1
 Bonvallet, G.A. **GTP 71**,
NW2 5
 Booth, Jean-Paul **GTP 16**,
GTP 31, **NW1 3**
 Booth, J.P. **ET1 5**
 Borbely, Joseph **GTP 6**
 Borg, Gerard G. **QWP 31**,
QWP 32
 Bose, Deepak **ET1 2**,
UR1 2, **UR1 5**
 Boswell, Rod **HT1 1**,
QWP 49, **YF2 3**
 Bouchoule, André **YF2 1**
 Boufendi, Laifa **XF1 1**
 Bowden, Mark **GTP 49**
 Boyle, Paul **ET1 6**, **ET1 6**
 Bradley, James W. **WF1 4**
 Braithwaite, Nick **GTP 34**,
GTP 53
 Brandenburg, Ronny
QWP 86
 Bratescu, Maria-Antoaneta
YF1 4
 Bray, Igor **GTP 6**
 Brinkmann, Ralf Peter
ET1 4
 Broers, J.L.V. **QWP 92**
 Brok, Wouter **QWP 80**
 Brooke IV, G. **QWP 29**,
RR2 4
 Brooks, N.H. **GTP 86**
 Brown, Michael **QWP 67**
 Brunger, Michael **RR2 1**
 Buckman, S.J. **SR2 4**
 Buckman, Stephen **RR2 3**
 Bulcourt, Nicolas **GTP 16**
 Bussiahn, René **WF2 1**
 Bychkov, Vyatcheslav
NW1 1
 Bychkov, Yuri **QWP 72**
- C**
 Campbell, S.A. **XF1 6**
 Campbell, Stephen **XF1 5**
 Cao, Jin **XF1 8**
 Cappelli, Mark **QWP 13**
 Carter, B. **SR1 6**
 Castrejon, A. **QWP 22**
 Caubet, V. **QWP 92**
- Cekic, Miodrag **QWP 79**
 Chabert, P. **ET1 5**, **RR1 2**
 Chabert, Pascal **GTP 31**,
NW1 3, **RR1 1**
 Chang, Chong H. **UR1 5**
 Chang, Hongyoung **GTP 30**
 Chang, Hong-Young
GTP 57
 Chang, H.Y. **QWP 62**
 Charles, Christine **GTP 21**,
QWP 49, **YF2 3**
 Cheng, C.H. **UR1 6**
 Chen, G.S. **UR1 6**
 Chen, Junhong **XF2 6**
 Chen, Zhiyu **QWP 84**
 Cherry, Robert **QWP 36**
 Chitaladze, Marika **YF1 7**
 Choe, W. **GTP 64**
 Choi, Joon-Sik **QWP 77**
 Choi, Shin Il **GTP 65**,
GTP 89
 Choi, Soo Seok **GTP 65**,
GTP 89
 Cho, Jung-Hyun **QWP 52**
 Christodoulatos, C. **UR2 4**
 Chung, Chinwook **GTP 30**
 Chung, Kyu-Sun **QWP 52**
 Chung, T.R. **GTP 33**
 Cicman, P. **QWP 9**
 Cigal, J.-C. **QWP 91**
 Cigal, Jean-Charles
QWP 93
 Coburn, J.W. **HT1 7**
 Cole, J. Vernon **HT1 4**
 Collaboration, Air Force
 Research Lab Kirtland
 AFB **WF2 5**
 Collaboration, CDL: Philips
 Central Development
 Lighting **QWP 80**
 Collaboration, French
 Research Ministry PPF
GTP 81
 Collaboration, FZR:
 Forschungszentrum
 Rossendorf Dresden
QWP 93
 Collaboration, Hong Kong
WF2 4
 Collaboration, Institute of
 Laser Information
 Technologies of Russian
 Academy of Sciences
QWP 66
 Collaboration, Plasma
 Processing Group **UR1 6**
 Collaboration, Plasma
 Sciences Laboratory
QWP 84
- Collaboration, P.N. Lebedev
 Physics Institute of
 Russian Academy of
 Sciences **QWP 66**,
WF2 5
 Collaboration, Shanghai
WF2 4
 Collaboration, Theoretical
 Electrical Engineering
ET1 4
 Collaboration, Troitsk
 Institute for Innovation
 and Fusion Research
WF2 5
 Collaboration, TUE:
 Eindhoven University of
 Technology **FT1 2**,
QWP 80, **QWP 93**
 Collaboration, UI:
 University of Illinois
FT1 2
 Collaboration, UT Plasma
 Sciences Laboratory
GTP 55, **YF2 4**
 Collaboration, UW-Madison
 USD Sheath **QWP 57**
 Collins, George **GTP 26**,
QWP 25
 Colombo, V. **FT2 7**
 Cornelis, R.A.A. **QWP 92**
 Corr, C.S. **RR1 4**
 Craig, Gary **QWP 21**
 Crowe, R. **UR2 4**
 Cruden, B.A. **HT2 4**,
UR1 3, **YF1 1**
 Cruden, Brett **NW1 2**
 Cruz, Nilson C. **GTP 17**,
GTP 18
 Cunha, M.D. **NW2 4**
 Curry, John J. **NW2 3**,
QWP 76
 Czarnetzki, U. **GTP 45**,
QWP 38, **UR1 4**
- D**
 Dantier, A. **XF2 3**
 Dasgupta, A. **GTP 7**
 Dateo, Christopher **ET2 4**,
TR2 3
 Dave, Bakul **GTP 93**
 Davidson, Jane **XF2 6**
 Davis, Ed **QWP 79**
 DeFrance, P. **QWP 10**
 DeJoseph Jr., C.A.
QWP 15, **QWP 70**
 Demyanov, A.V. **WF2 6**
 Denda, T. **QWP 35**
 Denifl, S. **QWP 9**
 Denning, C. Mark **XF2 4**
 Derkatch, A. **GTP 10**

- de Urquijo, J. **QWP 22**
 Deutsch, H. **QWP 10**
 Dhali, Shirshak **GTP 93**,
QWP 82
 Dias, F.M. **QWP 33**
 Dine, Sebastien **TR1 3**
 Dinh, T. **GTP 92**
 Djuric, Nada **TR2 2**
 Döbele, H.F. **GTP 51**,
GTP 52, **TR1 6**
 Doebele, H.F. **GTP 45**,
QWP 38, **UR1 4**
 Doll, G.L. **GTP 15**
 Domyslawska, Jolanta
GTP 6
 Dorn, Alexander **ET2 1**
 Dubin, D.H.E. **XF1 2**
 Ducree, Jens **WF1 3**
- E**
 Economou, Demetre J.
QWP 37, **UR1 7**, **WF1 2**
 El-Astal, A.H. **UR2 7**
 Ellappan, P. **HT1 5**
 Ellingboe, Albert R. **ET1 6**,
ET1 6, **GTP 35**, **GTP 38**,
QWP 59, **WF2 2**
 Endo, Harumi **QWP 83**
 Enloe, C.L. **QWP 87**
 Eom, G.S. **GTP 64**
- F**
 Fabrikant, I.I. **GTP 8**,
GTP 9
 Fanara, Carlo **FT2 6**
 Fang, Ziwei **QWP 24**
 Fan, Wai Yip **NW1 7**
 Faulkner, Ronan **QWP 59**
 Favia, Pietro **HT2 5**
 Feijen, Jaap **FT1 2**,
QWP 41
 Felch, Susan B. **QWP 24**
 Fernsler, Richard F. **FT1 3**,
GTP 54, **QWP 50**,
QWP 51
 Ferreira, C.M. **QWP 33**,
TR2 4
 Feuerstein, Bernold
QWP 7
 Fiegele, T. **QWP 9**
 Fischer, D. **QWP 12**
 Foest, R. **GTP 27**
 Fontcuberta i Morral, Anna
XF1 7
 Forelines, Robert **QWP 67**
 Foster, M. **QWP 12**
 Franklin, Raoul **FT1 1**
 Fraser, Gerald **NW1 1**
- Fraser, Stuart **WF1 4**
 Fredriksen, Åshild **QWP 49**
 Fresnet, F. **QWP 85**
 Fridman, Alexander **XF2 1**
- G**
 Gallagher, Alan **GTP 63**
 Ganciu, Mihai **GTP 81**
 Ganguly, Biswa N.
GTP 56, **QWP 67**
 Ganguly, B.N. **UR2 6**
 Gans, T. **GTP 51**,
GTP 52, **TR1 6**
 Ganter, Romain **QWP 13**
 Garscadden, A. **QWP 15**
 Garscadden, Alan **LW 1**
 Gavrilenko, V.P. **GTP 50**
 Geigl, Martin **QWP 64**
 Geller, Boris **QWP 79**
 Gendre, Maxime **QWP 80**
 Gerberich, W. **SR1 6**
 Ghedini, E. **FT2 7**
 Gherardi, Nicolas **QWP 86**
 Gidwani, A. **SR1 6**
 Gilgenbach, R.M. **GTP 15**
 Girshick, S. **SR1 6**
 Girshick, Steven **GTP 14**,
GTP 61, **XF1 4**
 Giuliani, J.L. **GTP 7**
 Giuliani, John **QWP 75**
 Glouchkov, Denis **GTP 87**
 Godyak, Valery **FT1 4**,
GTP 43
 Goeckner, M. **QWP 39**
 Goeckner, Matthew J.
GTP 22, **GTP 36**,
QWP 24, **WF1 5**
 Goeckner, M.J. **GTP 23**,
GTP 24
 Golde, Michael F. **GTP 11**
 Golubiantnikov, Guerman
NW1 1, **QWP 42**
 Golubovskii, Yu.B.
GTP 77, **GTP 78**,
QWP 47
 Golubovski, Y. **XF2 3**
 Gonzalvo, Y. Aranda
QWP 61
 Goodyear, Alec **GTP 53**
 Goree, J. **XF1 2**
 Goree, John **XF1 1**
 Gortchakov, Serguei
GTP 68, **QWP 72**,
WF2 1
 Goto, T. **QWP 35**
 Goto, Toshio **NW1 6**,
QWP 65
 Gousset, G. **GTP 46**
- Govindan, T.R. **ET1 2**,
UR1 2
 Goyette, Amanda **QWP 42**
 Graham, Bill **QWP 21**
 Graham, W.G. **RR1 4**,
UR2 7
 Grangeon, Frederic **XF1 7**
 Graves, David B. **HT1 7**
 Greene, Chris H. **TR2 1**
 Groetzschel, Rainer
QWP 93
 Groothuis, Charlotte **XF1 3**
 Grum-Grzhimailo, A.N.
ET2 3, **SR2 3**
 Gstir, B. **QWP 9**
 Guharay, Samar **GTP 19**
 Guillon, Jean **TR1 3**
 Guo, Wei **QWP 70**
- H**
 Haas, Fred **GTP 34**
 Hackett, Charles **FT2 3**
 Hager, G. **WF2 5**
 Hahn, J. W. **GTP 64**
 Hanel, G. **QWP 9**
 Hansen, R.W. **HT1 6**
 Happ, C.T. **HT1 5**
 Hara, Kenichiro **NW1 6**
 Harmon, Nicholas **QWP 6**
 Harris, Jeffrey H. **QWP 31**,
QWP 32
 Hash, David **NW1 2**
 Hatakeyama, Rikizo
QWP 48, **SR1 2**
 Hatton, P.J. **QWP 61**
 Haverlag, Marco **QWP 80**
 Haynes, M.A. **GTP 3**
 Heberlein, J. **SR1 6**
 Heberlein, Joachim **FT2 3**,
SR1 5, **UR2 3**
 Hebert, Michael **QWP 40**
 Hebner, G.A. **TR1 1**
 Hebner, Greg **FT1 6**,
GTP 59
 Hechtfisher, Ulrich
NW2 2, **NW2 3**
 Heggemeier, Jeffrey
QWP 70
 Henriques, J. **QWP 33**,
TR2 4
 Hernandez-Avila, J.L.
QWP 22
 Herrmann, Hans **GTP 84**
 Hershkowitz, Noah **FT1 5**,
QWP 55, **QWP 56**,
QWP 57
 Hess, Helmut **GTP 70**
 Hinojosa, G. **QWP 22**
- Hiramatsu, Mineo **QWP 65**
 Holik, M. **QWP 45**
 Honda, Roberto Y. **GTP 17**
 Hong, Sang-Hee **GTP 90**
 Hong, Sang Hee **GTP 65**,
GTP 89
 Hoogeveen, M.C.R. **WF2 6**
 Horanyi, Mihaly **GTP 60**
 Hori, Masaru **NW1 6**,
QWP 65
 Hoshimiya, Katsumi
GTP 26, **QWP 25**
 Howlader, Mostofa
GTP 55
 Huiskes, R. **QWP 91**
 Huo, Winifred **ET2 4**,
TR2 3
 Hur, Min **GTP 90**
- I**
 Ionikh, Y. **XF2 3**
 Ionin, A. **QWP 66**, **WF2 5**
 Irzyk, Michael **YF2 3**
 Ishigaki, Takuya **QWP 17**
 Ishii, Keiji **GTP 69**
 Ishii, Nobuo **NW1 6**
 Ito, Masahumi **NW1 6**
 Ivanov, S. **QWP 66**
 Ivanov, Vladimir **GTP 87**
- J**
 Jang, Bong-Chul **QWP 52**
 Japaridze, Josif **YF1 7**
 Jelisavcic, Milica **RR2 3**
 Jensen, T.H. **GTP 86**
 Jeon, Hyo-Sik **QWP 77**
 Jeon, Yong-Seog **QWP 77**
 Jiang, Tao **GTP 49**
 Jiao, C.Q. **QWP 15**
 Jindal, Ashish **GTP 36**
 Johnsen, Rainer **GTP 11**
 Johnston, M.D. **GTP 15**
 Jolly, Jacques **GTP 16**,
TR1 3
 Jones, M.C. **GTP 15**
 Jones, S. **GTP 2**, **QWP 2**,
QWP 12
 Jorand, F. **QWP 85**
 Joseph, E.A. **GTP 22**,
GTP 23, **GTP 24**
 Joseph, Eric A. **WF1 5**
 Joyce, Glenn **QWP 50**
 Junior, Sérgio C. **GTP 18**
 Jun, Sanghyun **GTP 57**
- K**
 Kadetov, V.A. **GTP 45**,
QWP 38, **UR1 4**

- Kado, Shigeru QWP 88
 Kadota, K. GTP 50,
 NW1 5
 Kaganovich, Igor D.
GTP 32, GTP 44,
QWP 18, QWP 37,
 UR1 7
 Kakalios, James GTP 62
 Kalhori, S. GTP 10
 Kalpat, S. HT1 5
 Kannadaguli, Nagesha
QWP 5
 Kano, T. GTP 82
 Kavlashvili, Nana YF1 7
 Kawakami, Satoshi NW1 6
 Kayama, Milton E. GTP 18
 Kedzierski, Wladek GTP 6
 Keller, John YF2 3
 Kessaratikoon, P. **QWP 29**
 Keto, John W. QWP 27
 Kettlitz, Manfred GTP 70
 Khampan, Catherine
 QWP 86
 Kho, Enny XF2 4
 Kikiani, Boris YF1 7
 Kim, Doosik WF1 2
 Kim, Gon-Ho **QWP 52**
 Kim, H.C. GTP 33
 Kim, Hyun-Jung QWP 77
 Kim, T. XF1 6
 Kim, Tae Won **TR1 2**
 Kimura, Mineo **GTP 4,**
QWP 3
 Kimura, T. **GTP 76**
 Kimura, Takashi GTP 80
 Kimura, Yoshihito SR1 3
 Kitajima, Masashi RR2 3
 Klein, Mason **UR2 5**
 Klimachev, Yu WF2 5
 Kobori, Hiroyuki **GTP 25**
 Kochetov, Igor WF2 4,
 YF1 5
 Ko, Eunsuk FT1 5,
QWP 55, QWP 56,
 QWP 57
 Koike, Shuji GTP 25
 Kokoouline, V. TR2 1
 Kolobov, Vladimir I.
GTP 79, HT1 4
 Kono, A. **GTP 82,**
QWP 54
 Koo, Bon-Woong QWP 24
 Kortor, Timothy NW1 1
 Kortshagen, U. XF1 6
 Kortshagen, Uwe GTP 61,
 GTP 62, QWP 40,
 UR2 3, XF1 4, XF1 5
 Koshelev, K.N. GTP 87
 Kotkov, A. QWP 66,
 WF2 5
 Kozlov, A. QWP 66
 Kozlov, Kirill V. QWP 86
 Kriha, Vitezslav **GTP 94**
 Kroesen, Gerrit FT1 2,
 GTP 49, QWP 41,
 QWP 80, QWP 93,
 XF1 3
 Kroesen, G.M.W. QWP 91
 Kroutilina, Valentina
QWP 64
 Kudrna, P. QWP 45,
 QWP 47
 Kunts, S. QWP 92
 Kurnosov, A. WF2 5
 Kushner, Mark J. ET1 1,
 FT1 2, GTP 67, UR1 8,
 WF2 3
- L**
 Lampe, Martin TR1 5
 Lange, Hartmut GTP 68,
 WF2 1
 Larson, M. GTP 10
 Lauer, J.L. **HT1 6**
 Lauro-Taroni, Laura
 GTP 34
 Lau, Y.Y. GTP 15
 Lavrich, Rich NW1 1
 Lawler, J.E. GTP 71,
 NW2 5
 Lazarides, A. GTP 15
 Lebedv, V. GTP 27
 Lee, Chan-Min GTP 90
 Lee, Chan Min GTP 65,
GTP 89
 Lee, D. S. QWP 62
 Lee, Ji-Young QWP 77
 Lee, J.K. GTP 33
 Lee, Sang-Won GTP 57
 Lei, Yu **QWP 24**
 Lenef, Alan **GTP 72**
 Leonhardt, Darrin GTP 54,
 QWP 51
 Leou, K.C. **UR1 6**
 Leprince, P. GTP 46
 Lezcano, Pedro QWP 79
 Liao, Feng **GTP 14**
 Lichtenberg, A.J. RR1 2
 Lieberman, M.A. **ET1 5,**
 RR1 2
 Lieberman, Michael A.
 GTP 31
 Linardakis, Peter **QWP 31,**
QWP 32
 Lin, Chun C. SR2 5
 Linnane, Shane **GTP 35**
- Lin, T.L. UR1 6
 Li, Peng NW1 7
 Lisovskiy, Valeriy TR1 3
 Liu, Bin **XF1 1**
 Liu, Yonghua GTP 22,
 GTP 23, GTP 24, WF1 5
 Loboiko, Alexander YF1 5
 Lo, Dennis **WF2 4**
 Loffhagen, Detlef GTP 68,
QWP 19, QWP 58
 Lohmann, B. GTP 3
 Lower, Julian RR2 3
 Luckowski, E.D. **HT1 5**
- M**
 MacAdam, Keith B.
 QWP 5
 MacAskill, John **GTP 6**
 Madani, Ramin **QWP 36**
 Madhan, Raja Chandra
 Mohan YF2 4
 Madison, D.H. GTP 2,
 GTP 3, QWP 2,
QWP 12
 Maerk, T. QWP 9,
 QWP 10
 Maeshige, K. FT1 7
 Mahajan, Satish GTP 73
 Maiorov, V.A. GTP 77,
 GTP 78
 Makabe, T. FT1 7, HT1 2,
 QWP 35, QWP 44
 Mangolini, Lorenzo **UR2 3**
 Marakhtanov, A.M. **RR1 2**
 Markhotok, A. QWP 29
 Marler, J.P. **SR2 4**
 Martinez, A. HT1 5
 Martin, Noel M. QWP 31
 Massines, Francoise
 QWP 86
 Matejcik, S. QWP 9
 Matsoukas, Themis XF1 8
 Matsuura, Haruaki GTP 25,
 QWP 68
 Matsuzaki, Mitsuo GTP 25
 Matt-Leubner, S. QWP 10
 Maurice, Carole **FT1 2,**
 QWP 41, QWP 93
 Maurice, C.Y.M. QWP 91
 Mayo, Robert M. QWP 63
 McCluskey, Craig W.
 QWP 27
 McConkey, William GTP 6
 McCord, J. WF2 5
 McCurdy, C. William
 QWP 4
 McKoy, Vincent GTP 5
 McLaughlin, T.E. QWP 87
- McMurry, P.H. SR1 6,
 XF1 6
 Mechtchanov, A. XF2 3
 Meger, Robert GTP 54,
 QWP 51
 Meichsner, Jürgen QWP 64
 Mentel, Juergen NW2 1
 Mentrelli, A. FT2 7
 Meyyappan, M. ET1 2,
 HT2 4, NW1 2, UR1 2,
 UR1 3, YF1 1
 Michel, Peter QWP 86
 Miller, M. HT1 5
 Mills, Randell L. **QWP 63**
 Mine, T. **QWP 44**
 Mitko, S.V. QWP 78,
 WF2 6
 Miyoshi, Y. QWP 35
 Moeller, C.P. GTP 86
 Moeller, Wolfhard QWP 93
 Mogul, R. HT2 4
 Mook, W. SR1 6
 Moore, J.J. QWP 46
 Morrow, T. UR2 7
 Morrow, Tom QWP 21
 Moselhy, Mohamed
 GTP 75, **QWP 73**
 Moshammer, R. QWP 12
 Moskowit, Phil **QWP 69**
 Moskwinski, L. **UR2 4**
 Moss, Richard S. **GTP 67**
 Mostaghimi, J. GTP 88
 Mukherjee, R. SR1 6
 Murakami, Yukio GTP 69
 Muratore, C. **QWP 46**
 Murphy, Donald QWP 51
 Muthuswami, Navin
QWP 82
 Muto, Nahoko QWP 88
- N**
 Nagai, Hisao **QWP 65**
 Naidis, G.V. FT2 5
 Nam, Jun Seok GTP 65
 Nanbu, K. UR1 1
 Napartovich, Anatoly
 WF2 4, WF2 5, YF1 5,
 YF1 6
 Neale, I.D. **QWP 61**
 Nehmzow, Bernd GTP 70
 Nelson, B. SR1 6
 Nordheden, Karen J. YF1 3
 Nosenko, V. **XF1 2**
 Nosenko, Vladimir XF1 1
 Nozaki, Tomohiro
QWP 88, SR1 3
 Nuamatha, Prasad **GTP 93**

O

Oda, A. GTP 76
 Oda, Akinori **GTP 80**,
 QWP 83
 Ohl, Andreas **HT2 1**
 Ohta, Takayuki **NW1 6**
 Okamoto, M. **NW1 5**
 Okazaki, Ken **QWP 88**,
 SR1 3, **XF2 2**
 Olthoff, James **QWP 42**
 Omi, T. **QWP 35**
 Onthong, U. **QWP 10**
 Onzawa, Tadao **FT2 4**
 Oohara, Wataru **QWP 48**
 Orel, A.E. **QWP 8**
 Orlando, Thomas **RR2 2**
 Orphal, Johannes **GTP 81**
 Overzet, L. **QWP 39**
 Overzet, Lawrence J.
 GTP 36, **QWP 24**,
 WF1 5
 Overzet, L.J. **GTP 22**,
 GTP 23, **GTP 24**

P

Panajotovic, Radmila
RR2 3
 Parajuli, R. **QWP 10**
 Park, Byeong-Ju **QWP 77**
 Park, C.W. **GTP 64**
 Park, S.E. **GTP 33**
 Park, S. E. **GTP 64**
 Park, Soonam **GTP 14**
 Pashaie, Bijan **GTP 93**,
 QWP 82
 Pasquiers, S. **QWP 85**
 Perrey, C. **SR1 6**
 Peters, John **FT2 3**
 Peters, P.J.M. **QWP 78**,
 WF2 6
 Petrov, George **QWP 75**,
 YF1 2
 Pfender, Emil **KW 1**
 Phelps, A.V. **QWP 14**,
 QWP 28
 Picatto, P.J. **UR2 4**
 Piscitelli, D. **QWP 89**
 Pitchford, L.C. **QWP 28**,
 QWP 89
 Plusquellic, David **NW1 1**
 Pointu, Anne-Marie
 GTP 81
 Polomarov, Oleg **GTP 40**
 Popović, S. **GTP 92**,
 QWP 29, **RR2 4**
 Porokhova, I. **XF2 3**
 Porokhova, I.A. **QWP 47**
 Pratti, L. **QWP 39**

Prideaux, A. **GTP 3**
 Probst, M. **QWP 10**

Q

Qi, B. **GTP 15**

R

Radovanov, Svetlana
YF2 5
 Radtke, Matthew T. **HT1 7**
 Radu, Ion **UR2 8**
 Rajaraman, Kapil **WF2 3**
 Ramaekers, F.C.S. **QWP 92**
 Ramamurthi, Badri
QWP 37, UR1 7
 Ramprasad, R. **HT1 5**
 Rangel, Elidiane C.
GTP 17, GTP 18
 Rao, M.V.V.S. **HT2 4**,
 NW1 2, **UR1 3**, YF1 1
 Rax, Jean-Marcel **GTP 31**
 Rax, J.M. **ET1 5**
 Raymond, M.V. **HT1 5**
 Ray, Paresh Chandra
QWP 63
 Rees, J.A. **QWP 46**,
 QWP 61
 Rimmel, T.P. **HT1 5**
 Remy, Jerome **XF1 3**
 Renault, T. **SR1 6**
 Rescigno, Thomas N.
QWP 4
 Revel, I. **QWP 89**
 Riemann, K.-U. **GTP 41**,
GTP 42, **GTP 87**
 Riley, M.E. **TR1 1**
 Riley, Merle E. **GTP 59**,
SR2 6
 Ritchie, A. Burke **SR2 6**
 Roberts, D.R. **HT1 5**
 Robertson, Scott **GTP 60**,
 TR1 5
 Roca i Cabarrocas, Pere
XF1 7
 Roepcke, J. **XF2 3**
 Röpcke, J. **QWP 85**
 Rosati, Richard E. **GTP 11**
 Rosen, S. **GTP 10**
 Rosocha, Louis **GTP 84**
 Roth, J. Reece **GTP 55**,
QWP 84, **YF2 4**
 Rousseau, A. **QWP 85**,
XF2 3
 Rozsa, Karoly **GTP 63**
 Ruckman, Mark **QWP 79**
 Ruemmele, M. **QWP 9**
 Russell, T.H. **QWP 61**
 Rusz, J. **QWP 45**

Rybin, Andrew **WF2 2**

S

Sadd, M. **HT1 5**
 Saito, Shigeki **FT2 4**
 Sakai, Y. **GTP 13**, **SR1 4**
 Sakai, Yosuke **GTP 29**,
QWP 17, **QWP 83**,
 YF1 4
 Sakamoto, Takeshi
QWP 68
 Sansonetti, Craig J. **NW2 3**
 Santos, Deborah C.R.
GTP 17
 Sant, Sanket **GTP 22**,
GTP 24
 Sasaki, K. **GTP 50**,
NW1 5
 Sato, Genta **QWP 48**
 Scharer, John E. **XF2 4**
 Scheier, P. **QWP 9**
 Schmidt, M. **GTP 27**
 Schoenbach, Karl H.
GTP 75, **QWP 73**
 Schrauwen, C.P.G. **RR1 3**
 Schulz, M. **QWP 12**
 Schulz-von der Gathen, V.
GTP 51, **GTP 52**, **TR1 6**
 Seleznev, L. **QWP 66**,
WF2 5
 Semaniak, J. **GTP 10**
 Sengupta, Debasis **GTP 79**
 Seo, Jun Ho **GTP 65**
 Severn, Greg **FT1 5**,
QWP 56, **QWP 57**
 Shangguan, Cheng **WF2 4**
 Shankaran, Arvind **FT1 2**
 Shan, Y. **GTP 88**
 Shard, A.G. **HT2 2**
 Sharma, S.P. **HT2 4**,
UR1 3
 Sharma, Surendra **NW1 2**,
YF1 1
 Shen, Z. **XF1 6**
 Sheu, J.C. **HT1 4**
 Shih, Han C. **SR1 1**
 Shiozawa, M. **UR1 1**
 Shi, Wenhui **GTP 75**
 Shnyrev, S. **WF2 5**
 Shohet, J.L. **HT1 6**
 Shon, C.H. **HT1 2**
 Shon, J.W. **GTP 33**
 Short, Robert D. **WF1 4**
 Sia, Joanne **YF1 3**
 Sieg, Michael **GTP 70**
 Sigener, Florian
QWP 19, **QWP 20**,
QWP 58

Silapunt, Rardchawadee
HT1 3
 Sin, Hojung **YF2 4**
 Sinitzyn, D. **WF2 5**
 Smith, D.J. **NW2 5**
 Soberon, Felipe **QWP 59**
 Sobolewski, Mark A.
NW1 4, **TR1 4**
 Sonnenfeld, A. **GTP 27**
 Sorokine, Mikhail **XF1 3**
 So, Soon-Youl **GTP 29**
 Srinivasan, S. **QWP 39**
 Stalder, Kenneth **GTP 83**,
XF2 5
 Stalder, K.R. **HT2 3**,
UR2 7
 Stamatovic, A. **QWP 9**
 Stano, M. **QWP 9**
 Starostin, S.A. **QWP 78**,
WF2 6
 Steen, P.G. **RR1 4**, **UR2 7**
 Steen, Philip **QWP 21**
 Steffen, H. **GTP 27**
 Steffens, Kristen L. **NW1 4**
 Stemile, B. **HT1 5**
 Sternberg, Natalia **FT1 4**,
GTP 43
 Sternovsky, Zoltan
GTP 60, **TR1 5**
 Stewart, M.D. **SR2 5**
 Stoffels, E. **QWP 91**,
QWP 92
 Stoffels, Winfred **XF1 3**
 Stoker, David S. **QWP 27**
 Straub, S. **HT1 5**
 Suda, Y. **GTP 13**, **SR1 4**
 Suganuma, Y. **GTP 13**,
SR1 4
 Sugawara, Hirotake
GTP 29, **QWP 17**
 Sugiyama, T. **GTP 82**
 Sullivan, J.P. **SR2 4**
 Surko, C.M. **SR2 4**
 Sutherland, Orson **YF2 3**

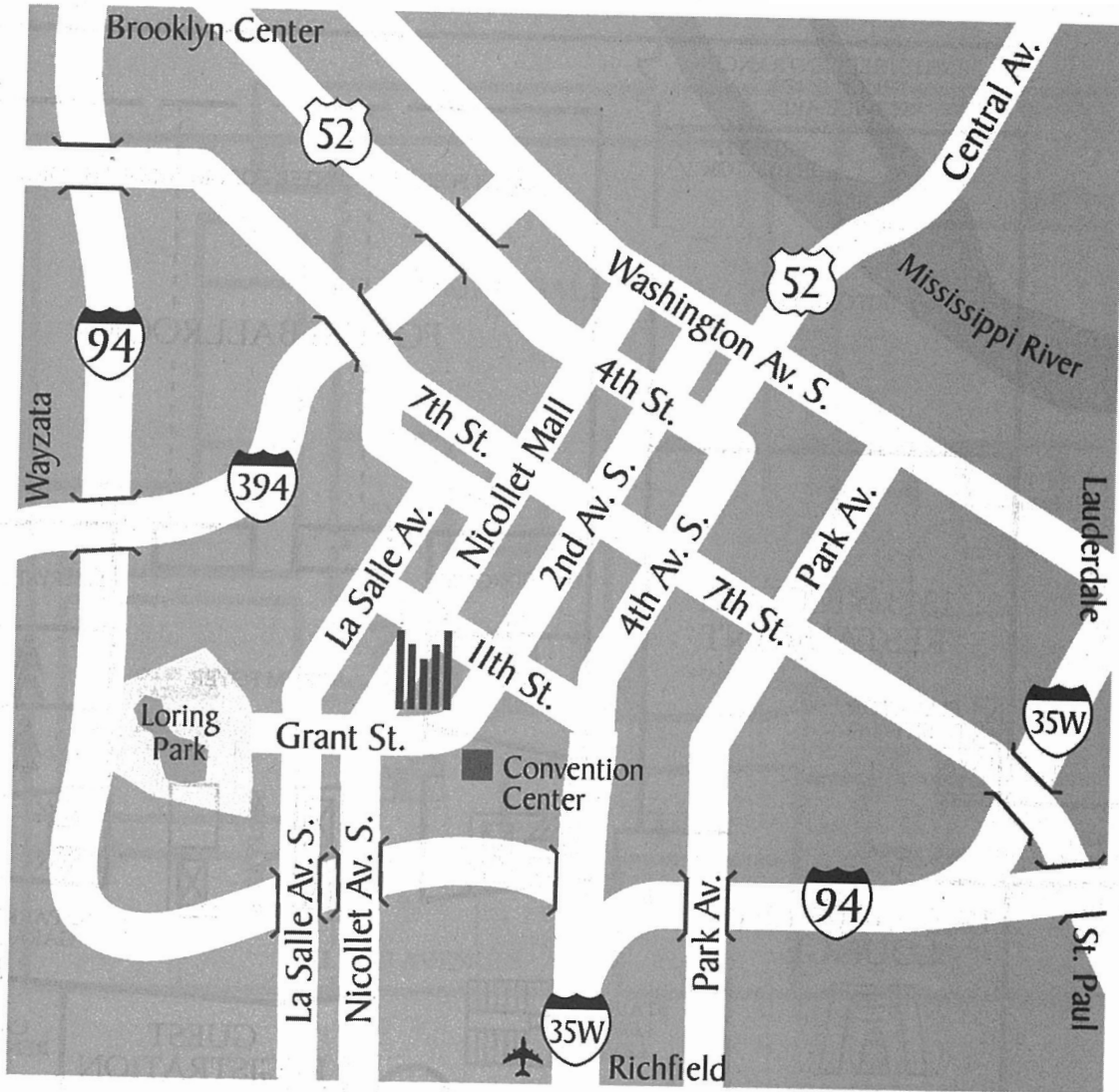
T

Tabacniks, Manfredo H.
GTP 18
 Tahara, Hirokazu **FT2 1**,
FT2 2, **GTP 47**, **YF2 2**
 Takada, M. **QWP 44**
 Takahashi, Kunio **FT2 4**
 Takano, Yoshimichi
GTP 69
 Takashima, Seigou
QWP 65
 Takizawa, K. **GTP 50**
 Tanaka, Hiroshi **RR2 3**

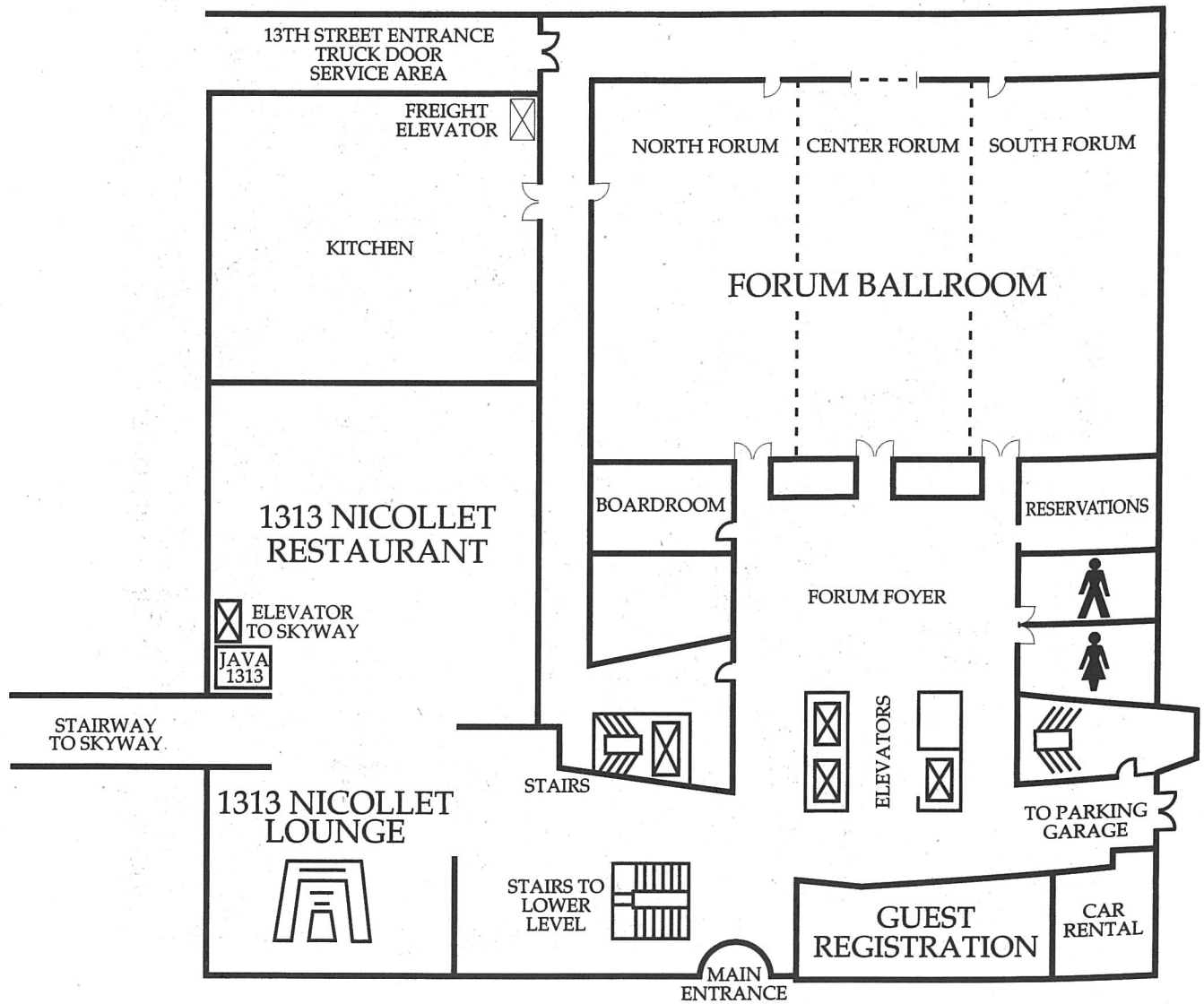
- Tatarova, E. **QWP 33**,
TR2 4
- Team, EPG **QWP 41**
- Team, Low Temperature
Plasma Physics **QWP 64**
- Team, Research laboratory
of atomic and molecular
physics of Tbilisi State
university **YF1 7**
- Team, Troitsk **WF2 4**
- Team, Yamaguchi
University **QWP 3**
- Teslow, Hilary **GTP 84**
- Theodosiou, Constantine
GTP 40, **QWP 6**
- Thompson, Catherine
QWP 21
- Thompson, Siri **GTP 62**
- Thumm, U. **GTP 8**,
GTP 9
- Thumm, Uwe **QWP 7**,
SR2 2, **WF1 3**
- Tichý, M. **QWP 45**,
QWP 47
- Tochikubo, Fumiyoshi
UR2 2
- Touzeau, Michel **GTP 81**
- Toyoda, Hirotaka **WF1 1**
- Toyoyoshi, Reo **QWP 68**
- Trunec, David **QWP 86**
- Trushkin, Nikolay **YF1 6**
- Turner, Miles M. **ET1 6**,
ET1 6, **GTP 31**, **GTP 38**
- Turner, M.M. **ET1 5**
- Tuszewski, M. **RR1 2**
- Tysk, Shane M. **XF2 4**
- U**
- Uchida, Satoshi **UR2 2**
- Udalov, Y.B. **WF2 6**
- Udalov, Yu.B. **QWP 78**
- Ueda, Masakazu **GTP 29**
- Ugglas, M.Af. **GTP 10**
- Uhm, H.S. **QWP 62**
- Uhrlandt, Dirk **GTP 68**,
QWP 30, **WF2 1**
- Ulrich, J. **QWP 12**
- V**
- van den Nieuwenhuizen,
Huub **QWP 80**
- van der Mullen, Joost
QWP 80
- van de Sanden, M.C.M.
RR1 3
- van Dijk, Jan **QWP 80**
- VanDyken, R.D. **QWP 87**
- van IJzendoorn, Leo
QWP 93
- van IJzendoorn, L.J.
QWP 91
- Vasenkov, Alex **ET1 1**,
UR1 8, **WF2 3**
- Vender, David **GTP 38**
- Vertuan, A. **FT2 7**
- Vervloet, Michel **GTP 81**
- Vidmar, Robert **GTP 83**,
XF2 5
- Viggiano, A.A. **GTP 10**
- Vilarinho, Louriel Oliveira
FT2 6
- Visser, Bram **GTP 49**
- Vos, Ted **QWP 80**
- Vušković, L. **GTP 92**,
QWP 29, **RR2 4**
- W**
- Wagenaars, E. **QWP 91**
- Wagenaars, Erik **QWP 93**
- Wagner, Hans-Erich
QWP 64, **QWP 86**,
UR2 1
- Wagner, Nicole **SR1 5**
- Walhout, Matthew **UR2 5**
- Walton, Scott **GTP 54**,
QWP 51
- Wang, X. **SR1 6**
- Wang, Xu **FT1 5**,
QWP 55, **QWP 56**,
QWP 57
- Wang, Yicheng **QWP 42**
- Warthesen, Sarah **GTP 61**
- Watanabe, Masahiro
GTP 26
- Watanabe, Shigeru **FT2 4**
- Watanabe, Sou **GTP 25**
- Watanabe, Tsuneo **UR2 2**
- Wellie, Th. **GTP 42**
- Wendt, Amy **HT1 3**
- Wertheimer, Michael
UR2 8
- Whelan, Colm T. **ET2 2**
- White, Ben O. **XF2 4**
- Williamson, James M.
GTP 56
- Winkler, Rolf **QWP 19**,
QWP 20, **QWP 58**
- Winstead, Carl **GTP 5**
- Woloszko, J. **HT2 3**
- Y**
- Yagisawa, T. **FT1 7**
- Yang, Yunqiang **GTP 55**
- Yastremsky, Arkady
QWP 72
- Yen, G.W. **UR1 6**
- Yi, Dechang **GTP 73**
- Yoo, Hyun-Jong **QWP 52**
- Yoshigoe, T. **GTP 76**
- Yoshikawa, Takao **FT2 1**,
FT2 2, **GTP 47**, **YF2 2**
- Yoshizaki, Yasunao **YF1 4**
- You, Shinjae **GTP 30**
- Yu, Zengqi **GTP 26**,
QWP 25
- Z**
- Zachariah, Michael **GTP 14**
- Zhang, Peng **UR2 3**
- Zhou, Baosuo **GTP 22**,
GTP 23, **GTP 24**,
WF1 5
- Zhou, Ning **ET1 3**
- Zorat, Roberto **GTP 38**
- Zurcher, P. **HT1 5**

NOTES

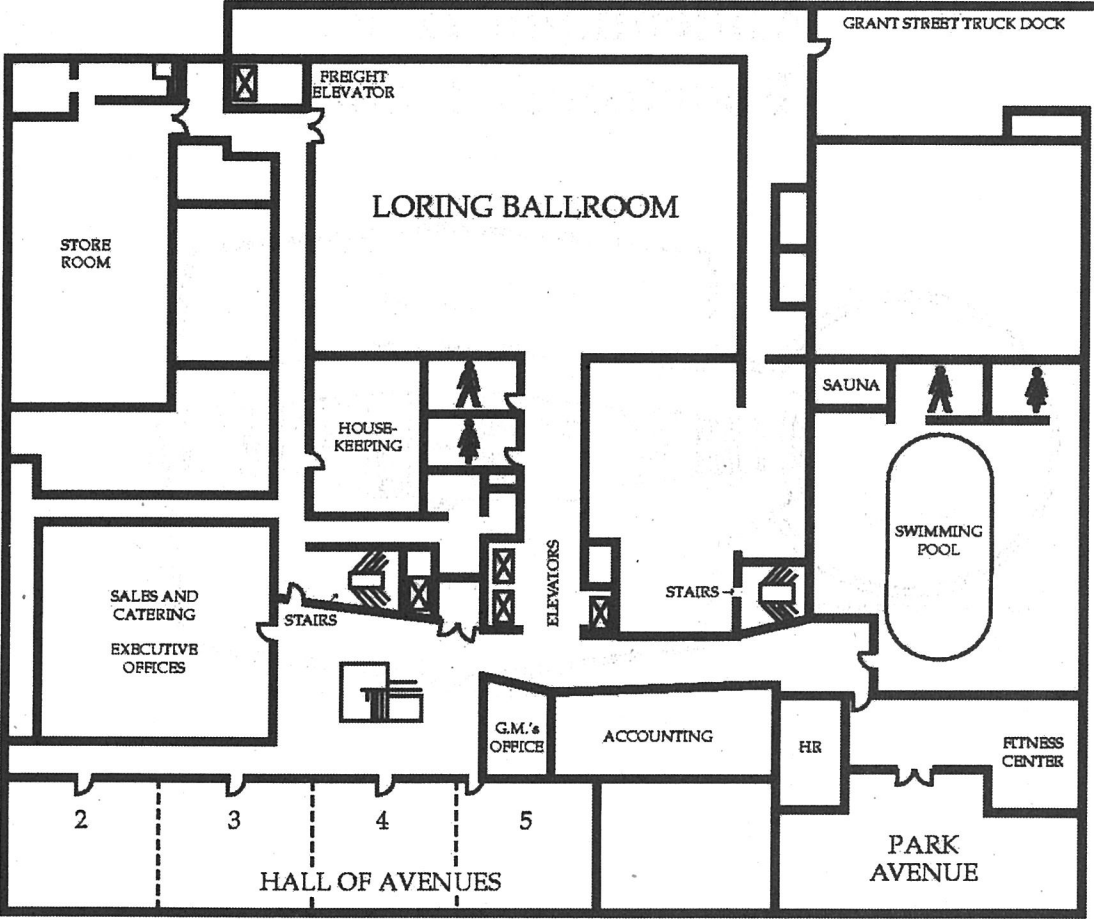
Downtown Minneapolis



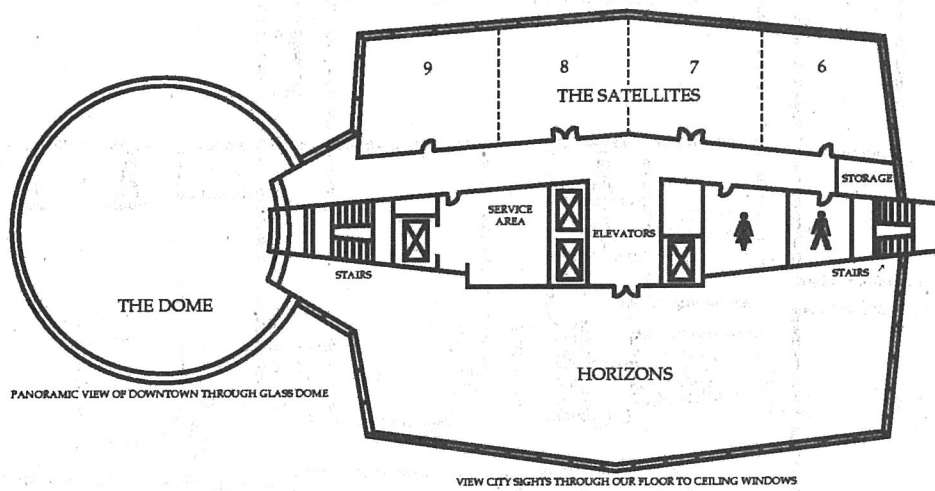
Millennium Hotel Lobby Level



Millennium Hotel Lower Level



Millennium Hotel Fourteenth Floor



On the Cover: Single-crystalline silicon nanoparticles synthesized in low-pressure inductive silane:helium discharge. Ameya Bapat, Uwe Kortshagen, Mechanical Engineering; Chris Perrey, C. Barry Carter, Chemical Engineering and Materials Science; Stephen A. Campbell, Electrical Engineering, University of Minnesota.

Epitome of the 55th Gaseous Electronics Conference of The American Physical Society

13:00 MONDAY AFTERNOON
14 OCTOBER 2002

AMT **Tutorial I: Biomedical Applications of Plasmas**
Satellites 6,7, Millennium Hotel

14:45 MONDAY AFTERNOON
14 OCTOBER 2002

BMT **Tutorial II: The Physics of Filamentary, Regularly-Patterned and Diffuse Barrier Discharges**
Satellites 6,7, Millennium Hotel

16:30 MONDAY AFTERNOON
14 OCTOBER 2002

CMT **Tutorial III: Nanoparticles and Plasmas**
Satellites 6,7, Millennium Hotel

19:00 MONDAY EVENING
14 OCTOBER 2002

DM **Reception and Registration**
Horizons/Dome, Millennium Hotel

8:00 TUESDAY MORNING
15 OCTOBER 2002

ET1 **Plasma Modeling**
North Forum, Millennium Hotel

ET2 **Ionization of Atoms and Molecules**
Dorn, Whelan
Center Forum, Millennium Hotel

10:00 TUESDAY MORNING
15 OCTOBER 2002

FT1 **Plasma Boundaries: Sheaths and Boundary Layers**
North Forum, Millennium Hotel

FT2 **Thermal Plasmas**
Center Forum, Millennium Hotel

13:15 TUESDAY AFTERNOON
15 OCTOBER 2002

GTP **Poster Session I**
Horizons/Satellites, Millennium Hotel

15:30 TUESDAY AFTERNOON
15 OCTOBER 2002

HT1 **Plasma Processing**
Boswell
North Forum, Millennium Hotel

HT2 **Biological and Emerging Applications of Plasmas**
Ohl, Shard, Favia
Center Forum, Millennium Hotel

19:15 TUESDAY EVENING
15 OCTOBER 2002

JTW **Workshop: The Bohm Criterion and Sheath Formation**
Dome, Millennium Hotel

8:15 WEDNESDAY MORNING
16 OCTOBER 2002

KW **GEC Foundation Talk**
Pfender
North/Center Forum, Millennium Hotel

10:00 WEDNESDAY MORNING
16 OCTOBER 2002

LW **APS Allis Prize Talk**
Garscadden
North/Center Forum, Millennium Hotel

11:15 WEDNESDAY MORNING
16 OCTOBER 2002

MW **GEC Business Meeting**
North/Center Forum, Millennium Hotel

13:15 WEDNESDAY AFTERNOON
16 OCTOBER 2002

NW1 **Diagnostics of Reactive Plasmas**
North Forum, Millennium Hotel

NW2 **Thermal Plasmas: Lamps and Electrodes**
Mentel, Hechtischer
Center Forum, Millennium Hotel

15:30 WEDNESDAY AFTERNOON
16 OCTOBER 2002

PW **Laboratory Tours**
University of Minnesota

19:15 WEDNESDAY EVENING
16 OCTOBER 2002

QWP **Poster Session II**
Horizons/Satellites, Millennium Hotel

8:00 THURSDAY MORNING
17 OCTOBER 2002

RR1 **Instabilities**
Chabert
North Forum, Millennium Hotel

RR2 **Collisions with Complex Targets**
Brunger, Orlando
Center Forum, Millennium Hotel

10:00 THURSDAY MORNING
17 OCTOBER 2002

SR1 **Plasmas for Nanostructured Materials**
Shih, Hatakeyama
North Forum, Millennium Hotel

SR2 **Near Threshold Processes**
Allan, Thumm
Center Forum, Millennium Hotel

13:30 THURSDAY AFTERNOON
17 OCTOBER 2002

TR1 **Plasma Diagnostics: Electrical and Optical**
North Forum, Millennium Hotel

TR2 **Recombination and Dissociation**
Greene, Djuric
Center Forum, Millennium Hotel

15:30 THURSDAY AFTERNOON
17 OCTOBER 2002

UR1 **Inductively Coupled Plasmas and Plasma Sources**
North Forum, Millennium Hotel

UR2 **Atmospheric Pressure Nonthermal Plasmas I**
Wagner
Center Forum, Millennium Hotel

18:45 THURSDAY EVENING
17 OCTOBER 2002

VR **Reception and Banquet**
Millennium Hotel

8:00 FRIDAY MORNING
18 OCTOBER 2002

WF1 **Plasma Surface Interactions**
Toyoda
North Forum, Millennium Hotel

WF2 **Nonequilibrium Light Sources**
Center Forum, Millennium Hotel

10:00 FRIDAY MORNING
18 OCTOBER 2002

XF1 **Plasmas for Nanostructures and Dusty Plasmas**
North Forum, Millennium Hotel

XF2 **Atmospheric Pressure Nonthermal Plasmas II**
Fridman, Okazaki
Center Forum, Millennium Hotel

13:30 FRIDAY AFTERNOON
18 OCTOBER 2002

YF1 **Plasma Diagnostics: Optical Emission**
North Forum, Millennium Hotel

YF2 **Plasma Propulsion and Plasma Aerodynamics**
Bouchoule
Center Forum, Millennium Hotel



0003-0503(200210)47:7;1-Z